1999

Interpenetrated and interlocked molecules via bis(pyridinium)ethanes.

James Andrew. Wisner
University of Windsor

INFORMATION TO USERS

This manuscript has been reproduced from the microfilm master. UMI films the text directly from the original or copy submitted. Thus, some thesis and dissertation copies are in typewriter face, while others may be from any type of computer printer.

The quality of this reproduction is dependent upon the quality of the copy submitted. Broken or indistinct print, colored or poor quality illustrations and photographs, print bleedthrough, substandard margins, and improper alignment can adversely affect reproduction.

In the unlikely event that the author did not send UMI a complete manuscript and there are missing pages, these will be noted. Also, if unauthorized copyright material had to be removed, a note will indicate the deletion.

Oversize materials (e.g., maps, drawings, charts) are reproduced by sectioning the original, beginning at the upper left-hand corner and continuing from left to right in equal sections with small overlaps.

Photographs included in the original manuscript have been reproduced xerographically in this copy. Higher quality 6" x 9" black and white photographic prints are available for any photographs or illustrations appearing in this copy for an additional charge. Contact UMI directly to order.

ProQuest Information and Learning
300 North Zeeb Road, Ann Arbor, MI 48106-1346 USA
800-521-0600

Interpenetrated and Interlocked Molecules Via Bis(pyridinium)ethanes

by

James A. Wisner

A Dissertation
Submitted to the
College of Graduate Studies and Research
Through the School of Physical Sciences,
Chemistry and Biochemistry
In Partial Fulfillment of the
Requirements for the Degree
Of Doctor of Philosophy at
The University of Windsor

Windsor, Ontario, Canada

ABSTRACT

This thesis deals with the synthesis of [2]pseudorotaxane, [2]-, and [3]rotaxane architectures utilizing bis(pyridinium)ethane dications and 24-membered crown ethers as templating agents.

Eight bis(pyridinium)ethane dications **2a-h** were synthesized and their complexation behaviour with six 24C8 derivatives **3a-f** was examined. All the dications formed [2]pseudorotaxane geometries in solution with the crown ethers except for **2c** which did not form a complex with any of **3a-f** due to steric constraints. Association constants for pseudorotaxane formation were determined by ^{1}H NMR spectroscopy for all the complexes formed and the thermodynamics of formation of the pseudorotaxanes involving **2g** and **3a-f**. The crystal structures of [2]pseudorotaxanes **2e:3c**, **2f:3c**, and **2g:3c** were determined.

[2]Pseudorotaxane **2e:3c** was converted to [2]rotaxanes **7** and **9** by two different synthetic routes. The ^{1}H NMR spectra were examined and the crystal structures of **7** and **9** were determined.

Two axle-shaped tetracations **11** and **12** were synthesized and converted, via benzylation in the presence of **3c**, to the respective [3]rotaxanes **14** and **15**, and [2]rotaxane molecular shuttles **16** and **17**. The ^{1}H NMR spectra of these compounds was examined and compared to the non-mechanically bonded benzylated products **18** and **19**. The dynamic behaviour of the [2]rotaxane shuttles was investigated by ^{1}H NMR spectroscopy to determine the free energy of activation. In addition, it was established

that molecular shuttle **17** displayed preference for one translational isomer. The crystal structures of **14** and **17** were also determined.

This work is dedicated to my mother and Suse.
My love to both of you.

So we make stories of our own,
in fevered and envious imitation of our Maker,
hoping that we'll tell, by chance, what God left untold.
And finishing our tale,
come to understand why we were born.

Clive Barker

Excerpt from the book *Sacrament*.

ACKNOWLEDGEMENTS

The first person I have to thank is undoubtedly my boss Steve Loeb. I picked him out on the basis of his literature presence and I count it one of the luckier developments of my life that he turned out to be a *truly great guy*. **No, Really**. When people told me before grad school that your boss ends up being one of your friends, I just couldn't imagine it. But here we are anyway.

Thanks also goes out to my lab mates and "chemistry" friends over the years: Chris Deslippe, Beth Cameron, Shannon Murphy, Jeff Hall, Jim Kickham, Clayton Price, Derek Beauchamp, Dave Tramontozzi, Norma Georges, Chantelle Bondy, Sarah Vella, Iavor Mihalkov, Amy Hubbard, Sam Murray, Silke Courtenay, and Nancy Yue. Good times all around. *I love you man.*

A deep thanks to Mike Feurth and Vivi Lazarescu for their technical support and the occasional dirty joke.

Finally, I would like to thank my family and Susan Roberts for their unconditional love and support. Ya just can't get things done without that.

TABLE OF CONTENTS

LIST OF FIGURES

LIST OF TABLES

LIST OF ABBREVIATIONS

Å	Angstrom
b	broad
Bu	butyl
°C	degrees Centigrade
d	doublet
δ	chemical shift
ESI	electrospray ionization
Et	ethyl
F_c	calculated structure factor
F_o	observed structure factor
fw	formula weight
g	grams
h	hours
Hz	Hertz
J	joule
K	degrees Kelvin
kJ	kilojoules
LSI	liquid secondary ionization
μ	absorption coefficient
m	multiplet
Me	methyl

MHz	megaHertz
min	minutes
mL	millilitres
mmol	millimoles
mol	moles
mp	melting point
MS	mass spectroscopy
ν	frequency
NMR	nuclear magnetic resonance
OTf	Trifluoromethane sulphonate
Ph	phenyl
ppm	parts per million
q	quartet
ρ	density
R	agreement factor
R_w	weighted agreement factor
s	singlet
t	triplet
T	temperature
t, tert	tertiary
TFA	Trifluoroacetic acid
X-ray	X-ray diffraction
V	unit cell volume

var	variables
Z	number of molecules in the unit cell

CHAPTER 1

1.1 INTRODUCTION

The advent of supramolecular chemistry is generally associated with the seminal paper by Pedersen in 1967 reporting his investigations into the interactions between cyclic polyethers (or *crown ethers*) and alkali metal salts.[1] The recognition that weak non-covalent forces can be harnessed to control the associative behaviour of two or more molecular entities and the application of this principle in practice secured Pedersen, Cram, and Lehn the 1987 Nobel Prize in Chemistry.[2,3,4] Thus, supramolecular chemistry deals with intermolecular forces rather than the manipulation of the covalent bonds that hold individual molecules together. This concept is expressed at its most sophisticated level in biological systems in which many different molecules interact to produce cooperative behaviour from the nanoscopic to macroscopic domains and between.

Peculiar to the field of supramolecular chemistry are molecules composed of two or more discrete components, which are irreversibly attached to each other via *mechanical bonds* rather than covalent links.[5] The two simplest forms of these types of *interlocked* molecules are the *catenane* (from the Latin *catena* meaning chain) and *rotaxane* (from the Latin *rota* and *axis* meaning wheel and axle respectively) examples of which are portrayed in Figure 1-1. A catenane is a molecule composed of two or more

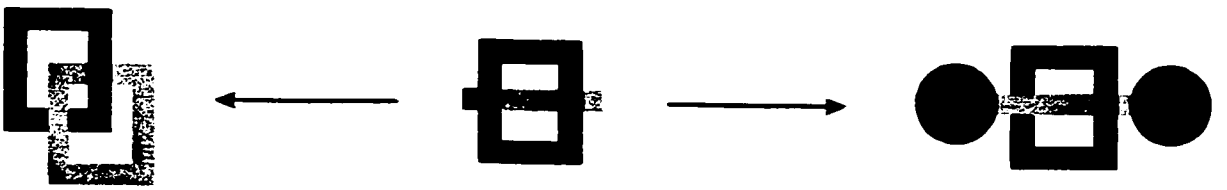

Figure 1-1. Some simple examples of interpenetrated and interlocked molecules.

interlocked rings, analogous to two links in a chain, inseparable but for the breakage of a covalent bond in one of the rings. Rotaxanes are composed of one or more rings threaded around a linear component (or thread) whose ends are "stoppered" to prevent the removal of the ring(s). If these stoppers are missing or of insufficient size to prevent the unthreading of the rings, the interpenetrated complex is referred to as a *pseudorotaxane* or *pre-catenane*. The nomenclature of these molecules involves placing the number of individual components in square brackets before the type of compound or complex. Hence, the two interlocked rings are termed a [2]catenane and the structure containing one dumbbell and one ring is termed a [2]rotaxane.

While rotaxanes and catenanes are both mechanically bonded, the catenane also contains a topological bond. No deformation of the components, aside from cleavage of a ring, can separate them. This is not true of the rotaxane, in which deformation of the ring component provides a route to the dissociation of the components. This theoretical distinction has real world consequences when the size of the stopper and the cavity of the ring in a rotaxane approach one another.[6]

As this thesis is primarily concerned with the synthesis of pseudorotaxanes and rotaxanes these will be the focus of this introduction. A comprehensive review of mechanically interlocked compounds, in general, is far beyond the scope of this offering.[7]

1.2 HISTORICAL PERSPECTIVES

The first pseudorotaxane reported in the literature was described by Lüttringhaus, Cramer, Prinzbach, and Henglein in 1958. This complex was composed of a cyclodextrin ring and a benzene nucleus appended with two alkanethiols as the thread (Figure 1-2).[8]

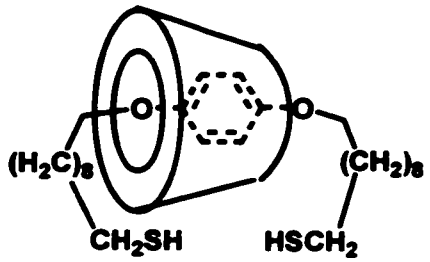

Figure 1-2. The first threaded molecular complex.

This was also the first planned attempt to form a catenane, by joining the ends of the thread via oxidation, which was unsuccessful.

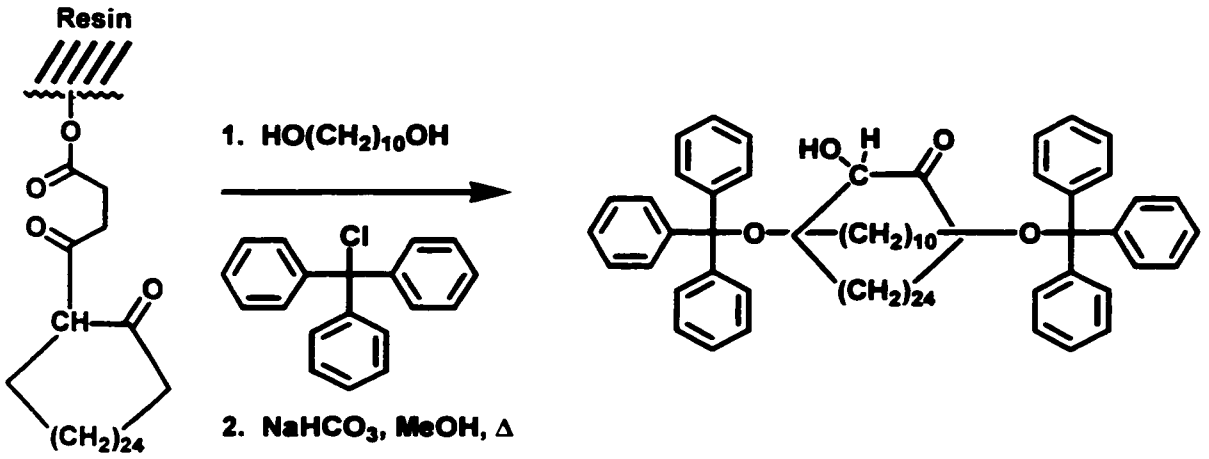

Figure 1-3. The statistical synthesis of the first rotaxane.

The first synthesis of a rotaxane was achieved by Harrison and Harrison in 1967 (Figure 1-3).[9] They used a statistical method in which a cyclic ketone attached to a Merrifield resin was washed repeatedly (70 times) with decane-1,10-diol and triphenylmethyl chloride. The rings were then cleaved from the resin and purified to yield the [2]rotaxane in 6% yield which was characterized using IR spectroscopy and degradation studies. They termed this rotaxane a "hooplane". I. T. Harrison later followed this work with investigations into the slippage of a mixture of cyclic hydrocarbons over the same triphenylmethoxy stoppered thread to form rotaxanes.[10,11] Reaction at 120 °C provided the necessary ring expansion to force the rings over the large

stoppers. At ambient temperature the rotaxanes involving a C_{26} macrocycle were stable to unthreading of the ring. Similar statistical methods were employed by Zilkha and Agam by threading mixtures of dibenzo crown ethers with poly(ethylene glycols) at

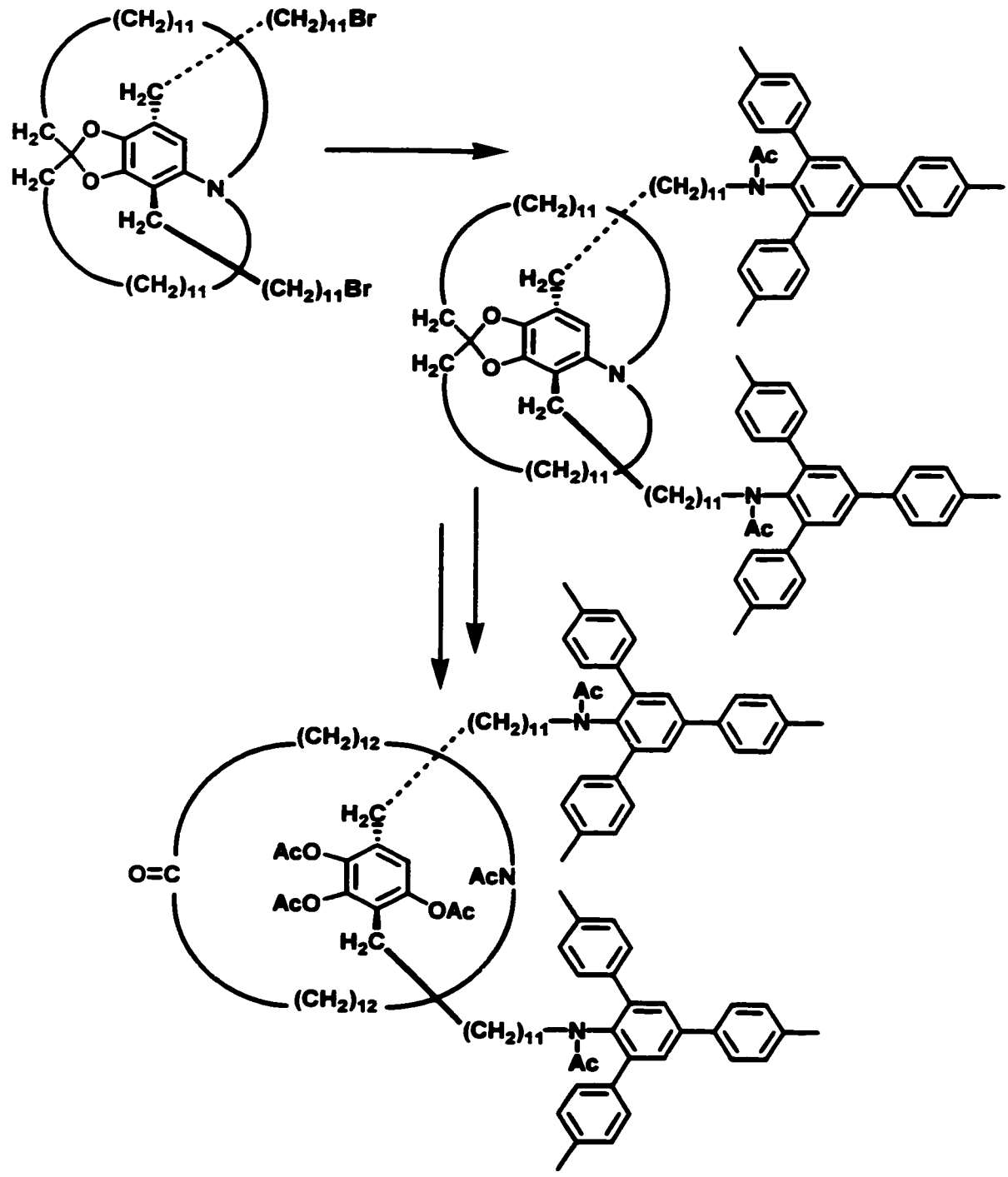

Figure 1-4. Schill's directed synthesis of a [2]rotaxane.

elevated temperatures to create rotaxanes in up to 15% yield.[12,13] It has been argued by Gibson that this approach was actually templated by hydrogen bonding between the diols and the crown ethers, which increased the yields above that normally seen in statistical syntheses.[14]

These statistical approaches are lacking, in that their success must always depend on chance events, and are therefore doomed to produce low yields at the best of times. One solution to this problem was the application of a "directed" synthesis, such as that espoused by Schill, initially in the construction of catenanes.[15] This method has been used to make rotaxanes as well, and takes advantage of the fact that the two alkyl chains connecting the ketal and the tertiary amine are disposed perpendicularly on either face of the benzene ring (Figure 1-4).[16] This also assures that the benzene ring and the other two alkyl chains run through the cavity that will be formed upon cleavage of the ketal and the amine from the aryl ring. Stoppering of the free ends of the alkyl chains and cleavage afford the rotaxane. Unfortunately, the length of the synthetic sequences, which reduce yields dramatically, and the technical expertise required leave much to be desired.

1.3 TEMPLATE DIRECTED SYNTHESIS

A drastic improvement in the synthesis of rotaxanes is realized when the concept of molecular recognition is brought to bear on the problem. By establishing the ways in which a rotaxane can be formed, one may approach the problem in a methodical manner (Figure 1-5). The components are then designed so that they assemble in the correct intermolecular arrangement (templation) prior to the final covalent attachment, which will produce the rotaxane.

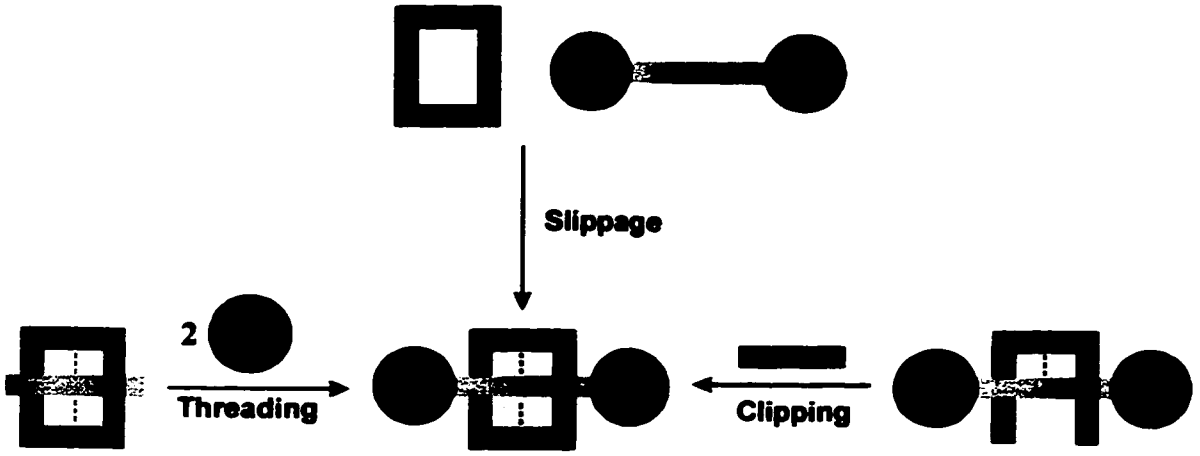

Figure 1-5. Methods of rotaxane formation via templation.

Threading and subsequent stoppering is perhaps the simplest method for construction of a rotaxane. This necessitates the formation of a pseudorotaxane intermediate at some point in the synthesis. It also assumes that the ends of the thread and the stoppers possess the appropriate functionality to be attached to one another without undue disruption of the interpenetrated geometry (see Section 3.1).

In a similar manner, the clipping method requires that the precyclic component of the rotaxane be organized around the dumbbell, such that reaction with a bis-functionalized connector yields the final product.

These two methods may be contrasted to the slippage approach. Here, reaction at elevated temperature provides the ring element with the kinetic energy to slip back and forth over the stoppers, which would otherwise be sterically insurmountable at ambient conditions. This design principle requires that the equilibrium between the separated components and rotaxane be biased in favour of the interlocked compound at high temperature due to an intermolecular interaction that lowers the energy of this state. All

three of these methods have been demonstrated in the literature as valid methods for rotaxane formation.[6,17,18]

1.4 ROTAXANES FORMED FROM CYCLODEXTRINS OR CUCURBITURIL

Cyclodextrins are an obvious choice for utilization in rotaxane synthesis, as they are readily available and include many rod-shaped compounds within their cavities in aqueous solution.[19] In fact, this topic has been reviewed recently by Stoddart and Nepogodiev.[20]

While the first pseudorotaxane was synthesized via the threading approach using a cyclodextrin, the certain formation of a low-molecular weight rotaxane from these compounds was not achieved until 1981 by Ogino (Figure 1-6).[21] Rotaxane formation

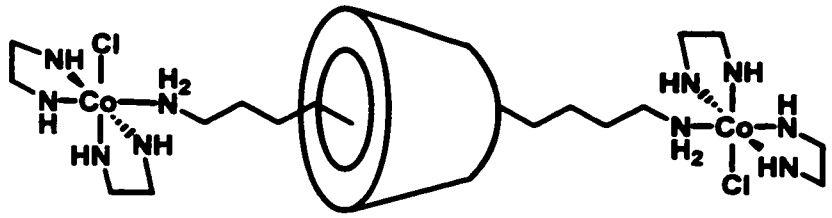

Figure 1-6. Ogino's cobalt(III) capped rotaxane.

with cyclodextrins is invariably a solvophobic process of inclusion of a hydrocarbon or aryl spacer element of the thread within the non-polar cyclodextrin cavity. If the ends of the thread are properly functionalized, addition of stoppers generally forms the rotaxane in a straight-forward manner. Aside from the use of stoppers linked to the ends of the threads via coordination bonds, covalent attachment of organic groups has also been successful.[22-29]

The use of cucurbituril as the cyclic component in a rotaxane has received attention recently in the literature primarily through the work of Kim et al., though the complexation of ammonium ions by this compound has been observed by others.[30-36]

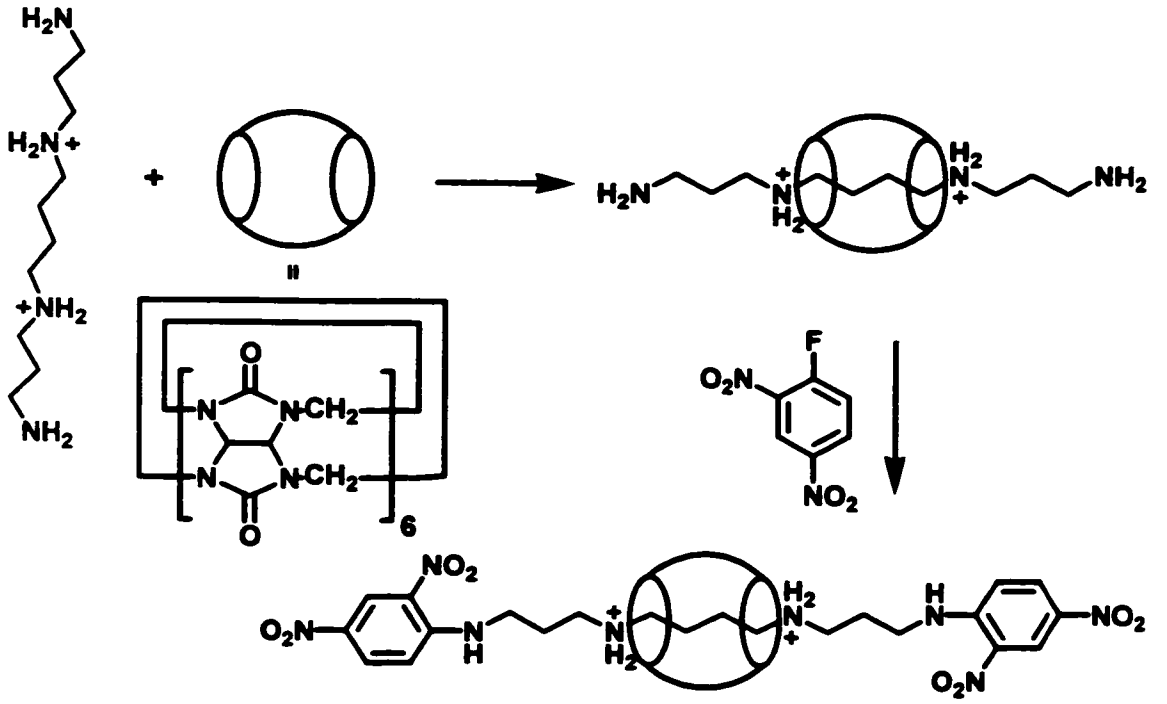

Figure 1-7. Kim's dinitrophenyl stoppered rotaxane.

Kim has used diammonium axles such as acidified spermine, onto which the cucurbituril "beads" are threaded (Figure 1-7). These complexes are then capped with either metal compounds or organic stoppers. The inclusion of these threads is a result of hydrogen bonding between the ammonium centers and the carbonyl functions of the cucurbituril ring.

While rotaxanes are readily formed from cyclodextrins and cucurbituril, these compounds are only viable in aqueous solution where they are most often formed. In addition, the relatively implacable nature of these cyclic components to any synthetic modification limit their usefulness in more advanced applications, such as construction of

molecular machines. The lack of specificity in the recognition between cyclodextrins and the thread components also limits their use in this capacity, as the vague nature of hydrophobic interactions make them difficult to modulate with external stimuli.

1.5 ROTAXANES FORMED FROM DIALKYL AMMONIUM SALTS

Stoddart and coworkers first reported in 1995 that secondary dialkylammonium salts were complexed by dibenzo-24-crown-8 (DB24C8) in a pseudorotaxane geometry.[37,38] These pseudorotaxanes are held together by hydrogen bonding between the oxygen atoms of the crown ether and the ammonium hydrogen atoms, as well as weaker hydrogen bonding interactions to the hydrogen atoms α to the ammonium center

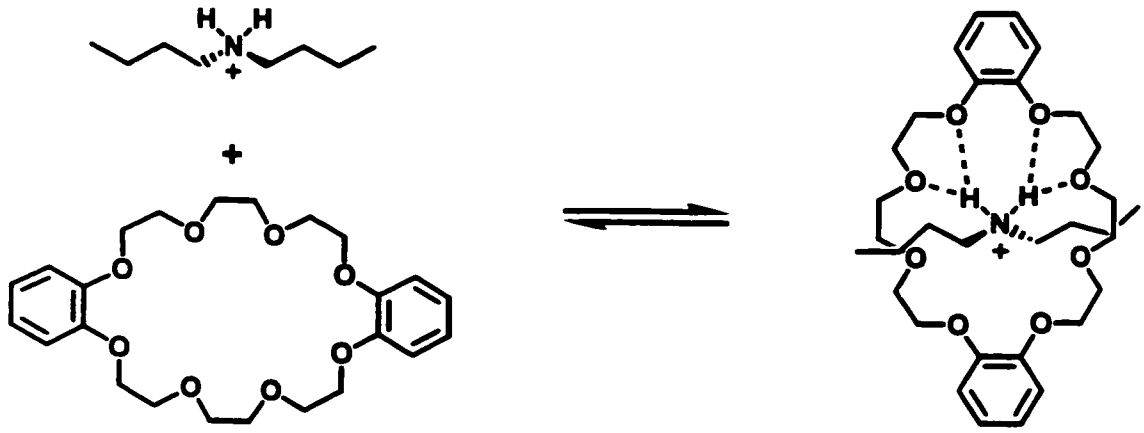

Figure 1-8. Threading of a dialkylammonium salt through the cavity of DB24C8.

(Figure 1-8). This pseudorotaxane geometry is not confined to DB24C8 and has been shown to exist for a range of other crown ether derivatives as well, although only the DB24C8 pseudorotaxanes have been converted into rotaxanes.[39-41] The conversion of these compounds into rotaxanes has been accomplished with the use of both threading/stoppering and slippage methodology by Stoddart and others.[42-45] This system is versatile, in that both the components are easily synthesized and amenable to a variety

of synthetic modifications. The recognition motif involved in formation of the interlocked and interpenetrated structures is relatively specific (i.e. the geometry of the complex has a predictable structure). This allows for more precise control over the position of the ring on the thread than cyclodextrin based rotaxanes.

1.6 ROTAXANES BASED ON AMIDES

In 1992 both Hunter and Vögtle, working independently, published the discovery of a series of catenanes obtained unexpectedly during the synthesis of cyclic amides.[46-50] This recognition motif has been modified to produce rotaxanes composed of both amides and sulphonamides via threading/stoppering and slippage.[51,52] The templation in this case involves hydrogen bonding between amide protons of a cyclic (sulphon)amide ring and the carbonyl(sulphonyl) oxygen atom of a (sulphon)amide based thread. Similar rotaxanes have been synthesized by Leigh et al. using different spacers in the macrocyclic ring.[53-54] These two series of rotaxanes possess very defined recognition motifs which control the location of the ring on the threads with a high degree of precision and are well understood. In addition, they are electronically neutral and do not require any charged centers or metal ions for templation or control over ring position. Ironically, these last two points may actually be a drawback. The presence of charged functionality and/or highly electron poor or rich centers provides for easily adaptable "handles" on the control of molecular motions in many other rotaxane species. This may be why there appears only one example of a rudimentary molecular machine derived from these motifs in the literature to date.[55] The tolerance of this particular architecture to synthetic modification will most likely overcome this concern in the long run.

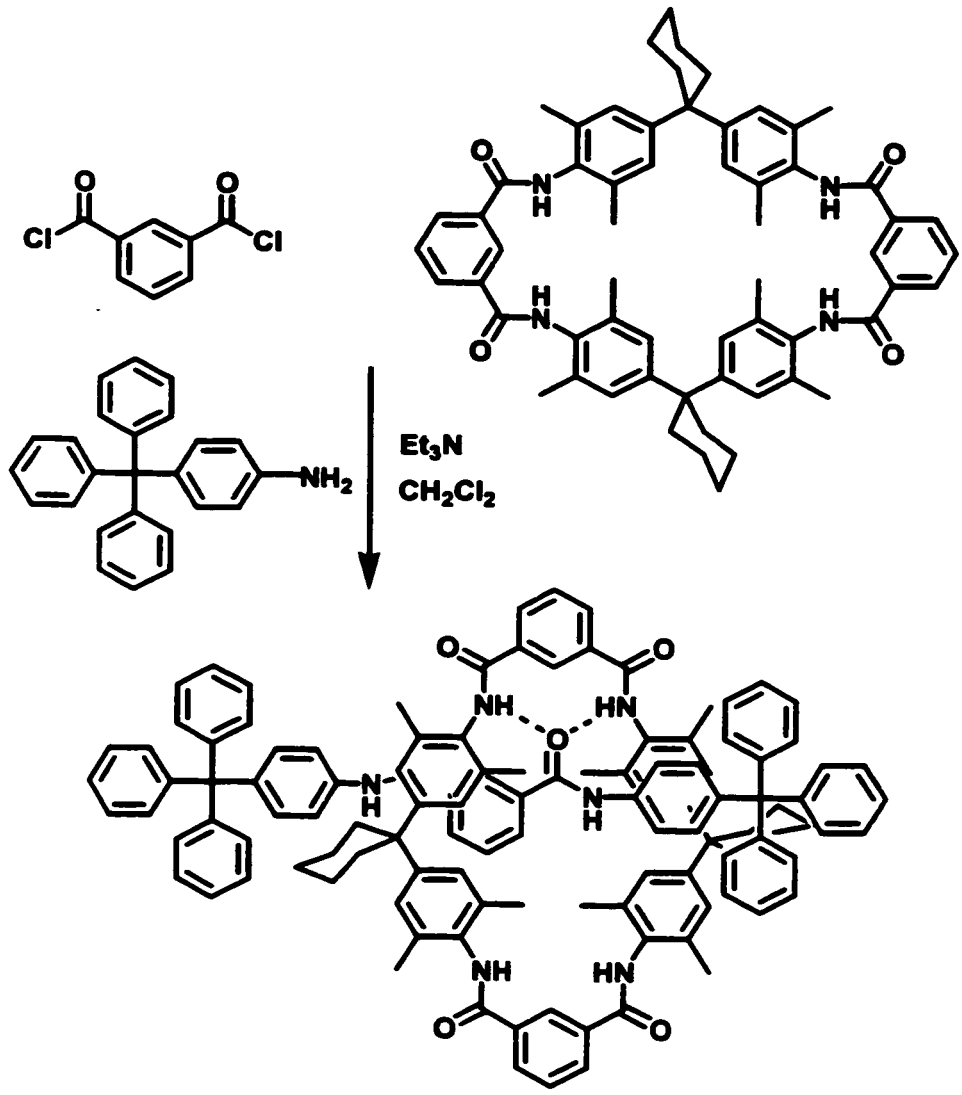

Figure 1-9. Vogtle's amide-based rotaxane.

1.7 ROTAXANES BASED ON METAL TEMPLATES

The use of metals to template the formation of catenanes and rotaxanes has largely been dominated by the work of Sauvage. He published the first synthesis of a catenate in 1983 (the term catenate is used to denote the continued presence of the metal ion in the structure, about which the two rings are still coordinated).[56] The same protocol used in the construction of the catenane species can be modified to produce rotaxanes

(Figure 1-10).[57,58] The Cu^+ template orients the ring and the thread perpendicularly to each other to ensure an intepenetrated geometry. In this sense, this method resembles

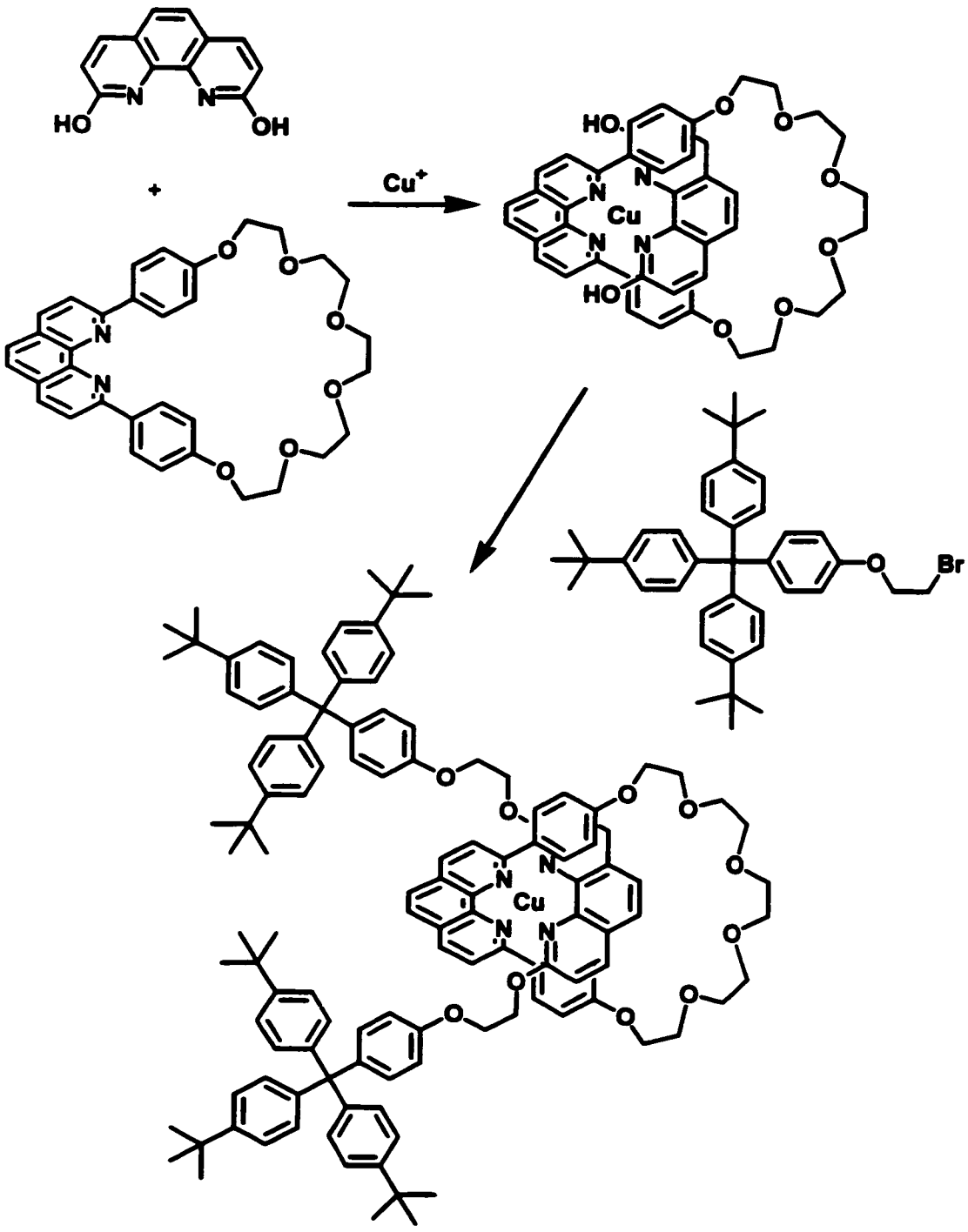

Figure 1-10. Sauvage's Cu^+ templated rotaxane synthesis.

that of Schill, but is much simpler synthetically. These rotaxanes can be demetallated with KCN after synthesis to yield the purely organic rotaxane if desired. However, the presence of the metal is usually desirable and has been used with some success in the control of ring position on a thread with two possible coordination sites, taking advantage of the different coordination geometries of the Cu^{+}/Cu^{2+} couple.[59] A variety of photo- and redox-active stoppers, such as fullerenes, porphyrins, and $Ru(terpy)_2$, have also been incorporated into these rotaxanes to determine their interactions within the mechanically bonded constructs.[60-66]

1.8 ROTAXANES BASED ON DONOR/ACCEPTOR TEMPLATES

By far the most successfully exploited method for creating mechanically bonded compounds is templation via π-electron-rich and π-electron poor aromatic building blocks. Stoddart and coworkers began developing this self-assembly approach in the late 1980's upon the realization that the common herbicide paraquat is bound by the cavity of the macrocyclic polyether bis(paraphenylene)-34-crown-10.[67] The complexation involves a combination of π-π stacking, $N^{+}\cdots O$ ion-dipole interactions, and $C\text{-}H\cdots O$ hydrogen bonding.[68-70] Stoddart's methods revolve around two related design methodologies.

The first approach for the construction of interpenetrated and interlocked molecules involves the complexation of linear paraquat-related species in the cavity of macrocyclic crown ethers (Figure 1-11).[71] This approach has been used to create a variety of pseudorotaxanes and rotaxanes by both slippage and threading/stoppering techniques.[72-77]

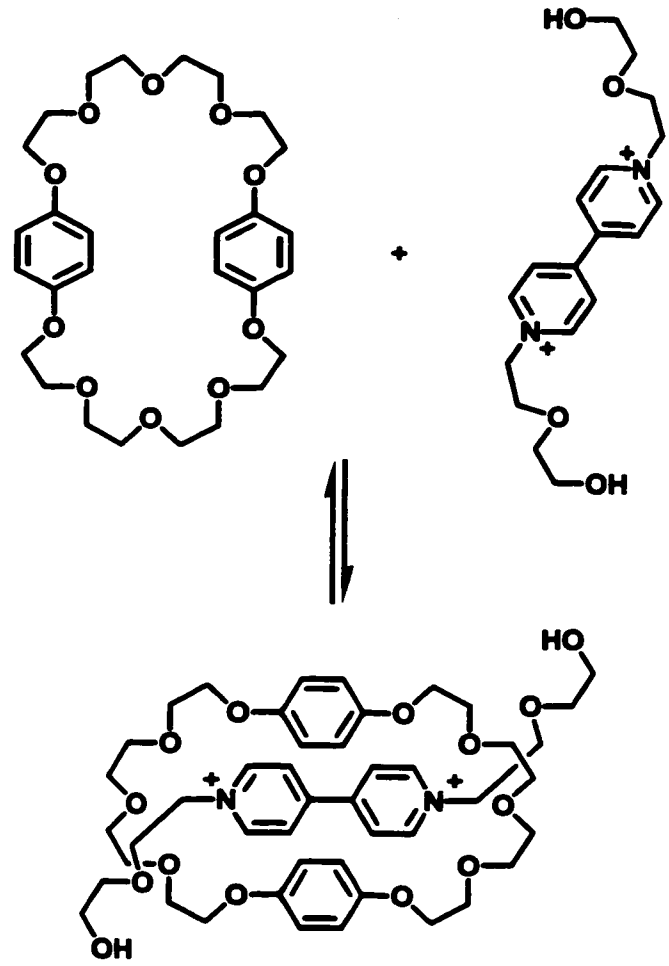

Figure 1-11. Pseudorotaxane formation involving an electron-poor thread and electron-rich ring.

The second design motif utilized by Stoddart employs an electron-poor cyclic component and an electron-rich thread to template rotaxane formation (Figure 1-12). In fact, the thread itself can be used as a template to form the electron-poor cycle from acyclic components.[78-84] This provides for clipping of the ring around the dumbbell-shaped thread as well as the threading/stoppering method.

Both of these techniques for rotaxane templation are highly flexible towards modification of the underlying frameworks. The templating forces are specific and result in well-defined geometries in the final compounds. These properties, coupled with the

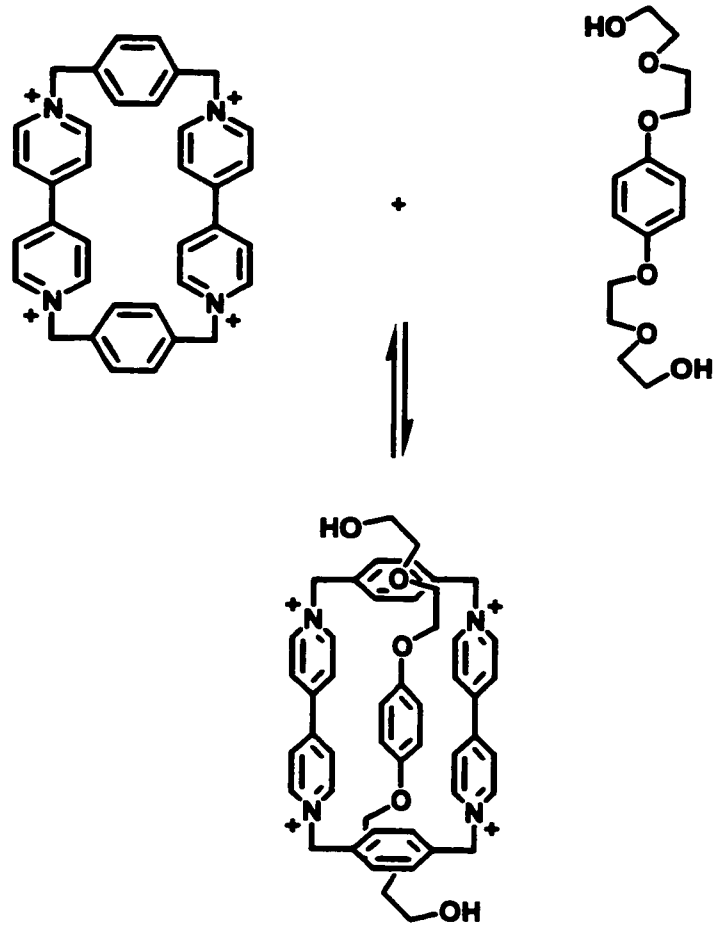

Figure 1-12. Pseudorotaxane formation involving an electron-rich thread and an electron-poor ring.

electron-rich/poor functions in these molecules and the redox activity associated with them, allow the programming of complex interlocked structures with predictable functions.

1.9 WHY MECHANICAL BONDING ?

The primary focus of research into the construction of mechanically bonded compounds has, until recently, primarily addressed the understanding of the processes which bring about the formation of such entities. This field has now begun to move

towards the goal of producing nanoscale entities engineered to perform specific functions or possess specific properties. Mechanically bonded molecules, by their very nature, combine the characteristics of covalently bonded compounds and supramolecular assemblies to form hybrid entities with some of the properties of both. This composite behaviour lends itself to two areas of investigation.

The extension of the rotaxane motif to the polymeric regime is particularly attractive. Many types of polyrotaxanes can be identified as possible targets for new materials (Figure 1-13). While the investigation into the synthesis of these materials is

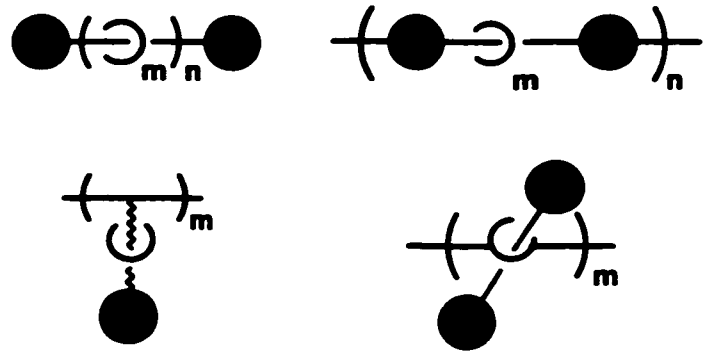

Figure 1-13. Examples of possible polyrotaxane architectures.

still in its infancy, they will undoubtedly possess different properties than traditional polymer formulations.[85]

The second major area of application emerging for interlocked compounds is in

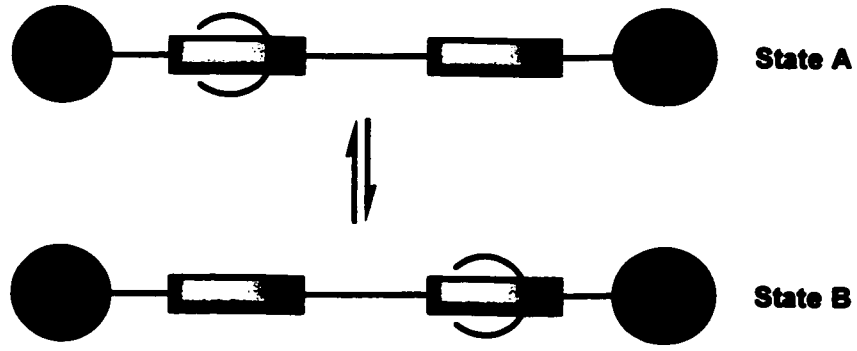

Figure 1-14. Schematic of a molecular shuttle.

the design of molecular machines. Rotaxanes with two or more recognition sites in the axle component but only one ring, termed molecular shuttles, have already been synthesized (Figure 1-14).[86] The perfection of control over the occupancy of one state over another via external stimuli has the potential to gain entry to the realm of molecular computers and extremely high-density storage devices. In fact, the initial steps towards these goals have recently been reported.[87]

1.10 SCOPE OF THE THESIS

This thesis describes the discovery of a new motif for the creation of a [2]pseudorotaxane geometry involving bis(pyridinium)ethanes and 24-membered crown ethers. The details of formation of these complexes and the factors governing their association were investigated. This knowledge was then used to construct two [2]rotaxanes by different routes and an examination undertaken of their properties. Finally, two [3]rotaxanes and two [2]rotaxane molecular shuttles were constructed based on this system. The properties of these compounds and the dynamics of the shuttling process are discussed.

CHAPTER 2

2.1 HYPOTHESIS AND LITERATURE PRECEDENT

It is well known that correctly designed aryl crown ethers complex alkyl pyridinium salts through a variety of intermolecular interactions.[41,88-90] While several recognition motifs have been established in these systems, with regard to complexation, the production of rotaxanes and catenanes utilizing these interactions has revolved around the use of only one particular geometry. In the course of his work on the molecular recognition of the common pesticide paraquat ($\mathbf{PQT^{2+}}$) by crown ethers, Stoddart found that it was included quite strongly in the cavity of BPP34C10 (Figure 2-1).[67] This complex exhibits all of the important bonding interactions involved in the vast array of

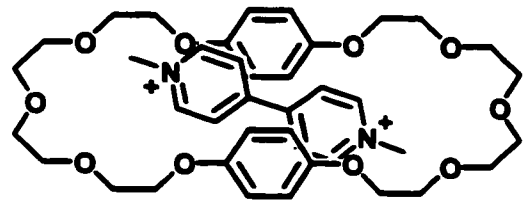

Figure 2-1. Complexation of paraquat dication in the cavity of BPP34C10.

interlocked and interpenetrated molecules derived from it, namely:

1) π-stacking between the electron poor pyridinium rings and the electron rich hydroquinol units of the crown ether.

2) $N^+\cdots O$ ion-dipole interactions.

3) C-H···O hydrogen bonding due to the highly polarized nature of the paraquat methyl groups.

This complexation is also a result of the stereochemical preorganization of the crown ether in regards to the positioning of its subunits spacially around the paraquat thread to allow these interactions to take place.[91]

This result led to our conjecture that an isomer of paraquat, 1,2-bis(pyridinium)ethane (**1a**), should interact in a similar manner with an appropriately designed crown ether. The formal charge separation in paraquat is approximately 7.00 Å while that of **1a** is only about 3.75 Å (Figure 2-2). This should increase the charge

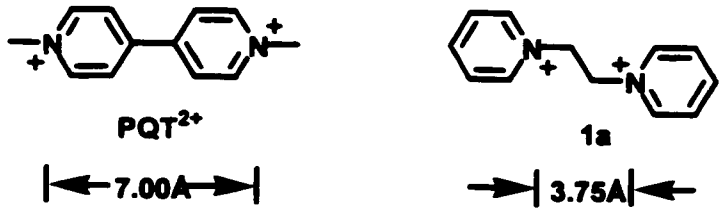

Figure 2-2. Comparison of the formal charge separation in $\mathbf{PQT}^{2+}$ and $\mathbf{1}^{2+}$.

density and polarization of the C-H bonds of the central ethylene unit of **1a**, with respect to those of paraquat's methyl groups. In addition, this conceptual isomerization would

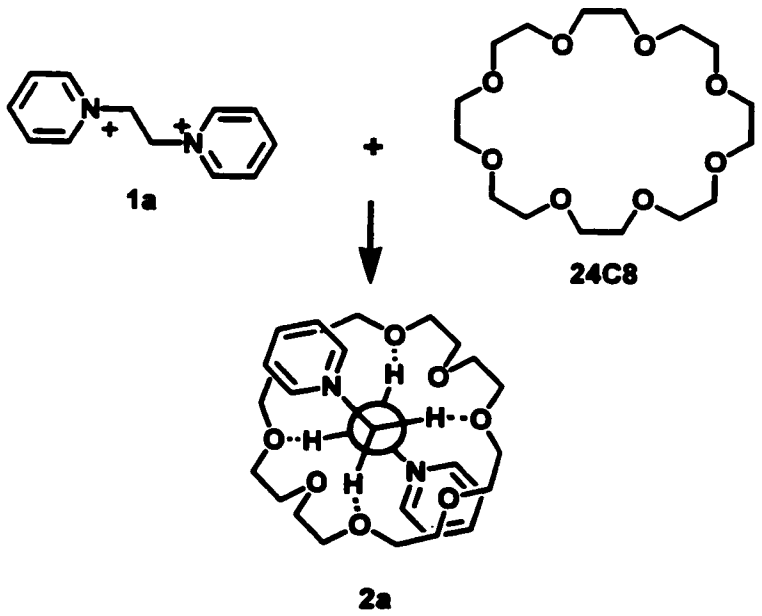

Figure 2-3. Potential non-covalent bonding interaction between **1a** and 24C8.

allow for the introduction of functionalities at the meta and para positions of the pyridinium rings, provided it did not interfere sterically with the complexation of the crown ether around the core of the molecule.

Analysis of CPK and computer models indicated that an excellent steric and stereochemical fit for pseudorotaxane formation with thread **1a** would be provided by a 24 membered crown ether wheel, the simplest being 24C8 (Figure 2-3). This binding motif places the oxygen atoms of the crown ether in close proximity and the correct orientation to maximize $N^{+}\cdots O$ and $C\text{-}H\cdots O$ interactions.

This proposition is supported in the literature by Stoddart *et al.* in their analyses of the interactions between dibenzo-24-crown-8 (DB24C8) and various pyridinium and dialkyl ammonium salts.

The addition of DB24C8 to a solution of N,N'-dimethyl-2,7-diazapyrenium dication in acetonitrile results in both a 1:1 (major) and a 2:1 (minor) complex with a first association constant of 840 M^{-1}. Diffusion of isopropyl ether into such a solution

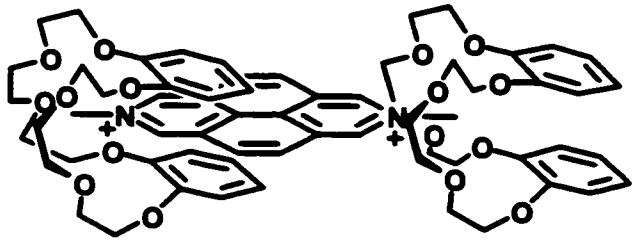

Figure 2-4. Structure of the 2:1 complex between DB24C8 and N,N'-dimethyl-2,7-diazapyrenium cation.

produces crystals of the 2:1 adduct (Figure 2-4).[92]

This structure can be regarded as [3]-pseudorotaxane in character, due to the interpenetration of the methyl groups through the cavities of both crown ether rings. The

contribution of C-H···O hydrogen bonding is evident in several short C···O contacts (2.56 – 3.23 Å) with the methyl groups (the hydrogen atoms were not located) and the aromatic C-H groups α to the N^+ centers. Additionally, there are proximal N^+···O interactions with both crown ether rings and further stabilization of one motif through π-stacking of the electron-rich catechol units above and below the electron poor diazapyrenium π-system. This final point suggests the possibility of incorporation of benzo- units in the 24C8 rings of our proposed 1,2-bis(pyridinium)ethane system.

Though the interaction of DB24C8 and paraquat is negligible, diquat dications form a strong 2:1 complex in acetone (K_a = 385 000 M^{-2}) with DB24C8. This prompted Stoddart to propose, in conjuction with other evidence, the solution structure pictured below (Figure 2-5).[88]

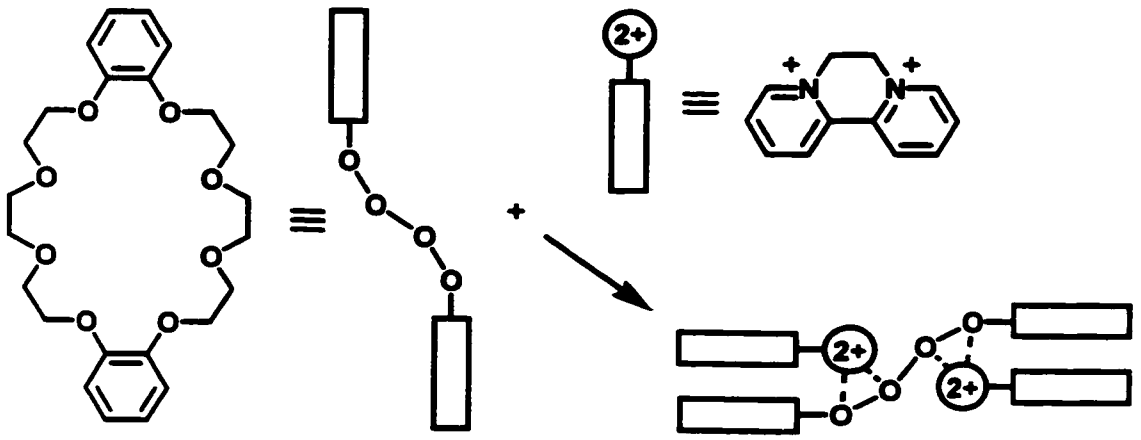

Figure 2-5. A possible solution structure for the 2:1 complex formed between diquat^{2+} and DB24C8.

The close structural similarity of diquat to **1a** infers the potential of similar intermolecular bond strengths and types to DB24C8, even if not in the same stereochemical arrangement.

Stoddart's group has also investigated, as previously mentioned, the formation of pseudorotaxanes between DB24C8 and various dialkylammonium salts (Figure 2-6).[37,38]

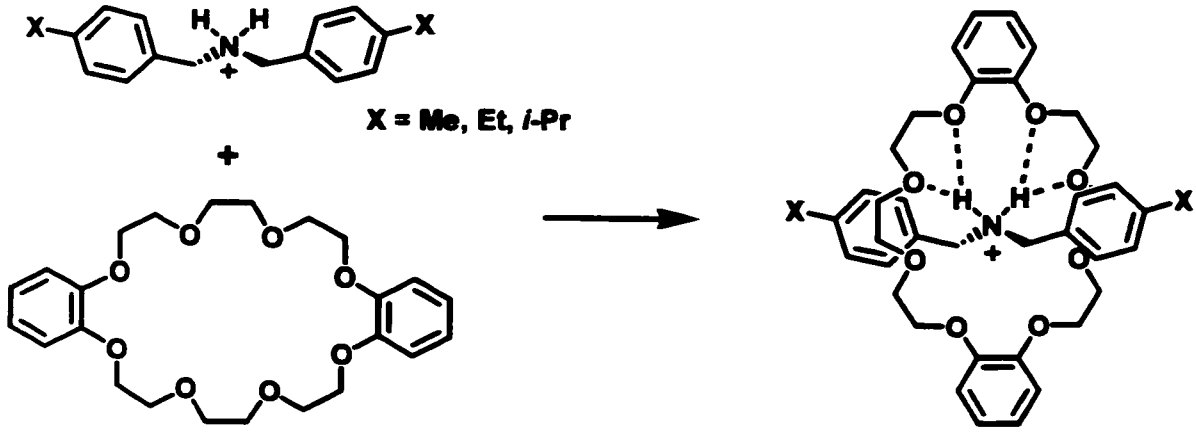

Figure 2-6. Threading of dialkyl ammonium salts through the cavity of DB24C8.

Their findings highlight the importance of steric bulk of a potential thread in its ability to penetrate the crown ether wheel. Specifically, they found that phenyl and substituted (Me, Et, *i*-Pr) phenyl rings were capable of passing through the crown's opening at room temperature.

These results are directly applicable to the proposed system, which is very similar sterically to those studied in their reports. The fact that functionalized phenyl rings were tolerated in Stoddart's work also lends credence to the possibility of similar modifications to the structure of **1a** without compromising the ability of the thread to form a pseudorotaxane.

2.2 EXPERIMENTAL

General Comments. 1,2-Dibromoethane, pyridine, 4-methylpyridine, 4-t-butylpyridine, 4-phenylpyridine, 4,4'-dipyridyl, nicotinic acid, and isonicotinic acid were purchased from Aldrich Chemicals and used as received. All deuterated solvents were purchased from Cambridge Isotope Laboratories and used as received. Ethyl nicotinate, ethyl isonicotinate and **[4][Br]** were synthesized from literature procedures.[93,94] Crown ethers **3a**, **3b**, and **3d-f** were synthesized according to literature methods.[1,95] The syntheses of compounds **2a**, **2b**, **2c**, **2d**, and **2e** have been reported in the literature.[94,96,97] LSI-MS spectra were recorded on a Kratos Profile mass spectrometer. ESI-MS spectra were recorded on an HP 1100 mass spectrometer at the University of Alberta. ^{1}H NMR spectra were recorded on Bruker Avance 300 and 500 instruments locked to the deuterated solvent operating at 300.1 and 500.1 MHz. All questionable assignments were verified by NOESY correlation. X-ray data for all compounds were collected on a Siemens SMART/CCD diffractometer and all solutions and refinements performed by Professor S. J. Loeb.

(i) **Preparation of $[2a][BF_4]_2$.** Pyridine (2.000 g, 25.28 mmol) and 1,2-dibromoethane (1.000 g, 5.323 mmol) were combined with 50 mL of acetonitrile and the solution refluxed for 24 hours. The resulting mixture was cooled to room temperature, filtered and washed with ether. Yield 0.378 g (20.5%) of white solid as the bromide salt. **^{1}H NMR (D_2O)**: δ (ppm) 8.80 (d, 4H, J = 5.99 Hz, ortho), 8.62 (t, 2H, J = 7.93 Hz, para), 8.08 (dd, 4H, meta), 5.30 (s, 4H, CH2). **LSI-MS**: 265 ($[M-Br]^+$). The bromide salt was combined with 10 mL of sat. aqueous NH_4BF_4 solution and brought to boiling until

the solid was completely dissolved. The resulting solution was immediately removed from heat and allowed to cool slowly to room temperature to yield the BF_4 salt of the cation as white crystals. **^{1}H NMR (CD_3CN)**: δ (ppm) 8.72 (d, 4H, J = 5.67 Hz, ortho), 8.63 (t, 2H, ^{2}J = 8.03 Hz, para), 8.12 (dd, 4H, meta), 5.12 (s, 4H, CH_2).

(ii) **Preparation of [2b][BF_4]$_2$.** 4-Methylpyridine (2.000 g, 21.48 mmol) and 1,2-dibromoethane (1.000 g, 5.323 mmol) were combined with 50 mL of acetonitrile and the solution refluxed for 24 hours. The resulting mixture was cooled to room temperature, filtered and washed with ether. Yield 0.771 g (38.7%) of white solid as the bromide salt. **^{1}H NMR (D_2O)**: δ (ppm) 8.53 (d, 4H, J = 6.64 Hz, ortho), 7.87 (d, 4H, meta), 5.17 (s, 4H, CH_2), 2.61 (s, 6H, CH_3). **LSI-MS**: 293 ([M]$^+$). The bromide salt was combined with 20 mL of sat. aqueous NH_4BF_4 solution and brought to boiling until the solid was completely dissolved. The resulting solution was immediately removed from heat and allowed to cool slowly to room temperature to yield the BF_4 salt of the cation as white crystals. **^{1}H NMR (CD_3CN)**: δ (ppm) 8.53 (d, 4H, J = 6.73 Hz, ortho), 7.88 (d, 4H, meta), 5.13 (s, 4H, CH_2), 2.67 (s, 6H, CH_3).

(iii) **Preparation of [2c][BF_4]$_2$.** 4-*t*-Butylpyridine (3.500 g, 25.89 mmol) and 1,2-dibromoethane (1.000 g, 5.323 mmol) were combined with 50 mL of acetonitrile and the solution heated to reflux for 48 hours. The resulting mixture was cooled to room temperature, filtered and washed with ether. Yield 1.148 g (47.1%) of white solid as the bromide salt. **^{1}H NMR (D_2O)**: δ (ppm) 8.56 (d, 4H, J = 6.09 Hz, ortho), 8.04 (d, 4H, meta), 5.17 (s, 4H, CH_2), 1.32 (s, 18H, CH_3). **LSI-MS**: 378 ([M-Br]$^+$). The bromide salt was combined with 20 mL of sat. aqueous NH_4BF_4 solution and brought to boiling until the solid was completely dissolved. The resulting solution was immediately removed

from heat and allowed to cool slowly to room temperature to yield the BF_4 salt of the cation as white crystals. **^{1}H NMR (CD_3CN):** δ (ppm) 8.61 (d, 4H, J = 6.54 Hz, ortho), 8.08 (d, 4H, meta), 5.04 (s, 4H, CH_2), 1.42 (s, 18H, CH_3).

(iv) **Preparation of [2d][BF_4]$_2$.** 4-Phenylpyridine (4.000 g, 25.77 mmol) and 1,2-dibromoethane (1.000 g, 5.323 mmol) were combined with 50 mL acetonitrile and the solution heated to reflux for 48 hours. The resulting mixture was cooled to room temperature, filtered and washed with ether. Yield 1.094 g (41.3%) of white solid as the bromide salt. **^{1}H NMR (D_2O):** δ (ppm) 8.73 (d, 4H, J = 6.75 Hz, ortho-Py), 8.32 (d, 4H, meta-Py), 7.90 (d, 4H, J = 6.79 Hz, ortho-Ph), 7.60 (m, 6H, meta and para-Ph), 5.27 (s, 4H, CH_2). The bromide salt was combined with 20 mL of sat. aqueous NH_4BF_4 solution and brought to boiling until the solid was completely dissolved. The resulting solution was immediately removed from the heat and allowed to cool slowly to room temperature to yield the BF_4 salt of the cation as white crystals. **^{1}H NMR (CD_3CN):** δ (ppm) 8.73 (d, 4H, J = 6.87 Hz, ortho-Py), 8.35 (d, 4H, meta-Py), 7.98 (d, 4H, J = 6.43 Hz, ortho-Ph), 7.67 (m, 6H, meta and para-Ph), 5.16 (s, 4H, CH_2). **LSI-MS**: 426 ([M-BF_4]$^+$).

(v) **Preparation of [4][Br].** Dipyridyl (5.000 g, 32.01 mmol) was dissolved in 1,2-dibromoethane (40 mL) and brought to reflux for 1 hour. The resulting mixture was filtered and washed with ether to remove residual dibromoethane. Yield 11.017 g (100%). **^{1}H NMR (D_2O):** δ (ppm) 8.92 (d, 2H, J = 6.78 Hz, ortho-N$^+$), 8.65 (d, 2H, J= 6.25 Hz, ortho-N), 8.34 (d, 2H, meta-N$^+$), 7.80 (d, 2H, meta-N), 4.99 (t, 2H, J = 5.74 Hz, CH_2-α-N$^+$), 3.93 (t, 2H, CH_2-β-N$^+$).

(vi) **Preparation of [2e][BF_4]$_2$.** 4,4'-Dipyridyl (1.300 g, 8.323 mmol) was combined with BrEtDIPY (0.640 g, 1.860 mmol) in 50 mL anhydrous ethanol and the

mixture brought to reflux. The production of a yellow-green precipitate was observed after 24 hours and this solid was filtered from the hot mixture after a period of 1 week to yield 0.690 g (74.1%) pure product as the bromide salt. **^{1}H NMR (D_2O)**: δ (ppm) 8.15 (d, 4H, J = 6.62 Hz, ortho-N^+), 7.93 (d, 4H, J = 5.95 Hz, ortho-N), 7.64 (d, 4H, meta-N^+), 7.07 (d, 4H, meta-N), 4.58 (s, 4H, CH_2). The bromide salt was combined with 15 mL of a saturated aqueous $NaBF_4$ solution and brought to boiling until the solid was completely dissolved. The resulting solution was allowed to cool slowly to room temperature to yield the BF_4 salt of the cation as a beige solid. **^{1}H NMR (CD_3CN)**: δ (ppm) 8.87 (d, 4H, J = 6.09 Hz, ortho-N), 8.76 (d, 4H, J = 6.89 Hz, ortho-N^+), 8.39 (d, 4H, meta-N^+), 7.82 (d, 4H, meta-N), 5.16 (s, 4H, CH_2). **LSI-MS**: 428 ($[M-BF_4]^+$).

(vii) Preparation of [2f][BF_4]$_2$. Ethyl isonicotinate (3.000 g, 19.85 mmol) was combined with 1,2-dibromoethane (1.000 g, 5.323 mmol) in 40 mL acetonitrile and refluxed for 3 days. The resulting mixture was cooled to room temperature, filtered and washed with ether to yield 0.193 g (7.4%) of white solid as the bromide salt. **^{1}H NMR (D_2O)**: δ (ppm) 9.02 (d, 4H, J = 6.20 Hz, ortho), 8.49 (d, 4H, meta), 5.34 (s, 4H, CH_2-α-N^+), 4.39 (q, 4H, J = 7.16 Hz, CH_2-α-O), 1.29 (t, 6H, CH_3). The bromide salt was combined with 5 mL of a saturated aqueous $NaBF_4$ solution and brought to boiling until the solid was completely dissolved. The resulting solution was allowed to cool slowly to room temperature to yield the BF_4 salt of the cation as white crystals. **^{1}H NMR (CD_3CN)**: δ (ppm) 8.96 (d, 4H, J = 6.69 Hz, ortho), 8.52 (d, 4H, meta), 5.24 (s, 4H, CH_2-α-N^+), 4.51 (q, 4H, J = 7.10 Hz, CH_2-α-O), 1.44 (t, 6H, CH_3). **LSI-MS**: 418 ($[M-BF_4]^+$).

(viii) Preparation of [2g][BF_4]$_2$. Ethyl nicotinate (3.000 g, 19.85 mmol) was combined with 1,2-dibromoethane (1.000 g, 5.323 mmol) in 40 mL acetonitrile and

refluxed for 3 days. The resulting mixture was cooled to room temperature, filtered and washed with ether to yield 0.237 g (9.1%) of white solid as the bromide salt. **^{1}H NMR (D_2O)**: δ (ppm) 9.50 (s, 2H, ortho-N^+ and -COOEt), 9.12 (m, 4H, ortho and para-N^+), 8.27 (dd, 2H, $J_{o,m} = J_{m,p} = 6.77$ Hz, meta-N^+), 5.41 (s, 4H, CH_2-α-N^+), 4.44 (q, 4H, J = 7.12 Hz, CH_2-α-O), 1.35 (t, 6H, CH_3). The bromide salt was combined with 6 mL of a saturated aqueous solution of $NaBF_4$ and brought to boiling until the solid was completely dissolved. The resulting solution was allowed to cool slowly to room temperature and filtered to yield the BF_4 salt of the cation as white crystals. **^{1}H NMR (CD_3CN)**: δ (ppm) 9.39 (s, 2H, ortho-N^+ and -COOEt), 9.07 (d, 2H, J = 8.77 Hz, para-N^+), 8.95 (d, 2H, J = 6.19 Hz, ortho-N^+), 8.26 (dd, 2H, meta-N^+), 5.22 (s, 4H, CH_2-α-N^+), 4.51 (q, 4H, J = 7.12 Hz, CH_2-α-O), 1.44 (t, 6H, CH_3). **LSI-MS**: 418 ($[M-BF_4]^+$).

(ix) Preparation of [5][Br]. Ethyl isonicotinate (2.000 g, 13.23 mmol) and 1,2-dibromoethane (21.80 g, 0.1160 mol) were combined with 20 mL of acetonitrile and the solution refluxed for 2 days. The reaction mixture was allowed to cool to room temperature and the acetonitrile removed under reduced pressure. The resulting liquid was triturated with 75 mL of ether and stirred for 2 hours. The precipitated white solid was then filtered and washed with ether. The solid was then redissolved in acetonitrile (50 mL) and filtered to remove any remaining solids. Rotoevaporation of the acetonitrile solution yielded 0.967 g (21.6%) of pure product as a white solid. **^{1}H NMR (D_2O)**: δ (ppm) 9.01 (d, 2H, J = 7.21 Hz, ortho), 8.48 (d, 2H, meta), 5.20 (t, 2H, J = 5.88 Hz, CH_2-α-N^+), 4.47 (q, 2H, J = 7.11 Hz, CH_2-α-O), 4.04 (d, 2H, CH_2-β-N^+), 1.42 (t, 3H, CH_3).

(x) Preparation of [2h][BF_4]$_2$. Ethyl nicotinate (2.000 g, 13.23 mmol) and (BrEtInic)(BF_4) (0.500 g, 1.475 mmol) were combined with 20 mL of acetonitrile and the

solution refluxed for 2 days. The reaction mixture was cooled to room temperature and the resulting solid filtered off and washed with acetonitrile to yield 76 mg (10.5%) of the bromide product as a white solid. **^{1}H NMR (D_2O)**: δ (ppm) 9.45 (s, 1H, ortho-N^+ and ortho–COOEt), 9.11 (d, 1H, J = 8.20 Hz, para-N^+), 9.07 (d, 2H and 1H unresolved, ortho-N^+ both rings), 8.55 (d, 2H, J = 6.63 Hz, meta-N^+), 8.24 (dd, 1H, $J_{o,m}$ = 6.27 Hz, meta-N^+), 5.38 (s, 4H, CH_2CH_2), 4.44 (m, 4H, CH_2-α-O), 1.35 (t, 3H, J = 7.16 Hz, CH_3-Nic), 1.33 (t, 3H, J = 7.15 Hz, CH_3-Inic). The bromide salt was combined with 5 mL of a saturated aqueous solution of $NaBF_4$ and brought to reflux until the solid had completely dissolved. The resulting solution was allowed to cool slowly to room temperature and the BF_4 salt of the cation was recovered as white crystals by filtration. **^{1}H NMR (CD_3CN)**: δ (ppm) 9.32 (s, 1H, ortho-N^+ and -COOEt), 9.05 (d, 1H, J = 8.12 Hz, para-N^+), 8.88 (d, 2H, J = 6.80 Hz, ortho-N^+),8.85 (d, 1H, J = 6.20 Hz, ortho-N^+), 8.52 (d, 2H, meta-N^+), 8.24 (dd, 1H, meta-N^+), 5.18 (s, 4H, CH_2CH_2), 4.50 (m, 2H, J = 7.11 Hz, CH_2-α-O nicotinium), 4.49 (q, 2H, J = 7.12 Hz , CH_2-α-O isonicotinium) 1.43 (t, 3H, J = 7.16 Hz, CH_3-nicotinium), 1.42 (t, 3H, J = 7.15 Hz, CH_3-isonicotinium). **LSI-MS**: 418 ([M-BF_4]$^+$).

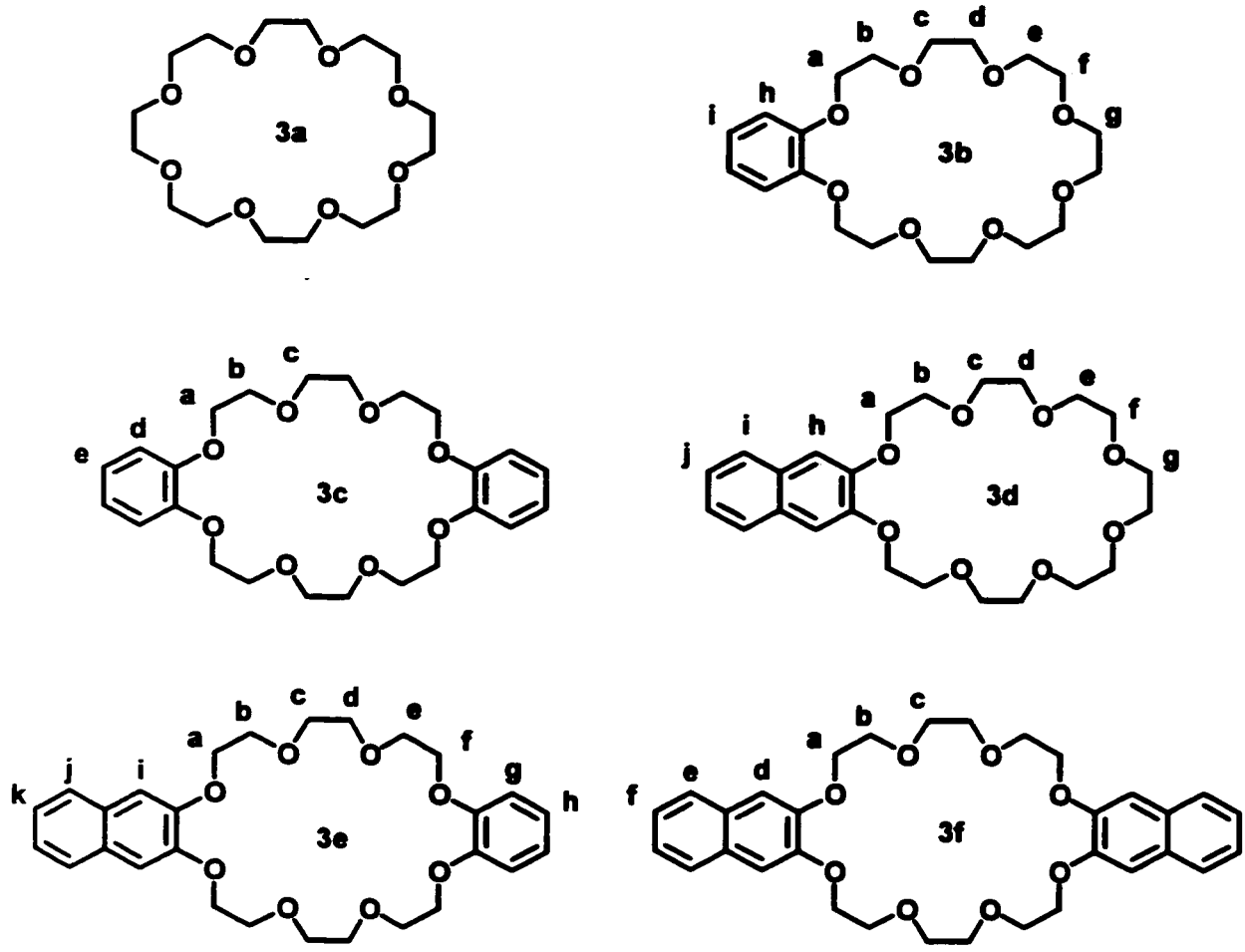

Figure 2-7. Crown ethers used in this study.

^{1}H NMR of Pseudorotaxane Complexes in CD_3CN.

(i) **2a:3a.** δ (ppm) **2a:** 9.02 (d, 4H, J = 5.70 Hz, ortho), 8.63 (t, 2H, J = 7.80 Hz, para), 8.14 (dd, 4H, meta), 5.29 (s, 4H, CH_2).

(ii) **2a:3b.** δ (ppm) **2a:** 8.98 (d, 4H, J = 6.27 Hz, ortho), 8.43 (t, 2H, J = 7.76 Hz, para), 7.99 (dd, 4H, meta), 5.31 (s, 4H, CH_2).

(iii) **2a:3c.** δ (ppm) **2a:** 8.99 (d, 4H, J = 5.77 Hz, ortho), 8.17 (t, 2H, J = 7.58 Hz, para), 7.80 (dd, 4H, meta), 5.39 (s, 4H, CH_2).

(iv) **2b:3a.** δ (ppm) **2b:** 8.77 (d, 4H, J = 6.56 Hz, ortho), 7.90 (d, 4H, meta), 5.16 (s, 4H, CH_2), 2.68 (s, 6H, CH_3).

(v) **2b:3b.** δ (ppm) **2b:** 8.77 (d, 4H, J = 6.54 Hz, ortho), 7.73 (d, 4H, meta), 5.22 (s, 4H, CH_2), 2.52 (s, 6H, CH_3).

(vi) **2b:3c.** δ (ppm) **2b:** 8.78 (d, 4H, J = 6.64 Hz, ortho), 7.54 (d, 4H, meta), 5.30 (s, 4H, CH_2), 2.31 (s, 6H, CH_3).

(vii) **2d:3a.** δ (ppm) **2d:** 9.08 (d, 4H J = 6.72 Hz, ortho-N^+), 8.39 (d, 4H, meta-N^+), 8.01 (d, 4H, J = 6.42 Hz, ortho-Ph), 7.69 (m, 6H, meta- and para-Ph), 5.34 (s, 4H, CH_2) **3a**: 3.53 (s, 32H, CH_2).

(viii) **2d:3b.** δ (ppm) **2d:** $PhPy_2Et$: 9.04 (d, 4H, J = 6.76 Hz, ortho-N^+), 8.18 (d, 4H, meta-N^+), 7.84 (d, 4H, J = 6.40 Hz, ortho-Ph), 7.69 (m, 6H, meta- and para-Ph), 5.39 (s, 4H, CH_2) **3b:** 6.76 (m, 2H, *h*), 6.64 (m, 2H, *i*), 4.08 (m, 4H, *a*), 3.94 (m, 4H, *b*), 3.81 (m, 8H, *c and d*), 3.65 (m, 4H, *e*), 3.48 (m, 4H, *f*), 3.27 (s, 4H, *g*).

(ix) **2d:3c.** δ (ppm) **2d:** 9.06 (d, 4H, J = 6.68 Hz, ortho-N^+), 7.96 (d, 4H, meta-N^+), 7.67 (m, 10H, ortho-, meta- and para-Ph), 5.51 (s, 4H, CH_2) **3c:** 6.68 (m, 4H, *d*), 6.57 (m, 4H, *e*), 4.06 (m, 8H, *a*), 3.99 (m, 16H, *b and c*).

(x) **2e:3a.** δ (ppm) **2e:** 9.18 (bd, 4H, ortho-N^+), 8.91 (d, 4H, J = 5.88 Hz, ortho-N), 8.46 (d, 4H, J = 6.55 Hz, meta-N^+), 7.88 (d, 4H, meta-N), 5.37 (bs, 4H, CH_2) **3a:** 3.57 (s, 32H, CH_2).

(xi) **2e:3b.** δ (ppm) **2e:** 9.16 (d, 4H, J = 5.78 Hz, ortho-N^+), 8.89 (d, 4H, J = 5.04 Hz, ortho-N), 8.25 (d, 4H, meta-N^+), 7.70 (d, 4H, meta-N), 5.43 (s, 4H, CH_2) **3b:**

6.74 (m, 2H, *h*), 6.64 (m, 2H, *i*), 4.02 (m, 4H, *a*), 3.94 (m, 4H, *b*), 3.83 (m, 8H, *c and d*), 3.63 (m, 4H, *e*), 3.45 (m, 4H, *f*), 3.18 (s, 4H, *g*).

(xii) .2e:3c. δ (ppm) **2e:** 9.19 (bs, 4H, ortho-N^+), 8.82 (bs, 4H, ortho-N), 8.04 (bs, 4H, meta-N^+), 7.50 (bs, 4H, meta-N), 5.56 (bs, 4H, CH_2) **3c:** 6.68 (m, 4H, *d*), 6.57 (m, 4H, *e*), 4.03 (m, 24H, *a, b and c*).

(xiii) 2e:3d. δ (ppm) **2e:** 9.15 (bs, 4H, ortho-N^+), 8.66 (bs, 4H, ortho-N), 8.20 (bs, 4H, meta-N^+), 7.44 (bs, 4H, meta-N), 5.45 (s, 4H, CH_2) **3d:** 7.44 (m, 2H, *j*), 7.22 (m, 2H, *i*), 7.04 (s, 2H, *h*), 4.19 (m, 4H, *a*), 4.04 (m, 4H, *b*), 3.88 (m, 8H, *c and d*), 3.59 (m, 4H, *e*), 3.44 (m, 4H, *f*), 3.17 (s, 4H, *g*).

(xiv) 2e:3e. δ (ppm) **2e:** 9.17 (bs, 4H, ortho-N^+), 8.61 (bs, 4H, ortho-N), 7.99 (bs, 4H, meta-N^+), 7.21 (bs, 4H, meta-N), 5.45 (s, 4H, CH_2) **3e:** 7.43 (m, 2H, *j*), 7.21 (m, 2H, *k*), 6.99 (s, 2H, *i*), 6.65 (bs, 2H, *g*), 6.54 (bs, 2H, *h*), 4.04 (m, 24H, *a, b, c, d, e, and f*).

(xv) 2f:3a. δ (ppm) **2f:** 9.27 (d, 4H, J = 6.75 Hz, ortho-N^+), 8.56 (d, 4H, meta-N^+), 5.40 (s, 4H, CH_2-α-N^+), 4.51 (q, 4H, J = 7.08 Hz, CH_2-α-O), 1.44 (t, 6H, CH_3) **3a:** 3.50 (s, 32H, CH_2).

(xvi) 2f:3b. . δ (ppm) **2f:** 9.24 (d, 4H, J = 6.44 Hz, ortho-N^+), 8.36 (d, 4H, meta-N^+), 5.46 (s, 4H, CH_2-α-N^+), 4.47 (q, 4H, J = 7.15 Hz, CH_2-α-O), 1.45 (t, 6H, CH_3) **3b:** 6.82 (m, 2H, *h*), 6.77 (m, 2H, *i*), 4.02 (m, 4H, *a*), 3.94 (m, 4H, *b*), 3.83 (m, 8H, *c and d*), 3.63 (m, 4H, *e*), 3.44 (m, 4H, *f*), 3.18 (s, 4H, *g*).

(xvii) 2f:3c. δ (ppm) **2f:** 9.25 (d, 4H, J = 6.56 Hz, ortho-N^+), 8.14 (d, 4H, meta-N^+), 5.58 (s, 4H, CH_2-α-N^+), 4.40 (q, 4H, J = 7.13 Hz, CH_2-α-O), 1.43 (t, 6H, CH_3) **3c:** 6.76 (m, 4H, *h*), 6.70 (m, 4H, *i*), 4.00 (m, 24H, *a, b and c*).

(xviii) 2f:3d. δ (ppm) **2f:** 9.25 (d, 4H, J = 6.15 Hz, ortho-N^+), 8.31 (d, 4H, meta-N^+), 5.46 (s, 4H, CH_2-α-N^+), 4.18 (q, 4H, J = 7.16 Hz, CH_2-α-O), 1.29 (t, 6H, CH_3) **3d:** 7.67 (m, 2H, *i*), 7.37 (m, 2H, *j*), 7.08 (s, 2H, *h*), 4.14 (m, 4H, *a*), 4.00 (m, 4H, *b*), 3.88 (m, 8H, *c and d*), 3.62 (m, 4H, *e*), 3.41 (m, 4H, *f*), 3.13 (s, 4H, *g*).

(xix) 2f:3e. δ (ppm) **2f:** 9.25 (d, 4H, J = 6.38 Hz, ortho-N^+), 8.09 (d, 4H, meta-N^+), 5.59 (s, 4H, CH_2-α-N^+), 4.09 (q, 4H, J = 7.07 Hz, CH_2-α-O), 1.27 (t, 6H, CH_3) **3e:** 7.64 (m, 2H, *j*), 7.36 (m, 2H, *k*), 7.04 (s, 2H, *i*), 6.73 (m, 2H, *g*), 6.68 (m, 2H, *h*), 4.01 (m, 24H, *a, b, c, d, e and f*).

(xx) 2f:3f. δ (ppm) **2f:** 9.28 (d, 4H, J = 6.60 Hz, ortho-N^+), 8.07 (d, 4H, meta-N^+), 5.61 (s, 4H, CH_2-α-N^+), 3.82 (q, 4H, J = 7.11 Hz, CH_2-α-O), 1.12 (t, 6H, CH_3) **3f:** 7.63 (m, 4H, *e*), 7.34 (m, 4H, *f*), 7.03 (s, 4H, *d*), 4.14 (m, 8H, *a*), 4.05 (m, 16H, *b and c*).

(xxi) 2g:3a. δ (ppm) **2g:** 9.71 (s, 2H, ortho-N^+ and -COOEt), 9.28 (d, 2H, J = 5.17 Hz, ortho-N^+), 9.06 (d, 2H, J = 7.80 Hz, para-N^+), 8.27 (dd, 2H, meta-N^+), 5.40 (s, 4H, CH_2-α-N^+), 4.54 (bm, 4H, CH_2-α-O), 1.45 (bm, 6H, CH_3) **3a:** 3.51 (s, 32H, CH_2).

(xxii) 2g:3b. δ (ppm) **2g:** 9.70 (s, 2H, ortho-N^+ and -COOEt), 9.28 (d, 2H, J = 6.01 Hz, ortho-N^+), 8.78 (d, 2H, J = 8.01 Hz, para-N^+), 8.12 (dd, 2H, meta-N^+), 5.48 (s, 4H, CH_2-α-N^+), 4.51 (q, 4H, J = 7.11 Hz, CH_2-α-O), 1.45 (t, 6H, CH_3) **3b:** 6.85 (m, 2H, *h*), 6.72 (m, 2H, *i*), 4.00 (m, 4H, *a*), 3.96 (m, 4H, *b*), 3.88 (m, 8H, *c and d*), 3.65 (m, 4H, *e*), 3.42 (m, 4H, *f*), 3.14 (s, 4H, *g*).

(xxiii) 2g:3c. δ (ppm) **2g:** 9.71 (s, 2H, ortho-N^+ and -COOEt), 9.29 (d, 2H, J = 6.08 Hz, ortho-N^+), 8.43 (d, 2H, J = 8.15 Hz, para-N^+), 7.92 (dd, 2H, meta-N^+), 5.63 (s, 4H, CH_2-α-N^+), 4.49 (q, 4H, J = 7.08 Hz, CH_2-α-O), 1.46 (t, 6H, CH_3) **3c:** 6.80 (m, 4H, *h*), 6.66 (m, 4H, *i*), 4.06 (m, 8H, *a*), 3.99 (m, 16H, *b and c*).

(xxiv) 2g:3d. δ (ppm) **2g:** 9.69 (s, 2H, ortho-N^+ and -COOEt), 9.30 (d, 2H, J = 5.81 Hz, ortho-N^+), 8.64 (d, 2H, J = 7.79 Hz, para-N^+), 8.12 (dd, 2H, meta-N^+), 5.48 (s, 4H, CH_2-α-N^+), 4.37 (q, 4H, J = 7.08 Hz, CH_2-α-O), 1.33 (t, 6H, CH_3) **3d:** 7.69 (m, 2H, *i*), 7.34 (m, 2H, *j*), 7.05 (s, 2H, *h*), 4.13 (m, 4H, *a*), 4.01 (m, 4H, *b*), 3.88 (m, 8H, *c and d*), 3.64 (m, 4H, *e*), 3.40 (m, 4H, *f*), 3.12 (s, 4H, *g*).

(xxv) 2g:3e. δ (ppm) **2g:** 9.71 (s, 2H, ortho-N^+ and -COOEt), 9.30 (d, 2H, J = 6.00 Hz, ortho-N^+), 8.28 (d, 2H, J = 8.15 Hz, para-N^+), 7.91 (dd, 2H, meta-N^+), 5.63 (s, 4H, CH_2-α-N^+), 4.37 (q, 4H, J = 7.10 Hz, CH_2-α-O), 1.34 (t, 6H, CH_3) **3e:** 7.65 (m, 2H, *j*), 7.36 (m, 2H, *k*), 7.00 (s, 2H, *i*), 6.76 (m, 2H, *g*), 6.64 (m, 2H, *h*), 4.12 (m, 4H, *a*), 4.06 (m, 12H, *b,e and f*), 3.98 (m, 8H, *c and d*).

(xxvi) 2g:3f. δ (ppm) **2g:** 9.72 (s, 2H, ortho-N^+/-COOEt), 9.33 (d, 2H, J = 6.11 Hz, ortho-N^+/para-COOEt), 8.15 (d, 2H, J = 8.11 Hz, para-N^+), 7.92 (dd, 2H, meta-N^+), 5.66 (s, 4H, CH_2-α-N^+), 4.27 (q, 4H, J = 7.12 Hz, CH_2-α-O), 1.24 (t, 6H, CH_3) **3f:** 7.64 (m, 4H, *e*),7.35 (m, 4H, *f*), 7.00 (s, 4H, *d*), 4.12 (m, 8H, *a*), 4.09 (m, 8H, *c*), 4.05 (m, 8H, *b*).

(xxvii) 2h:3a. δ (ppm) **2h:** 9.69 (s, 1H, ortho-N^+/-COOEt), 9.26 (br, 3H, ortho-N^+/para-COOEt and ortho-N^+/meta-COOEt), 9.05 (d, 1H, J = 8.49 Hz, para-N^+), 8.56 (br, 2H, meta-N^+/ortho-COOEt), 8.24 (br, 1H, meta-N^+/-COOEt), 5.39 (s, 4H, CH_2-α-N^+), 4.49 (br, 4H, CH_2-α-O), 1.43 (br, 6H, CH_3) **3a:** 3.49 (s, 32H, CH_2).

(xxviii)2h:3b. δ (ppm) **2h:** 9.66 (s, 1H, ortho-N^+/-COOEt), 9.29 (d, 1H, J = 5.58 Hz, ortho-N^+/para-COOEt), 9.21 (d, 2H, J = 6.37 Hz, ortho-N^+/meta-COOEt), 8.75 (d, 1H, J = 7.64 Hz, para-N^+), 8.36 (d, 2H, meta-N^+/ortho-COOEt), 8.09 (dd, 1H, meta-N^+/-COOEt), 5.46 (s, 4H, CH_2-α-N^+), 4.49 (m, 4H, CH_2-α-O), 1.43 (m, 6H, CH_3) **3b:** 6.82

(m, 2H, *h*), 6.73 (m, 2H, *i*), 4.01 (br, 4H, *a*), 3.92 (br, 4H, *b*), 3.83 (br, 8H, *c and d*), 3.56 (br, 4H, *e*), 3.41 (br, 4H, *f*), 3.15 (br, 4H, *g*).

(xxix) 2h:3c. δ (ppm) 2h: 9.66 (s, 1H, ortho-N^+/-COOEt), 9.27 (d, 1H, J = 6.45 Hz, ortho-N^+/para-COOEt), 9.25 (d, 2H, J = 6.67 Hz, meta-COOEt/ortho-N^+), 8.37 (d, 1H, J = 7.33 Hz, para-N^+), 8.17 (d, 2H, meta-N^+/ortho-COOEt), 7.86 (dd, 1H, meta-N^+/-COOEt), 5.59 (s, 4H, CH_2-α-N^+), 4.46 (q, 2H, J = 7.64 Hz, CH_2-α-O-nicotinium), 4.41 (q, 2H, J = 7.37 Hz, CH_2-α-O-isonicotinium), 1.44 (t, 3H, CH_3-nicotinium), 1.43 (t, 3H, CH_3-isonicotinium) **3c**: 6.77 (m, 4H, *d*), 6.66 (m, 4H, *e*), 4.02 (s, 8H, *c*), 3.98 (m, 16H, *a and b*).

(xxx) 2h:3d. δ (ppm) **2h:** 9.69 (s, 1H, ortho-N^+/-COOEt), 9.32 (d, 1H, J = 6.80 Hz, ortho-N^+/para-COOEt), 9.24 (d, 2H, J = 6.28 Hz, ortho-N^+/meta-COOEt), 8.67 (d, 1H, J = 7.80 Hz, para-N^+), 8.30 (d, 2H, meta-N^+/ortho-COOEt), 8.13 (dd, 1H, meta-N^+/-COOEt), 5.47 (s, 4H, CH_2-α-N^+), 4.39 (q, 2H, J = 6.77 Hz, CH_2-α-O-nicotinium), 4.17 (q, 2H, J = 7.47 Hz, CH_2-α-O-isonicotinium), 1.33 (t, 3H, CH_3-nicotinium), 1.28 (t, 3H, CH_3-nicotinium) **3d:** 7.68 (m, 2H, *j*), 7.38 (m, 2H, *i*), 7.07 (s, 2H, *h*), 4.14 (m, 4H, *a*), 4.01 (m, 4H, *b*), 3.88 (m, 4H, *c*), 3.63 (m, 4H, *d*), 3.57 (m, 4H, *e*), 3.40 (m, 4H, *f*), 3.12 (m, 4H, *g*).

(xxxi) 2h:3e. δ (ppm) **2h:** 9.68 (s, 1H, ortho-N^+/-COOEt), 9.30 (d, 1H, J = 6.37 Hz, ortho-N^+/para-COOEt), 9.27 (d, 2H, J = 6.53 Hz, ortho-N^+/meta-COOEt), 8.28 (d, 1H, J = 8.65 Hz, para-N^+), 8.12 (d, 2H, meta-N^+/ortho-COOEt), 7.91 (dd, 1H, meta-N^+/-COOEt), 5.62 (s, 4H, CH_2-α-N^+), 4.34 (q, 2H, J = 7.75 Hz, CH_2-α-O-nicotinium), 4.17 (q, 2H, J = 6.35 Hz, CH_2-α-O-isonicotinium), 1.33 (t, 3H, CH_3-nicotinium), 1.27 (t, 3H,

CH_3-nicotinium) **3e:** 7.65 (m, 2H, *k*), 7.36 (m, 2H, *j*), 7.02 (s, 2H, *i*), 6.76 (m, 2H, *g*), 6.66 (m, 2H, *h*), 4.01 (m, 24H, *a, b, c, d, e and f*).

(xxxii) 2h:3f. δ (ppm) **2h:** 9.70 (s, 1H, ortho-N^+/-COOEt), 9.33 (d, 1H, J = 6.66 Hz, ortho-N^+/para-COOEt), 9.28 (d, 2H, J = 6.59 Hz, ortho-N^+/meta-COOEt), 8.19 (d, 1H, J = 7.72 Hz, para-N^+), 8.07 (d, 2H, meta-N^+/ortho-COOEt), 7.94 (dd, 1H, meta-N^+/-COOEt), 5.63 (s, 4H, CH_2-α-N^+), 4.15 (q, 2H, J = 7.76 Hz, CH_2-α-O-nicotinium), 3.83 (q, 2H, J = 6.66 Hz, CH_2-α-O-isonicotinium), 1.21 (t, 3H, CH_3-nicotinium), 1.13 (t, 3H, CH_3-nicotinium) **3f:** 7.64 (m, 4H, *f*), 7.36 (m, 4H, *e*), 7.01 (s, 4H, *d*), 4.08 (m, 24H, *a, b and c*).

2.3 RESULTS AND DISCUSSION

SYNTHESIS

The reaction of an amine and an alkyl halide to produce a quaternized nitrogen center is generally referred to as the *Menshutkin* reaction.[98] The reaction kinetics are sensitive to temperature, pressure and solvent polarity, as are many S_N2 type transformations. This procedure was used to construct all of the threads studied in this thesis. Figure 2-8 outlines the general route to compounds **2a-g**.

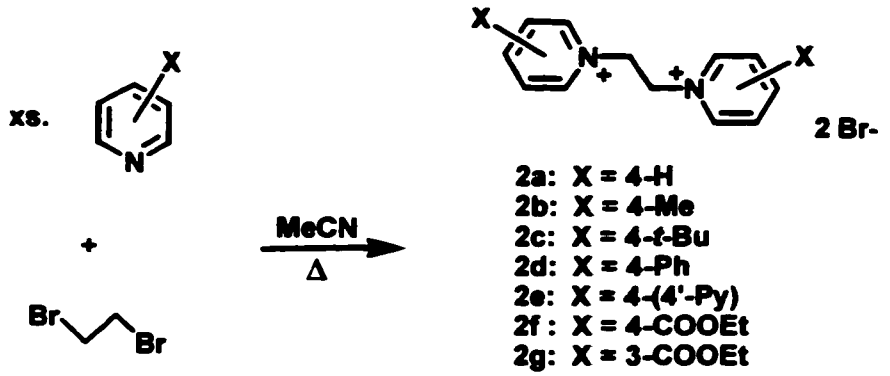

Figure 2-8. General synthesis of threads **2a-g**.

An excess of the amine reactant was used to accelerate the formation of product due to the low rate of the reaction. Reaction times in excess of 3-4 days usually resulted in contamination of the products and were therefore avoided. The use of solvents such as $MeNO_2$, MeCN, and EtOH in these reactions leads to much cleaner products and higher yields than those observed when conducted in more polar solvents such as DMF and DMSO. Yields ranged from 7.4% (**2f**) to 47.1% (**2c**) with no apparent trends observed with regard to the substituent on the pyridine ring. Luckily, the relative inexpense of the starting materials and the need for only small amounts of product rendered these poor yields acceptable in this application.

The exception to the previous reaction scheme was the synthesis of compound **2e**. While the one-pot synthesis depicted in Figure 2-9 is a facile method for its construction, a stepwise route provides this product in much higher yields (Figure 2-9). Though the

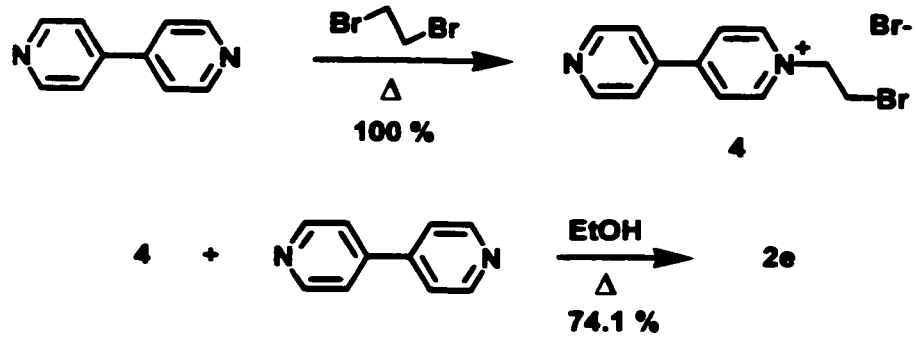

Figure 2-9. Synthesis of **2e** via two step method.

yield of **4** reported in the literature for the initial reaction is only 25%, reproduction of these conditions in our laboratory results in the quantitative isolation of this compound from the reaction mixture. Subsequent reaction with excess 4,4'-dipyridyl generates **2f** in 74.1% yield overall. While this method works well for compound **2e**, attempts to duplicate this approach for the other threads resulted in intractable tars during the initial bromoethylation.

In order to synthesize the unsymmetrical thread **2h** a two-step procedure similar

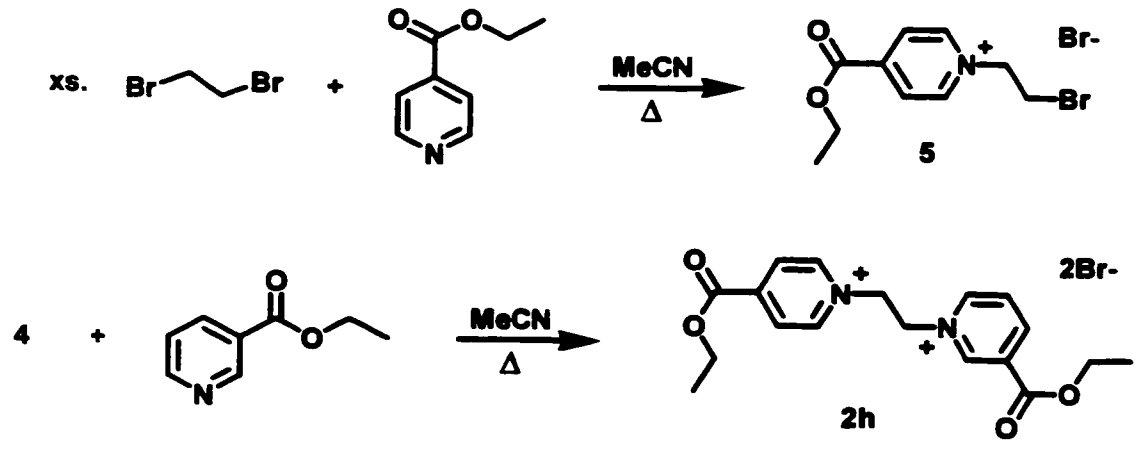

Figure 2-10. Synthesis of **2h**.

to that of **2e** was developed (Figure 2-10). Reaction of ethyl isonicotinate with a large excess of 1,2-dibromoethane in MeCN at reflux resulted in the formation of compound **5**. Further treatment of **5** with ethyl nicotinate in MeCN gave **2h** in 2.2 % yield from the initial ester.

Compounds **2a-h** were precipitated from aqueous $NaBF_4$ or NH_4BF_4 solutions in order to exchange the bromide anions for the less coordinating BF_4^- anion which also rendered the threads more soluble in organic solvents for study by ^1H NMR.

Once the threads had been synthesized, the process of forming pseudorotaxanes with them involved simply dissolving the desired thread and crown ether in an appropriate solvent (Figure 2-11). This is an equilibrium phenomenon, and as such, the

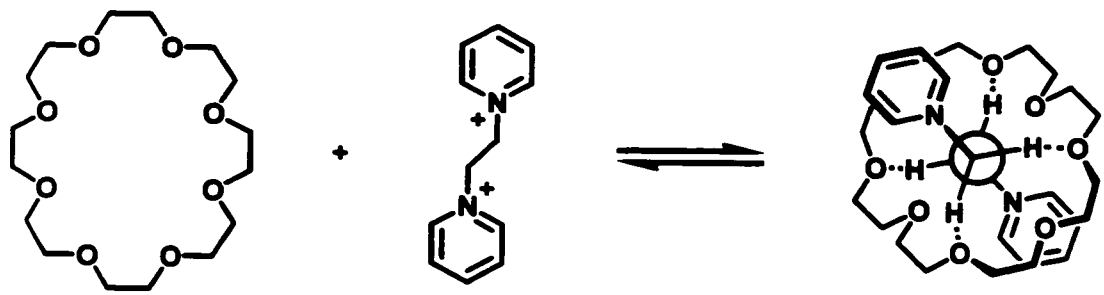

Figure 2-11. Equilibrium formation of a pseudorotaxane.

amount of pseudorotaxane present in solution is dependent on the ratios of the concentrations of the thread and crown in a predictable manner. This dependence can be formulated as an *association constant* (K_a) in the following equation:

$$K_a = \frac{[\text{Thread:Crown}]}{[\text{Thread}][\text{Crown}]}$$

While an *equimolar* solution of each component will never quantitatively form the respective pseudrotaxane, increasing the amount of either thread or crown will result in an increase of pseudorotaxane formed, with respect to the limiting reactant. Thus, it is

possible to "quantitatively" form a pseudorotaxane from a particular thread by adding a large excess of crown to the solution. The amount needed is proportional to the association constant of the formation reaction and could be calculated if the need arose.

^{1}H NMR SPECTROSCOPY

Analysis of the ^{1}H NMR spectra of the pseudorotaxane complexes was performed in MeCN-d_3 due to the universal solubility of all the species studied (crowns and threads) in this solvent. Low solubility of the threads in more non-polar solvents, and solvent competition with the crown for the thread, as well as crown insolubility, in more polar solvents rendered any meaningful scrutiny in these media impossible. $MeNO_2$ exhibits similar properties to MeCN, with regards to this system, the almost identical behaviour of the pseudorotaxanes in these two solvents during initial testing indicated the investigation of these complexes in both environments was redundant.

The dissolution of a thread (**2a-h**) and a crown (**3a-f**) together in MeCN results in a complexation induced shift of the ^{1}H NMR chemical shifts of both species. The shifts of the central methylene protons of the complexed threads are summarized in Table 2-1.

As can been seen in Table 2-1, all of the methylene resonances shift downfield upon interpenetration of the crown ether ring. Downfield shifts of this type are characteristic of hydrogen-bonding interactions due to a weakening of the C-H bond by the oxygen donors of the crowns. This conclusion is borne out by the weakening of this effect in **2b** via the electron donating methyl unit, which should decrease the polarization of the methylene C-H bonds. Conversely, the threads with electron-withdrawing substituents tend to have higher downfield shifts. The absence of any shift whatsoever

Table 2-1. Shifts (in ppm) of the central methylene protons of the thread component upon pseudorotaxane formation

	3a	**3b**	**3c**	**3d**	**3e**	**3f**
2a	0.17	0.19	0.27	-	-	-
2b	0.03	0.09	0.17	-	-	-
2c	0.00	0.00	0.00	-	-	-
2d	0.18	0.21	0.33	-	-	-
2e	0.21	0.27	0.40	0.29	0.29	0.29
2f	0.16	0.22	0.34	0.22	0.35	0.37
2g	0.18	0.26	0.41	0.26	0.41	0.44
2h	0.19	0.26	0.40	0.28	0.43	0.45

in the *t*-butyl-substituted thread **2c** would indicate that this group prevents threading of the dication through the crown ether cavity. Furthermore, this implies that the shifts observed in the other cases *are* the result of an interpenetrated geometry. If the complexation of the threads is of a non-pseudorotaxane geometry, then *at least in the case of* **2c:3a** there is no reason that the *t*-butyl substituents should eliminate the bonding interaction, as they are sufficiently distant from the central methylene units as to be of no steric consequence.

These observations may be reiterated upon inspection of the shifts of the ortho-N^+ protons of the pyridinium rings (Table 2-2). These protons all experience a downfield shift when complexed with **3a-f**, presumably as a result of hydrogen-bonding as well. The major difference between these two sets of shifts is their behaviour as benzo or naphtho groups are introduced to the crown ether component. In the case of the central methylene protons, the addition of an aryl group to the crown ether results in a general

increase in the magnitude of the downfield shift. Assuming that the aryl groups are π-stacking with the pyridinium rings (see section 2.5) and that this interaction is a positive one, then it may be reasonable to conclude that this π-stacking effect orients the crown ether oxygen atoms in a more favourable manner for hydrogen-bonding with the central methylene protons. Likewise, the decrease in conformational flexibility of the crown due to these aryl units may also play a role in preorganizing the oxygen atoms in a complementary fashion.

Table 2-2. Shifts (in ppm) of ortho-N^+ protons of the thread component upon pseudorotaxane formation.

	3a	**3b**	**3c**	**3d**	**3e**	**3f**
2a	0.30	0.26	0.27	-	-	-
2b	0.24	0.24	0.25	-	-	-
2c	0.00	0.00	0.00	-	-	-
2d	0.35	0.31	0.33	-	-	-
2e	0.42	0.40	0.43	0.39	0.41	0.41
2f	0.31	0.28	0.29	0.29	0.29	0.32
2g (o-COOEt/N^+)	0.32	0.31	0.32	0.30	0.32	0.33
(o-N^+)	0.21	0.21	0.22	0.23	0.23	0.26
2h (o-COOEt/N^+)	0.37	0.34	0.34	0.37	0.36	0.38
(o-N^+/p-COOEt)	0.41	0.44	0.42	0.47	0.45	0.48
(o-N^+/m-COOEt)	0.38	0.33	0.37	0.36	0.39	0.40

This pattern does not hold for the ortho-N^+ protons of the pyridinium rings. Introduction of aryl units into the crown ethers generally results in a reduction in the downfield shifts of these protons indicating a mildly destructive effect, if any, in most cases.

The presence of π-stacking in solution between the benzo or naphtho components of the crown ethers and the pyridinium rings is further observed in the shifts of the meta-

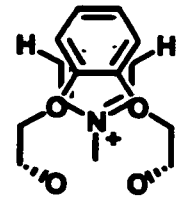

Figure 2-12. π-Stacking of a benzo group over a pyridinium ring.

and para-N^+ protons (where present) of the threads. In all cases, these protons shift upfield upon threading through crown ethers **3b-e**. This may be accounted for by noting that these protons should spend, on average, the majority of their time in close proximity to the influence of the aryl ring current of the crown ether (Figure 2-12). In exactly the same manner, the benzo and naphtho protons of the crown ethers shift upfield as well. This is demonstrated in Table 2-3 with **3c** and threads **2d-h**. The complexes of **2a** and **2b** with **3a-c** have a short lifetime on the NMR timescale and limiting shifts of these threads were determined by the titration method (this will be elaborated further on). Determining the limiting shifts of the crowns would have required dissolution of large amounts of the threads in some samples, which was physically impossible. In addition, examination of the shifts of the crowns in these two instances is of questionable value in light of the other data.

Table 2-3. Shifts of the benzo protons of **3c** upon complexation with **2d-h**.

		2d	**2e**	**2f**	**2g**	**2h**
3c	(d)	6.68	6.68	6.76	6.80	6.77
3c	(e)	6.57	6.57	6.70	6.66	6.66

The OCH_2 protons of the crown ethers are generally shifted upfield as a result of pseudorotaxane formation though no definite pattern results from an analysis of these shifts.

As mentioned above, the complexes formed between **2a** or **2b** and **3a-c** have lifetimes that are short on the NMR timescale. In other words, over the time of the observation of the decay of the RF pulse the components associate and dissociate many times. This results in the shifts of the thread and crown protons in such a solution appearing as a weighted average of the complexed and uncomplexed species. Thus, in order to determine the shifts of these protons in the complexed form, one component must be present in great excess in order that the equilibrium for the other is biased almost entirely towards the complexed state (Figure 2-6). This can be demonstrated by

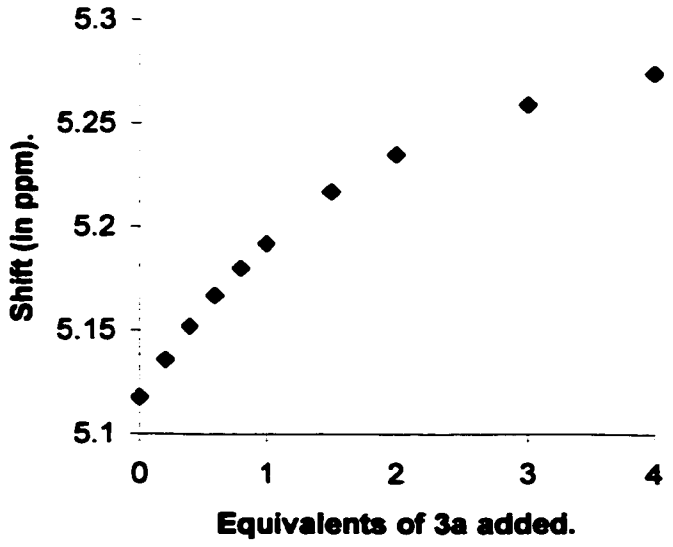

Figure 2-13. Variation of the shift of the central methylene protons of 2a with increasing 3a.

inspecting the shift of the central methylene protons of **2a** upon addition of increasing amounts of **3a** (Figure 2-13). In this example, it is evident that the limiting shift value for the protons in question, as a result of complexation, is 5.28 ppm at a crown to thread ratio of approximately 8:1. In this manner, the shifts of the thread in its complexed state may be determined.

In addition to providing this information, a titration such as that of Figure 2-8 can also yield an accurate value for the association constant for the equilibrium being observed. The fact that the observed shift is a *weighted average* of the free and complexed states allows us to fit the experimental data to those calculated by a non-linear least-squares refinement program. In our case, the program EQNMR was used to perform this function.[99] This program formulates the problem as shown below:

$$\delta_{calc} = \frac{\delta_{uc}[Thread]_{uc}}{[Thread]_{Total}} + \frac{\delta_c K_a [Thread]_{uc}[Crown]_{uc}}{[Thread]_{Total}}$$

Input requires starting concentrations of crown and thread, observed proton shifts, and initial guesses of the association constant, complexed and uncomplexed shifts of the probe proton. Output consists of calculated values for the proton shifts and association constant, as well as a goodness of fit between the experimental and calculated values.

The situation for pseudorotaxane formation between **2d-h** and **3a-f** is considerably different. The rate of association and dissociation is slow with respect to the NMR timescale. This results in the observation of both the complexed and uncomplexed species *simultaneously* in the ^{1}H NMR spectrum. A spectrum of a 1:1 mixture of **2f** and **3c** is shown in Figure 2-14. This transition in the rates of the complexation reaction from **2a** and **b** to **2d-h** further suggests that the nature of the complexation geometry in solution is that of a pseudorotaxane. Most likely, this change

in behaviour is a result of the increased steric bulk of the substituents of **2d-h** compared to the other two threads. This observation also lends weight to the conclusion that the *t*-

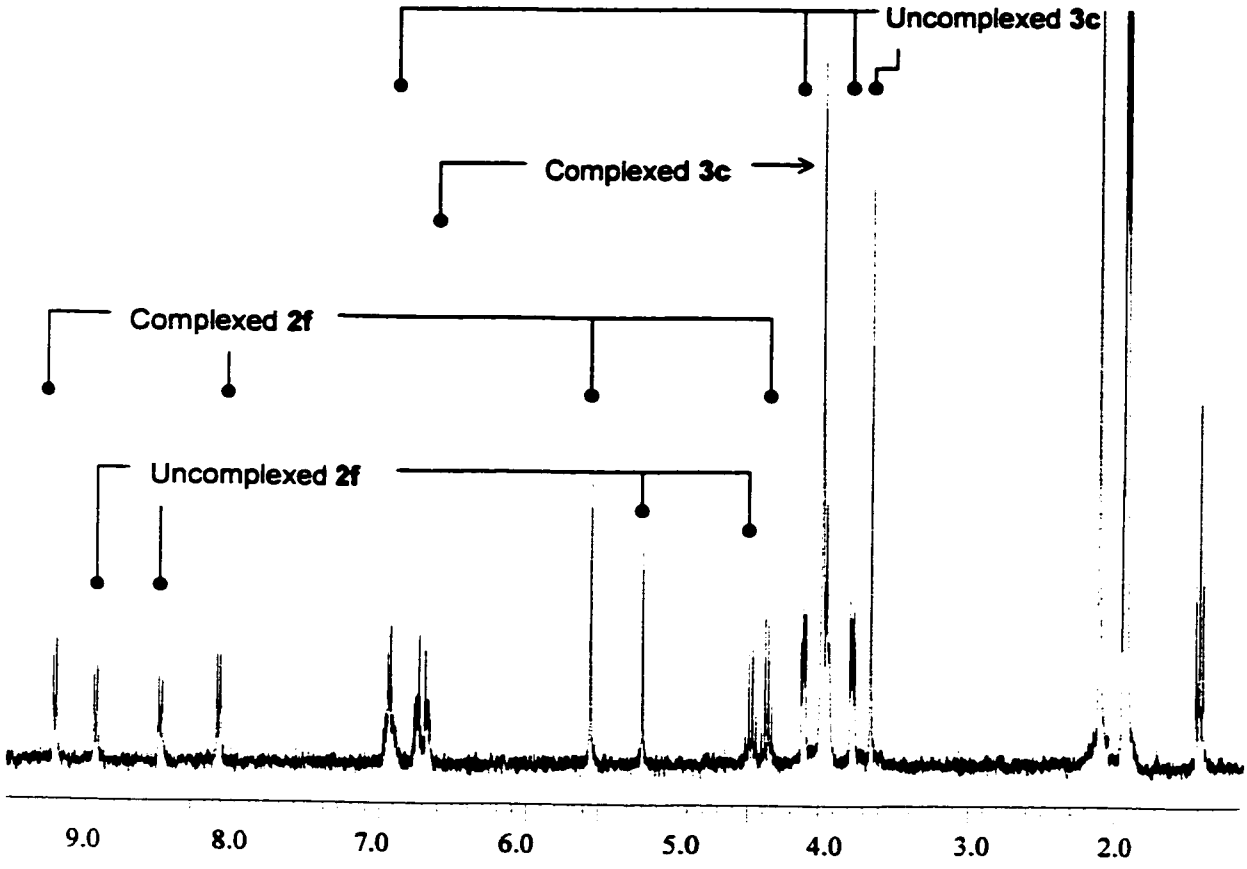

Figure 2-14. ^{1}H NMR spectrum of a 1:1 mixture of **2f** and **3c**.

butyl group of **2c** prevents threading due to an insurmountable steric barrier. This group is larger, on average, than the substituents on the other threads, which can lie in the plane of the pyridinium ring to allow the crown to thread over them.

The static nature of these spectra is convenient, in that the shifts of the complexed protons can be deduced from a single sample. Furthermore, if the initial concentrations of the components are known, integration of the complexed and uncomplexed peaks yields the relative amounts of these species in solution and thus the association constant.

Using the example of **2f:3c**, if the integrals for the central methylene protons of the complexed (δ = 5.58) and uncomplexed (δ = 5.23) thread are 1 and 0.870 respectively, and the initial concentrations of thread and crown are 2 x 10^{-3} M, then:

$$K_a = \frac{[\text{Thread:Crown}]}{[\text{Thread}][\text{Crown}]} = \frac{\frac{1}{1.870} \times 2 \times 10^{-3}\ \text{M}}{\left(\frac{0.870}{1.870} \times 2 \times 10^{-3}\ \text{M}\right)^2} = 1200\ \text{M}^{-1}$$

Utilizing the previous two procedures for the determination of the association constants, we calculated selected values for all of the threads with all of the crowns (Table 2-4).

Table 2-4. Association constants (M^{-1}) and ΔG° (kJ/mol) values for the pseudorotaxanes formed between **2a-h** and **3a-f** at 298 K.

	2a	**2b**	**2c**	**2d**	**2e**	**2f**	**2g**	**2h**
3a K_a	165	105	0	160	300	320	670	370
ΔG°	-12.7	-11.6	0	-12.6	-14.1	-14.3	-16.1	-14.7
3b K_a	195	205	0	300	630	740	2480	1140
ΔG°	-13.1	-13.2	0	-14.2	-16.0	-16.4	-19.4	-17.5
3c K_a	180	230	0	320	920	1200	3640	1800
ΔG°	-12.9	-13.5	0	-14.3	-16.9	-17.6	-20.3	-18.6
3d K_a	-	-	0	-	390	580	1220	960
ΔG°	-	-	0	-	-14.8	-15.8	-17.6	-17.0
3e K_a	-	-	0	-	830	1000	2440	1540
ΔG°	-	-	0	-	-16.7	-17.2	-19.3	-18.2
3f K_a	-	-	0	-	-	970	2350	2100
ΔG°	-	-	0	-	-	-17.1	-19.2	-18.8

Several trends are evident upon examination of the association constants for these pseudorotaxanes. The threads **2a, 2b** and **2d** exhibit increases in the free energy of

association with the addition of one or two benzo groups to the crown ether ring.

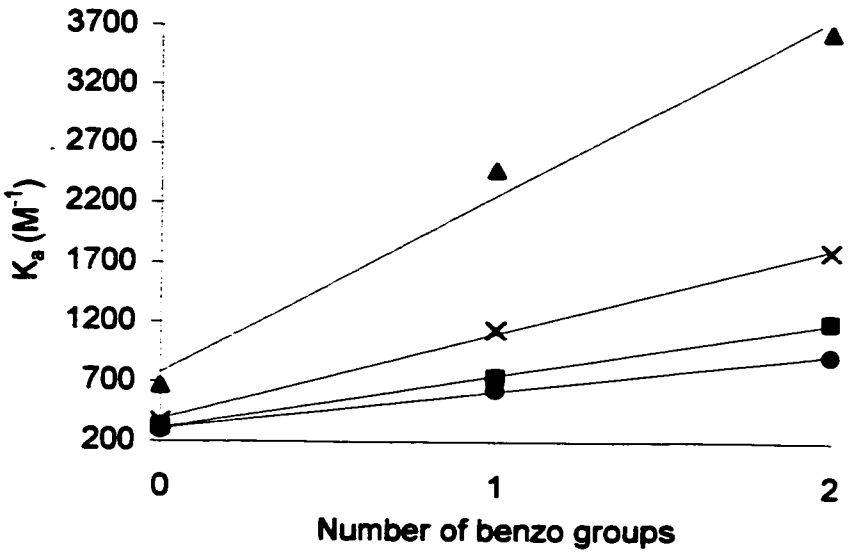

Figure 2-15. Variation of K_a values (M^{-1}) of threads **2e**(•), **2f**(■), **2g**(▲) and **2h**(×) with the number of benzo groups present in **3a-c.**

However these gains are minimal and indicate that the stabilization gained from π-stacking and/or macrocyclic preorganization of the crown has little significance in these cases. The situation is much different for the pyridyl and ester substituted threads **2e-h**. Pseudorotaxane formation, as a function of the association constants, increases monotonically with the number of benzo or naphtho groups present in the crown ether (Figures 2-15 and 2-16), though some deviation appears present in the naphtho series. This constant variation suggests that the effect that annulating the crown with benzo or naphtho groups has on the formation of these complexes is independent of the type or position of substituent present on the pyridinium moiety, except in magnitude. It further indicates that the solution geometries of the threads and their associated pseudorotaxanes

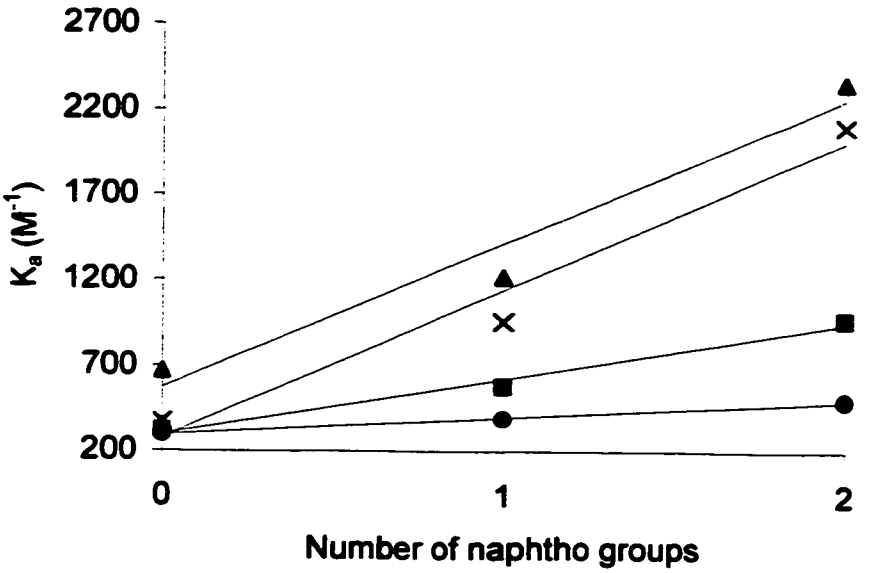

Figure 2-16. Variation of Ka values (M^{-1}) of threads **2e**(•), **2f**(■), **2g**(▲) and **2h**(×) with the number of naphtho groups present in **3a, d,** and **f.**

are highly similar. Most likely, this result holds for threads **2a**, **2b**, and **2d**, but the effect is so weak that it has become difficult to discern within experimental error.

The strongest interactions overall occur with the threads containing electron withdrawing substituents. This is to be predicted, due to the increase in polarization these groups induce in the pyridinium ring and the protons of the central ethylene unit. The benzo-annulated crowns generally confer more stabilization to the complexes than those containing naphtho groups.

Thread **2h** has a structure which incorporates one "half" of each of **2f** and **2g** and could be expected to display an average of the individual stability exhibited by the complexes formed from these two components. Unfortunately, this pattern is not displayed in the complexes formed with either the benzo or naphtho series of crowns,

though the association constants fall within the range between the two symmetric threads. The reason for this discrepancy is unclear and indicates that some other phenomenon is occurring to alter the stability of these complexes.

In a similar manner to **2h**, crown **3e** can be considered an amalgam of the structures of **3c** and **3f**. Thus, the association behaviour of **3e** with the threads could be expected to manifest itself as an average of the symmetric crowns. Of the threads measured, the stability constants of **3e** with **2e-g** do fall between the values of the corresponding complexes involving **3c** and **3f**. However, with none of these threads is the "average" value midway between the other two.

The convenience of the single point determination of association constants in the static cases discussed above allows for a relatively simple determination of the

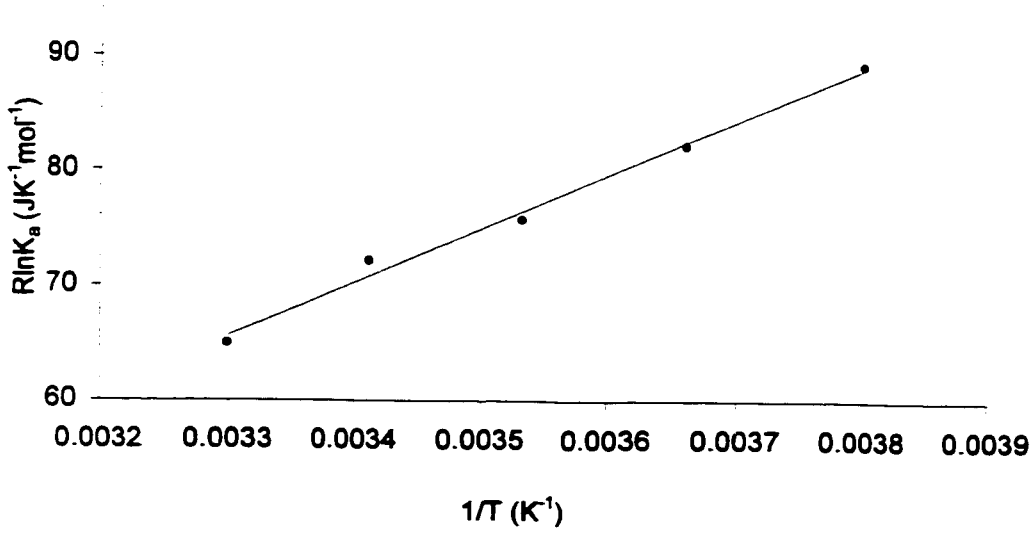

Figure 2-17. Van't Hoff plot of pseudorotaxane formation between **2g** and **3c**.

thermodynamic parameters of the association process. Utilizing a standard van't Hoff analysis of the association constants of 1:1 mixtures of **2g** and **3a-f** at different temperatures via variable temperature ^{1}H NMR spectroscopy (VTNMR), the values of -

$\Delta H°$ and $\Delta S°$ may be extracted.[100] As an example, the association constants from the VTNMR investigation of pseudorotaxane formation between **2g** and **3c** are plotted as $RlnK_a$ versus the reciprocal temperature (Figure 2-17). The slope of the line of best fit and its intercept give values for $\Delta H° = -46.5$ kJ mol^{-1} and $\Delta S° = -87.9$ J mol^{-1} K^{-1} respectively. This method works well for the pseudorotaxanes formed between **2g** and **3b-f** within the temperature range studied (–10°C to 30°C) and assumes, accurately, that the $\Delta H°$ and $\Delta S°$ contributions to complexation are temperature-invariant.

In the case of the complexation of **2g** by **3a** the van't Hoff plot results in a nonlinear relationship unlike that with the other crowns (Figure 2-18). This suggests that

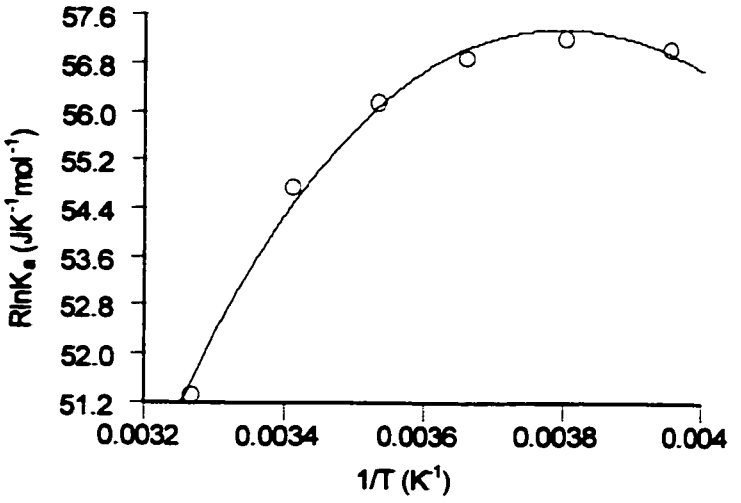

Figure 2-18. Van't Hoff plot for pseudorotaxane formation between **2g** and **3a** with Dougherty's best fit.

the thermodynamics of pseudorotaxane formation in this instance are affected by a non-negligible heat capacity. Similar behaviour has been observed by Stoddart's group in the formation of pseudorotaxanes from dialkyl ammonium salts and DB24C8. This deviance from linearity was treated by employing Dougherty and co-workers' expansion of the usual van't Hoff equation by the inclusion of a heat capacity term ($\Delta C_p°$):[101]

$$\Delta G^\circ = -RT\ln K_a = \Delta H^\circ - T\Delta S^\circ$$

$$\Delta H^\circ = \Delta H_0 + T\Delta C_p^\circ$$

$$\Delta S^\circ = \Delta S_0 + \Delta C_p^\circ \ln T$$

$$R\ln K_a = -\left(\frac{\Delta H_0}{T}\right) + \Delta C_p^\circ \ln T + (\Delta S_0 - \Delta C_p^\circ)$$

This modified equation fits the data quite well (R = 0.9964) and results in values for $\Delta H_0 = 108.2$ kJ mol^{-1}, $\Delta C_p^\circ = -409.7$ J mol^{-1} K^{-1}, and $\Delta S_0 = 2.342$ kJ mol^{-1} K^{-1}. Using these parameters, the change in ΔH° and $-T\Delta S^\circ$ can be plotted as a function of temperature, in order to obtain a clearer picture of their individual contributions over the

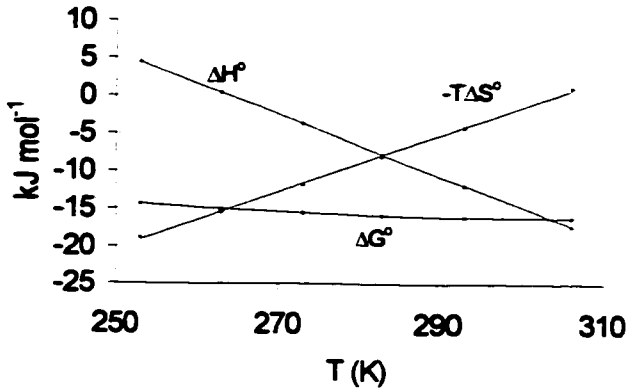

Figure 2-19. Plot of the variation of ΔG°, ΔH°, and $-T\Delta S^\circ$ versus temperature.

range of observation (Figure 2-19). At low temperature (-20°C), pseudorotaxane formation is driven primarily by entropic forces, while at higher temperature (30°C) this process is entirely enthalpic in nature. These two compensating forces combine to render the free energy of complexation relatively unchanged over the temperature range studied, similar to behaviour seen in biological systems with large heat capacities.[102] This enthalpic dependence on temperature in the case of **3a** could be viewed as a result of the lower preorganization of this crown with respect to **3b-f**, which would require less

conformational change prior to, or during complexation. Annulation of the crown ether ring with aromatic groups would be expected to hold the cavity of the crown in a more accessible conformation than that of **3a**, facilitating penetration of the thread through the opening.

Combining the above two methods for the calculation of the enthalpic and entropic considerations, we may compare the room temperature contributions of each towards complexation with each of the crown ethers and **2g** (Table 2-5).

Table 2-5. Thermodynamic parameters of the complexation of **2g** with **3a-f** at 298 K (kJ $mole^{-1}$).

	ΔG°	ΔH°	-TΔS°
3a	-16.1	-13.9	-2.18
3b	-19.4	-33.4	14.0
3c	-20.3	-46.5	26.2
3d	-17.6	-24.4	6.8
3e	-19.3	-33.2	13.9
3f	-19.2	-32.2	13.0

The formation of all six pseudorotaxanes is definitely a result of molecular recognition, as indicated by the entirely enthalpic character of the complexation process in these cases. The relatively large and unfavourable entropic terms present with crowns **3b-f** are not surprising. Other highly preorganized hosts, which bind *neutral* guests, have been found to demand a sizable entropic consideration in organic solvents in order to bring the two species together as one. The relatively non-coordinating BF_4^- anion and

polar solvent would be expected to largely reduce to negligible any ion pair effects that might normally appear in a situation involving a charged guest such as ours.

X-RAY CRYSTALLOGRAPHY

Inspection of the previously determined crystal structure of **3c** obtained from a

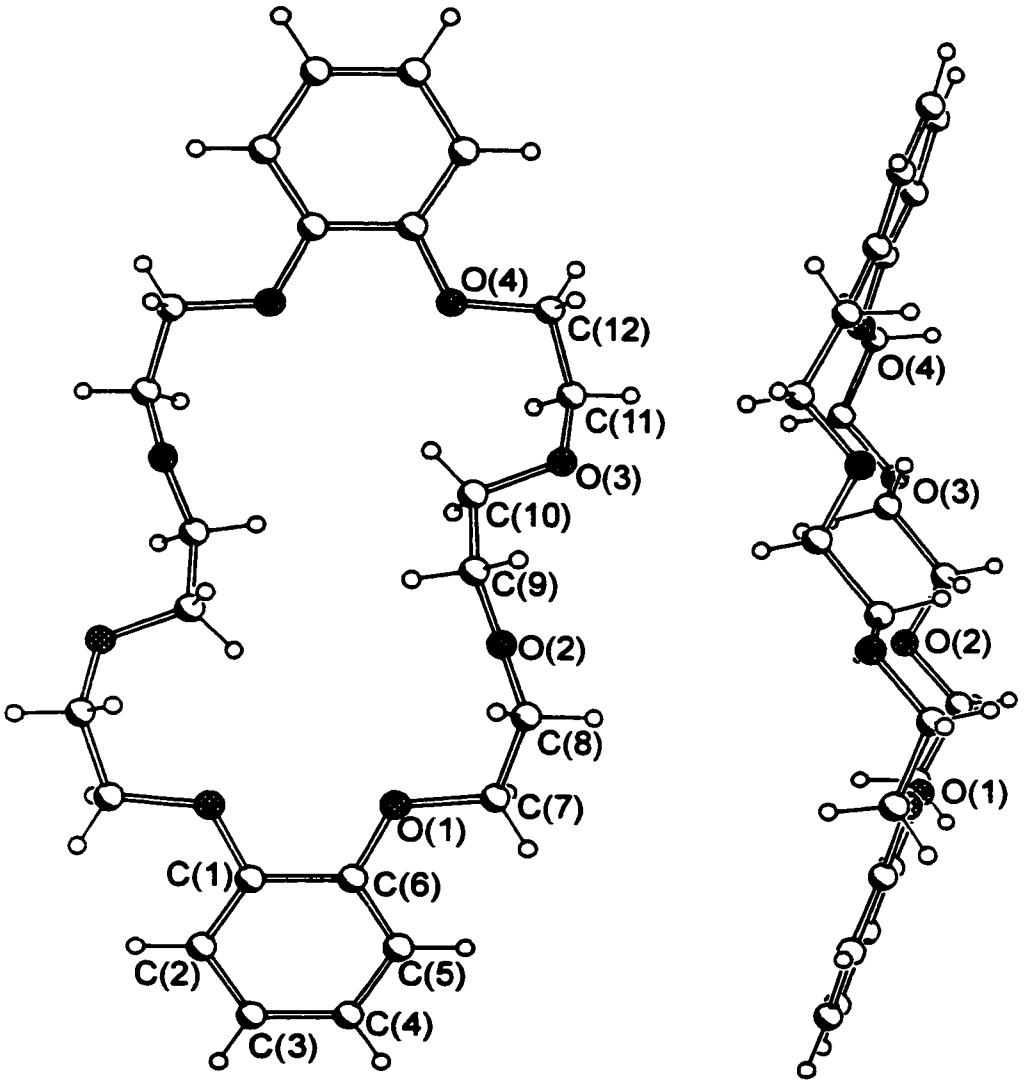

Figure 2-20. Two views of the crystal structure of **3c**.

dichloromethane/ethanol solution reveals a largely open structure (Figure 2-20).[103] There are two molecules in a monoclinic unit cell having space group $P2_1/c$, resulting in each being related and centrosymmetric. The molecule takes on an S-shaped conformation in the crystal similar to that envisioned by Stoddart upon binding two diquat dications (Figure 2-6). The plane of the catecholate rings extends to C7 and C12 (C1-C6-O1-C7 = 174.6(5) and C6-C1-O4-C12 = -172.3(5)), presumably in order to extend the π-system of the aryl rings to include partially sp^2-hybridized oxygen atoms attached to them. The adjacent carbon atoms in the polyether chain (β-methylenes) are included in this plane as well (C6-O1-C7-C8 = -175° and C1-O4-C12-C11 = 177°). This conformation is common in aryl crown ethers of this type and generally results in structures (in the solid state at least) of an open form such as this.

It is interesting to compare the structure of **3c** to that of the pseudorotaxane formed between **2e** and **3c**, which was crystallized from acetonitrile/isopropyl ether (Figure 2-21). The conformation of the crown in the complex **2e:3c** is identical in many ways to that of the free compound **3c**. The major difference between the two is the orientation of the γ-methylene groups of the polyether chain. In the free compound, these groups are positioned to partially fill the cavity, most likely in an attempt to fill the free space, which would otherwise be unoccupied. These groups have swung, necessarily, out of the cavity in the complex, to allow both occupation of the cavity by the thread, as well as hydrogen bonding and $N^+\cdots O$ ion-dipole interactions. The position of the α- and β-methylene units of the interpenetrated crown are very similar to those of free **3a**, lying in the plane of the catechol rings (C(12)-C(17)-O(1)-C(18) = 170.2°, C(17)-O(1)-C(18)-C(19) = -176.6°, C(17)-C(12)-O(4)-C(23) = -172.9°, C(12)-O(4)-C(23)-C(22)' = 177.4°).

The complex **2e:3c** is held together by a combination of $N^{+}\cdots O$ ion-dipole interactions, C-H···O hydrogen bonding, and π-stacking. It crystallized with two complexes per unit cell in the monoclinic space group $P2_1/c$, requiring the solution of

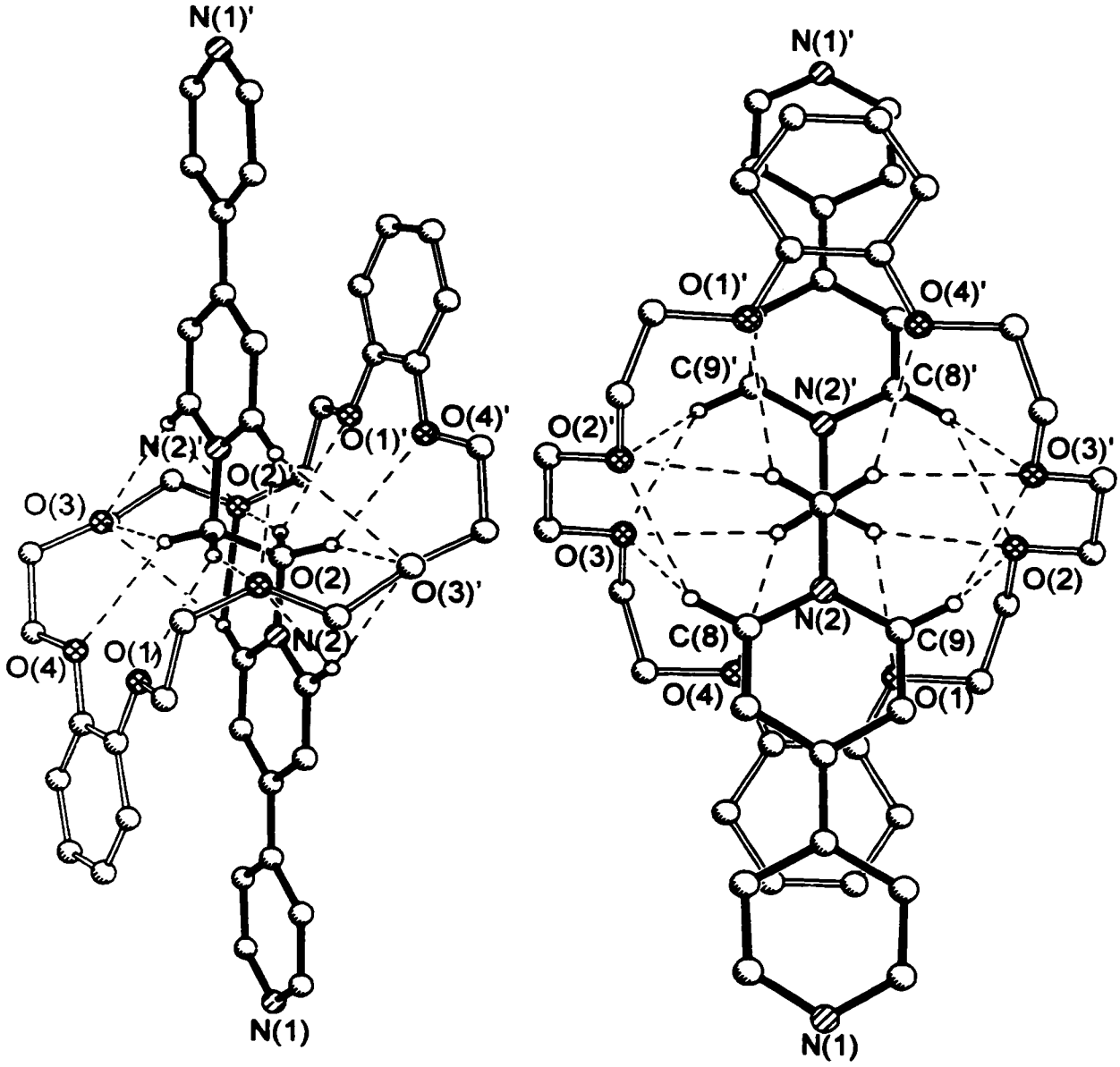

Figure 2-21. Two views of the crystal structure of the pseudorotaxane formed from **2e** and **3c**.

only half of one centrosymmetric pseudorotaxane, the rest of the cell being related by symmetry. $N^{+}\cdots O$ ion-dipole stabilization is evident from a series of close to medium

contacts between the quaternized dipyridinium nitrogen atoms and the ether oxygens (N2···O4 = 3.48 Å, N2···O1 = 3.57 Å, N2···O3 = 3.70 Å, N2···O2A = 3.74 Å). These contributions are reinforced by the presence of 16 hydrogen bonds involving the central methylene and ortho-N^+ hydrogen atoms of the thread and the crown ether (Table 2-6).

Table 2-6. Hydrogen bonding parameters in the crystal structure of pseudorotaxane **2e:3c**.

Hydrogen Bonded Atoms	Distance (Å)	C-H···O Angle (°)
O1'···H11A	2.631	129.8
O2'···H11A	2.341	156.7
O2···H9A	3.045	132.0
O3···H9A	2.435	145.8
O2'···H8A	2.493	144.1
O3'···H8A	2.915	130.5
O3···H11B	2.444	141.7
O4'···H11B	2.545	138.0

All eight oxygen atoms are involved in the hydrogen bonding motif, with the alkyl oxygen atoms bonded to multiple hydrogen sites in the thread.

The catecholate rings of the crown ether are engaged in π-stacking over the center of the dipyridinium ring system with an interplanar distance of ca. 3.5 Å apart, typical of this type of interaction. The dipyridinium rings are nearly co-planar, canted at an angle of 3.9°, the two of which adopt an average interplanar angle with the catechol ring of 4.0°. As expected, the thread is arranged about its center in an anti conformation, due to

the intramolecular repulsion of the positively charged nitrogen atoms. The long axis of the crown describes an angle of 1.8°, nearly coincident with that of the thread.

A similar complexation geometry is discovered when the pseudorotaxane formed from **2f** and **3c** is crystallized from acetonitrile/isopropyl ether (Figure 2-22). The

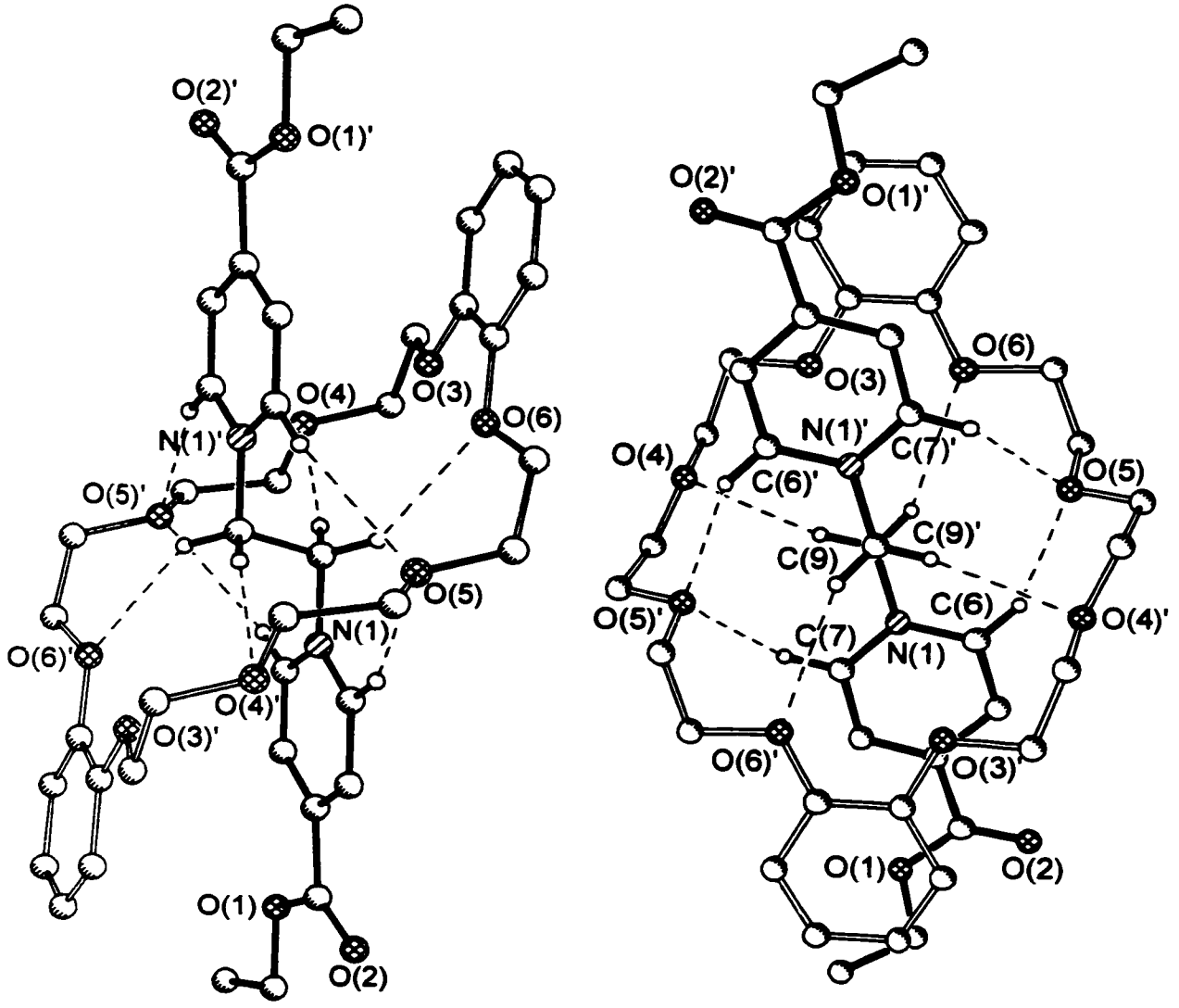

Figure 2-22. Two views of the crystal structure of the pseudorotaxane formed between **2f** and **3c**.

complex again crystallizes in the space group $P2_1/c$ with two centrosymmetric pseudorotaxanes per unit cell.

The crown ether takes up an S-shaped conformation comparable to that in the previous two structures (C(10-C(15)-O(3)-C(16) = -168.0°, C(15)-O(3)-C(16)-C(17) = 172.8°, C(15)-C(10)-O(6)-C(21) = 169.7°, C(10)-O(6)-C(21)-C(20) = 176.4°), including the α- and β-methylene units in the plane of the catechol rings. The thread also takes on the predictable anti conformation seen in the foregoing example. However, in this structure the long axes of the crown and thread are inclined to one another by 19.6° and indicate a more coherent set of ion-dipole and hydrogen bonding interactions.

In this case, alternating oxygen atoms in the crown ether are responsible for hydrogen bonding to the central methylene components of the thread (Table 2-7). The

Table 2-7. Hydrogen bonding parameters for the crystal structure of pseudorotaxane **2f:3c**.

Hydrogen Bonded Atoms	Distance (Å)	C-H···O Angle (°)
O4···H9A	2.54	165.0
O6···H9B	2.66	150.0
O5'···H7A	2.54	141.0
O5···H6A	2.36	154.2

remaining alkyl oxygen atoms in the crown are left to bifurcate the ortho-N^+ hydrogen atoms of the isonicotinium rings on either side of the thread. In general, the alkyl oxygen atoms display shorter H···O distances than their aryl counterparts, most probably as a result of their greater basicity.

The misalignment of the long axes of the crown and thread does not impede the ion-dipole interactions of the crown with the quaternized nitrogen atoms of the thread.

Several short to medium contacts of this type are still in evidence (Table 2-8) and indicate some stabilization of the structure by this type of interaction.

Table 2-8. $N^{+}\cdots O$ contacts in the crystal structure of pseudorotaxane **2f:3c**.

Atoms	Distance (Å)
N1···O5	3.76
N1···O3'	3.46
N1···O4'	3.87
N1···O5'	3.80
N1···O6'	3.55

π-Stacking interactions are apparent in this structure as well. The catecholate ring lies at a 10.8° interplanar angle to that of the pyridinium ring system. In this instance however, the crown ether is interacting more directly with the conjugated portion of the thread's ester substituent than with the quaternized ring. This results in an average distance of these atoms (O1, O2, C3, and C4) to the mean plane of the catechol ring of 3.71 Å.

The recognition motif of the previous structure is mirrored by that of the pseudorotaxane formed from **2g** and **3c** (Figure 2-23). Orthorhombic crystals of the space group *Pbca* were obtained from a solution of acetonitrile/isopropyl ether including four centrosymmetric pseudorotaxanes per unit cell.

The long axes of the crown ether and the thread are offset by 30.1°, slightly more in comparison to those of **2f:3c**. Nevertheless, the complexation geometry is very

similar, involving hydrogen bonding, ion-dipole interactions and π-stacking between the two components.

The oxygen atoms of the crown ether are again hydrogen bonded to the central methylene protons of the thread in an alternating pattern (Table 2-9). The alkyl oxygen atoms display shorter intramolecular contacts than their aryl counterparts and the

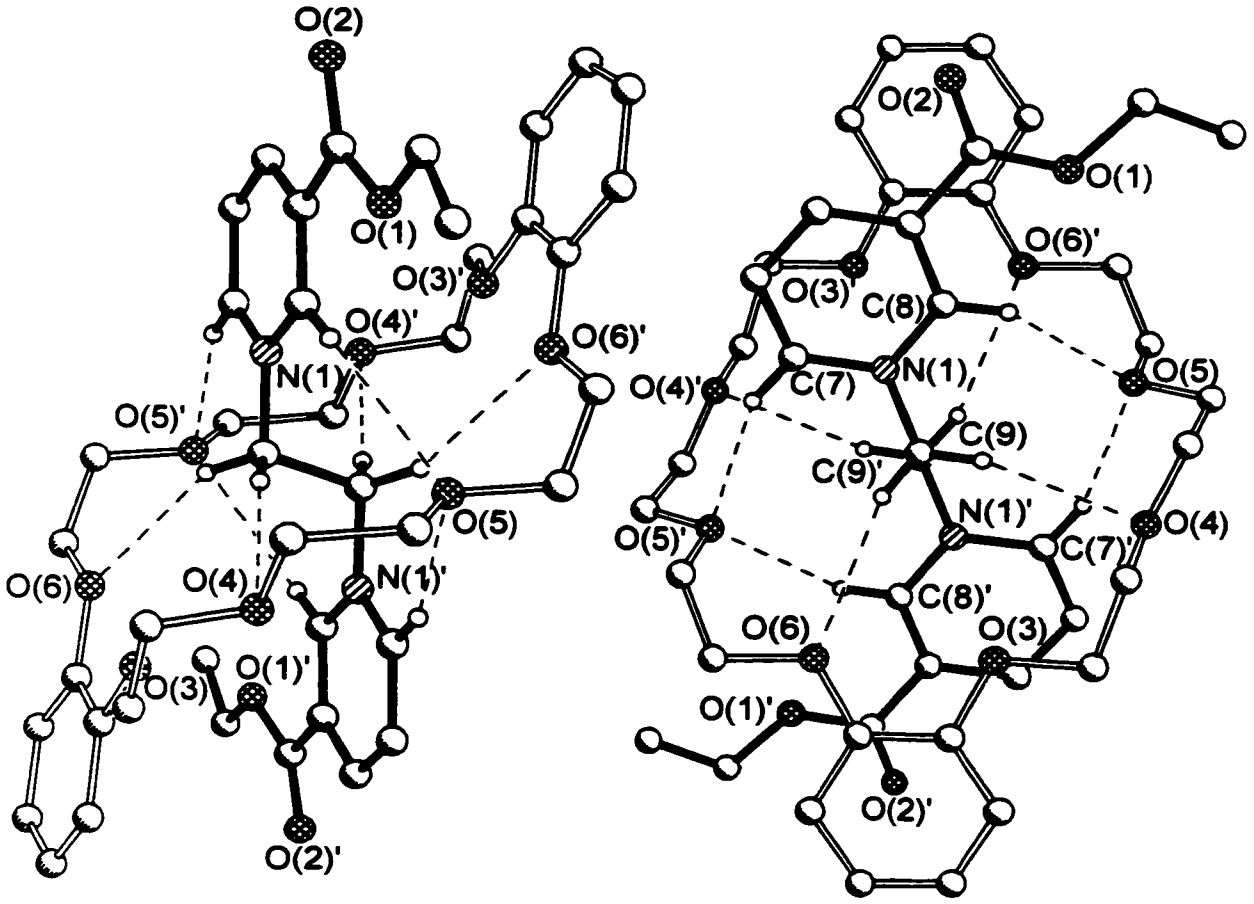

Figure 2-23. Two views of the crystal structure of the pseudorotaxane formed between **2g** and **3c**.

remaining alkyl oxygen atoms bifurcate the ortho-N^+ hydrogen atoms of the nicotinium rings. In this case however, there is a difference between the ortho-N^+ hydrogen atoms of each pyidinium ring owing to the unsymmetrical attachment of the ester group. Surprisingly, the shorter hydrogen bond involves the proton para to the ester function

rather than the more electropositive hydrogen atom situated between it and the quaternized nitrogen center.

Table 2-9. Hydrogen bonding parameters in the crystal structure of **2g:3c** pseudorotaxane.

Hydrogen Bonded Atoms	Distance (Å)	Angle (°)
O6···H9A	2.721	157.6
O4···H9B	2.546	161.3
O5'···H7A	2.350	157.4
O5···H8A	2.661	144.4

The ion-dipole interactions present in the previous structures remain, but this stabilizing force is now more obviously the domain of the non-hydrogen bonded ether oxygen atom O(3)'(Table 2-10).

Table 2-10. N^+···O contacts in the crystal structure of **2g:3c** pseudorotaxane.

Atoms	Distance (Å)
N1···O5	3.894
N1···O3'	3.365
N1···O4'	3.814
N1···O5'	3.794
N1···O6'	3.816

Again, the catecholate ring is π-stacked over the conjugated ester function at a mean interplanar angle of 10.6° to the pyridinium ring. The atoms of the thread involved in this interaction average 3.53 Å from the mean plane of the crown's aryl component.

These three structures indicate that in the case of the pseudorotaxane **2e:3c** the highly directional hydrogen bonding forces are compromised with the tendency of the crown ether to maximize the potential π-stacking interactions. In the ester substituted cases the π-stacking influence is either well accommodated by the alternating hydrogen bonding scheme or "loses out" as these contributions have become dominating in the overall geometry of the complex. It would appear that these structures contribute much to the solution state of the complexes as the NMR spectroscopic evidence is consistent with the intramolecular forces evident in the solid state.

2.4 SUMMARY AND CONCLUSIONS

The interactions between the six 24-crown-8 ethers **3a-f** and the eight bis(pyridinium)ethane threads **2a-h** were investigated. Of the complexes formed, the strength of the recognition event is dependent on both the identity of the substituent attached to the pyridinium rings and the degree of benz- or naphthannulation of the crown ether. More specifically, substitution of the pyridinium rings with electron withdrawing groups tends to increase the amount of pseudorotaxane formed. Regiochemical change in the position of the substituent also has an effect, as demonstrated by the complexes formed by **2g**. Monotonic increases in the association constants of the two components were observed as one and two aryl groups were added to the crown ether. The thermodynamic data extracted for some of the complexes confirmed that the formation of pseudorotaxanes, in the case of **2g** and **3a-f**, is a result of molecular recognition, rather than solvophobic forces, indicated by nearly exclusive enthalpic contributions to the free energy of association. In addition, three solid state pseudorotaxane structures were

characterized and the intramolecular forces contributing their formation determined. While none of the data presented directly confirms the existence of a pseudorotaxane geometry for the complexes in solution, there is a preponderance of evidence to warrant such a conclusion.

CHAPTER 3

3.1 HYPOTHESIS AND LITERATURE PRECEDENT

Once the investigation in the previous chapter had established that the complexes formed between **2a-h** and **3a-f** were of a pseudorotaxane geometry, the obvious extension of this system was the conversion of these interpenetrated species into the corresponding interlocked analogs. Of the eight threads examined in the previous chapter, the only one amenable to direct modification *without disruption of the integrity of the necessary pseudorotaxane intermediate* is the dipyridinium dication **2e**. Post-functionalization of any pseudorotaxane to form a rotaxane product must be achieved within the following restrictions:

a) Functionalization must proceed under reaction conditions which do not compromise the pseudorotaxane superstructure (e.g. room temperature or lower, appropriate solvents).

b) Reagents must be inert towards all of the functionality present in the pseudorotaxane except the site of derivatization (e.g. pyridinium compounds are very sensitive to basic reagents).

c) In the case of symmetric pseudorotaxanes, functionalization of one terminus of the thread cannot disrupt the intepenetrated geometry, as this will result in de-threading before the other extremity is capped.

d) The functionalization reaction must proceed at a reasonable rate.

In view of these restraints, two capping regimens were proposed in order to form a rotaxane from the pseudorotaxane **2e:3c** (Figure 3-1). Only one crown compound was investigated in this context, due to the similar nature of pseudorotaxane formation

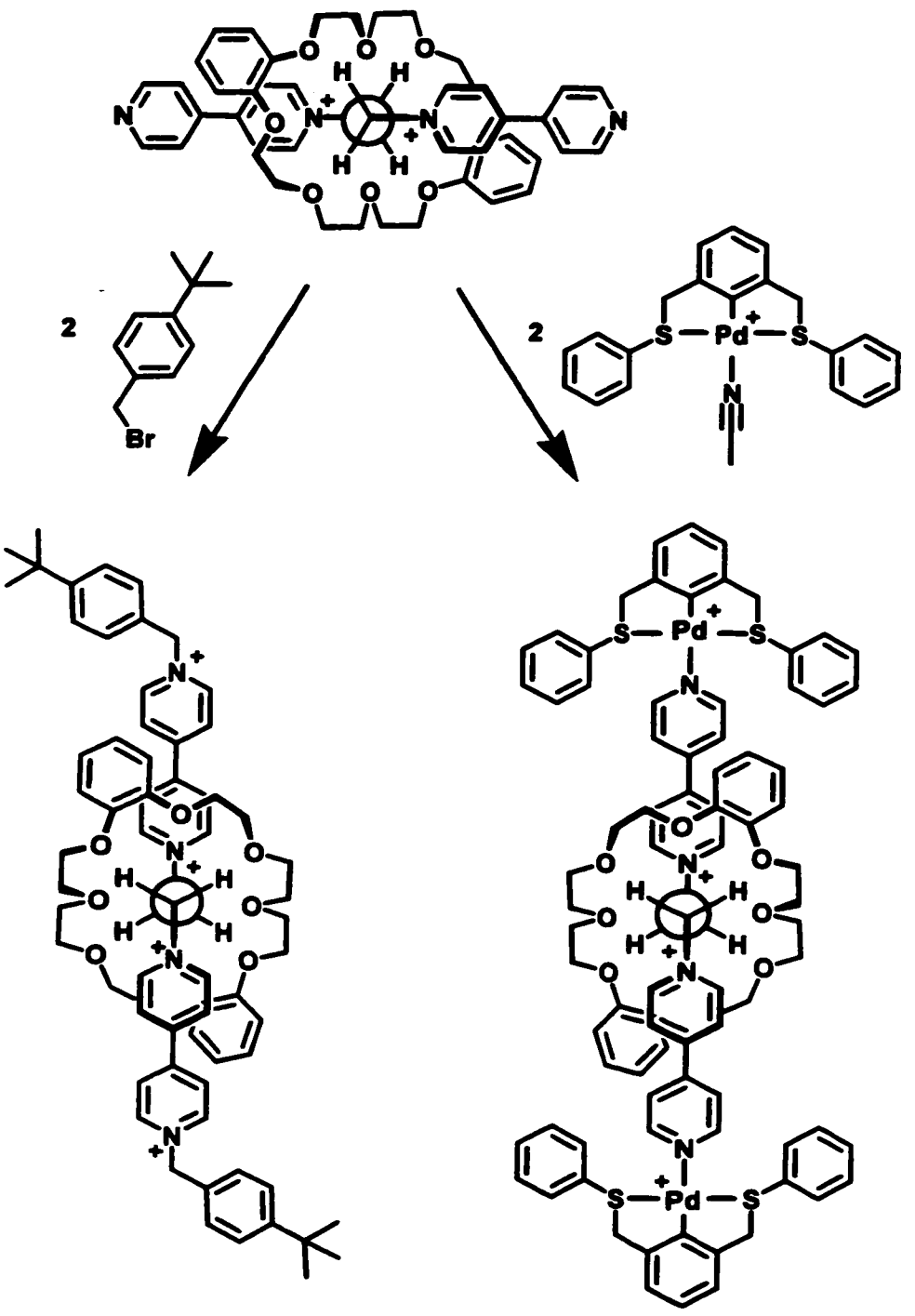

Figure 3-1. Two routes to the formation of a rotaxane from the pseudorotaxane **2e:3c**.

between this thread and all six crowns **3a-f** and the ready availability of **3c**. It can be reasonably expected that the results of rotaxane formation, in this particular case, are

general for the entire series of crowns. The capping reactions, by their very nature, are designed to have little or no effect on the underlying molecular recognition.

Benzylation of exogenous aryl nitrogen centers has been employed by Stoddart and co-workers to produce a variety of rotaxane and catenane species (Figure 3-2).[72,83]

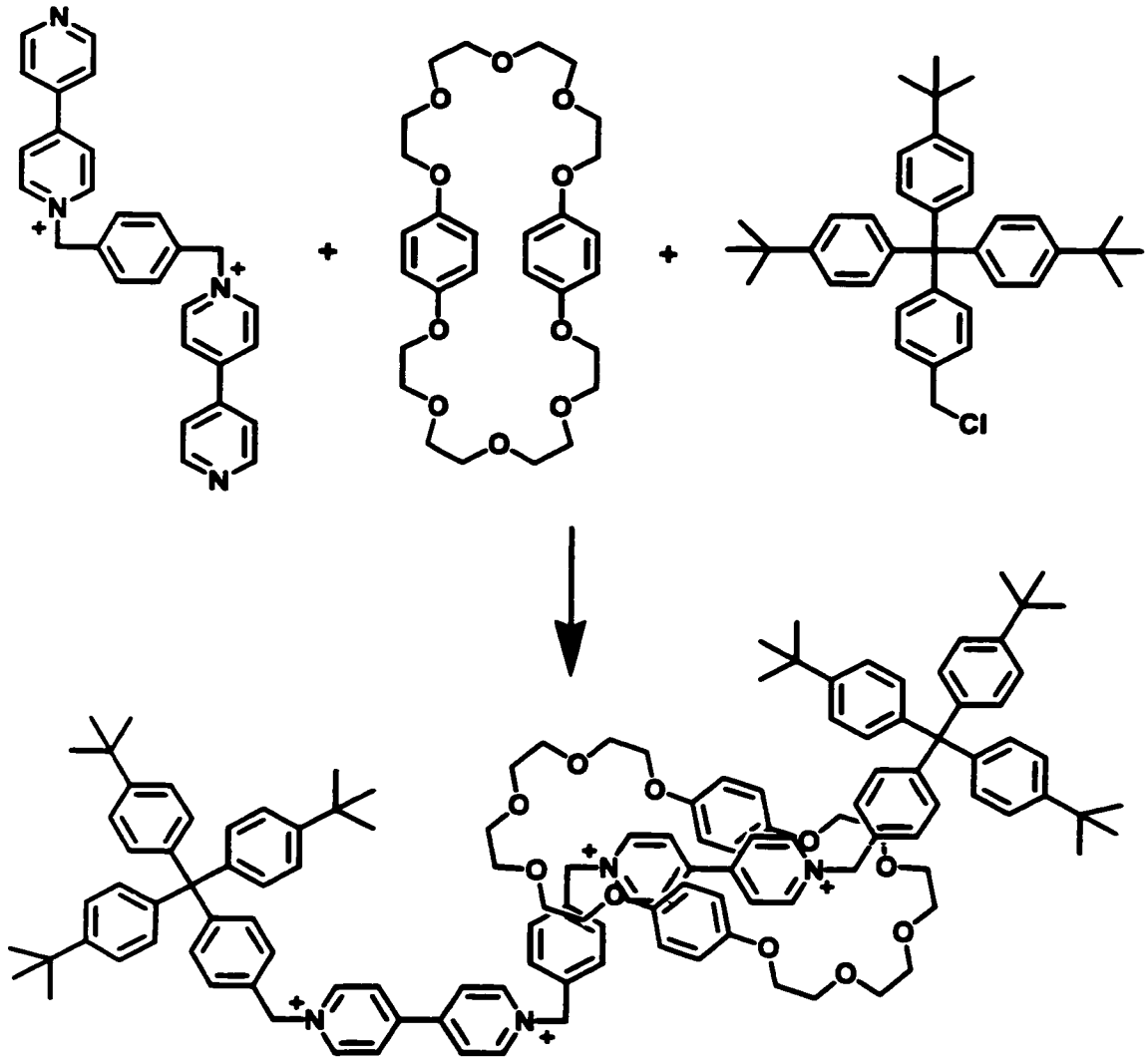

Figure 3-2. Example of a benzylation reaction employed by Stoddart to generate a rotaxane.

The high degree of similarity between the systems investigated by this group and that described here suggests that this capping reaction should be compatible with our own system. These investigators have extensively utilized very large alkyl substituted 4-

(triphenylmethyl)benzyl chlorides for this derivatization, owing to the large cavities of the crown ethers used to generate the pseudorotaxanes in their systems. In our system, we already have evidence, from the pseudorotaxane studies, that the steric bulk of 4-*t*-butylbenzyl group should be sufficient to prevent the unthreading of the crown ether **3c**. The inability of any of the crown ethers studied in the previous chapter to form a pseudorotaxane with **2c** indicates that the *t*-butylphenyl function is insurmountable to threading (or conversely de-threading) of a 24-membered ring. In addition, the nitrogen center of **2e** that will be derivatized is far enough from the site of recognition that reaction at this point will leave the pseudorotaxane motif unperturbed.

The use of coordination compounds as stoppers for preformed pseudorotaxanes has received little attention in the literature, aside from work involving cyclodextrin complexes.[21-26] The aqueous threading of α,ω-diamino alkanes through the cavity of β-cyclodextrin was used by Ogino to produce intermediate pseudorotaxanes, which were

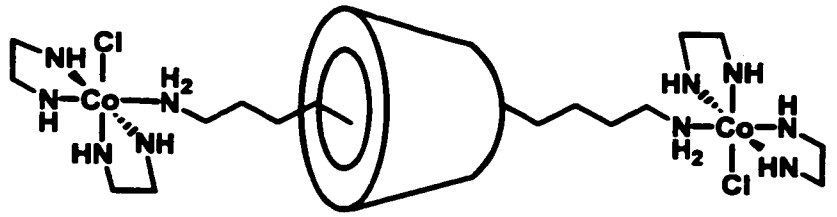

Figure 3-3. Ogino's cobalt(III) capped rotaxane.

then stoppered with cobalt(III) complexes (Figure 3-3). Macartney has employed a similar method for the construction of $[Fe(CN)_5]^{3-}$ capped rotaxanes involving α-cyclodextrin (Figure 3-4). In this case, addition of the cyclodextrin wheel to a solution of the thread with the metal stoppers already attached to the ends still results in the formation of the rotaxane species, indicating the lability of the bond between the thread and the metal.

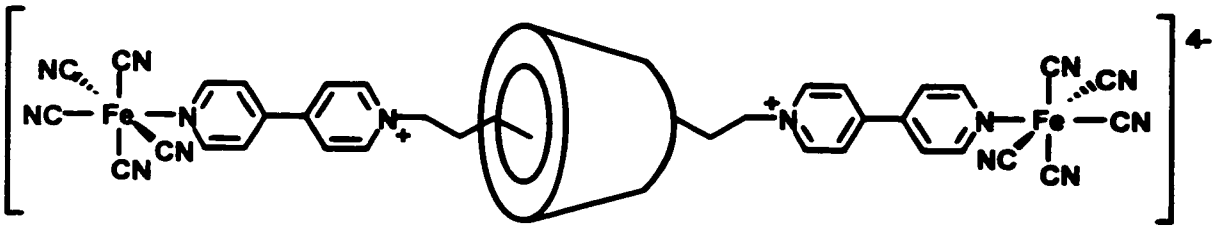

Figure 3-4. Macartney's $[Fe(II)(CN)_5]^{3-}$ capped rotaxane.

$Ru(terpy)^{2+}$ stoppers have been used by Sauvage to cap a $Cu(phen)_2^{+}$ templated pseudorotaxane (Figure 3-5).[62] The inert nature of the $Ru(terpy)_2^{2+}$ centers enabled the removal of the Cu template without loss of the rotaxane superstructure.

More recently, Kim and coworkers have threaded dialkyl secondary ammonium

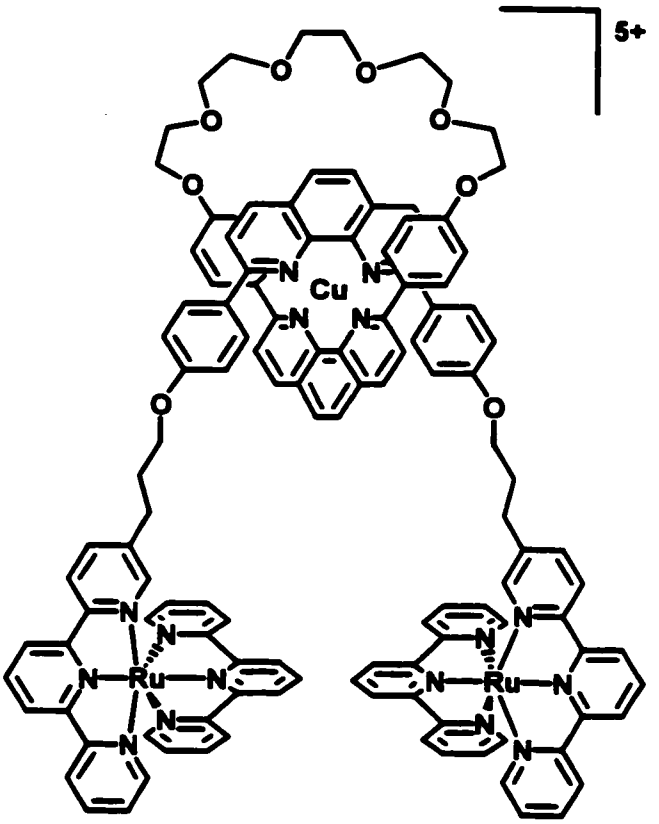

Figure 3-5. Sauvage's $Ru(terpy)_2^{2+}$ capped rotaxane.

salts through the cavity of curcurbituril via hydrophobic and hydrogen bonding interactions.[30-34] By appending the ends of the alkylammonium chains with pyridyl

groups they were able cap the threads with transition metal ions to produce polyrotaxanes and a cyclic "molecular necklace" (Figure 3-6).

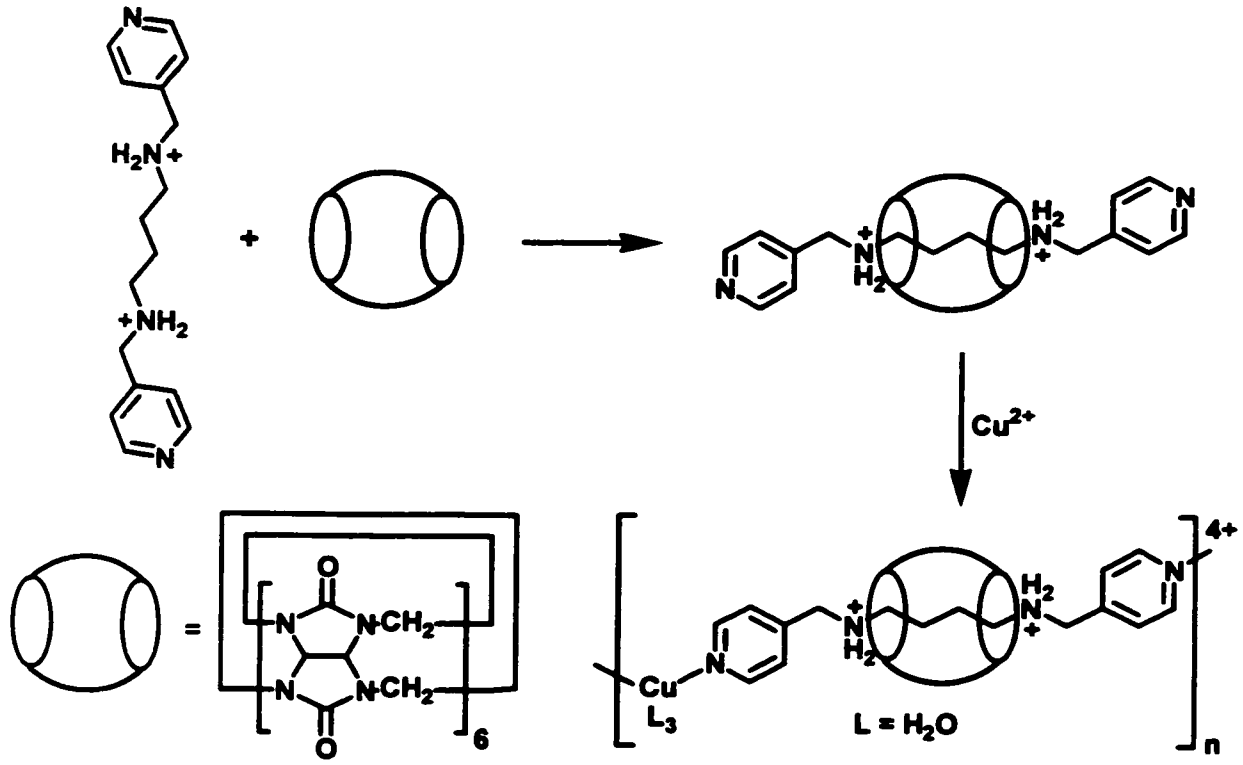

Figure 3-6. Kim's Cu^{2+} stoppered polyrotaxane.

Unfortunately, all of these examples, except for that of Sauvage, are aqueous preparations. We decided to use the cyclopalladated α,α'-di(phenylthio)xylene fragment pictured in Figure **3-1** to stopper **2e**, as our group has used this type of complex extensively in other published work.[104,105] This complex is durable and relatively inert to redox reactions and ligand substitution at the SCS bracket, leaving only one site trans to the carbon donor for ligation of the divergent nitrogen centers of **2e**. Examination of molecular models indicated that the complex is easily large enough to prevent de-threading of the crown ether from the rotaxane.

3.2 EXPERIMENTAL

General Comments. 4-*t*-Butylbenzylbromide was purchased from Aldrich Chemicals and used as received. Compound **8** was prepared as per the literature method.[105]

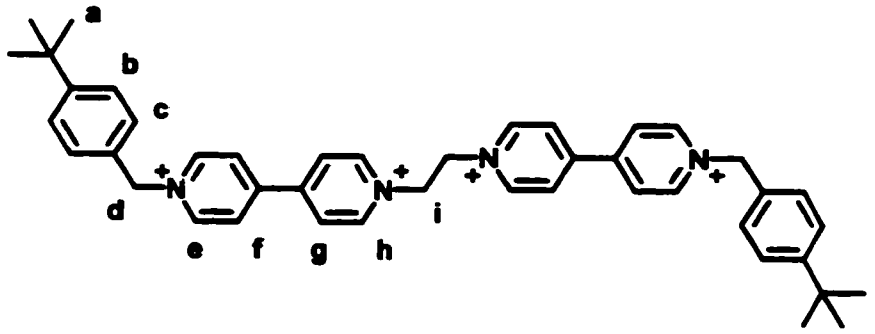

i) **Preparation of [6][BF_4]$_4$: 2e** (100 mg, 0.194 mmol) and 4-*t*-butylbenzylbromide (177 mg, 0.778 mmol) were dissolved in 20 mL acetonitrile and stirred for 48 hours. The reaction mixture was filtered to remove insolubles and the solvent evaporated to approximately 5 mL. 50 mL diethyl ether was added and the resulting white precipitate collected by vacuum filtration and washed with additional ether (2 x 5 mL) to yield 39 mg (20.4%) of pure product. **^{1}H NMR (CD_3CN)**: δ (ppm) 9.00 (d, 4H, J = 6.95 Hz, *e*), 8.98 (d, 4H, J = 6.95 Hz, *h*), 8.47 (d, 4H, *g*), 8.42 (d, 4H, *f*), 7.55 (d, 4H, J = 8.43 Hz, *b*), 7.45 (d, 4H, *c*), 5.80 (s, 4H, *d*), 5.27 (s, 4H, *i*), 1.33 (s, 18H, *a*). **LSI-MS**: 896 ([M-BF_4]$^+$).

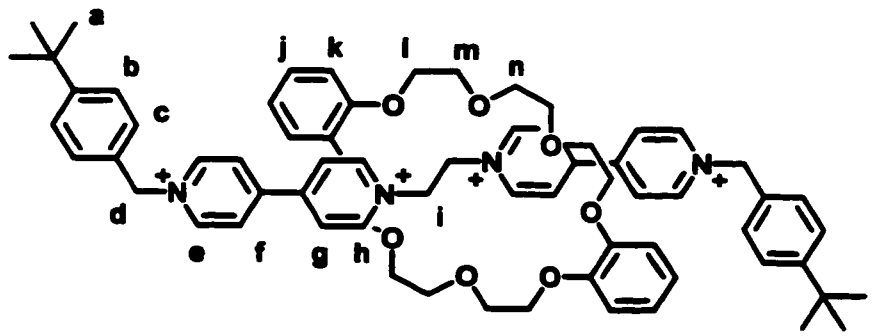

ii) **Preparation of [7][BF_4]$_4$ (Method A)**: **2e** (50 mg, 0.0972 mmol) and **3c** (131 mg, 0.292 mmol) were dissolved in acetonitrile (25 mL) with stirring. After 10 min. 4-*t*-butylbenzylbromide (133 mg, 0.584 mmol) was added and the solution stirred for another 48 hours. The resulting orange mixture was filtered to remove insolubles and the filtrate evaporated to yield an orange oil. The oil was dissolved in 10 mL CH_2Cl_2 and 50 mL diethyl ether added to precipitate 46 mg (32.7%) of the pure product. X-ray quality crystals were grown from slow cooling of a hot aqueous solution. **(Method B)**: 4-*t*-Butylbenzylbromide (133 mg, 0.584 mmol) was added to a mixture of **2e** (50 mg, 0.0972 mmol) and **3c** (131 mg, 0.292 mmol) dissolved in nitromethane. Saturated aqueous $NaBF_4$ (25 mL) was layered on top of the solution and the two-phase mixture stirred for 48 hours. The aqueous layer was then separated from the mixture and the nitromethane evaporated to leave an orange oil. The crude rotaxane was dissolved in CH_2Cl_2 (25 mL), dried with $MgSO_4$ and filtered to yield a red/orange solution. Addition of diethyl ether (50 mL) to this solution precipitated the rotaxane as 65 mg (46.2%) of a pure orange solid. **^{1}H NMR (CD_3CN)**: δ (ppm) 9.32 (d, 4H, J = 6.76 Hz, *h*), 8.97 (d, 4H, J = 6.68 Hz, *e*), 8.20 (d, 4H, *g*), 8.15 (d, 4H, *f*), 7.59 (d, 4H, J = 8.31 Hz, *b*), 7.49 (d, 4H, *c*), 6.65 (m, 4H, *k*), 6.40 (m, 4H, *j*), 5.81 (s, 4H, *d*), 5.60 (s, 4H, *i*), 4.03 (m, 24H, *l,m,n*), 1.33 (s, 18H, *a*). **ES-MS**: 1344 ([M-BF_4]$^+$).

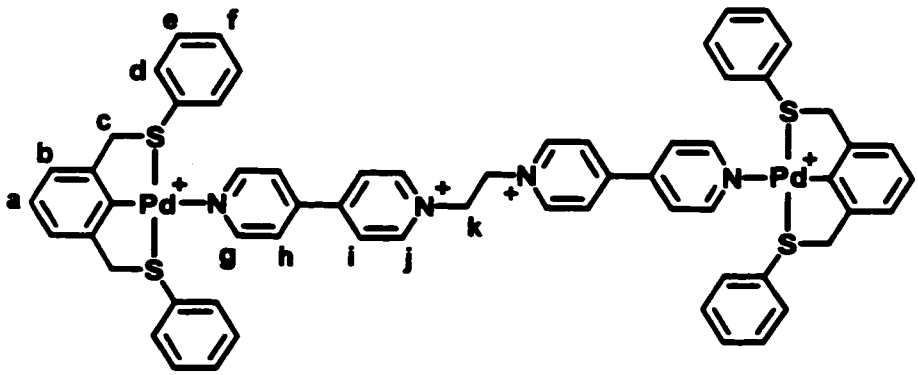

iii) Preparation of [10][BF_4]$_4$: **2e** (42.8 mg, 0.0832 mmol) and **8** (100 mg, 0.166 mmol) were dissolved in acetonitrile (20 mL) and stirred for 15 min. Diethyl ether was added (50 mL) and 117 mg (81.9%) of a pale yellow solid was isolated as pure complex. **^{1}H NMR (CD_3CN):** δ (ppm) 8.84 (b, 4H, *g*), 8.76 (d, 4H, J = 6.90 Hz, *j*), 8.38 (d, 4H, i), 7.82 (m, 12H, *d,h*), 7.50 (m, 12H, *e,f*), 7.09 (m, 6H, *a,b*), 5.16 (s, 4H, *k*), 4.74 (b, 8H, *c*). **LSI-MS:** 1455 ([M-BF_4]$^+$).

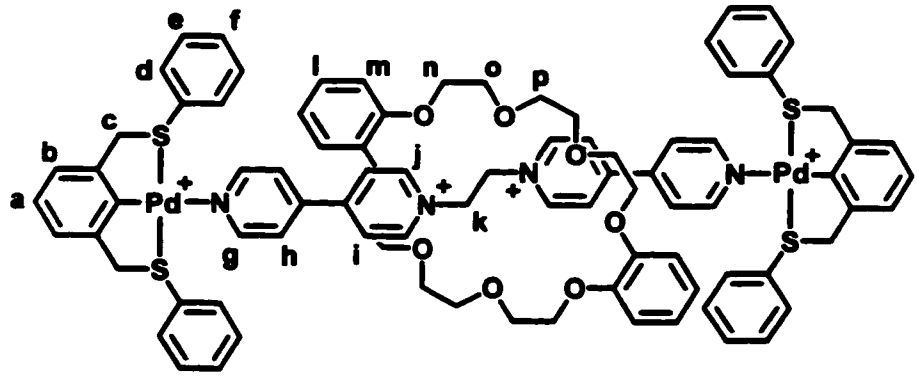

iv) Preparation of [9][BF_4]$_4$: **2e** (50 mg, 0.0972 mmol), **8** (117 mg, 0.194 mmol), and **3c** (131 mg, 0.292 mmol) were dissolved in acetonitrile (25 mL) and stirred for 10 min. Evaporation of a 2 mL aliquot of the solution and dissolution of the residue in acetonitrile-d_3 produced a ^{1}H NMR spectrum indicating quantitative formation of the [2]rotaxane in solution. X-ray quality crystals were grown by vapour diffusion of diisopropyl ether into the remaining solution. **^{1}H NMR (CD_3CN):** δ (ppm) 9.18 (b, 4H, *j*), 8.60 (b, 4H, *g*), 8.00 (b, 4H, *i*), 7.81 (m, 8H, *d*), 7.50 (m, 16H, *e,f,h*), 7.11 (m, 6H, *a,b*), 6.60 (b, 4H, *m*), 6.33 (b, 4H, *l*), 5.54 (s, 4H, *k*), 4.80 (b, 8H, *c*), 4.00 (m, 24H, *n,o,p*). **LSI-MS:** 1390 ([M-**6**-BF_4]$^+$).

3.3 RESULTS AND DISCUSSION

SYNTHESIS

As demonstrated in the preceding chapter, formation of a pseudorotaxane is determined by the equilibrium between the free components and the interpenetrated product. However, the covalent attachment of bulky end groups to form a rotaxane is a process under kinetic control, provided the bond forming reaction is irreversible. Thus, the benzylation reaction outlined in section 3.1 could be viewed as a kinetic "sink" removing components from the pseudorotaxane equilibrium (Figure 3-7). Ideally, the presence of excess crown ether in the reaction mixture would result in the equilibrium lying far to the right, and as such, produce the rotaxane as the major product. This expectation has one major difficulty in practice. The stoppering reaction produces bromide counterions as a result of displacement of the benzylic bromides by the reactive nitrogen centers. This has the effect of precipitating one equivalent of **2e** as the bromide salt, which is quite insoluble, for every **6** and/or **7** produced. The consequence of this is the effective reduction in the maximum possible yield of rotaxane to 50%. Nevertheless, the yield of rotaxane from this reaction is still 33%, or 66% considered from the amount of material that actually reacts. Attempts to modify the reaction conditions to rectify this situation met with only minor increases in yield. The acetonitrile solvent system was exchanged for nitromethane, which is immiscible with water. This modification allowed the addition of a saturated aqueous $NaBF_4$ layer to form a two-phase mixture, in anticipation that the bromide counterions produced might be exchanged in situ and allow all of the **2e** present to participate in rotaxane formation. Reaction under these conditions improved the yield by roughly half to 46%.

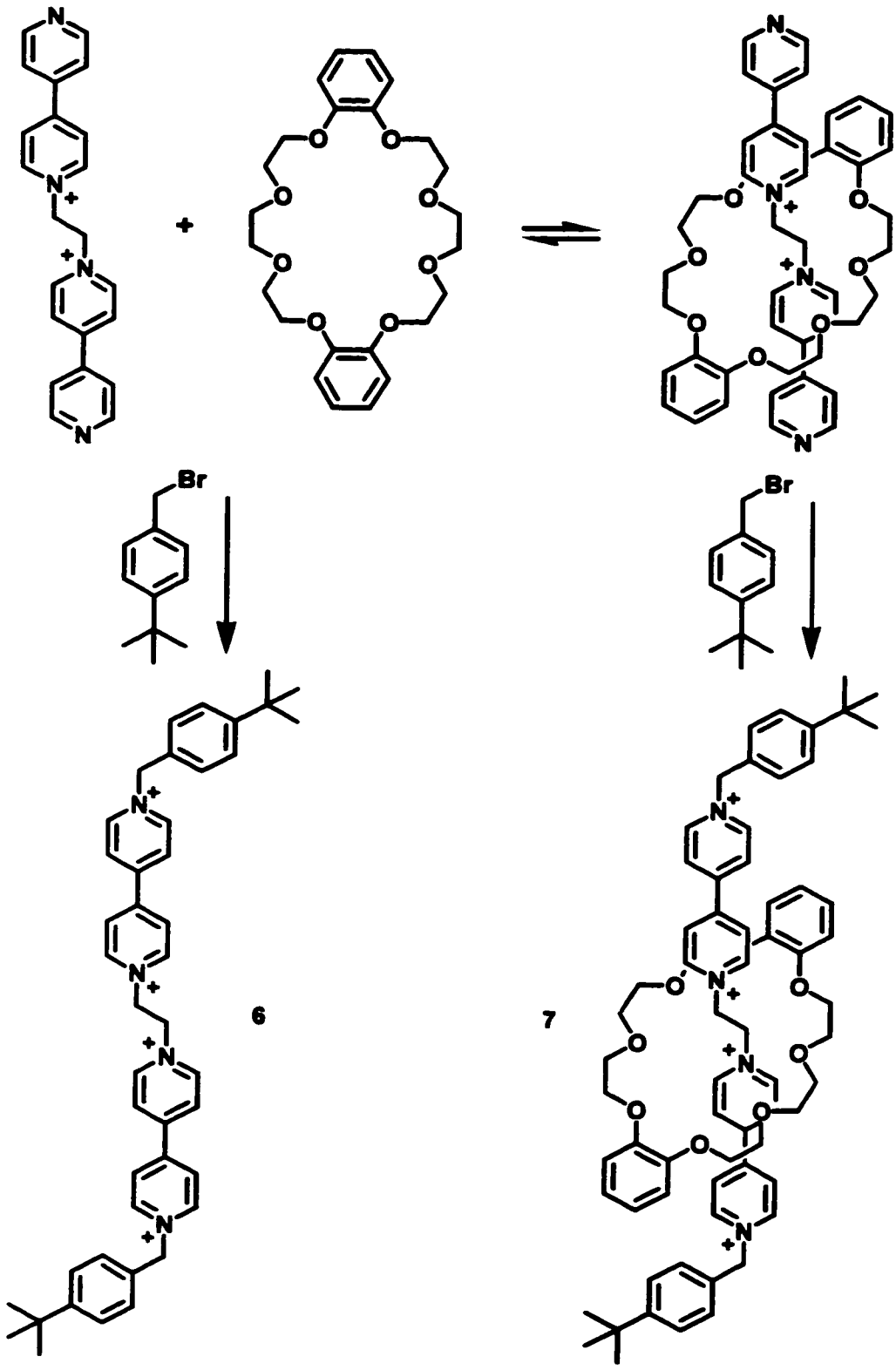

Figure 3-7. The reaction of 4-*t*-butylbenzylbromide with the pseudorotaxane and its components.

The synthetic scheme pictured in Figure 3-7 is actually a simplified view, neglecting the presence of an intermediate in the reaction where only one of the ends of the thread has been stoppered (Figure 3-8). In fact, this should have a negligible effect on

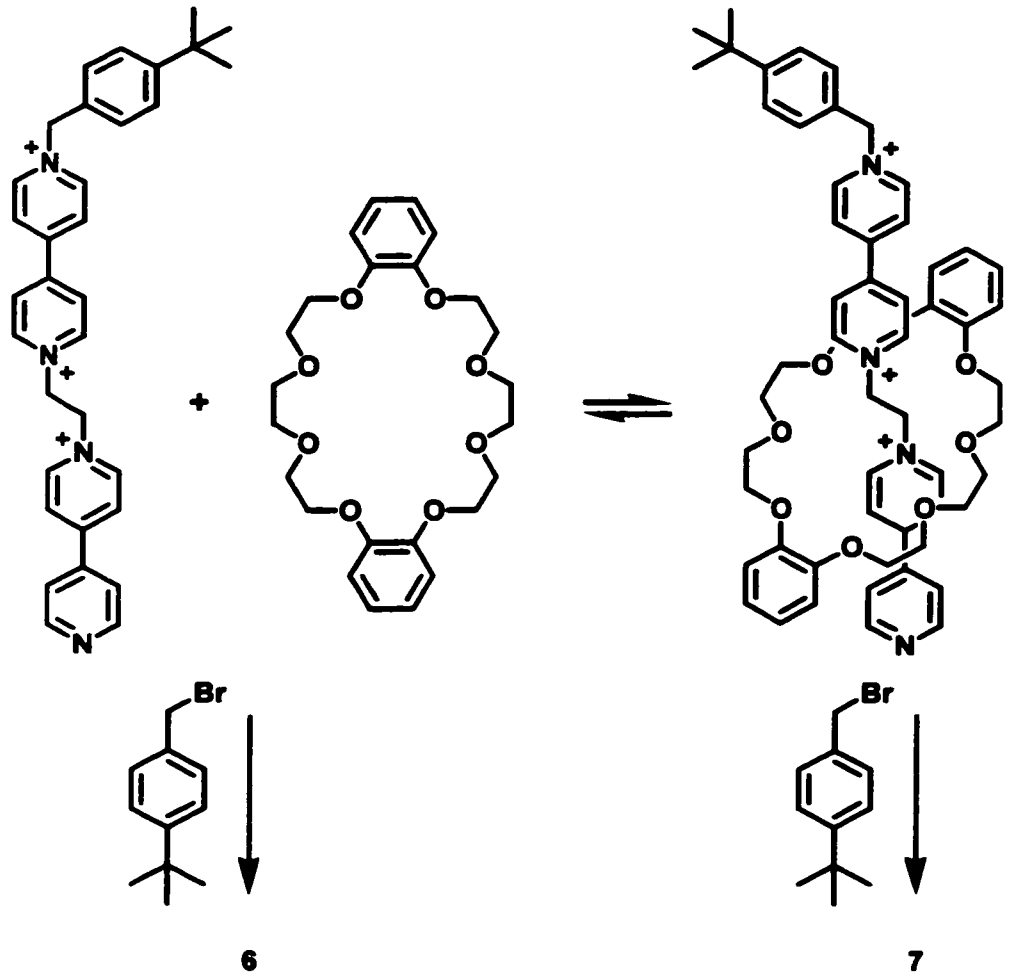

Figure 3-8. Benzylation of the singly stoppered intermediate during the reaction to form a rotaxane.

the outcome of the synthesis, as the consequence of benzylating one end of the thread should have positive repercussions in the association between the crown and thread. Quaternization of one end of **2e** should merely increase the polarization of the central dication and hence the strength of the complexation with **3c**. More likely, the pseudorotaxane pictured in Figure 3-8, for whatever reason, presents a less reactive target

than the free thread for the second benzyl stopper. Though less than expected on an intuitive level, the yield of rotaxane in our case is not unusual when compared with similar systems.[72]

Construction of the organopalladium stoppered rotaxane is a simple process in comparison to **7**. Dissolution of all the components, with the crown ether in excess, in acetonitrile produced the rotaxane **9** in quantitative yield when viewed by ^{1}H NMR spectroscopy of the resulting solution (Figure 3-9). Unfortunately, the lability of the

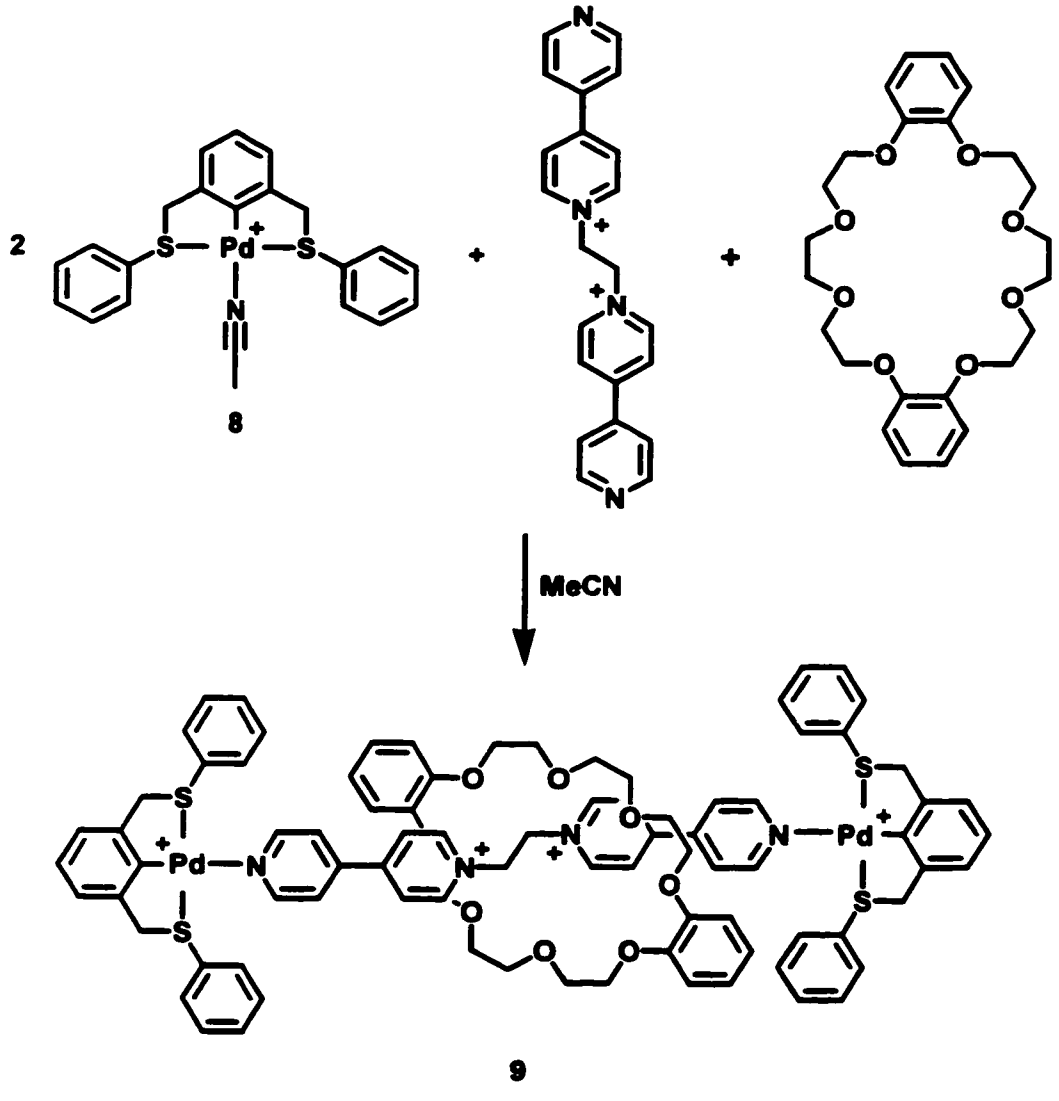

Figure 3-9. Formation of the palladium stoppered rotaxane.

bond formed between the pyridyl nitrogen atoms of the thread and the organopalladium stopper **8** in acetonitrile is readily apparent. Solubilization of a crystalline sample of the rotaxane in acetonitrile resulted in a mixture of rotaxane, stoppered thread **10**, and free crown. Addition of excess crown to this solution immediately produced the rotaxane quantitatively. This behaviour was identical in nitromethane and indicates that ligand dissociation in these solvents occurs readily on, at least, the time scale of the threading process. This is further observed in comparison of the appearance of the ^{1}H NMR spectra of the pseudorotaxane precursor and the organopalladium stoppered rotaxane. Both exhibit similarly broad slow-exchange peaks for the thread and crown. If the stoppers were impeding the unthreading of the crown in solution, these resonances would be expected to sharpen. Attempts to solubilize the rotaxane in less competitive solvents, such as chloroform or methylene chloride, to reduce or eliminate ligand dissociation were unsuccessful due to the complete insolubility of **2e** in these media.

^{1}H NMR SPECTROSCOPY

Examination of the ^{1}H NMR spectrum of rotaxane **7** in comparison to the stoppered thread **6** reveals similar shift patterns to those seen upon pseudorotaxane formation between **2e** and **3c** (Figure 3-10). Those trends are exaggerated in this case due to the fixation of the crown ether about the thread. Downfield shifts are observed for the C-H$\cdots$O hydrogen-bonded protons of the thread *h* and *i* with $\Delta\delta$ of 0.34 and 0.33 ppm respectively. Upfield shifts indicative of π-stacking occur in both the thread and the crown ether. Protons *f* and *g* of the thread move -0.28 and -0.27 ppm while the aryl crown ether protons shift -0.26 (ortho) and -0.50 (meta) ppm. The remaining alkyl

protons of the crown ether shift in an identical manner as those of the related pseudorotaxane. The benzylic protons *a, b, c,* and *d* show little or no change in chemical

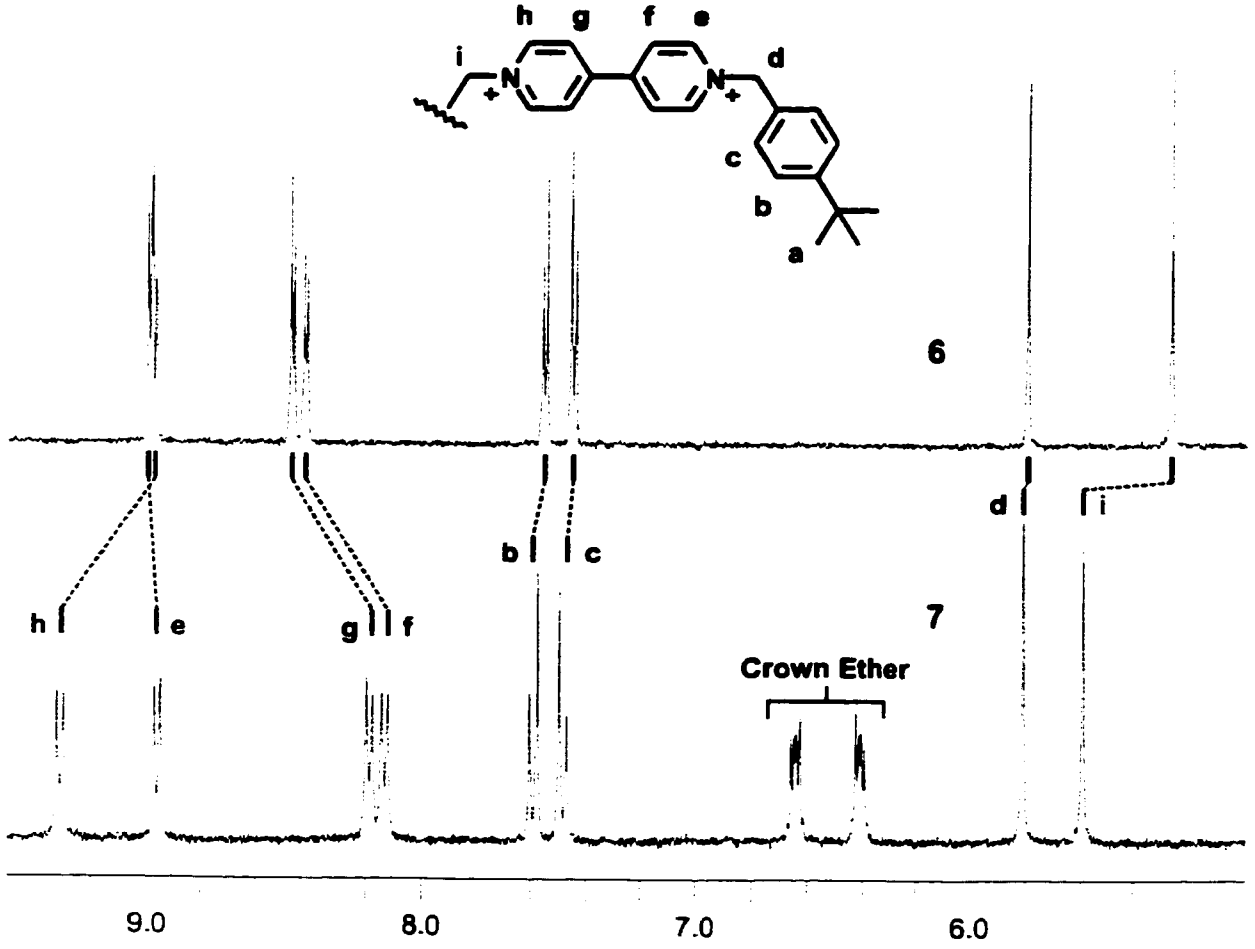

Figure 3-10. Partial ^{1}H NMR spectra of **6** and **7** in MeCN-d_3.

shift due to the presence of the encircled crown. This would indicate that the crown ether component of the rotaxane spends all or the majority of time located at the recognition site in the center of the thread. This is to be expected since **3c** and dibenzyl paraquat show negligible affinity for one another. The lack of exchange broadening that would be associated with any significant occupancy of the benzyl site (see shuttles in Chapter 4) reinforces this conclusion.

As mentioned in the synthetic section, the organopalladium stoppered rotaxane suffers in solution from an overt lability of the bond connecting the stopper and the ends of the thread. Whereas the benzyl stoppers impede any movement of the crown off the

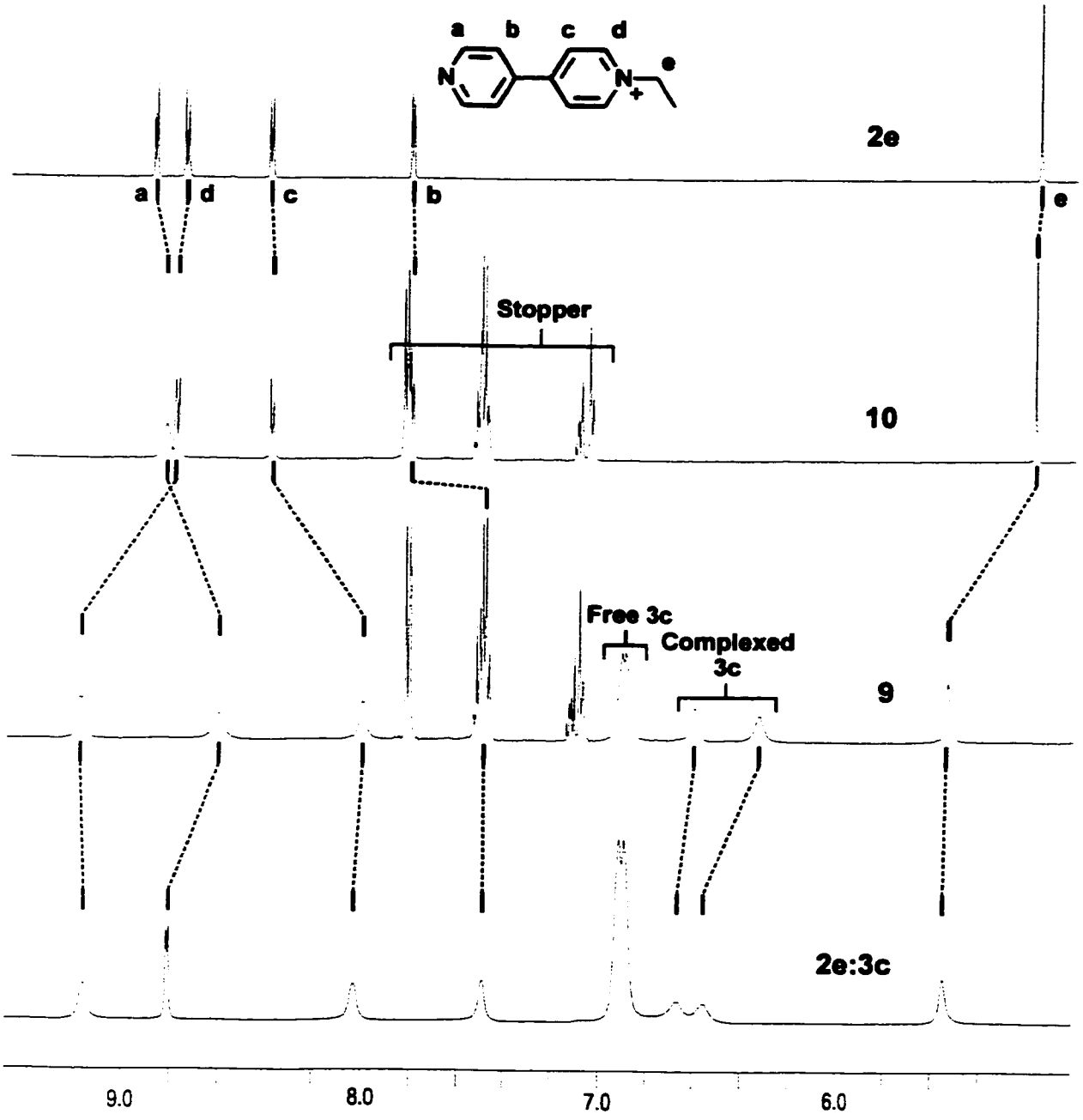

Figure 3-11. Partial ^{1}H NMR spectra of **2e**, **9**, **10**, and **2e:3c**.

thread, the rate of the threading/unthreading process for **9** and **10** is most likely very similar that of the pseudorotaxane. Thus, we could expect similar shifts and spectral appearance to the thread as well. Indeed, this is what is observed (Figure 3-11). Addition of the organopalladium stoppers to **2e** produces a slight coordination induced shift (-0.04 ppm) and broadening in the protons ortho to the ligating nitrogen atom but has little other effect on the spectrum of the thread. Stoppering the pseudorotaxane **2e:3c** generates a somewhat larger shift upfield for these protons ($\Delta\delta$ = -0.22 ppm). The aryl crown ether protons shift upfield further in **9** ($\Delta\delta$ = -0.30 and –0.57 ppm) than in **2e:3c** and even **7**. This could indicate that the benzo groups of the crown ether spend a portion of the time interacting with the organopalladium stoppers.

X-RAY CRYSTALLOGRAPHY

Rotaxane **7** was crystallized from water in the triclinic space group *P-1*. The unit cell contains two non-centrosymmetric rotaxane molecules related by a center of inversion. The most obvious difference between this structure and that of the pseudorotaxane **2e:3c** is the angle described between the long axes of the crown and thread through the central carbon-carbon bond of the thread at 13.5°. In the pseudorotaxane these lines are almost coincident (Figure 3-12). The rotaxane exhibits a definite rotation of the crown away from this orientation more similar to that seen in the pseudorotaxanes **2f:3c** and **2g:3c**. Alternating oxygen atoms of the crown ether are involved in hydrogen bonding with the central methylene protons of the thread. The remaining alkyl oxygen atoms engage in hydrogen bonding with the ortho-N^+ hydrogen atoms of the inner pyridinium rings (Table 3-1). Several of the oxygen atoms are also

employed in $N^{+}\cdots O$ interactions (Table 3-2). Though offset more than the rings of the pseudorotaxane **2e:3c**, the catechol and inner pyridinium rings of the thread are also π-

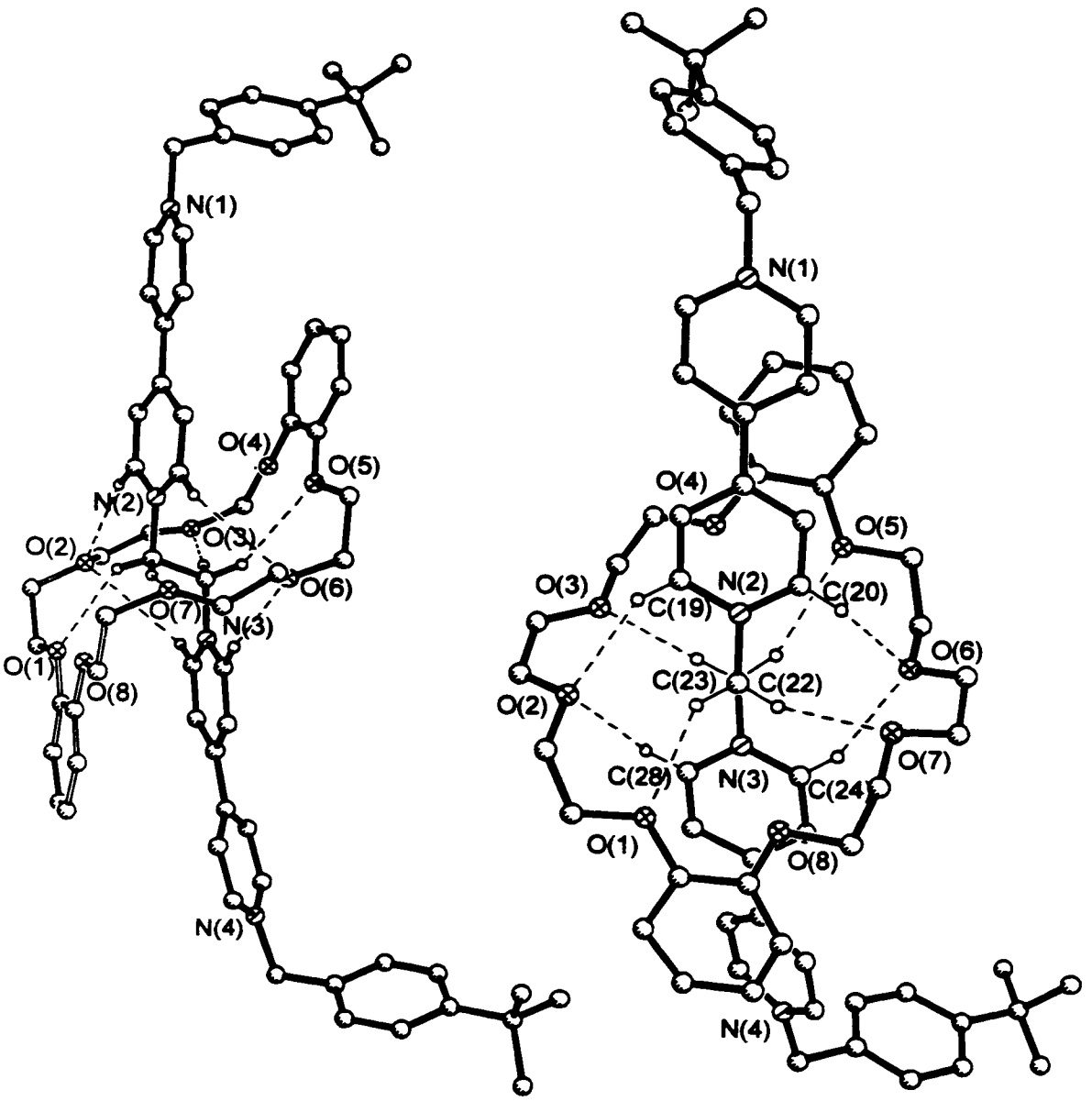

Figure 3-12. Two views of the crystal structure of rotaxane **7**.

stacked in this structure at a distance of approximately 3.5 Å with interplanar angles of 7.1° (N(2) ring) and 6.8° (N(3) ring). One of the adjacent pyridyl rings of the rotaxane is not coplanar and lies at a dihedral angle of 35.9° (N(3)-N(4)). The inner pyridinium rings

are also not coplanar to each other and have an interplanar angle of 10.9°. The nitrogen atoms of the central recognition motif are positioned anti with respect to the central ethylene carbon-carbon bond at a dihedral angle of 175.7°.

Table 3-1. Hydrogen bonding parameters in the crystal structure of rotaxane **7**.

Hydrogen Bonded Atoms	Distance (Å)	C-H···O Angle (°)
O2···H19A	2.449	151.9
O6···H20A	2.890	133.9
O6···H24A	2.315	148.8
O2···H28A	3.014	128.8
O1···H22A	2.489	140.7
O7···H22A	2.344	161.6
O3···H23B	2.282	171.7
O5···H23B	2.668	151.3

Examination of the entire unit cell of the crystal uncovers a further product of the recognition motif in the rotaxane. Each unit cell contains a intermolecularly π-stacked dimer of **7** (Figure 3-13). The two molecules lie face to face in such a manner as to form a four-layer sandwich structure of alternating π-donor/π-acceptor rings. The *t*-butylbenzyl stoppers are positioned away from the abutting faces of the two molecules to allow this phenomenon to take place. This additional ordering in the solid state is not surprising in view of the complementary S-shape of the rotaxane. Furthermore, this type

Table 3-2. $N^{+}\cdots O$ contacts in the crystal structure of rotaxane **7**.

Atoms	Distance (Å)
N2···O4	3.412
N2···O5	3.584
N3···O1	3.428
N3···O8	3.653

of motif has been observed in many other π-donor/π-acceptor systems of this sort.[106] In fact, it is surprising that this type of behaviour is *not* witnessed in the pseudorotaxane structures of the previous chapter. The fact that this structure was obtained via crystallization from aqueous solution rather than acetonitrile could attest to the

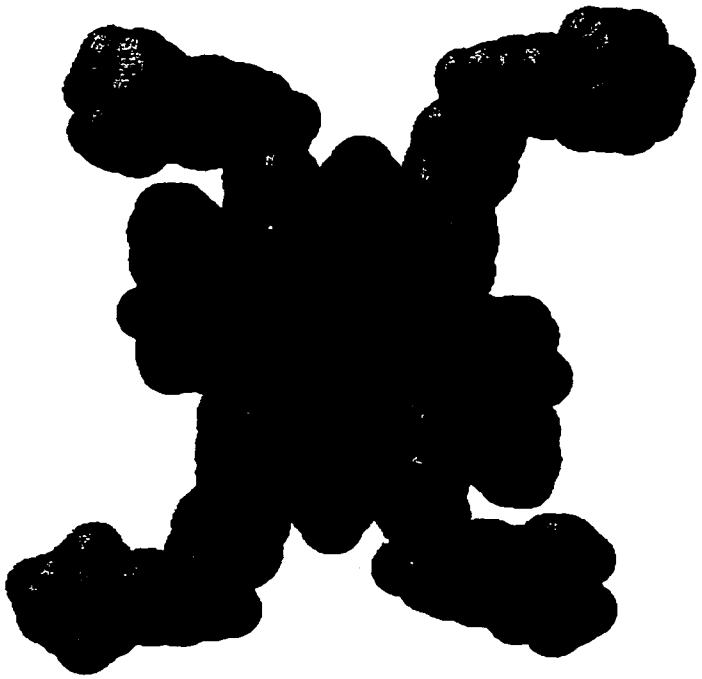

Figure 3-13. Space filling model of the packing of two adjacent rotaxanes **7** in the unit cell.

hydrophobic character generally associated with π-stacking interactions.

Rotaxane **9** was crystallized via slow diffusion of isopropyl ether into an acetonitrile solution of the compound. Two rotaxane molecules occupied the unit cell in

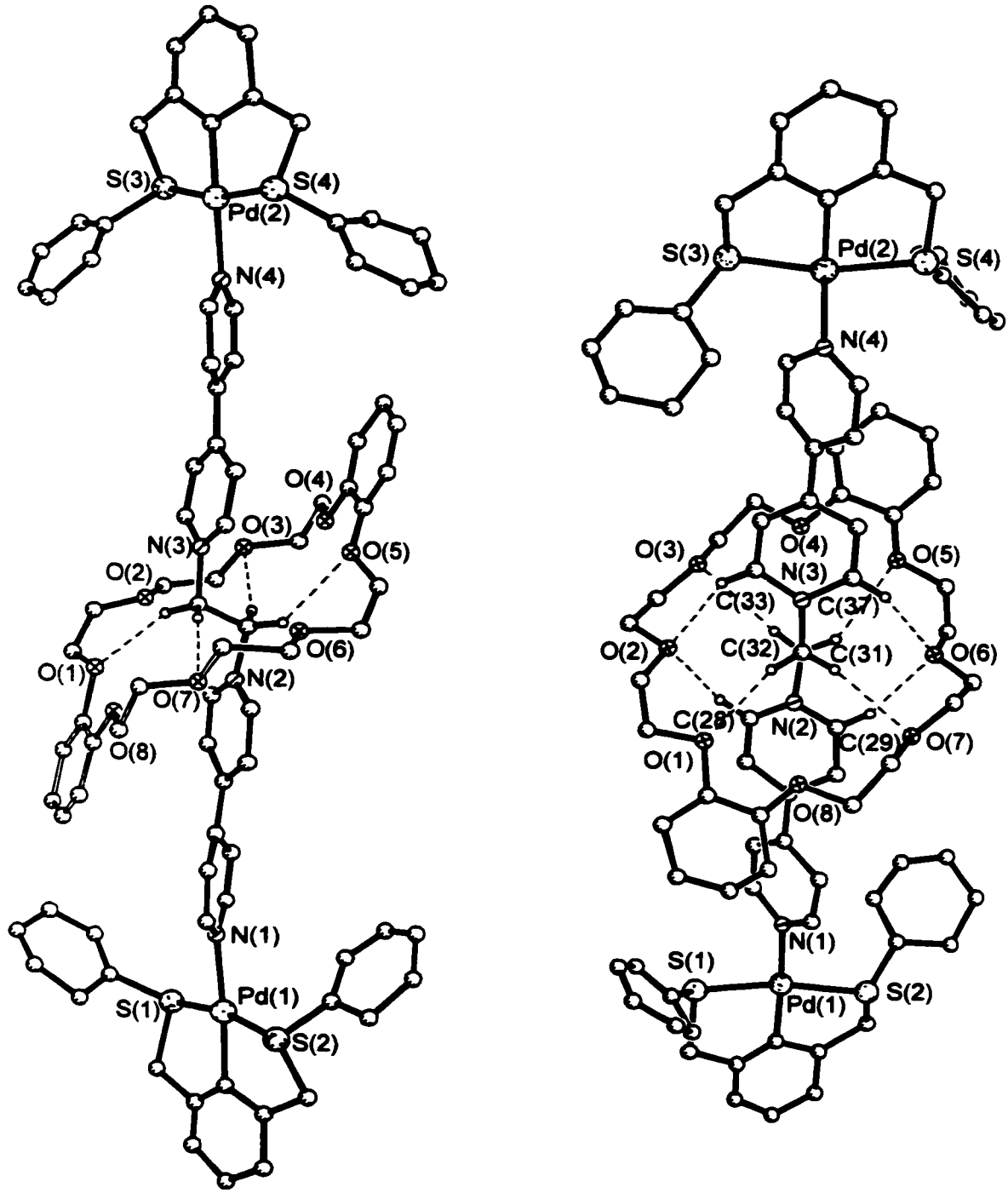

Figure 3-14. Two views of the crystal structure of rotaxane **9**.

the space group *Pc* requiring the solution of the entire rotaxane molecule. The structure exhibits many of the same interactions in the solid state observed in the parent pseudorotaxane and the rotaxane **7** discussed above (Figure 3-14). As witnessed in the structure of **7**, the long axes of the crown and thread are canted to one another when viewed along the central ethylene carbon-carbon bond at an angle of 18.3°. This orientation provides for hydrogen bonding between the alternating oxygen atoms of the crown ether and the central ethylene unit in an array such as that found in **7** (Table 3-3).

Table 3-3. Hydrogen bonding parameters in the crystal structure of rotaxane **9**.

Hydrogen Bonded Atoms	Distance (Å)	C-H···O Angle (°)
O1···H32B	2.521	158.9
O2···H28A	2.504	145.2
O2···H33A	2.343	149.5
O3···H31A	2.677	162.9
O5···H31B	2.627	141.5
O6···H29A	2.386	159.9
O6···H37A	2.665	139.1
O7···H32A	2.567	162.7

The remaining alkyl oxygen atoms are, again, hydrogen bonded to the ortho-N^+ hydrogen atoms of the inner pyridinium rings. The structure is further stabilized by several short N^+···O contacts similar to those observed in the other structures (Table 3-4). The central pyridinium nitrogen atoms are situated anti about the central ethylene carbon-carbon bond at a dihedral angle of 171.4°. The inner pyridinium rings are also nearly coplanar at

Table 3-4 $N^{+}\cdots O$ contacts in the crystal structure of rotaxane **9**

Atoms	Distance (Å)
N2···O1	3.512
N2···O8	3.549
N3···O4	3.541
N3···O5	3.576

an interplanar angle of only 3.5°. These two rings are π-stacked with the catechol components of the crown ether at approximately 3.5 Å and interplanar angles of 14.7° (N(2)) and 8.9° (N(3)). Both of the outer pyridyl rings are twisted with respect to the adjacent rings of each dipyridinium moiety at angles of 37.6° (N(1)-N(2)) and 38.9° (N(3)-N(4)) which is allowed by the offset of the catechol rings of the crown.

The thread is coordinated to the organopalladium stoppers via the exogenous nitrogen atoms of the thread as expected (N(1)-Pd(1)-C(1) = 176.3° and N(4)-Pd(2)-C(43) = 178.0°). The metallated carbon atoms exhibit typical N-Pd distances of 2.18 Å (Pd(1)-N(1)) and 2.11 Å (Pd(2)-N(4)). The stoppers themselves demonstrate similar bond lengths, bond angles, and conformations to several structures detailed elsewhere by our group. It is clear from visual inspection of the crystal structure that the stoppers are much too large to allow the escape of the crown ether from the thread.

3.4 SUMMARY AND CONCLUSIONS

The work presented in this chapter details the construction of two [2]rotaxane compounds **7** and **9** from the [2]pseudorotaxane **2e:3c** and the full characterization of both. Each of the compounds demonstrate similar ^{1}H NMR shifts and X-ray structural data to the parent pseudorotaxane. In the case of rotaxane **7**, these shifts are exaggerated due to the irreversibly interlocked nature of the components of the rotaxane molecule. This exaggeration is not observed in rotaxane **9** owing to the lability of the bond formed between the thread and the stopper in solution. However, this lability does not preclude the isolation of a pure sample of the rotaxane from solution. This would indicate, in conjunction with coordination induced shifts in the thread, that the components spend at least some amount of time in this form in solution.

The results of this chapter directly establish the formation of a pseudorotaxane complex from **2e** and **3c** in solution via kinetic trapping of this intermediate to form rotaxane **7**. This further verifies the conclusions made in the previous chapter from the indirect evidence presented there. In addition, these demonstrations of rotaxane formation provide a potential avenue to higher order structures such as polyrotaxanes, molecular necklaces, and catenanes.

CHAPTER 4

4.1 HYPOTHESIS AND LITERATURE PRECEDENT

With the success of the rotaxane synthesis of the previous chapter, the next step in our investigation led us to consider the possibility of synthesizing [2]- and [3]rotaxanes utilizing threads incorporating two recognition sites. Two dumbbell-shaped compounds were identified as targets for constructing these rotaxanes (Figure 4-1). Both threads

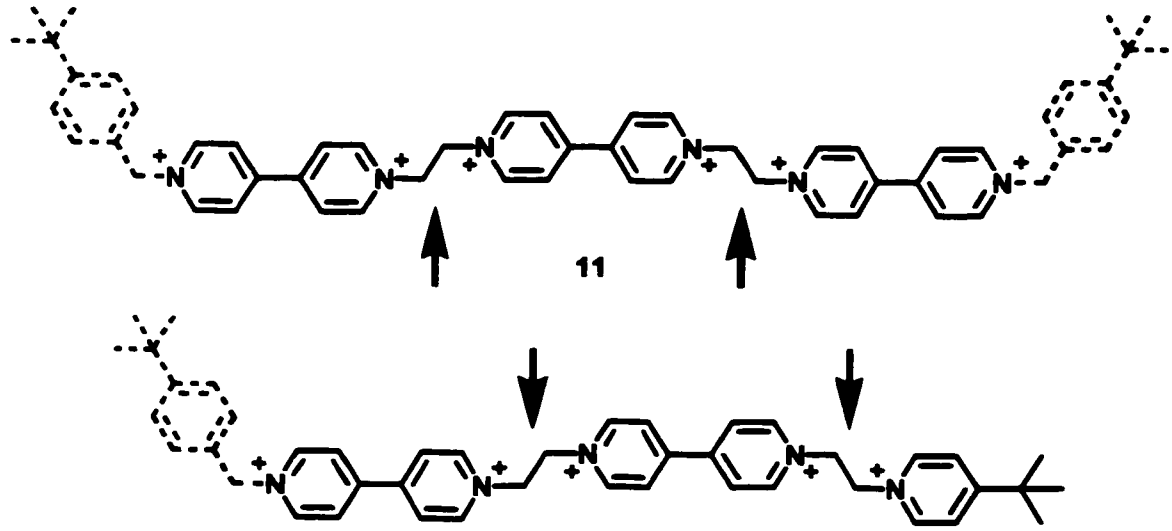

Figure 4-1. Two dumbbell-shaped molecules for the construction of [2]- and [3]rotaxanes.

contain two bis(pyridinium)ethane sites for complexation of a crown ether. The sites in **11** are degenerate and similar to that present in rotaxane **7**, but are sharing a common central dipyridinium subunit. The sites in **12** are inequivalent with one bearing resemblance to that of **7** and the other combined from a dipyridinium and a 4-*t*-butylpyridinium subunit. Again, these two inequivalent sites share a common central dipyridinium moiety. It was hoped that the inclusion of a shared central spacer in the

design of **11** and **12** would result in negative cooperativity during the threading process. Addition of a crown ether at one site of the thread could destabilize the addition of the second by decreasing the ability of the second crown ether to π-stack with the open face of the central dipyridinium ring. This type of behaviour would assist in the synthesis of the [2]rotaxanes and still allow the construction of the [3]rotaxanes. Any deficiency in formation of the [3]pseudorotaxane intermediates during synthesis could be overcome by the addition of more crown to the solution in order to push the equilibrium further in that direction.

A [2]rotaxane with two possible sites of occupation on the thread is generally referred to as a molecular shuttle, owing to the shuttling motion of the ring back and forth between the two sites. The [2]rotaxanes formed from **11** and **12** should exhibit this type of behaviour, although in the case of **11** this shuttling motion would be degenerate. The [2]rotaxane formed from **12** should display preference for the bis(dipyridinium)ethane site over the other. This is due to the expectation that the large *t*-butyl substituent located at the other site would hamper the ability of the crown to π-stack over the 4-*t*-butylpridinium ring. In addition, the electron donating effect of the *t*-butyl group should decrease the polarization at this site and hence the attraction for the crown, as demonstrated in the investigation of pseudorotaxane formation in Chapter 2.

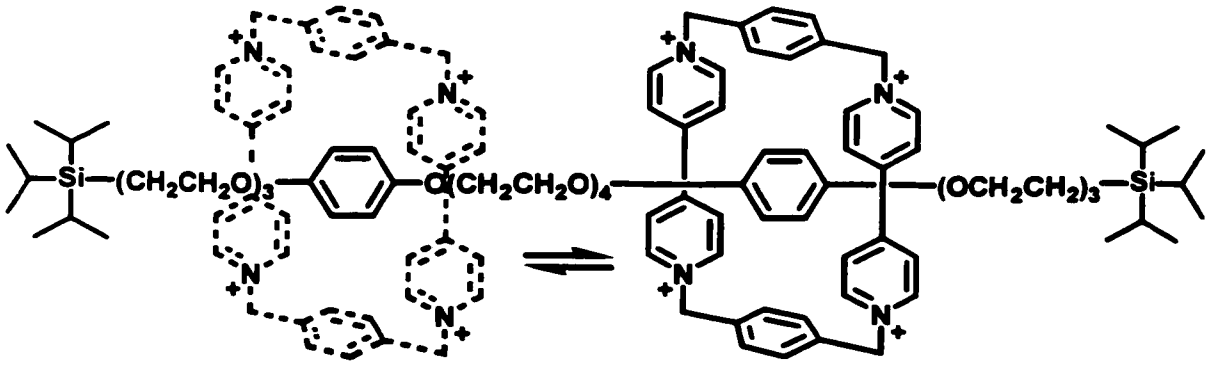

Figure 4-1. The first molecular shuttle.

The first molecular shuttle was described by Stoddart in 1991 and involved the shuttling of an electron-poor ring between two degenerate electron-rich sites of a thread

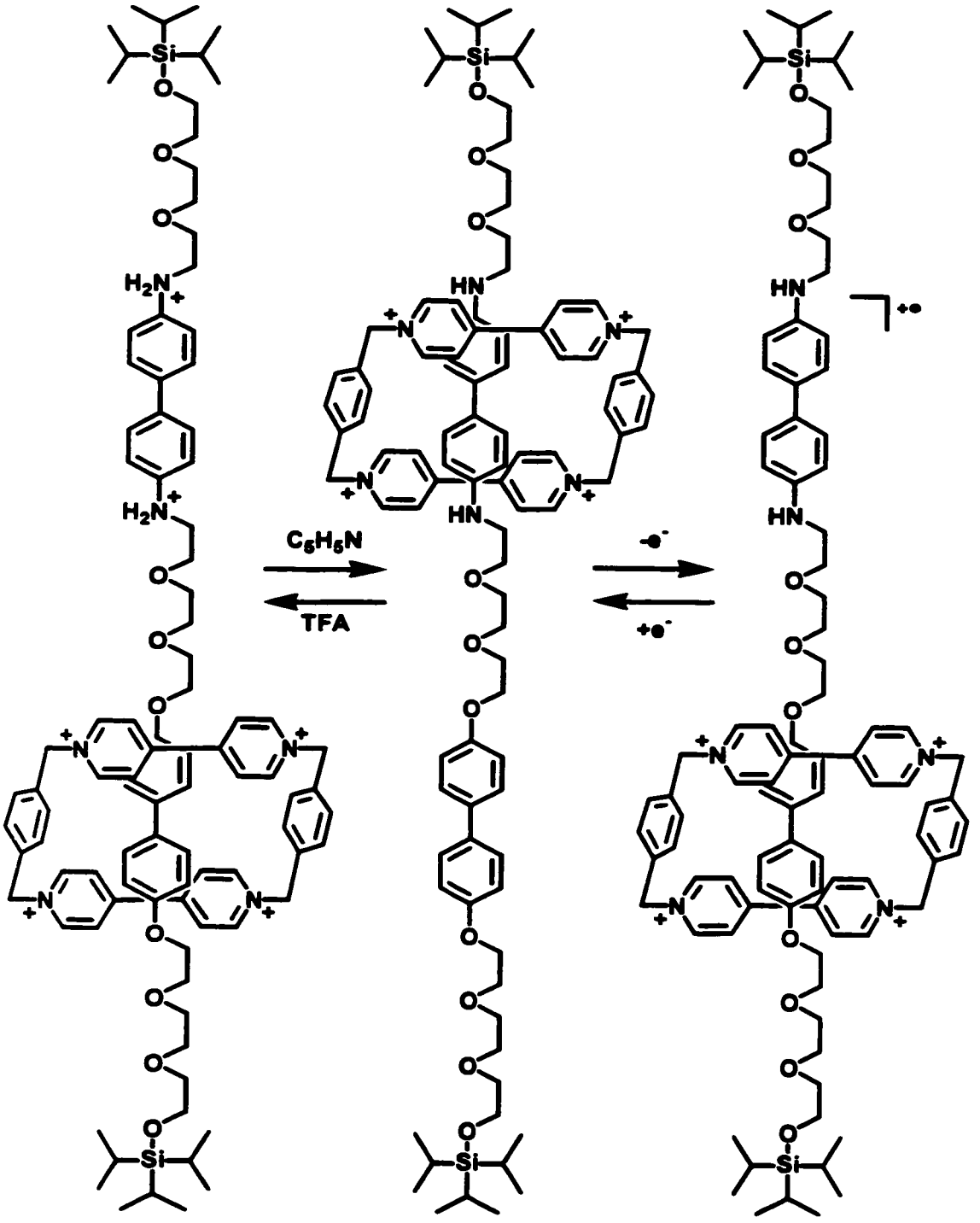

Figure 4-3. A chemically and electrochemically switchable shuttle.

(Figure 4-2).[107] Variable temperature NMR experiments determined that the ring was moving between the two stations at a rate of approximately 500 times per second. This research was followed by the construction of desymmetrized threads containing two different sites.[108] These shuttles displayed definite preferences for the occupation of one site over the other, termed translational isomerism. Though no definite correlation was obtained, the more electron rich site on the thread was generally preferred. It has also been shown that small differences in site structure can have a large effect on preference (e.g. hydroquinone >> resorcinol).

Stoddart has also demonstrated control over site occupancy in rotaxane shuttles via chemical and electrochemical switching (Figure 4-3).[109] In this example, the tetracationic ring shows a preference for the benzidine ring over the biphenol moiety of 84:16 in acetonitrile. Electrochemical oxidation of the benzidine ring system causes the tetracation to move to the biphenol site exclusively. This movement can be reversed by reducing the benzidine radical cation back to its original state. The same motion may be induced by doubly protonating the benzidine nitrogen atoms. The newly created dication repulses the tetracation which takes up the position at the biphenol station. Addition of pyridine reverses this effect.

Though our proposed system is effectively a reversal of these examples (i.e. an electron-poor thread and electron-rich ring), its behaviour is expected to be similar as the interactions involved bear close resemblance to those employed above. If this is the case, it should be possible to design systems which may be switched to one state or another via similar methods.

4.2 EXPERIMENTAL

General Comments. NaOTf was purchased from Aldrich Chemical Co. and used as received.

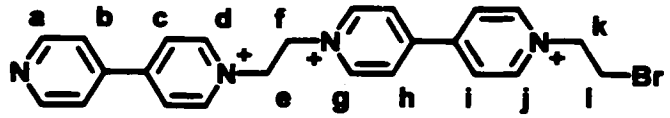

i) **Preparation of [13][BF_4]$_3$:** **4** (5.000 g, 14.53 mmol) was combined with absolute ethanol (100 mL) and refluxed with stirring for 1 week. The resulting bright yellow precipitate was filtered from the hot solution to yield 2.738 g of crude DEDE[Br]$_3$. The solid was dissolved in hot aqueous sat. $NaBF_4$ solution and allowed to cool to room temperature. The product crystallized from solution as 2.104 g (40.9%) of a beige solid and was removed by filtration and washing with distilled water. **^{1}H NMR (CD_3CN):** δ (ppm) 8.98 (d, 2H, J = 7.63 Hz, *g*), 8.95 (d, 2H, J = 6.54 Hz, *a*), 8.88 (d, 2H, J = 5.45 Hz, *d*), 8.83 (d, 2H, J = 6.54 Hz, *j*), 8.50 (d, 2H, *h*), 8.49 (d, 2H, *i*), 8.42 (d, 2H, *c*), 7.86 (d, 2H, *b*), 5.21 (m, 4H, *e and f*), 5.05 (t, 2H, J = 5.99 Hz, *k*), 4.00 (t, 2H, *l*). **ESI-MS:** 621.2 ([M-BF_4]$^+$).

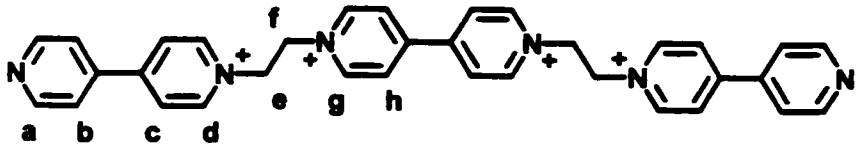

ii) **Preparation of [11][OTf]$_4$:** [13][BF_4]$_3$ (800 mg, 1.13 mmol) and 4,4'-dipyridyl (1.000 g, 6.405 mmol) were dissolved in nitromethane (50 mL) and heated to 60° C for 3 days. The resulting solution was filtered hot to yield 249 mg crude DEDED[Br]$_4$ as a beige solid. The solid was dissolved in hot aqueous sat. NaOTf solution and cooled slowly to room temperature. The final product was filtered off and

washed with distilled water as 227 mg (17.9%) of a light brown solid. **^{1}H NMR (CD_3CN)**: δ (ppm) 9.00 (d, 4H, J = 7.36 Hz, *g*), 8.88 (d, 4H, J = 7.00 Hz, *a*), 8.87 (d, 4H, J = 6.52 Hz, *d*), 8.54 (d, 4H, *h*), 8.42 (d, 4H, *c*), 7.83 (d, 4H, *b*), 5.26 (m, 8H, *e and f*). **ESI-MS**: 971.0 ($[M\text{-}OTf]^+$).

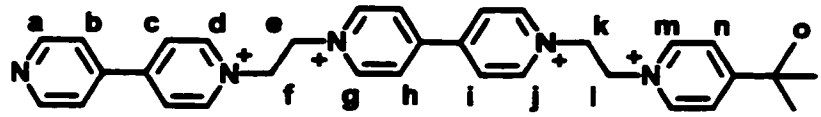

iii) Preparation of $[12][BF_4]_4$: $[13][BF_4]_3$ (800 mg, 1.13 mmol) and 4-*t*-butylpyridine (1.000 g, 7.396 mmol) were dissolved in acetonitrile (50 mL) and heated to 60° C for three days. The resulting grey solid was filtered from the hot reaction mixture to yield 478 mg of crude $[12][Br]_4$. The solid was dissolved in hot aqueous sat. $NaBF_4$ solution and allowed to cool slowly to room temperature. The final pure product was filtered from this mixture and washed with distilled water as 438 mg (45.6%) of a brown solid. **^{1}H NMR (CD_3NO_2)**: δ (ppm) 9.18 (d, 2H, J = 6.39 Hz, *g*), 9.15 (d, 2H, J = 6.39 Hz, *j*), 9.06 (d, 2H, J = 6.36 Hz, *d*), 8.94 (d, 2H, J = 4.12 Hz, *a*), 8.79 (d, 2H, J = 6.31 Hz, *m*), 8.65 (d, 4H, *i and h*), 8.57 (d, 2H, *c*), 8.21 (d, 2H, *n*), 8.06 (d, 2H, *b*), 5.53 (m, 4H, *e and f*), 5.47 (m, 2H, *k*), 5.37 (m, 2H, *l*), 1.47 (m, 9H, *o*). **ESI-MS**: 764.3 ($[M\text{-}BF_4]^+$).

iv) Preparation of $[18][BF_4]_6$: $[11][OTf]_4$ (100 mg, 0.0893 mmol) and 4-*t*-

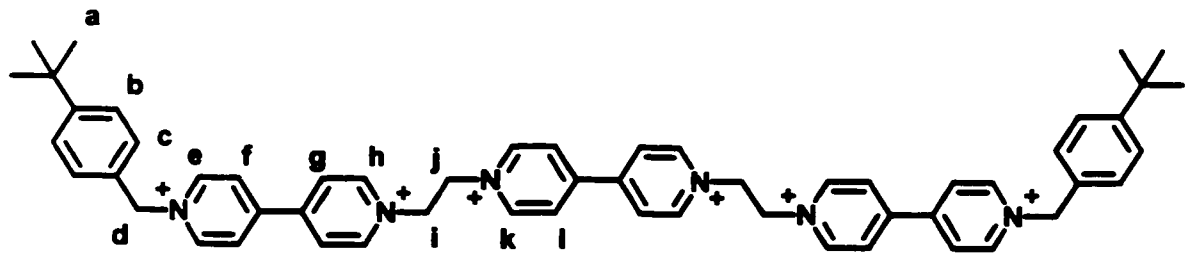

butylbenzylbromide (203 mg, 0.893 mmol) were combined in nitromethane (25 mL) and heated to 60° C for 24 hours. The resulting mixture was filtered hot and the solvent

evaporated under vacuum. The oily residue was taken up in acetonitrile (10 mL) and the pure product precipitated with diethyl ether (50 mL) to yield 34 mg (22.2%) of beige solid. **^{1}H NMR (CD_3CN)**: δ (ppm) 9.00 (d, 8H, J = 6.54 Hz, *h and k*), 8.98 (d, 4H, J = 6.54 Hz, *e*), 8.53 (d, 4H, *l*). 8.48 (d, 4H, *g*), 8.42 (d, 4H, *f*), 7.56 (d, 4H, J = 8.28 Hz, *b*), 7.45 (d, 4H, *c*), 5.80 (s, 4H, *d*), 5.27 (s, 8H, *i and j*), 1.32 (s, 18H, *a*). **ESI-MS**: 1563.4 ($[M-BF_4]^+$).

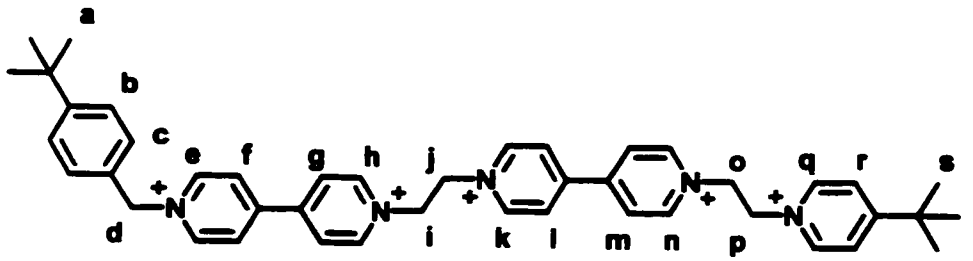

v) **Preparation of [19][BF_4]$_5$**: [12][BF_4]$_4$ (100 mg, 0.118 mmol) and 4-*t*-butylbenzylbromide (134 mg, 0.590 mmol) were dissolved in nitromethane (20 mL) and heated to 60° C for 24 hours. The resulting mixture was filtered hot and the filtrate concentrated to 5 mL under vacuum. The addition of diethyl ether (50 mL) precipitated the pure compound as 32 mg (25.0%) of light beige solid. **^{1}H NMR (CD_3CN)**: δ (ppm) . 8.99 (m, 6H, *e, h, andk*), 8.94 (d, 2H, J = 5.45 Hz, *n*), 8.60 (d, 2H, J = 5.45 Hz, *q*), 8.51 (m, 4H, *l and m*), 8.48 (d, 2H, *g*), 8.43 (d, 2H, *f*), 8.09 (d, 2H, *r*), 7.56 (d, 2H, J = 8.72 Hz, *b*), 7.45 (d, 2H, *c*), 5.80 (s, 2H, *d*), 5.28 (s, 4H, *i and j*), 5.19 (m, 2H, *o*), 5.10 (m, 2H, *p*), 1.42 (s, 9H, *s*), 1.32 (s, 9H, *a*). **ESI-MS** 998.3 ($[M-BF_4]^+$).

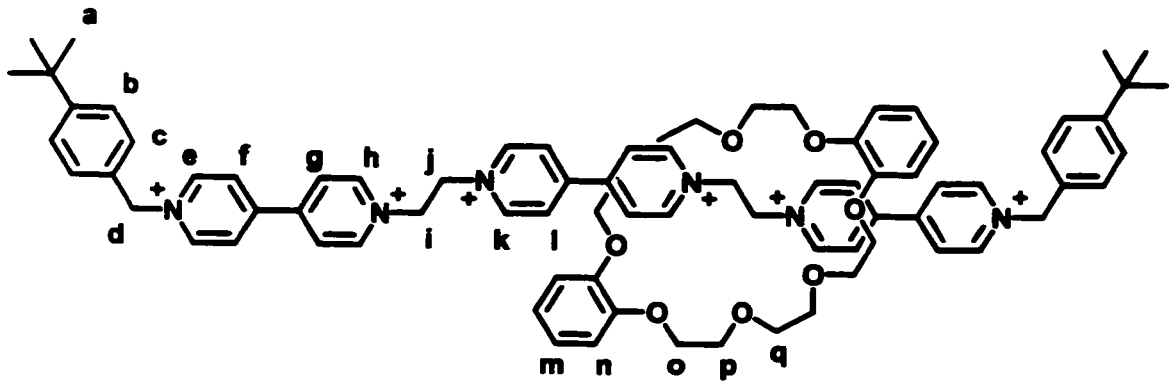

vi) **Preparation of [16][OTf]$_6$:** [11][OTf]$_4$ (100 mg, 0.0892 mmol) and **3c** (80 mg, 0.178 mmol) were dissolved in acetonitrile (15 mL) and stirred for 5 min. to produce an orange solution. 4-*t*-Butylbenzylbromide (81 mg, 0.357 mmol) was added to the solution and stirring continued for 2 days. The resulting mixture was concentrated to 5 mL and diethyl ether (50 mL) added to precipitate the salts. The solid was then chromatographed [SiO_2:MeOH-NH_4Cl(2M aq.)-$MeNO_2$ (6:2:2), R_f = 0.35]. The fractions containing the product (as monitored by TLC) were evaporated under vacuum and the remaining solid dissolved in water (10 mL). Addition of aqueous sat. NaOTf (5 mL) precipitated the pure product as 25 mg (13.0%) of orange solid. **^{1}H NMR (CD_3CN):** δ (ppm) 9.22 (b, 8H, *h and k*), 9.00 (d, 4H, J = 7.63 Hz, *e*), 8.35 (b, 8H, *g and l*), 8.28 (d, 4H, *f*), 7.57 (d, 4H, J = 8.72 Hz, *b*), 7.47 (d, 4H, *c*), 6.68 (m, 4H, *n*), 6.49 (m, 4H, *m*), 5.81 (s, 4H, *d*), 5.48 (b, 8H, *i and j*), 4.03 (m, 24H, *o, p, and q*), 1.33 (s, 18H, *a*). **ESI-MS:** 2012.7 ([M-OTf]$^+$).

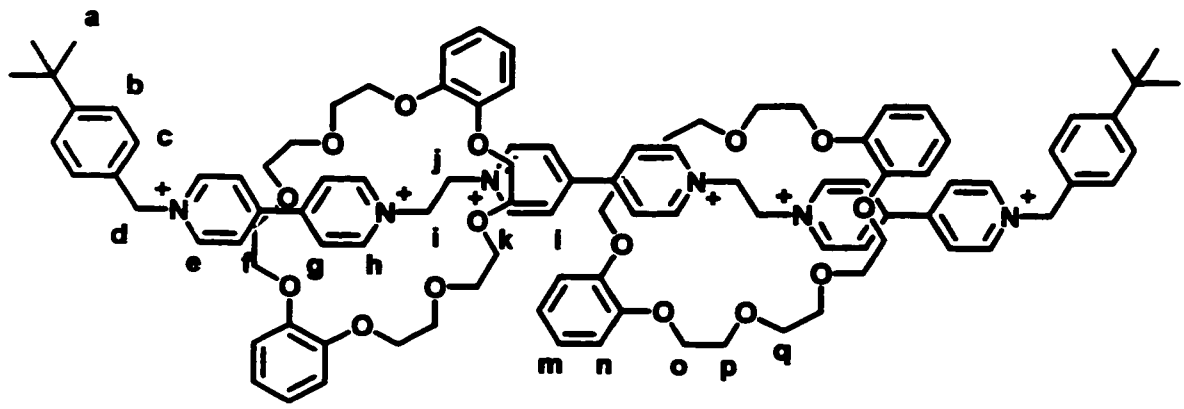

vii) **Preparation of [14][OTf]$_6$**: [11][OTf]$_4$ (100 mg, 0.0892 mmol) and **3c** (160 mg, 0.356 mmol) were dissolved in acetonitrile (15 mL) and stirred for 5 min. to produce an orange solution. 4-*t*-Butylbenzylbromide (81 mg, 0.357 mmol) was added to the solution and stirring continued for 2 days. The resulting mixture was concentrated to 5 mL and diethyl ether (50 mL) added to precipitate the salts. The solid was then chromatographed [SiO_2: MeOH-NH_4Cl(2M aq.)-$MeNO_2$ (6:2:2), R_f = 0.47]. The fractions containing the product (as monitored by TLC) were evaporated under vacuum and the remaining solid dissolved in water (10 mL). Addition of aqueous sat. NaOTf (5 mL) precipitated the pure product as 34 mg (14.6%) of orange solid. **^{1}H NMR (CD_3CN)**: δ (ppm) 9.33 (d, 4H, J = 6.84 Hz, *h*), 9.30 (d, 4H, J = 6.84 Hz, *k*), 8.95 (d, 4H, J = 6.84, *e*), 8.14 (d, 4H, *g*), 8.10 (d, 8H, *f and l*), 7.60 (d, 4H, J = 7.81 Hz, *b*), 7.49 (d, 4H, *c*), 6.68 (m, 8H, *n*), 6.49 (m, 8H, *m*), 5.81 (s, 4H, *d*), 5.48 (s, 8H, *i and j*), 4.07 (m, 48H, *o, p, and q*), 1.34 (s, 18H, *a*). **ESI-MS**: 2459.4 ([M-OTf]$^+$).

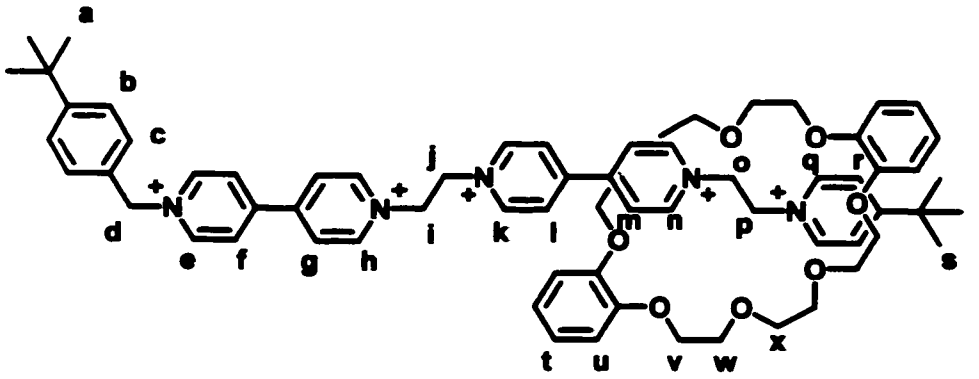

viii) Preparation of [17][BF_4]$_5$: [**12**][BF_4]$_4$ (100 mg, 0.118 mmol) and **3c** (105 mg, 0.235 mmol) were dissolved in acetonitrile (15 mL) and stirred for 5 min. to produce an orange solution. 4-*t*-Butylbenzylbromide (53 mg, 0.235 mmol) was added to the solution and stirring continued for 2 days. The resulting mixture was concentrated to 5 mL and diethyl ether (50 mL) added to precipitate the salts. The solid was then chromatographed [SiO_2: MeOH-NH_4Cl(2M aq.)-$MeNO_2$ (6:2:2), R_f = 0.31]. The fractions containing the product (as monitored by TLC) were evaporated under vacuum and the remaining solid dissolved in water (10 mL). Addition of aqueous sat. NaOTf (5 mL) precipitated the pure product as 35 mg (19.3%) of orange solid. **^{1}H NMR (CD_3CN)** δ (ppm) 9.28 (b, 4H, *h and k*), 9.12 (b, 2H, *n*), 9.01 (d, 2H, *e*), 8.83 (b, 2H, *q*), 8.28 (b, 8H, *f, g, l, and m*), 8.06 (b, 2H, *r*), 7.59 (d, 2H, J = 8.29 Hz, *b*), 7.50 (d, 2H, *c*), 6.69 (m, 4H, *u*), 6.54 (m, 4H, *t*), 5.83 (s, 2H, *d*), 5.55 (b, 4H, *i and j*), 5.35 (b, 2H, *o*), 5.28 (b, 2H, *p*), 4.06 (m, 24H, *v, w, and x*), 1.38 (s, 9H, *s*), 1.34 (s, 9H, *a*). **ESI-MS**: 1446.6 ([M-BF_4]$^+$)

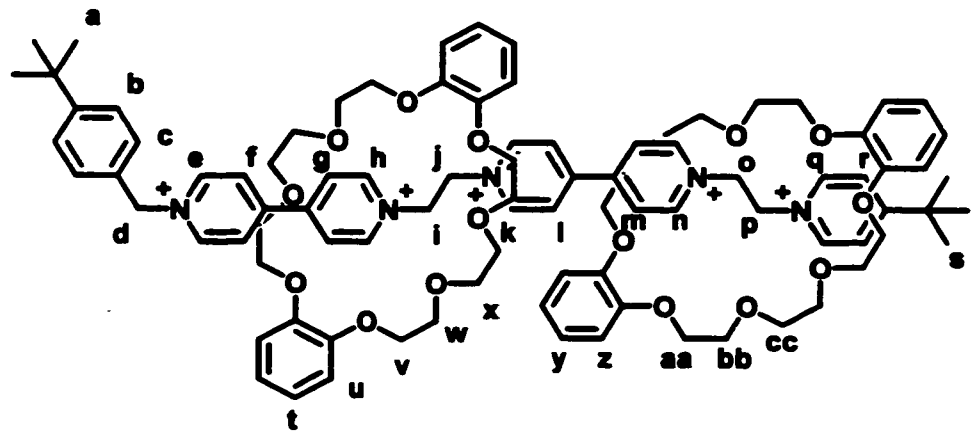

ix) Preparation of [15][BF_4]$_5$: [12][BF_4]$_4$ (100 mg, 0.118 mmol) and **3c** (210 mg, 0.470 mmol) were dissolved in acetonitrile (15 mL) and stirred for 5 min. to produce an orange solution. 4-*t*-Butylbenzylbromide (53 mg, 0.235 mmol) was added to the solution and stirring continued for 2 days. The resulting mixture was concentrated to 5 mL and diethyl ether (50 mL) added to precipitate the salts. The solid was then chromatographed [SiO_2: MeOH-NH_4Cl(2M aq.)-$MeNO_2$ (6:2:2), R_f = 0.44]. The fractions containing the product (as monitored by TLC) were evaporated under vacuum and the remaining solid dissolved in water (10 mL). Addition of aqueous sat. NaOTf (5 mL) precipitated the pure product as 42 mg (18.0%) of orange solid. **^{1}H NMR (CD_3CN)** δ (ppm) 9.30 (m, 6H, *h, k, and n*), 8.95 (m, 4H, *e and q*), 8.13 (d, 2H, J = 6.72 Hz, *g*), 8.08 (d, 2H, J = 6.76, *f*), 7.95 (m, 4H, *l and m*), 7.75 (d, 2H, J = 6.85 Hz, *r*), 7.59 (d, 2H, J = 8.44 Hz, *b*), 7.48 (d, 2H, *c*), 6.74 (m, 8H, *y and z*), 6.68 (m, 4H, *u*), 6.51 (m, 4H, *t*), 5.82 (s, 2H, *d*), 5.61 (m, 6H, *i, j, and o*), 5.45 (m, 2H, *p*), 4.04 (m, 48H, *v, w, x, aa, bb, and cc*), 1.34 (s, 9H, *a*), 1.18 (s, 9H, *s*). **ESI-MS:** 1894.8 ([M-BF_4]$^+$).

4.3 RESULTS AND DISCUSSION

SYNTHESIS

The first step in the construction of threads **11** and **12** was the synthesis of the intermediate **13** from the reaction of **4** with itself in refluxing ethanol. The reaction produces **13** exclusively due to the immediate insolubility of the trication in ethanol.

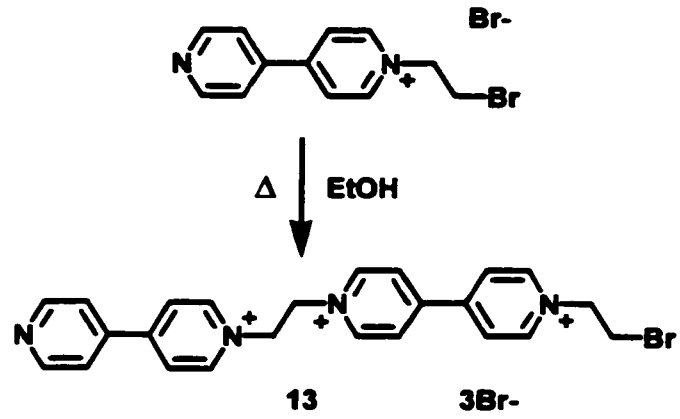

Figure 4-4. Synthesis of intermediate **13**.

This intermediate is convenient, in that it provides a direct route to both **11** and **12** as well as numerous other threads of this type, depending on the nitrogen base reacted with the remaining alkyl bromide. Conversion of **13** to the BF_4 salt was required to solubilize it for further reaction in acetonitrile and nitromethane.

Reaction of **13** in acetonitrile with 4-*t*-butylpyridine gave **12** in 45.6% yield after recrystallization as the BF_4^- salt (Figure 4-5). Similarly, reaction of **13** in nitromethane with 4,4'-dipyridyl produced **11** in 17.9% yield, recrystallized as the triflate salt due to insolubility of the BF_4^- compound in acetonitrile and nitromethane.

Synthesis of the [3]rotaxanes **14** and **15** was accomplished in a similar manner to that of **7** in the presence of an excess of crown (Figure 4-6). Production of bromide counterions is not as serious a problem as in **7** as only 33% and 20% mole fractions of

counterions are produced during reaction of **11** and **12** respectively with 4-*t*-butylbenzylbromide. Yields were acceptable at 14.6% and 18%. These are not

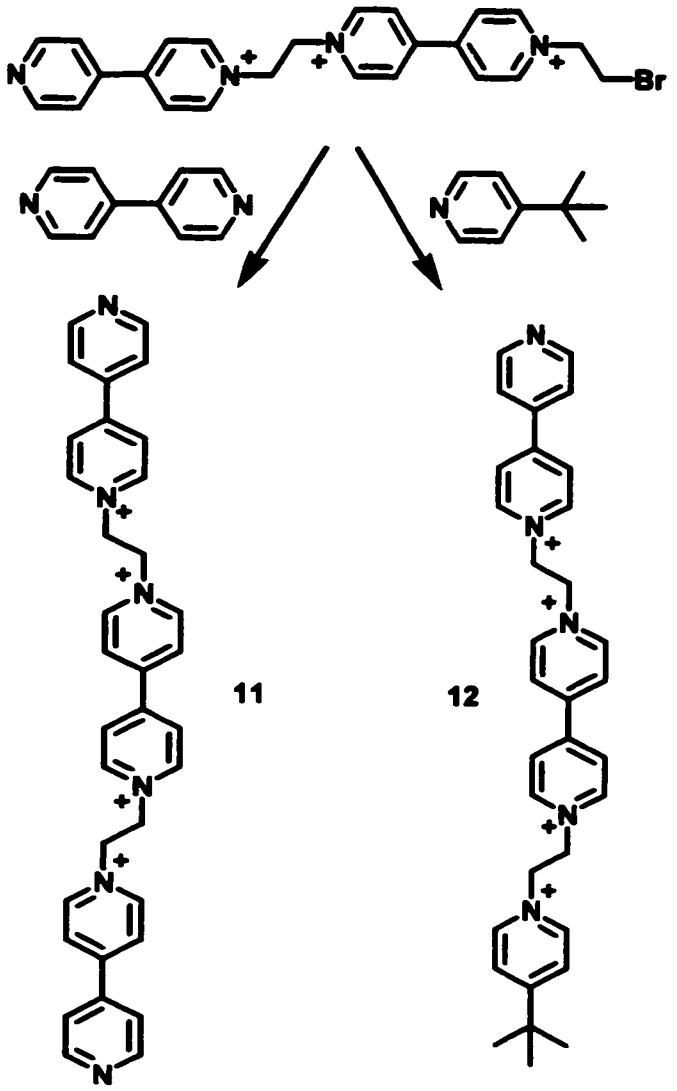

Figure 4-5. Synthesis of threads **11** and **12**.

unreasonable for the formation of [3]rotaxanes in general, though much higher yields have been reported in one case.[44] A small amount of [2]rotaxane is obtained in both of these syntheses (4% and 6%) as a by-product. Isolation of these species was effected using column chromatography in conjunction with Stoddart's MeOH:NH_4Cl:$MeNO_2$ solvent system. This provides excellent separation of the products in both cases.

Prior to synthesizing the [2]rotaxane shuttles from **11** and **12** an attempt was made to titrate both threads with **3c** to determine the optimum concentration of crown to

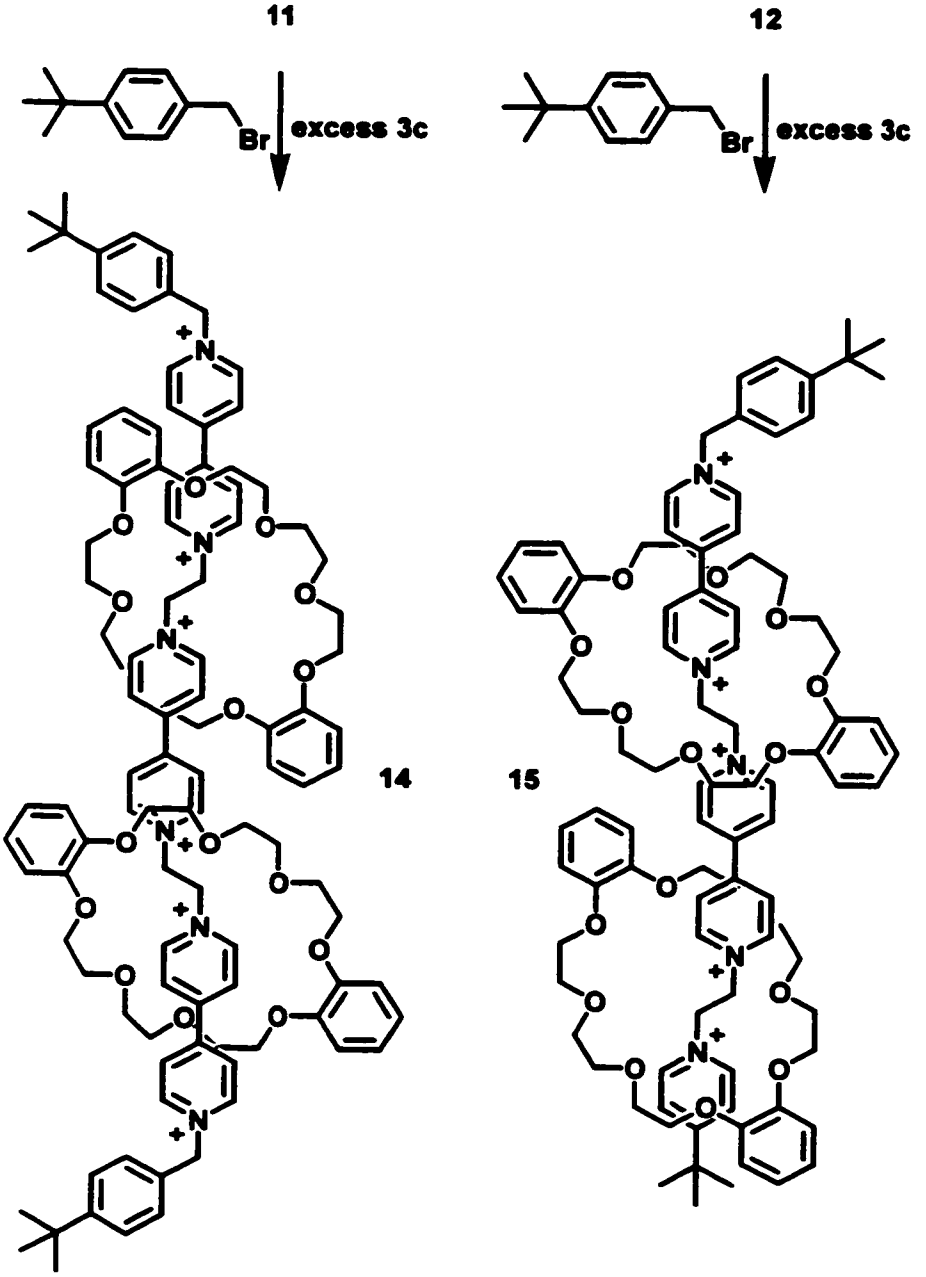

Figure 4-6. Synthesis of [3]rotaxanes **14** and **15**.

produce the [2]pseudorotaxanes. Unfortunately, the results obtained were extremely complex for both cases. Though the process of threading and dethreading is a slow exchange phenomenon at room temperature, the shuttling motion between sites once the

crown ether is threaded is a fast exchange event (see the next section). This complication makes interpretation of the results nearly impossible due to spectral overlap coupled with exchange broadening. In light of this fact, synthesis of the [2]rotaxanes was carried out using two molar equivalents of **3c**, assuming that this ratio would produce a reasonable amount of [2]pseudorotaxane in solution. Yields using this method were comparable with those obtained in the [3]rotaxane syntheses.

^{1}H NMR SPECTROSCOPY

The [3]rotaxanes **14** and **15** exhibit similar trends in spectral shifts as the pseudorotaxanes and rotaxanes of the previous chapters. A comparison of the ^{1}H NMR spectra of **14** and the free stoppered thread **18** reveals the expected downfield shifts for the hydrogen-bonded protons h-k and upfield shifts for the π-stacked protons f, g, and l (Figure 4-7). The aryl crown ether protons are similarly shifted upfield. The two crown ethers appear identical in the spectrum as a result of the symmetry of the thread. Though more complicated because of the asymmetry of the thread, the spectrum of **15** in relation to the free stoppered thread **19** also exhibits shifts due to the interlocked crown ethers (Figure 4-8). All of the ortho-N^+ and α-N^+ protons (h, i, j, k, n, o, p, and q) shift downfield as a consequence of hydrogen-bonding with the crown ethers except for e and d which remain unaffected as expected. Upfield shifts are observed for the π-stacked protons of the thread (f, g, l, m, and r) and the crown ether (t, u, y, and z). As predicted, the 4-*t*-butylpyridinium group inhibits π-stacking somewhat, resulting in less of an upfield shift for the aryl crown protons involved with this site (y, and z) than those associated with the bis(dipyridinium)ethane center. This inhibition is also demonstrated

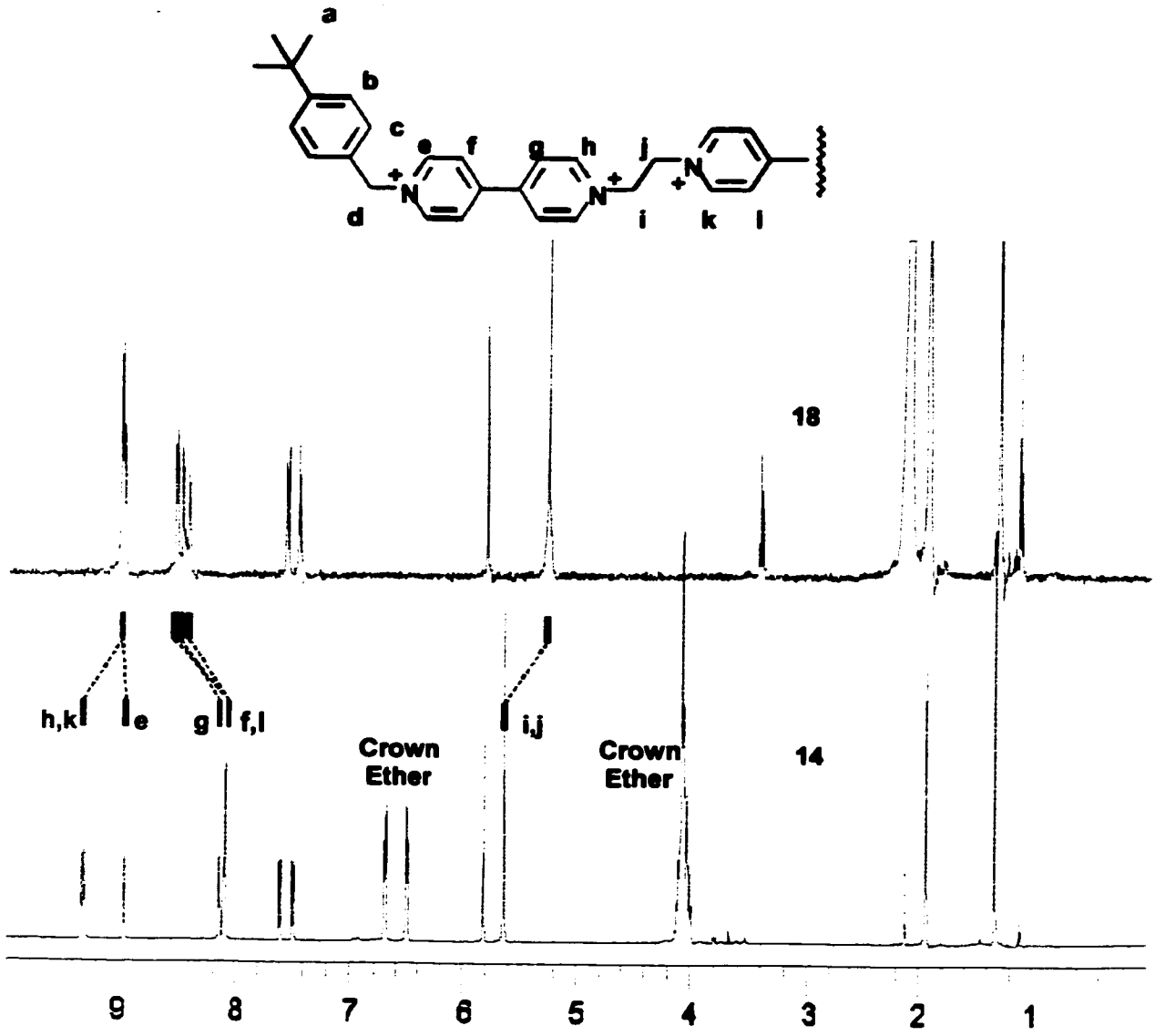

Figure 4-7. ^{1}H NMR spectra of **14** and **18**.

by an upfield shift in the *t*-butyl protons of the 4-*t*-butylpyridinium moiety, presumably because these protons point on average into the aryl ring current of the crown ether as it attempts to π-stack over the pyridinium rings.

The situation is much different for the [2]rotaxane shuttles **16** and **17**. Both of these spectra display only a single set of peaks for each compound. If the crown ether was in slow exchange on the NMR timescale between the two possible sites of the

threads we would expect to see two sets of resonances in both spectra, one for each translational isomer present. Thus, the crown ether must be undergoing fast exchange between sites at room temperature. Exchange broadening of the protons of the threads associated with the crown supports this conclusion further.

As an example, the spectrum of **17** is shown in Figure 4-9. In this case, one site

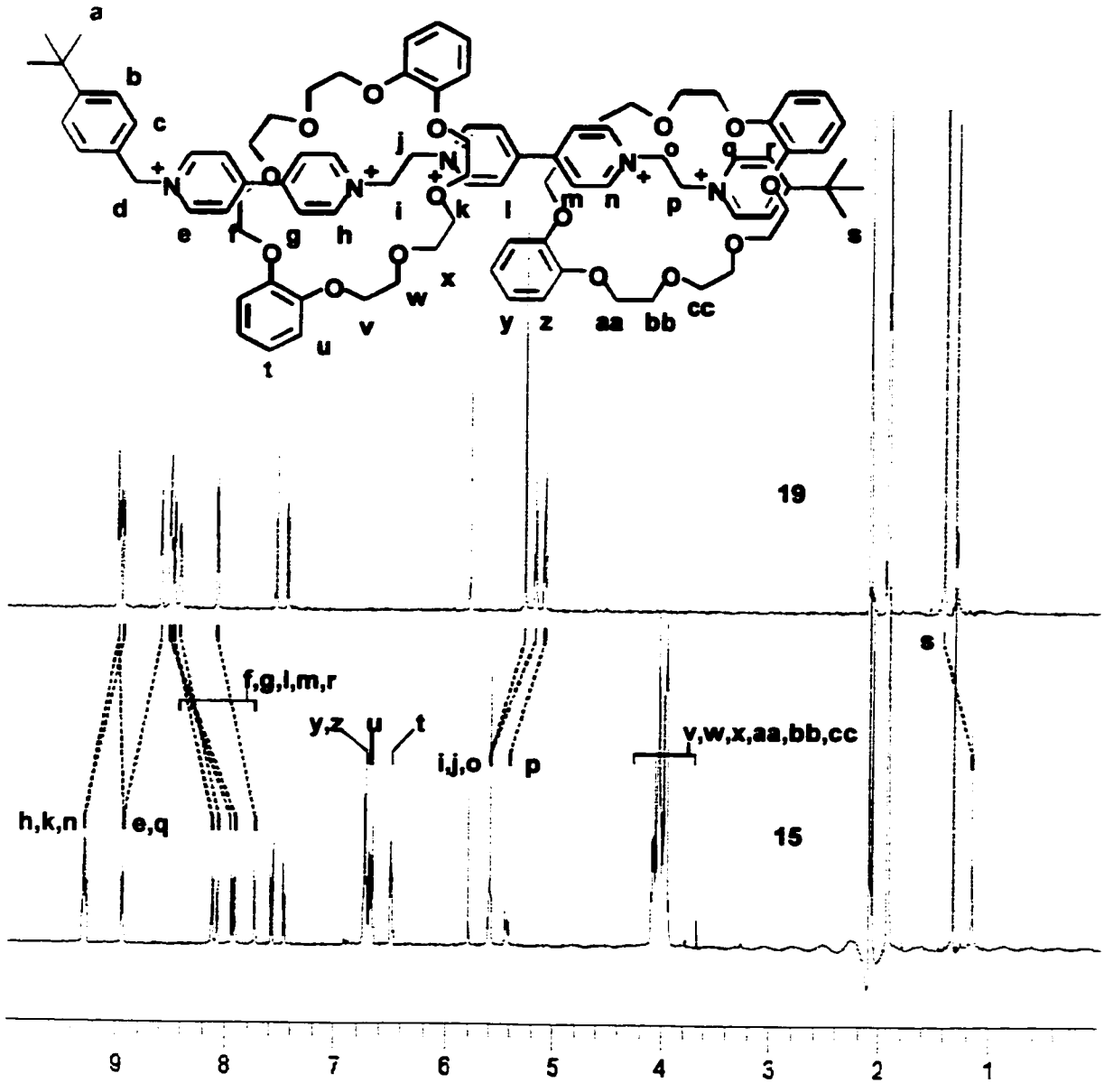

Figure 4-8. ^{1}H NMR spectra of **12** and **15**.

should be preferred over the other. However, we cannot determine the ratio of occupancy at this temperature by simple integration.

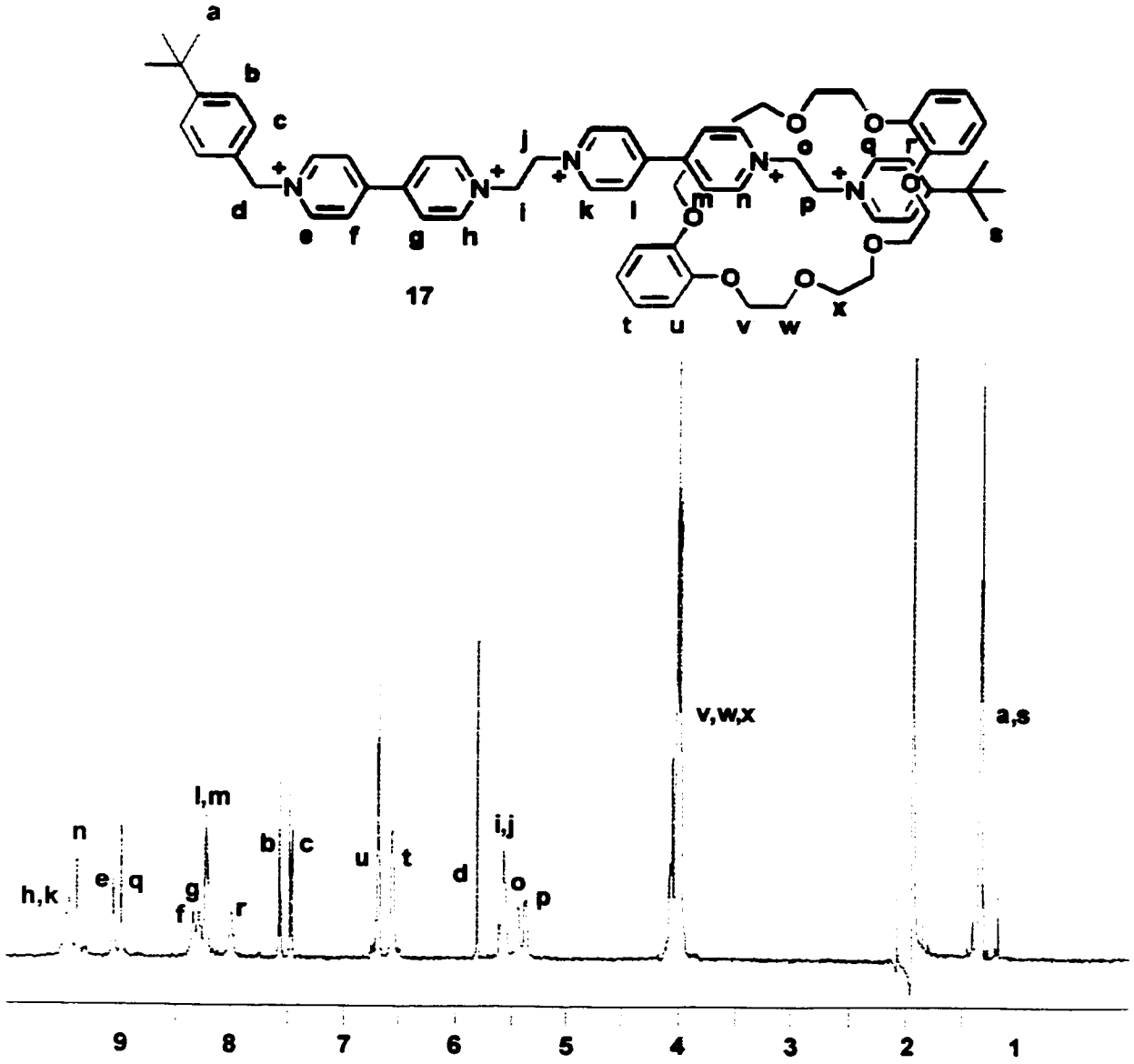

Figure 4-9. ^{1}H NMR spectrum of **17** at 298 K.

In order to determine this value a VT NMR study was undertaken with the expectation that the shuttling motion would shift to a slow exchange situation at low temperature, allowing the integration of the signals of each translational isomer to yield the occupancy.

This investigation was successful, the spectrum separating into two isomeric sets of resonances at 243 K. The aryl crown ether resonances were used to determine the occupancy of each site as they exhibited the least sign of overlap between isomers (Figure 4-10). Integration of these signals at 243 K yielded a 65:35 ratio of occupancy

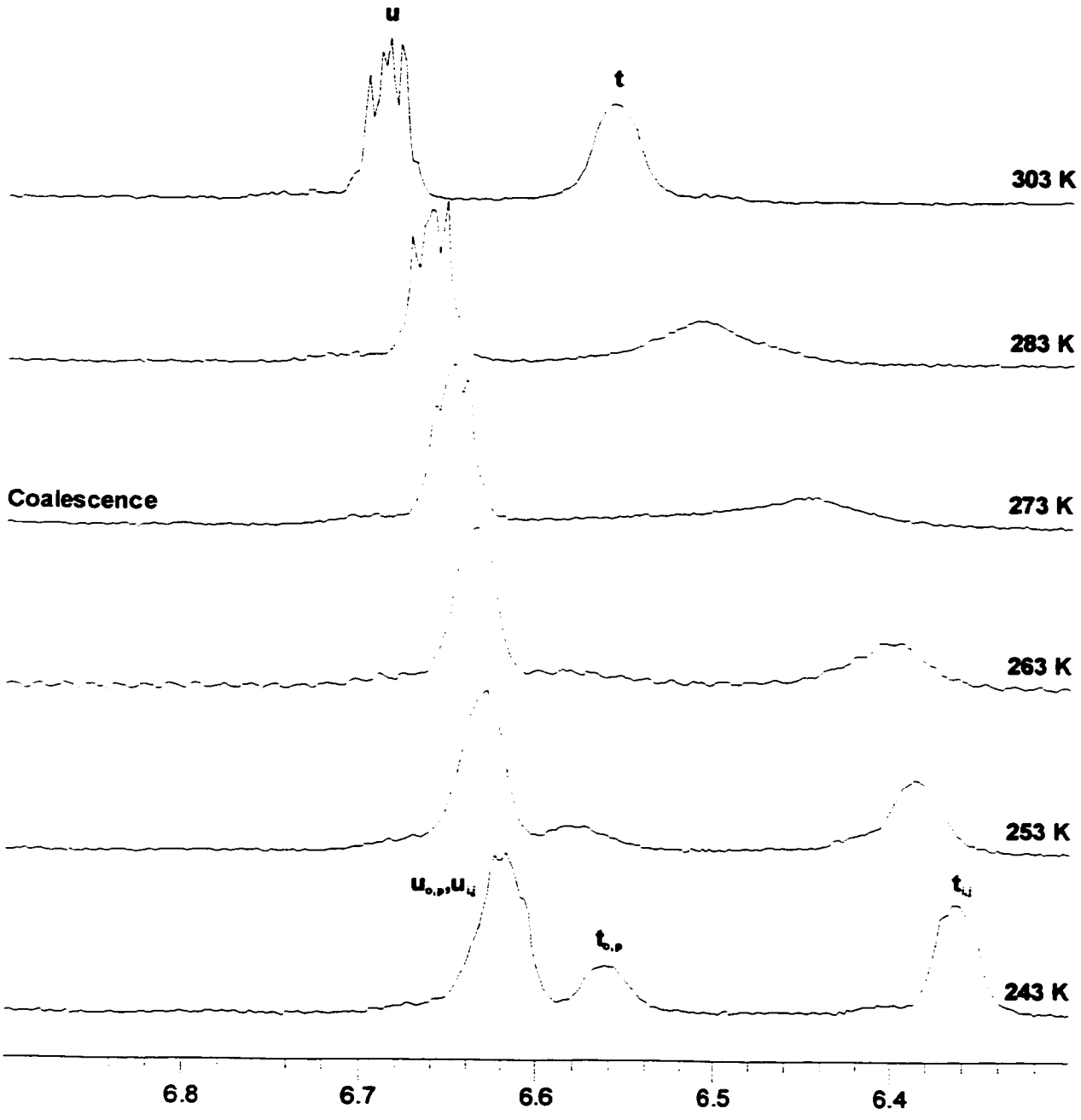

Figure 4-10. Partial variable temperature ^{1}H NMR spectra of **17**.

for the crown ether at the i,j and o,p sites respectively, at this temperature.

The VT NMR data supply another piece of information. It is possible to calculate the barrier energy for transfer of the crown from one site to the other, at the coalescence temperature (T_c).[110] At coalescence, an approximate expression for the rate at which this process occurs is given by:

$$k_{coal.} = 2.22\ \Delta\delta$$

where $\Delta\delta$ is the difference in the frequency (Hz) of the coalescing signals in the absence of exchange. This rate may then be substituted into the Eyring equation to give the expression:

$$\Delta G^{\ddagger} = 0.0191 T_c(9.97 + \log (T_c/\Delta\delta))\ \text{kJ mole}^{-1}$$

for the free energy of activation ($\Delta G^{\ddagger}$). Using this equation ($\Delta\delta$ = 100 Hz) we find that the rate of exchange at 273 K for **17** is 222 Hz and $\Delta G^{\ddagger}$ = 54.3 kJ mole^{-1}. A similar treatment for **16** which coalesces at 293 K and $\Delta\delta$ = 144 Hz gives a rate of exchange at this temperature of 320 Hz and $\Delta G^{\ddagger}$ = 57.5 kJ mole^{-1}. These values are comparable to those observed in similar processes in the literature.

X-RAY CRYSTALLOGRAPHY

The [3]rotaxane **14** was crystallized from the slow evaporation of an ethanol/water solution. It crystallized in the space group $P2_1/n$ with 2 centrosymmetric rotaxane molecules per unit cell requiring the solution of half of one molecule (Figure 4-11). This compound displays a similar molecular geometry to that of **7**, with two S-shaped crown ethers encircling both sites of the thread. The crown ether is offset from

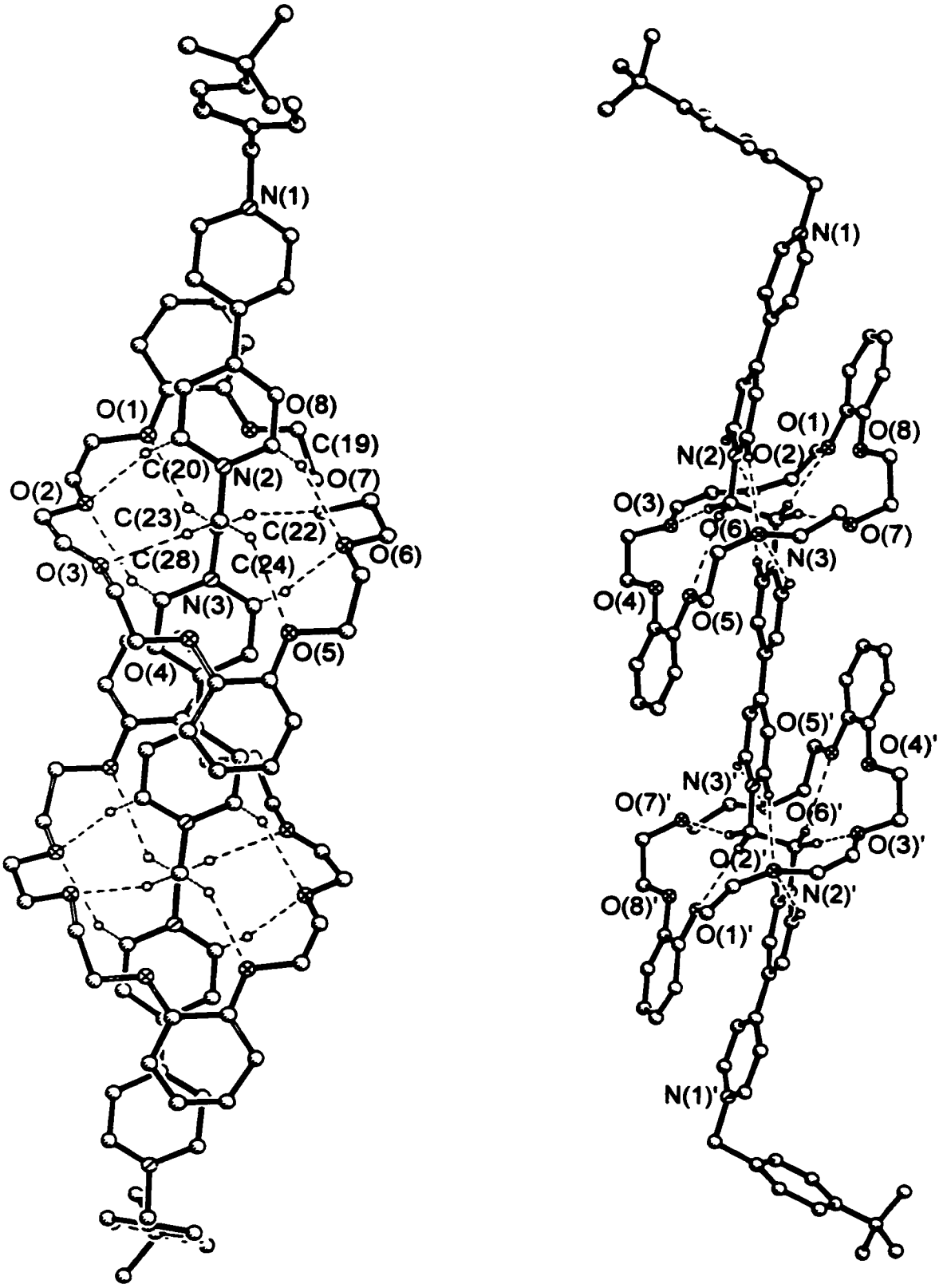

Figure 4-11. Two views of the crystal structure of **14**.

the long axis of the thread by 10.6° with a comparable hydrogen-bonding array and $N^+\cdots O$ interactions to that of **7** (Tables 4-1 and 4-2).

Table 4-1. Hydrogen bonding parameters in the crystal structure of rotaxane **14**.

Hydrogen Bonded Atoms	Distance (Å)	C-H···O Angle (°)
O6···H19A	2.516	149.8
O2···H20A	2.573	142.4
O5···H22A	2.773	140.9
O3···H22B	2.351	169.2
O7···H23A	2.261	162.0
O1···H23B	2.446	152.6
O6···H24A	2.531	140.8
O2···H28A	2.483	154.7

Table 4-2. $N^+\cdots O$ contacts in the crystal structure of rotaxane **14**.

Atoms	Distance (Å)
N2···O1	3.649
N2···O8	3.609
N3···O4	3.528
N3···O5	3.510

The aryl rings of the crown ethers are π-stacked over both the outer dipyridinium rings and the central dipyridinium ring system at an average distance of approximately

3.5 Å in all cases and interplanar angles of 14.1° (N(3)), 10.1° (N(2)), and 0.9° (N(3)). This forms a triple π-stack around the central dipyridinium ring in which the two pyridinium rings are perfectly coplanar. The outer pyridinium rings lie at an angle of 9.3° to each other and those connected to the ethylene unit at an angle of 8.3°. No significant packing effects were observed.

[2]rotaxane **17** was crystallized from slow evaporation of a saturated aqueous $NaBF_4$ solution. The rotaxane crystallized as 4 molecules per unit cell in space group *Cc* requiring solution of the whole molecule (Figure 4-12). Again, the crown ether is offset from the long axis of the thread by an angle of 15.8° presenting the same type of hydrogen-bonding array and $N^+\cdots O$ interactions as **7** and **14** (Tables 4-3 and 4-4).

Table 4-1. Hydrogen bonding parameters in the crystal structure of rotaxane **17**.

Hydrogen Bonded Atoms	Distance (Å)	C-H···O Angle (°)
O3···H19A	2.633	135.0
O7···H20A	2.467	151.2
O2···H22A	2.520	163.5
O8···H22B	2.698	148.7
O4···H23A	2.651	147.3
O6···H23B	2.595	166.1
O3···H24A	2.326	155.3
O7···H28A	2.568	138.5

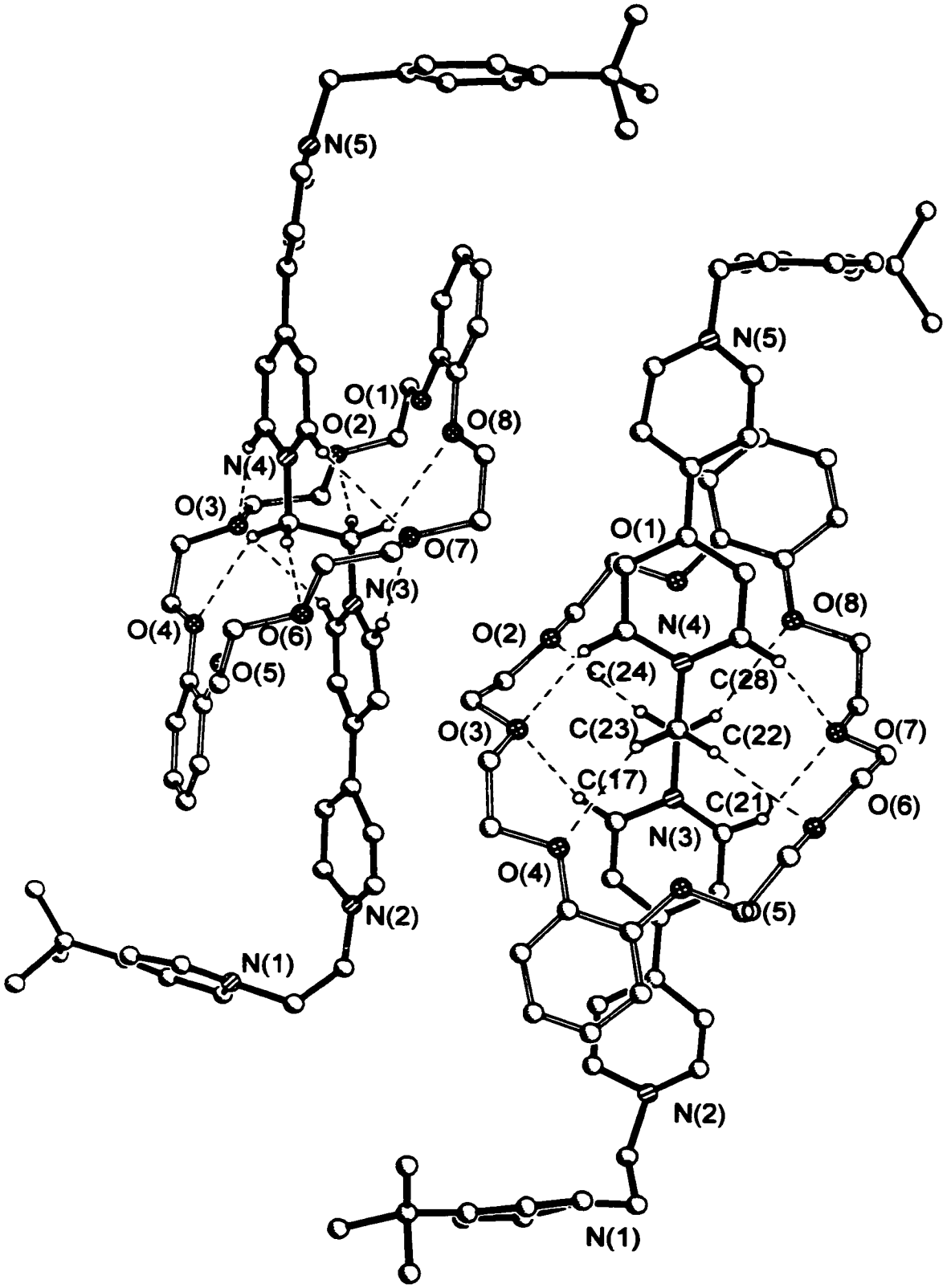

Figure 4-12. Two views of the crystal structure of **17**.

Table 4-4. $N^{+}\cdots O$ contacts in the crystal structure of rotaxane **17**.

Atoms	Distance (Å)
N3···O4	3.536
N3···O5	3.481
N4···O1	3.564
N4···O8	3.550

As predicted from the NMR data, the crown ether is bound to the bis(dipyridinium)ethane site rather than the other less attractive one. The crown ether rings are π-stacked over the dipyridinium components at an average distance of 3.5 Å and interplanar angles of 13.3° (N(2)), 9.2° (N(3)), 10.7° (N(4)), and 14.9° (N(5)). The two dipyridinium ring systems are situated perfectly anti to each other at a dihedral angle of 179.2° (N(3)-C(22)-C(23)-N(4)) with each set of rings nearly coplanar at 7.6° (N(2)-N(3)) and 23.9° (N(4)-N(5)). The uncomplexed pyridinum sites lie in a gauche conformation of 76.6° about the shared ethylene unit.

4.4 SUMMARY AND CONCLUSIONS

Two thread shaped molecules for potential [3]rotaxane and [2]rotaxane shuttle formation were synthesized and used to construct [3]rotaxanes **14** and **15** as well as [2]rotaxanes **16** and **17**. The [3]rotaxanes presented similar NMR behaviour and, in the case of **14** x-ray crystallographic details to the [2]rotaxane **7** presented in the previous chapter. Analysis of the [2]rotaxanes **16** and **17** revealed that the crown ether mechanically bonded to the threads shuttles back and forth between the two possible sites

of occupancy, the frequency and free energy of the transition state having been derived from VT NMR data. Furthermore, it was found that in the non-degenerate case of **17**, the crown ether displays a preference for one site over the other which could be rationalized from the trends observed in the pseudorotaxanes examined in the second chapter.

These results demonstrate that this system has the potential for the design of interlocked molecules with information content beyond simple two-component host-guest complexation. The research presented here bodes well for the construction of molecules, based on the underlying principles investigated, in which translational isomerism may be controlled by chemical, electrochemical, or photochemical means.

APPENDIX 1

Table A-1. Details of X-ray Data Collection, Solution and Refinement for [2]Pseudorotaxane **2e:3c**

Empirical formula	$C_{46}H_{46}B_2F_8N_4O_8$
Formula weight	956.49
Temperature, K	293(2)
Wavelength, Å	0.71073
Crystal system	Monoclinic
Space group	$P2_1/c$ (No. 14)
a, Å	10.5068(3)
b, Å	12.0843(3)
c, Å	21.5489(7)
β, °	102.703(1)
V, Å^3	2669.0(1)
Z	2
ρ_{calcd}, Mg m^{-3}	1.190
μ, mm^{-1}	0.099
F(000)	992
Crystal size, mm	0.22 x 0.26 x 0.34
θ–range for data collection, °	1.94 to 22.00
Limiting indices	$-14 \le h \le 14$, $-15 \le k \le 10$, $-28 \le l \le 27$
Reflections collected	9883
Independent reflections	3241 [R(int) = 0.0616]
Refinement method	Full-matrix least-squares on F^2
Data / restraints / parameters	3235 / 0 / 315
Goodness-of-fit on F^2	0.979
Final R indices [$I>2\sigma(I)$]	$R_1 = 0.0814$, $wR_2 = 0.2156$
R indices (all data)	$R_1 = 0.1300$, $wR_2 = 0.2540$
Largest differences; peak and hole	0.492 and -0.391 eÅ^{-3}

Table A-2. Atomic coordinates (x10^4) and equivalent isotropic displacement parameters (Å^2 x 10^3) for [2]Pseudorotaxane **2e:3c**.

Atom	x	y	z	U(eq)
N(1)	3148(6)	11930(4)	793(3)	85(2)
N(2)	5016(4)	6538(3)	110(2)	50(1)
O(1)	1664(3)	5812(3)	-43(2)	66(1)
O(2)	2187(3)	4830(3)	-1224(2)	64(1)
O(3)	4429(3)	5613(3)	-1568(2)	66(1)
O(4)	3036(4)	5625(3)	1111(2)	67(1)
C(1)	3930(8)	11307(6)	1221(3)	95(2)

C(2)	4303(6)	10238(5)	1118(3)	77(2)
C(3)	3840(5)	9753(4)	532(2)	49(1)
C(4)	3008(5)	10388(5)	89(3)	63(2)
C(5)	2699(5)	11458(5)	243(3)	73(2)
C(6)	4220(4)	8626(4)	394(2)	46(1)
C(7)	5042(5)	7982(4)	842(2)	56(1)
C(8)	5422(5)	6960(4)	701(2)	57(1)
C(9)	4216(5)	7123(5)	-334(2)	55(1)
C(10)	3824(5)	8147(5)	-203(2)	57(1)
C(11)	5486(5)	5443(4)	-35(3)	58(1)
C(12)	2289(5)	6550(5)	987(3)	56(1)
C(13)	2229(5)	7361(5)	1425(3)	68(2)
C(14)	1462(6)	8288(6)	1244(3)	78(2)
C(15)	764(5)	8400(5)	641(3)	76(2)
C(16)	808(5)	7597(5)	193(3)	69(2)
C(17)	1559(5)	6657(5)	368(3)	59(1)
C(18)	772(5)	5816(5)	-647(2)	69(2)
C(19)	994(5)	4800(5)	-1003(3)	71(2)
C(20)	2119(5)	5457(5)	-1785(3)	66(2)
C(21)	3346(5)	5297(5)	-2026(2)	70(2)
C(22)	5613(6)	5645(5)	-1791(3)	79(2)
C(23)	3687(6)	5421(5)	1762(3)	74(2)
F(1)	8732(7)	1079(10)	1337(3)	266(5)
F(2)	7346(5)	123(4)	1657(3)	179(2)
F(3)	9061(5)	657(4)	2353(2)	149(2)
F(4)	7651(9)	1817(5)	1873(4)	249(4)
B(1)	8223(8)	867(4)	1823(2)	106(3)
O(1S)	13223(4)	2520(2)	2765(1)	86(1)
C(1S)	12052(3)	2697(2)	2625(1)	72(2)
C(2S)	11282(4)	2749(2)	3118(2)	99(2)
C(3S)	11362(7)	2898(6)	1968(3)	107(2)

Table A-3. Bonding Parameters for [2]Pseudorotaxane **2e:3c**.

Bond	Distance (Å)	Bond	Distance (Å)
N(1)-C(5)	1.307(7)	C(7)-C(8)	1.353(7)
N(1)-C(1)	1.326(8)	C(9)-C(10)	1.353(7)
N(2)-C(9)	1.330(6)	C(11)-C(11)'	1.510(10)
N(2)-C(8)	1.350(6)	C(12)-C(13)	1.373(7)
N(2)-C(11)	1.471(6)	C(12)-C(17)	1.391(7)
O(1)-C(17)	1.372(6)	C(13)-C(14)	1.384(8)
O(1)-C(18)	1.427(6)	C(14)-C(15)	1.353(8)
O(2)-C(20)	1.414(6)	C(15)-C(16)	1.377(8)
O(2)-C(19)	1.436(6)	C(16)-C(17)	1.387(7)

O(3)-C(21)	1.385(6)	C(18)-C(19)	1.493(7)
O(3)-C(22)	1.429(6)	C(20)-C(21)	1.505(7)
O(4)-C(12)	1.359(6)	C(22)-C(23)'	1.478(8)
O(4)-C(23)	1.442(6)	C(23)-C(22)'	1.478(8)
C(1)-C(2)	1.383(9)	F(1)-B(1)	1.300(6)
C(2)-C(3)	1.379(7)	F(2)-B(1)	1.281(9)
C(3)-C(4)	1.378(7)	F(3)-B(1)	1.304(7)
C(3)-C(6)	1.468(7)	F(4)-B(1)	1.312(7)
C(4)-C(5)	1.391(8)	O(1S)-C(1S)	1.219(2)
C(6)-C(7)	1.385(6)	C(1S)-C(3S)	1.463(7)
C(6)-C(10)	1.388(6)	C(1S)-C(2S)	1.471(3)

Bonds	Angle (°)	Bonds	Angle (°)
C(5)-N(1)-C(1)	115.4(5)	O(4)-C(12)-C(17)	116.0(5)
C(9)-N(2)-C(8)	119.8(4)	C(13)-C(12)-C(17)	119.6(5)
C(9)-N(2)-C(11)	120.9(4)	C(12)-C(13)-C(14)	119.7(5)
C(8)-N(2)-C(11)	119.3(4)	C(15)-C(14)-C(13)	120.8(6)
C(17)-O(1)-C(18)	117.1(4)	C(14)-C(15)-C(16)	120.6(6)
C(20)-O(2)-C(19)	114.4(4)	C(15)-C(16)-C(17)	119.4(6)
C(21)-O(3)-C(22)	114.1(4)	O(1)-C(17)-C(16)	123.8(5)
C(12)-O(4)-C(23)	117.5(4)	O(1)-C(17)-C(12)	116.3(5)
N(1)-C(1)-C(2)	124.9(6)	C(16)-C(17)-C(12)	119.9(5)
C(3)-C(2)-C(1)	119.3(6)	O(1)-C(18)-C(19)	108.7(4)
C(4)-C(3)-C(2)	116.1(5)	O(2)-C(19)-C(18)	113.4(5)
C(4)-C(3)-C(6)	122.3(5)	O(2)-C(20)-C(21)	109.9(4)
C(2)-C(3)-C(6)	121.6(5)	O(3)-C(21)-C(20)	110.6(4)
C(3)-C(4)-C(5)	119.9(5)	O(3)-C(22)-C(23)'	115.0(5)
N(1)-C(5)-C(4)	124.4(6)	O(4)-C(23)-C(22)'	108.4(5)
C(7)-C(6)-C(10)	115.2(5)	F(2)-B(1)-F(1)	108.2(6)
C(7)-C(6)-C(3)	122.3(4)	F(2)-B(1)-F(3)	114.4(4)
C(10)-C(6)-C(3)	122.4(5)	F(1)-B(1)-F(3)	115.1(7)
C(8)-C(7)-C(6)	121.7(5)	F(2)-B(1)-F(4)	108.8(7)
N(2)-C(8)-C(7)	120.6(5)	F(1)-B(1)-F(4)	99.8(7)
N(2)-C(9)-C(10)	120.6(4)	F(3)-B(1)-F(4)	109.4(6)
C(9)-C(10)-C(6)	122.1(5)	O(1S)-C(1S)-C(3S)	121.8(3)
N(2)-C(11)-C(11)'	110.5(5)	O(1S)-C(1S)-C(2S)	120.9
O(4)-C(12)-C(13)	124.4(5)	C(3S)-C(1S)-C(2S)	117.2(3)

Symmetry transformation used to generate equivalent atoms: -x+1,-y+1,-z

Table A-4. Anisotropic thermal parameters ($Å^2 \times 10^3$) for [2]Pseudorotaxane **2e:3c**.

Atom	U_{11}	U_{22}	U_{33}	U_{23}	U_{13}	U_{12}
N(1)	84(4)	71(3)	104(4)	-12(4)	32(3)	7(3)
N(2)	40(2)	54(3)	61(3)	-1(2)	21(2)	0(2)
O(1)	46(2)	87(3)	66(2)	-3(2)	14(2)	13(2)
O(2)	48(2)	81(3)	65(2)	6(2)	16(2)	10(2)
O(3)	48(2)	86(3)	63(2)	2(2)	11(2)	0(2)
O(4)	57(2)	83(3)	63(2)	-2(2)	22(2)	12(2)
C(1)	116(6)	83(5)	78(4)	-17(4)	9(4)	12(5)
C(2)	89(5)	66(4)	71(4)	-9(3)	9(3)	10(3)
C(3)	34(3)	50(3)	65(3)	3(3)	19(3)	1(3)
C(4)	44(3)	63(4)	83(4)	-12(3)	17(3)	4(3)
C(5)	49(4)	70(4)	102(5)	8(4)	19(3)	13(3)
C(6)	29(3)	56(3)	56(3)	0(3)	16(2)	-6(2)
C(7)	44(3)	67(4)	54(3)	-3(3)	7(3)	9(3)
C(8)	51(3)	65(4)	54(3)	5(3)	8(3)	13(3)
C(9)	42(3)	65(4)	55(3)	-4(3)	6(3)	6(3)
C(10)	48(3)	64(4)	57(3)	9(3)	6(3)	6(3)
C(11)	50(3)	56(3)	73(3)	-5(3)	24(3)	10(2)
C(12)	35(3)	69(4)	72(4)	-5(3)	29(3)	0(3)
C(13)	43(3)	92(5)	73(4)	-7(4)	24(3)	0(3)
C(14)	54(4)	89(5)	102(5)	-25(4)	38(4)	-4(4)
C(15)	43(3)	82(4)	106(5)	-1(4)	21(4)	9(3)
C(16)	44(3)	84(4)	85(4)	-3(4)	23(3)	10(3)
C(17)	31(3)	78(4)	73(4)	0(3)	26(3)	-3(3)
C(18)	33(3)	101(5)	73(4)	-4(3)	13(3)	9(3)
C(19)	52(4)	91(4)	71(3)	3(3)	16(3)	1(3)
C(20)	51(3)	72(4)	72(3)	11(3)	8(3)	5(3)
C(21)	62(4)	94(4)	55(3)	3(3)	11(3)	-5(3)
C(22)	64(4)	96(5)	81(4)	24(3)	25(3)	-1(4)
C(23)	61(4)	103(5)	64(4)	9(3)	24(3)	7(4)
F(1)	165(6)	526(16)	106(4)	46(6)	29(4)	-105(8)
F(2)	109(4)	113(4)	283(7)	-6(4)	-25(4)	-24(3)
F(3)	153(4)	164(4)	104(3)	20(3)	-31(3)	-7(3)
F(4)	354(11)	107(4)	227(7)	-15(4)	-64(7)	58(6)
B(1)	137(9)	66(6)	98(7)	14(5)	-13(6)	-19(6)

The anisotropic displacement factor exponent takes the form: $-2\pi^2[h^2\, a^{*2}\, U11 + ... + 2hka^*b^*U12]$

Table A-5. Hydrogen coordinates (x 10^4) and isotropic thermal parameters $Å^2$ x 10^3 for [2]Pseudorotaxane **2e:3c**.

Atom	x	y	z	U(eq)
H(1A)	4253(8)	11614(6)	1621(3)	114
H(2A)	4860(6)	9849(5)	1440(3)	92
H(4A)	2653(5)	10101(5)	-312(3)	75
H(5A)	2136(5)	11866(5)	-67(3)	88
H(7A)	5341(5)	8259(4)	1251(2)	67
H(8A)	5967(5)	6544(4)	1014(2)	68
H(9A)	3922(5)	6825(5)	-738(2)	66
H(10A)	3272(5)	8542(5)	-523(2)	69
H(11A)	6317(5)	5289(4)	251(3)	70
H(11B)	5618(5)	5439(4)	-467(3)	70
H(13A)	2700(5)	7288(5)	1842(3)	81
H(14A)	1427(6)	8839(6)	1541(3)	94
H(15A)	250(5)	9026(5)	527(3)	91
H(16A)	339(5)	7684(5)	-224(3)	83
H(18A)	907(5)	6471(5)	-885(2)	83
H(18B)	-118(5)	5827(5)	-589(2)	83
H(19A)	1009(5)	4162(5)	-728(3)	85
H(19B)	269(5)	4708(5)	-1365(3)	85
H(20A)	2013(5)	6235(5)	-1696(3)	79
H(20B)	1370(5)	5225(5)	-2107(3)	79
H(21A)	3428(5)	4526(5)	-2134(2)	85
H(21B)	3299(5)	5735(5)	-2407(2)	85
H(22A)	6192(6)	6185(5)	-1541(3)	95
H(22B)	5414(6)	5901(5)	-2229(3)	95
H(23A)	3054(6)	5392(5)	2029(3)	89
H(23B)	4299(6)	6013(5)	1916(3)	89
H(2SA)	11838(3)	2605(2)	3527(2)	148
H(2SB)	10600(4)	2205(2)	3030(1)	148
H(2SC)	10904(4)	3473(3)	3118(2)	148
H(3SA)	11964(7)	2842(6)	1692(3)	161
H(3SB)	10986(7)	3625(6)	1934(3)	161
H(3SC)	10683(7)	2358(6)	1845(3)	161

Table A-6. Details of X-ray Data Collection, Solution and Refinement for [2]Pseudorotaxane **2f:3c**.

Empirical formula	$C_{40}H_{54}B_2F_8N_2O_{12}$
Formula weight	928.47
Temperature, K	293(2)
Wavelength, Å	0.71073
Crystal system	Orthorhombic
Space group	*Pbca* (No. 62)
a, Å	9.3357(1)
b, Å	22.4319(3)
c, Å	25.0932(2)
V, Å^3	5255.0(1)
Z	4
ρ_{calcd}, Mg m^{-3}	1.174
μ, mm^{-1}	0.103
F(000)	1944
Crystal size, mm	0.18 x 0.26 x 0.32
θ–range for data collection, °	1.62 to 22.00
Limiting indices	$-10 \le h \le 12$, $-29 \le k \le 22$, $-26 \le l \le 32$
Reflections collected	15012
Independent reflections	2448 [R(int) = 0.1350]
Refinement method	Full-matrix least-squares on F^2
Data / restraints / parameters	2440 / 0 / 361
Goodness-of-fit on F^2	1.262
Final R indices [$I>2\sigma(I)$]	$R_1 = 0.1300$, $wR_2 = 0.2637$
R indices (all data)	$R_1 = 0.1648$, $wR_2 = 0.2961$
Largest differences; peak and hole	0.220 and -0.260 eÅ^{-3}

Table A-7. Atomic coordinates (x 10^4) and equivalent isotropic displacement parameters (Å^2 x 10^3) for [2]Pseudorotaxane **2f:3c**.

Atom	x	y	z	U(eq)
O(1)	2857(8)	6349(3)	6523(3)	75(2)
O(2)	829(9)	6772(4)	6245(3)	96(3)
O(3)	5340(7)	3382(3)	5302(3)	56(2)
O(4)	5831(7)	4181(3)	6243(2)	57(2)
O(5)	6432(7)	5411(3)	6169(3)	65(2)
O(6)	4011(7)	3492(3)	4393(3)	63(2)
O(7)	12360(18)	7278(7)	3062(5)	190(6)
O(8)	10531(20)	7102(7)	2590(7)	227(8)
N(1)	3232(7)	5349(3)	5175(3)	39(2)
N(2)	11664(17)	6936(9)	2777(6)	128(5)
C(1)	3712(18)	6431(8)	7402(6)	140(6)

C(2)	2748(18)	6640(7)	7041(5)	126(6)
C(3)	1844(14)	6440(5)	6169(5)	70(3)
C(4)	2051(10)	6100(4)	5667(4)	45(2)
C(5)	1179(11)	6211(5)	5239(5)	65(3)
C(6)	1307(10)	5886(5)	4786(5)	64(3)
C(7)	2353(11)	5452(4)	4756(4)	53(3)
C(8)	3090(10)	5681(4)	5625(4)	47(2)
C(9)	4334(8)	4877(4)	5136(4)	45(2)
C(10)	4911(10)	3008(5)	4452(5)	54(3)
C(11)	5099(12)	2567(6)	4054(4)	69(3)
C(12)	6028(14)	2092(5)	4153(6)	80(4)
C(13)	6733(13)	2051(6)	4627(6)	76(3)
C(14)	6537(10)	2472(5)	5006(5)	63(3)
C(15)	5602(10)	2945(5)	4928(4)	49(3)
C(16)	5649(12)	3219(4)	5851(4)	66(3)
C(17)	4956(11)	3668(4)	6231(4)	63(3)
C(18)	5363(11)	4596(5)	6638(4)	67(3)
C(19)	6398(11)	5111(5)	6663(4)	63(3)
C(20)	7430(12)	5900(5)	6139(5)	87(4)
C(21)	3238(13)	3544(5)	3899(5)	84(4)
C(22)	12143(19)	6361(7)	2652(7)	147(7)
B(1)	9098(21)	5320(9)	3510(8)	85(5)
F(1)	8209(9)	5450(4)	3940(4)	154(4)
F(2)	9948(31)	4966(13)	3802(10)	145(9)
F(2A)	8568(35)	5631(26)	3125(13)	256(20)
F(3)	8279(29)	4999(22)	3210(17)	187(15)
F(3A)	10429(24)	5531(27)	3608(13)	209(22)
F(4)	9747(42)	5764(11)	3321(14)	165(11)
F(4A)	9324(54)	4817(21)	3298(20)	243(18)

Table A-8. Bonding Parameters for [2]Pseudorotaxane **2f:3c**.

Bond	Distance (Å)	Bond	Distance (Å)
O(1)-C(3)	1.313(13)	C(10)-C(15)	1.364(13)
O(1)-C(2)	1.458(12)	C(10)-C(11)	1.416(14)
O(2)-C(3)	1.219(11)	C(11)-C(12)	1.40(2)
O(3)-C(15)	1.379(11)	C(12)-C(13)	1.36(2)
O(3)-C(16)	1.453(11)	C(13)-C(14)	1.353(14)
O(4)-C(17)	1.412(10)	C(14)-C(15)	1.389(13)
O(4)-C(18)	1.428(11)	C(16)-C(17)	1.531(13)
O(5)-C(19)	1.411(11)	C(18)-C(19)	1.506(13)
O(5)-C(20)	1.441(12)	C(20)-C(21)'	1.398(14)
O(6)-C(10)	1.381(11)	C(21)-C(20)'	1.398(14)
O(6)-C(21)	1.439(11)	B(1)-F(4)	1.26(2)
O(7)-N(2)	1.23(2)	B(1)-F(4A)	1.27(4)

O(8)-N(2)	1.22(2)	B(1)-F(2A)	1.29(3)
N(1)-C(7)	1.354(11)	B(1)-F(3)	1.29(3)
N(1)-C(8)	1.358(11)	B(1)-F(2)	1.34(3)
N(1)-C(9)	1.480(10)	B(1)-F(3A)	1.35(3)
N(2)-C(22)	1.40(2)	B(1)-F(1)	1.39(2)
C(1)-C(2)	1.36(2)	F(2)-F(4A)	1.43(5)
C(3)-C(4)	1.486(14)	F(2)-F(3A)	1.43(5)
C(4)-C(8)	1.356(12)	F(2A)-F(4)	1.24(4)
C(4)-C(5)	1.371(13)	F(2A)-F(3)	1.46(5)
C(5)-C(6)	1.356(13)	F(3)-F(4A)	1.08(4)
C(6)-C(7)	1.381(13)	F(3A)-F(4)	1.09(4)
C(9)-C(9)'	1.52(2)		

Bonds	Angle (°)	Bonds	Angle (°)
C(3)-O(1)-C(2)	118.9(10)	C(12)-C(11)-C(10)	119.0(11)
C(15)-O(3)-C(16)	115.6(8)	C(13)-C(12)-C(11)	120.5(12)
C(17)-O(4)-C(18)	111.7(7)	C(14)-C(13)-C(12)	120.1(12)
C(19)-O(5)-C(20)	115.1(7)	C(13)-C(14)-C(15)	121.3(11)
C(10)-O(6)-C(21)	117.5(9)	C(10)-C(15)-O(3)	116.1(9)
C(7)-N(1)-C(8)	119.5(8)	C(10)-C(15)-C(14)	119.9(10)
C(7)-N(1)-C(9)	119.5(8)	O(3)-C(15)-C(14)	123.9(10)
C(8)-N(1)-C(9)	121.0(8)	O(3)-C(16)-C(17)	109.9(8)
O(8)-N(2)-O(7)	120(2)	O(4)-C(17)-C(16)	107.9(8)
O(8)-N(2)-C(22)	118(2)	O(4)-C(18)-C(19)	109.4(8)
O(7)-N(2)-C(22)	122(2)	O(5)-C(19)-C(18)	110.1(8)
C(1)-C(2)-O(1)	113.3(13)	C(21)'-C(20)-O(5)	113.2(9)
O(2)-C(3)-O(1)	123.3(11)	C(20)'-C(21)-O(6)	110.9(10)
O(2)-C(3)-C(4)	123.1(12)	F(4A)-B(1)-F(2A)	103(4)
O(1)-C(3)-C(4)	113.6(10)	F(4)-B(1)-F(3)	120(3)
C(8)-C(4)-C(5)	119.3(9)	F(4)-B(1)-F(2)	113(3)
C(8)-C(4)-C(3)	121.0(10)	F(3)-B(1)-F(2)	110(3)
C(5)-C(4)-C(3)	119.7(11)	F(4A)-B(1)-F(3A)	104(3)
C(6)-C(5)-C(4)	120.4(9)	F(2A)-B(1)-F(3A)	108(3)
C(5)-C(6)-C(7)	119.2(10)	F(4)-B(1)-F(1)	114(2)
N(1)-C(7)-C(6)	120.4(9)	F(4A)-B(1)-F(1)	128(3)
C(4)-C(8)-N(1)	121.0(9)	F(2A)-B(1)-F(1)	104(2)
N(1)-C(9)-C(9)'	109.7(8)	F(3)-B(1)-F(1)	102(2)
C(15)-C(10)-O(6)	117.5(10)	F(2)-B(1)-F(1)	93(2)
C(15)-C(10)-C(11)	119.1(10)	F(3A)-B(1)-F(1)	110(2)
O(6)-C(10)-C(11)	123.3(10)		

Symmetry transformation used to generate equivalent atoms: -x+1,-y+1,-z+1

Table A-9. Anisotropic thermal parameters ($Å^2 \times 10^3$) for [2]-Pseudorotaxane **2f:3c**.

Atom	U_{11}	U_{22}	U_{33}	U_{23}	U_{13}	U_{12}
O(1)	67(5)	93(6)	66(5)	-13(5)	-1(4)	11(5)
O(2)	92(6)	94(6)	103(6)	-24(5)	11(5)	37(6)
O(3)	59(4)	56(4)	55(4)	8(4)	-16(3)	-1(3)
O(4)	59(4)	61(5)	51(4)	-7(4)	4(3)	-15(4)
O(5)	67(5)	61(5)	66(5)	19(4)	-31(4)	-14(4)
O(6)	59(4)	63(5)	67(5)	13(4)	-17(4)	-6(4)
O(7)	215(14)	209(14)	146(11)	-71(10)	-35(10)	-11(11)
O(8)	223(17)	228(17)	231(16)	3(13)	-67(14)	83(14)
N(1)	27(4)	46(5)	43(5)	6(5)	4(4)	4(4)
N(2)	114(11)	175(17)	95(10)	21(11)	-21(9)	15(12)
C(1)	132(14)	220(19)	69(10)	-18(12)	4(10)	24(13)
C(2)	157(15)	163(15)	58(9)	-60(10)	24(10)	20(12)
C(3)	63(8)	57(8)	91(10)	10(7)	24(8)	27(7)
C(4)	37(6)	54(7)	45(7)	-5(6)	7(5)	0(6)
C(5)	53(7)	52(7)	91(9)	0(7)	0(7)	22(5)
C(6)	38(7)	73(8)	81(9)	0(7)	-16(6)	14(6)
C(7)	48(6)	57(7)	54(7)	-1(6)	-3(6)	0(6)
C(8)	36(6)	56(7)	49(7)	3(6)	10(5)	-6(6)
C(9)	32(5)	37(5)	68(7)	11(5)	0(4)	13(5)
C(10)	45(6)	53(7)	64(8)	14(7)	-1(6)	-9(6)
C(11)	69(8)	84(9)	52(7)	-9(7)	2(6)	-19(8)
C(12)	67(8)	54(8)	120(13)	-5(8)	48(9)	-14(7)
C(13)	64(8)	67(9)	96(10)	-7(9)	18(8)	4(7)
C(14)	45(6)	68(8)	76(8)	8(7)	7(6)	0(6)
C(15)	36(6)	54(7)	58(8)	-7(6)	1(5)	-9(6)
C(16)	76(8)	52(7)	69(8)	12(6)	-15(6)	-8(6)
C(17)	75(7)	60(7)	54(7)	4(6)	1(6)	-31(7)
C(18)	60(7)	72(8)	68(8)	9(7)	-6(6)	-2(7)
C(19)	60(7)	71(8)	58(7)	-22(6)	-7(5)	1(6)
C(20)	58(7)	69(9)	133(11)	7(8)	-52(7)	-13(7)
C(21)	75(8)	79(9)	98(10)	29(7)	-40(7)	-13(7)
C(22)	162(16)	91(12)	189(18)	-11(12)	-53(13)	38(12)
B(1)	75(14)	78(13)	102(14)	-4(13)	6(13)	3(14)
F(1)	111(7)	158(8)	194(9)	-13(7)	39(7)	-12(6)
F(2)	100(16)	142(18)	192(24)	82(19)	11(15)	56(14)
F(2A)	134(24)	420(57)	215(27)	196(35)	-74(20)	-10(32)
F(3)	109(18)	218(33)	235(30)	-118(27)	4(21)	-90(24)
F(3A)	45(13)	444(64)	137(24)	-107(31)	0(12)	-67(21)
F(4)	153(28)	144(18)	198(29)	68(18)	-3(21)	-91(20)
F(4A)	204(38)	232(36)	294(45)	-123(30)	-53(40)	29(32)

The anisotropic displacement factor exponent takes the form: $-2\pi^2[h^2 a^{*2} U11 + ... + 2hka^*b^*U12]$

Table A-10. Hydrogen coordinates (x 10^4) and isotropic thermal parameters $Å^2$ x 10^3 for [2]Pseudorotaxane **2f:3c**.

Atom	x	y	z	U(eq)
H(1A)	3591(18)	6638(8)	7734(6)	211
H(1B)	4666(18)	6496(8)	7271(6)	211
H(1C)	3561(18)	6012(8)	7457(6)	211
H(2A)	2893(18)	7065(7)	6996(5)	151
H(2B)	1789(18)	6581(7)	7180(5)	151
H(5A)	495(11)	6512(5)	5259(5)	78
H(6A)	699(10)	5954(5)	4499(5)	77
H(7A)	2454(11)	5229(4)	4446(4)	64
H(8A)	3715(10)	5620(4)	5908(4)	57
H(9A)	3961(8)	4543(4)	4933(4)	55
H(9B)	4579(8)	4735(4)	5490(4)	55
H(11A)	4612(12)	2593(6)	3732(4)	82
H(12A)	6166(14)	1801(5)	3894(6)	96
H(13A)	7350(13)	1733(6)	4690(6)	91
H(14A)	7038(10)	2443(5)	5325(5)	75
H(16A)	6677(12)	3213(4)	5907(4)	79
H(16B)	5279(12)	2823(4)	5923(4)	79
H(17A)	4003(11)	3771(4)	6107(4)	75
H(17B)	4876(11)	3498(4)	6585(4)	75
H(18A)	5314(11)	4401(5)	6983(4)	80
H(18B)	4414(11)	4742(5)	6549(4)	80
H(19A)	6107(11)	5385(5)	6942(4)	76
H(19B)	7348(11)	4964(5)	6749(4)	76
H(20A)	8033(12)	5895(5)	6454(5)	104
H(20B)	8044(12)	5844(5)	5832(5)	104
H(21A)	3894(13)	3493(5)	3603(5)	101
H(21B)	2521(13)	3232(5)	3878(5)	101
H(22A)	13044(19)	6289(7)	2825(7)	221
H(22B)	12262(19)	6327(7)	2273(7)	221
H(22C)	11453(19)	6074(7)	2772(7)	221

Table A-11. Details of X-ray Data Collection, Solution and Refinement for [2]Pseudorotaxane **2g:3c**.

Empirical formula	$C_{40}H_{54}B_2F_8N_2O_{12}$
Formula weight	928.47
Temperature, K	293(2)
Wavelength, Å	0.71073
Crystal system	Orthorhombic
Space group	*Pbca* (No. 62)
a, Å	9.3357(1)
b, Å	22.4319(3)
c, Å	25.0932(2)
V, Å^3	5255.0(1)
Z	4
ρ_{calcd}, Mg m^{-3}	1.174
μ, mm^{-1}	0.103
F(000)	1944
Crystal size, mm	0.18 x 0.26 x 0.32
θ–range for data collection, °	1.62 to 22.00
Limiting indices	$-10 \le h \le 12$, $-29 \le k \le 22$, $-26 \le l \le 32$
Reflections collected	15012
Independent reflections	2448 [R(int) = 0.1350]
Refinement method	Full-matrix least-squares on F^2
Data / restraints / parameters	2440 / 0 / 361
Goodness-of-fit on F^2	1.262
Final R indices [$I>2\sigma(I)$]	$R_1 = 0.1300$, $wR_2 = 0.2637$
R indices (all data)	$R_1 = 0.1648$, $wR_2 = 0.2961$
Largest differences; peak and hole	0.220 and -0.260 eÅ^{-3}

Table A-12. Atomic coordinates (x 10^4) and equivalent isotropic displacement parameters (Å^2 x 10^3) for [2]Pseudorotaxane **2g:3c**.

Atom	x	y	z	U(eq)
O(1)	2857(8)	6349(3)	6523(3)	75(2)
O(2)	829(9)	6772(4)	6245(3)	96(3)
O(3)	5340(7)	3382(3)	5302(3)	56(2)
O(4)	5831(7)	4181(3)	6243(2)	57(2)
O(5)	6432(7)	5411(3)	6169(3)	65(2)
O(6)	4011(7)	3492(3)	4393(3)	63(2)
O(7)	12360(18)	7278(7)	3062(5)	190(6)
O(8)	10531(20)	7102(7)	2590(7)	227(8)
N(1)	3232(7)	5349(3)	5175(3)	39(2)
N(2)	11664(17)	6936(9)	2777(6)	128(5)
C(1)	3712(18)	6431(8)	7402(6)	140(6)

C(2)	2748(18)	6640(7)	7041(5)	126(6)
C(3)	1844(14)	6440(5)	6169(5)	70(3)
C(4)	2051(10)	6100(4)	5667(4)	45(2)
C(5)	1179(11)	6211(5)	5239(5)	65(3)
C(6)	1307(10)	5886(5)	4786(5)	64(3)
C(7)	2353(11)	5452(4)	4756(4)	53(3)
C(8)	3090(10)	5681(4)	5625(4)	47(2)
C(9)	4334(8)	4877(4)	5136(4)	45(2)
C(10)	4911(10)	3008(5)	4452(5)	54(3)
C(11)	5099(12)	2567(6)	4054(4)	69(3)
C(12)	6028(14)	2092(5)	4153(6)	80(4)
C(13)	6733(13)	2051(6)	4627(6)	76(3)
C(14)	6537(10)	2472(5)	5006(5)	63(3)
C(15)	5602(10)	2945(5)	4928(4)	49(3)
C(16)	5649(12)	3219(4)	5851(4)	66(3)
C(17)	4956(11)	3668(4)	6231(4)	63(3)
C(18)	5363(11)	4596(5)	6638(4)	67(3)
C(19)	6398(11)	5111(5)	6663(4)	63(3)
C(20)	7430(12)	5900(5)	6139(5)	87(4)
C(21)	3238(13)	3544(5)	3899(5)	84(4)
C(22)	12143(19)	6361(7)	2652(7)	147(7)
B(1)	9098(21)	5320(9)	3510(8)	85(5)
F(1)	8209(9)	5450(4)	3940(4)	154(4)
F(2)	9948(31)	4966(13)	3802(10)	145(9)
F(2A)	8568(35)	5631(26)	3125(13)	256(20)
F(3)	8279(29)	4999(22)	3210(17)	187(15)
F(3A)	10429(24)	5531(27)	3608(13)	209(22)
F(4)	9747(42)	5764(11)	3321(14)	165(11)
F(4A)	9324(54)	4817(21)	3298(20)	243(18)

Table A-13. Bonding Parameters for [2]Pseudorotaxane **2g:3c**.

Bond	Distance (Å)	Bond	Distance (Å)
O(1)-C(3)	1.313(13)	C(10)-C(15)	1.364(13)
O(1)-C(2)	1.458(12)	C(10)-C(11)	1.416(14)
O(2)-C(3)	1.219(11)	C(11)-C(12)	1.40(2)
O(3)-C(15)	1.379(11)	C(12)-C(13)	1.36(2)
O(3)-C(16)	1.453(11)	C(13)-C(14)	1.353(14)
O(4)-C(17)	1.412(10)	C(14)-C(15)	1.389(13)
O(4)-C(18)	1.428(11)	C(16)-C(17)	1.531(13)
O(5)-C(19)	1.411(11)	C(18)-C(19)	1.506(13)
O(5)-C(20)	1.441(12)	C(20)-C(21)'	1.398(14)
O(6)-C(10)	1.381(11)	C(21)-C(20)'	1.398(14)
O(6)-C(21)	1.439(11)	B(1)-F(4)	1.26(2)
O(7)-N(2)	1.23(2)	B(1)-F(4A)	1.27(4)

O(8)-N(2)	1.22(2)	B(1)-F(2A)	1.29(3)
N(1)-C(7)	1.354(11)	B(1)-F(3)	1.29(3)
N(1)-C(8)	1.358(11)	B(1)-F(2)	1.34(3)
N(1)-C(9)	1.480(10)	B(1)-F(3A)	1.35(3)
N(2)-C(22)	1.40(2)	B(1)-F(1)	1.39(2)
C(1)-C(2)	1.36(2)	F(2)-F(4A)	1.43(5)
C(3)-C(4)	1.486(14)	F(2)-F(3A)	1.43(5)
C(4)-C(8)	1.356(12)	F(2A)-F(4)	1.24(4)
C(4)-C(5)	1.371(13)	F(2A)-F(3)	1.46(5)
C(5)-C(6)	1.356(13)	F(3)-F(4A)	1.08(4)
C(6)-C(7)	1.381(13)	F(3A)-F(4)	1.09(4)
C(9)-C(9)'	1.52(2)		

Bonds	Angle (°)	Bonds	Angle (°)
C(3)-O(1)-C(2)	118.9(10)	C(12)-C(11)-C(10)	119.0(11)
C(15)-O(3)-C(16)	115.6(8)	C(13)-C(12)-C(11)	120.5(12)
C(17)-O(4)-C(18)	111.7(7)	C(14)-C(13)-C(12)	120.1(12)
C(19)-O(5)-C(20)	115.1(7)	C(13)-C(14)-C(15)	121.3(11)
C(10)-O(6)-C(21)	117.5(9)	C(10)-C(15)-O(3)	116.1(9)
C(7)-N(1)-C(8)	119.5(8)	C(10)-C(15)-C(14)	119.9(10)
C(7)-N(1)-C(9)	119.5(8)	O(3)-C(15)-C(14)	123.9(10)
C(8)-N(1)-C(9)	121.0(8)	O(3)-C(16)-C(17)	109.9(8)
O(8)-N(2)-O(7)	120(2)	O(4)-C(17)-C(16)	107.9(8)
O(8)-N(2)-C(22)	118(2)	O(4)-C(18)-C(19)	109.4(8)
O(7)-N(2)-C(22)	122(2)	O(5)-C(19)-C(18)	110.1(8)
C(1)-C(2)-O(1)	113.3(13)	C(21)'-C(20)-O(5)	113.2(9)
O(2)-C(3)-O(1)	123.3(11)	C(20)'-C(21)-O(6)	110.9(10)
O(2)-C(3)-C(4)	123.1(12)	F(4A)-B(1)-F(2A)	103(4)
O(1)-C(3)-C(4)	113.6(10)	F(4)-B(1)-F(3)	120(3)
C(8)-C(4)-C(5)	119.3(9)	F(4)-B(1)-F(2)	113(3)
C(8)-C(4)-C(3)	121.0(10)	F(3)-B(1)-F(2)	110(3)
C(5)-C(4)-C(3)	119.7(11)	F(4A)-B(1)-F(3A)	104(3)
C(6)-C(5)-C(4)	120.4(9)	F(2A)-B(1)-F(3A)	108(3)
C(5)-C(6)-C(7)	119.2(10)	F(4)-B(1)-F(1)	114(2)
N(1)-C(7)-C(6)	120.4(9)	F(4A)-B(1)-F(1)	128(3)
C(4)-C(8)-N(1)	121.0(9)	F(2A)-B(1)-F(1)	104(2)
N(1)-C(9)-C(9)'	109.7(8)	F(3)-B(1)-F(1)	102(2)
C(15)-C(10)-O(6)	117.5(10)	F(2)-B(1)-F(1)	93(2)
C(15)-C(10)-C(11)	119.1(10)	F(3A)-B(1)-F(1)	110(2)
O(6)-C(10)-C(11)	123.3(10)		

Symmetry transformation used to generate equivalent atoms: -x+1,-y+1,-z+1

Table A-14. Anisotropic thermal parameters ($Å^2 \times 10^3$) for [2]-Pseudorotaxane **2g:3c**.

Atom	U_{11}	U_{22}	U_{33}	U_{23}	U_{13}	U_{12}
O(1)	67(5)	93(6)	66(5)	-13(5)	-1(4)	11(5)
O(2)	92(6)	94(6)	103(6)	-24(5)	11(5)	37(6)
O(3)	59(4)	56(4)	55(4)	8(4)	-16(3)	-1(3)
O(4)	59(4)	61(5)	51(4)	-7(4)	4(3)	-15(4)
O(5)	67(5)	61(5)	66(5)	19(4)	-31(4)	-14(4)
O(6)	59(4)	63(5)	67(5)	13(4)	-17(4)	-6(4)
O(7)	215(14)	209(14)	146(11)	-71(10)	-35(10)	-11(11)
O(8)	223(17)	228(17)	231(16)	3(13)	-67(14)	83(14)
N(1)	27(4)	46(5)	43(5)	6(5)	4(4)	4(4)
N(2)	114(11)	175(17)	95(10)	21(11)	-21(9)	15(12)
C(1)	132(14)	220(19)	69(10)	-18(12)	4(10)	24(13)
C(2)	157(15)	163(15)	58(9)	-60(10)	24(10)	20(12)
C(3)	63(8)	57(8)	91(10)	10(7)	24(8)	27(7)
C(4)	37(6)	54(7)	45(7)	-5(6)	7(5)	0(6)
C(5)	53(7)	52(7)	91(9)	0(7)	0(7)	22(5)
C(6)	38(7)	73(8)	81(9)	0(7)	-16(6)	14(6)
C(7)	48(6)	57(7)	54(7)	-1(6)	-3(6)	0(6)
C(8)	36(6)	56(7)	49(7)	3(6)	10(5)	-6(6)
C(9)	32(5)	37(5)	68(7)	11(5)	0(4)	13(5)
C(10)	45(6)	53(7)	64(8)	14(7)	-1(6)	-9(6)
C(11)	69(8)	84(9)	52(7)	-9(7)	2(6)	-19(8)
C(12)	67(8)	54(8)	120(13)	-5(8)	48(9)	-14(7)
C(13)	64(8)	67(9)	96(10)	-7(9)	18(8)	4(7)
C(14)	45(6)	68(8)	76(8)	8(7)	7(6)	0(6)
C(15)	36(6)	54(7)	58(8)	-7(6)	1(5)	-9(6)
C(16)	76(8)	52(7)	69(8)	12(6)	-15(6)	-8(6)
C(17)	75(7)	60(7)	54(7)	4(6)	1(6)	-31(7)
C(18)	60(7)	72(8)	68(8)	9(7)	-6(6)	-2(7)
C(19)	60(7)	71(8)	58(7)	-22(6)	-7(5)	1(6)
C(20)	58(7)	69(9)	133(11)	7(8)	-52(7)	-13(7)
C(21)	75(8)	79(9)	98(10)	29(7)	-40(7)	-13(7)
C(22)	162(16)	91(12)	189(18)	-11(12)	-53(13)	38(12)
B(1)	75(14)	78(13)	102(14)	-4(13)	6(13)	3(14)
F(1)	111(7)	158(8)	194(9)	-13(7)	39(7)	-12(6)
F(2)	100(16)	142(18)	192(24)	82(19)	11(15)	56(14)
F(2A)	134(24)	420(57)	215(27)	196(35)	-74(20)	-10(32)
F(3)	109(18)	218(33)	235(30)	-118(27)	4(21)	-90(24)
F(3A)	45(13)	444(64)	137(24)	-107(31)	0(12)	-67(21)
F(4)	153(28)	144(18)	198(29)	68(18)	-3(21)	-91(20)
F(4A)	204(38)	232(36)	294(45)	-123(30)	-53(40)	29(32)

The anisotropic displacement factor exponent takes the form: $-2\pi^2[h^2\, a^{*2}\, U11 + ... + 2hka^*b^*U12]$

Table A-15. Hydrogen coordinates (x 10^4) and isotropic thermal parameters $Å^2$ x 10^3 for [2]Pseudorotaxane **2g:3c**.

Atom	x	y	z	U(eq)
H(1A)	3591(18)	6638(8)	7734(6)	211
H(1B)	4666(18)	6496(8)	7271(6)	211
H(1C)	3561(18)	6012(8)	7457(6)	211
H(2A)	2893(18)	7065(7)	6996(5)	151
H(2B)	1789(18)	6581(7)	7180(5)	151
H(5A)	495(11)	6512(5)	5259(5)	78
H(6A)	699(10)	5954(5)	4499(5)	77
H(7A)	2454(11)	5229(4)	4446(4)	64
H(8A)	3715(10)	5620(4)	5908(4)	57
H(9A)	3961(8)	4543(4)	4933(4)	55
H(9B)	4579(8)	4735(4)	5490(4)	55
H(11A)	4612(12)	2593(6)	3732(4)	82
H(12A)	6166(14)	1801(5)	3894(6)	96
H(13A)	7350(13)	1733(6)	4690(6)	91
H(14A)	7038(10)	2443(5)	5325(5)	75
H(16A)	6677(12)	3213(4)	5907(4)	79
H(16B)	5279(12)	2823(4)	5923(4)	79
H(17A)	4003(11)	3771(4)	6107(4)	75
H(17B)	4876(11)	3498(4)	6585(4)	75
H(18A)	5314(11)	4401(5)	6983(4)	80
H(18B)	4414(11)	4742(5)	6549(4)	80
H(19A)	6107(11)	5385(5)	6942(4)	76
H(19B)	7348(11)	4964(5)	6749(4)	76
H(20A)	8033(12)	5895(5)	6454(5)	104
H(20B)	8044(12)	5844(5)	5832(5)	104
H(21A)	3894(13)	3493(5)	3603(5)	101
H(21B)	2521(13)	3232(5)	3878(5)	101
H(22A)	13044(19)	6289(7)	2825(7)	221
H(22B)	12262(19)	6327(7)	2273(7)	221
H(22C)	11453(19)	6074(7)	2772(7)	221

Table A-16. Details of X-ray Data Collection, Solution and Refinement for [2]-Rotaxane 7.

Empirical formula	$C_{68}H_{82}B_4F_{16}N_4O_8$
Crystal	Orange blocks
Formula weight	1430.62
Temperature	293(2) K
Wavelength, , Å	0.71073
Crystal system	Triclinic
Space group	*P-1* (No.2)
A, Å	13.9669(3)
b, Å	17.0627(3)
c, Å	17.0640(3)
α, °	86.686(1)
β, °	80.281(1)
γ, °	75.390(1)
V, Å^3	3878.1(1)
Z	2
ρ_{calcd}, Mg m^{-3}	1.225
μ, mm^{-1}	0.099
F(000)	1492
Crystal size, mm	0.24 x 0.26 x 0.34
θ–range for data collection, °	1.21 to 22.50
Limiting indices	$-16 \le h \le 18$, $-22 \le k \le 22$, $-22 \le k \le 17$
Reflections collected	15271
Independent reflections	9521 [R(int) = 0.0293]
Refinement method	Full-matrix least-squares (F^2)
Data / restraints / parameters	9509 / 795 / 973
Goodness-of-fit on F^2	0.908
Final R indices [I>2σ(I)]	R_1 = 0.1297, *w*R2 = 0.3690
R indices (all data)	R_1 = 0.1847, *w*R2 = 0.4310
Largest difference peak and hole	0.934 and -0.607 e Å^{-3}

Table A-18. Atomic coordinates (x 10^4) and equivalent isotropic displacement parameters (Å^2 x 10^3) for [2]-Rotaxane 7.

Atom	x	y	z	*U*(eq)
O(1)	4481(6)	3216(4)	-29(3)	101(2)
O(2)	6388(5)	3082(5)	608(4)	126(2)
O(3)	6692(6)	2928(4)	2172(5)	138(3)
O(4)	5880(5)	4239(4)	3318(3)	103(2)
O(5)	4057(5)	5112(3)	3743(3)	92(2)
O(6)	2245(4)	5097(3)	3060(4)	101(2)

O(7)	2134(5)	5599(4)	1477(5)	116(2)
O(8)	2775(5)	4302(5)	281(3)	101(2)
N(1)	7398(6)	7866(4)	2539(4)	81(2)
N(2)	4917(4)	5012(3)	1645(3)	58(1)
N(3)	3759(4)	3229(3)	1992(3)	59(1)
N(4)	789(5)	511(4)	1953(4)	81(2)
C(1)	9888(7)	7282(6)	5523(5)	98(3)
C(2)	9593(13)	6415(10)	5809(9)	201(7)
C(3)	9453(10)	7863(8)	6196(7)	156(5)
C(4)	10961(9)	7087(13)	5387(8)	220(9)
C(5)	9412(6)	7567(5)	4792(5)	79(2)
C(6)	8374(6)	7738(6)	4821(5)	103(3)
C(7)	7935(7)	8006(6)	4180(5)	104(3)
C(8)	8461(6)	8136(4)	3458(5)	80(2)
C(9)	9477(7)	7971(5)	3413(5)	91(2)
C(10)	9949(6)	7687(5)	4065(5)	88(2)
C(11)	7968(7)	8452(5)	2738(5)	97(3)
C(12)	7929(6)	7116(5)	2306(5)	87(2)
C(13)	7458(5)	6549(4)	2121(4)	73(2)
C(14)	6431(5)	6731(4)	2192(4)	58(2)
C(15)	5898(6)	7510(4)	2437(5)	80(2)
C(16)	6410(7)	8065(4)	2586(5)	88(2)
C(17)	5891(5)	6131(3)	2006(3)	51(2)
C(18)	6405(5)	5399(4)	1657(4)	66(2)
C(19)	5902(5)	4850(4)	1487(4)	69(2)
C(20)	4397(5)	5711(4)	1971(4)	71(2)
C(21)	4857(5)	6282(4)	2168(4)	69(2)
C(22)	4372(5)	4404(4)	1457(4)	70(2)
C(23)	4354(5)	3797(4)	2131(4)	70(2)
C(24)	2771(6)	3475(4)	2105(4)	71(2)
C(25)	2169(5)	2961(4)	2014(4)	69(2)
C(26)	2630(5)	2160(4)	1836(4)	59(2)
C(27)	3663(5)	1922(4)	1710(4)	69(2)
C(28)	4203(5)	2469(4)	1781(4)	67(2)
C(29)	2003(5)	1558(4)	1828(4)	63(2)
C(30)	2306(6)	791(4)	2112(5)	87(2)
C(31)	1692(7)	263(4)	2172(6)	105(3)
C(32)	475(5)	1257(5)	1655(4)	75(2)
C(33)	1066(5)	1794(4)	1605(4)	75(2)
C(34)	98(6)	-50(5)	2066(6)	96(3)
C(35)	-660(6)	136(4)	2805(6)	91(3)
C(36)	-375(7)	-33(6)	3555(8)	108(3)
C(37)	-1065(8)	84(6)	4231(7)	112(3)
C(38)	-2086(6)	435(5)	4221(6)	92(3)
C(39)	-2355(6)	599(5)	3469(7)	98(3)
C(40)	-1660(6)	454(5)	2774(6)	91(2)

C(41)	-2883(7)	626(5)	4974(6)	100(3)
C(42)	-3300(10)	1527(7)	5061(8)	157(4)
C(43)	-2475(10)	248(10)	5745(9)	190(6)
C(44)	-3748(8)	244(8)	4916(8)	153(4)
C(45)	2697(10)	3597(8)	48(5)	108(3)
C(46)	1839(10)	3373(10)	-60(6)	142(4)
C(47)	1781(21)	2666(20)	-269(11)	237(14)
C(48)	2679(19)	2057(12)	-398(9)	181(9)
C(49)	3619(12)	2198(7)	-330(5)	145(4)
C(50)	3602(12)	3008(7)	-105(5)	108(3)
C(51)	5443(10)	2633(7)	-272(5)	126(4)
C(52)	6229(8)	3025(8)	-202(5)	122(3)
C(53)	7162(8)	2521(6)	874(7)	119(3)
C(54)	7339(8)	2530(8)	1616(8)	138(4)
C(55)	6816(10)	2906(7)	2979(7)	141(4)
C(56)	6720(10)	3602(9)	3333(7)	153(5)
C(57)	5762(9)	4952(6)	3706(5)	93(3)
C(58)	6571(8)	5227(8)	3848(6)	120(3)
C(59)	6407(13)	5961(9)	4235(7)	132(4)
C(60)	5428(14)	6422(8)	4461(6)	135(4)
C(61)	4677(9)	6144(7)	4310(6)	115(3)
C(62)	4825(8)	5406(6)	3926(5)	91(2)
C(63)	3077(7)	5502(6)	4085(5)	101(3)
C(64)	2386(8)	5013(6)	3859(6)	110(3)
C(65)	1544(8)	5826(6)	2864(6)	117(3)
C(66)	1286(9)	5784(7)	2078(9)	142(4)
C(67)	1962(9)	5616(8)	646(8)	145(4)
C(68)	1836(11)	4881(11)	409(8)	153(5)
B(1)	2592(8)	7926(6)	2584(8)	119(3)
F(1)	2499(9)	7464(6)	1994(5)	250(5)
F(2)	3368(5)	8245(5)	2340(7)	232(4)
F(3)	2791(7)	7367(5)	3155(5)	218(4)
F(4)	1774(4)	8486(3)	2841(4)	151(2)
B(2)	4124(9)	1993(8)	3802(7)	129(4)
F(5)	5017(5)	1845(7)	3317(5)	225(4)
F(6)	3613(9)	2764(5)	3654(5)	246(5)
F(7)	3576(8)	1521(7)	3558(5)	239(4)
F(8)	4168(5)	1866(5)	4566(4)	174(3)
B(3)	-785(11)	4334(12)	1776(12)	135(6)
F(9)	-641(11)	4981(8)	1318(9)	176(5)
F(10)	-1212(13)	4558(10)	2512(8)	185(6)
F(11)	-1428(13)	4060(12)	1411(11)	181(6)
F(12)	106(11)	3788(11)	1713(16)	226(10)
B(3A)	-624(15)	4051(13)	1758(13)	172(8)
F(9A)	-719(10)	3421(8)	2247(10)	187(6)
F(10A)	-344(25)	3784(16)	1015(11)	299(12)

F(11A)	138(13)	4283(11)	1995(16)	212(9)
F(12A)	-1463(12)	4603(11)	1852(19)	255(11)
B(4)	-151(17)	1670(15)	-702(13)	322(11)
F(13)	-907(14)	1292(15)	-714(16)	502(14)
F(14)	-224(15)	2239(11)	-1274(8)	366(8)
F(15)	-354(13)	1939(16)	51(8)	487(14)
F(16)	743(12)	1120(10)	-806(14)	431(11)
O(1W)	5307(14)	56(7)	2780(11)	305(8)
O(2W)	5987(14)	722(11)	1218(20)	446(18)
O(3W)	-1549(20)	486(12)	653(13)	422(14)

Table A-19. Bonding parameters for [2]-Rotaxane **7**.

Bond	Distance (Å)	Bond	Distance (Å)
O(1)-C(50)	1.388(12)	C(29)-C(30)	1.358(9)
O(1)-C(51)	1.467(12)	C(29)-C(33)	1.380(9)
O(2)-C(53)	1.373(12)	C(30)-C(31)	1.380(10)
O(2)-C(52)	1.449(11)	C(32)-C(33)	1.371(9)
O(3)-C(54)	1.285(12)	C(34)-C(35)	1.496(12)
O(3)-C(55)	1.414(11)	C(35)-C(40)	1.374(11)
O(4)-C(56)	1.386(12)	C(35)-C(36)	1.397(13)
O(4)-C(57)	1.379(11)	C(36)-C(37)	1.361(14)
O(5)-C(62)	1.380(11)	C(37)-C(38)	1.403(12)
O(5)-C(63)	1.404(10)	C(38)-C(39)	1.391(12)
O(6)-C(65)	1.438(11)	C(38)-C(41)	1.544(13)
O(6)-C(64)	1.405(11)	C(39)-C(40)	1.391(12)
O(7)-C(66)	1.413(13)	C(41)-C(42)	1.506(14)
O(7)-C(67)	1.475(14)	C(41)-C(44)	1.529(13)
O(8)-C(45)	1.323(11)	C(41)-C(43)	1.562(14)
O(8)-C(68)	1.42(2)	C(45)-C(46)	1.39(2)
N(1)-C(16)	1.325(9)	C(45)-C(50)	1.398(14)
N(1)-C(12)	1.351(10)	C(46)-C(47)	1.30(3)
N(1)-C(11)	1.511(9)	C(47)-C(48)	1.41(3)
N(2)-C(19)	1.316(8)	C(48)-C(49)	1.42(2)
N(2)-C(20)	1.327(8)	C(49)-C(50)	1.450(14)
N(2)-C(22)	1.508(8)	C(51)-C(52)	1.446(14)
N(3)-C(24)	1.321(8)	C(53)-C(54)	1.332(14)
N(3)-C(28)	1.330(8)	C(55)-C(56)	1.33(2)
N(3)-C(23)	1.478(8)	C(57)-C(62)	1.345(12)
N(4)-C(32)	1.337(9)	C(57)-C(58)	1.389(14)
N(4)-C(31)	1.334(10)	C(58)-C(59)	1.40(2)
N(4)-C(34)	1.506(9)	C(59)-C(60)	1.40(2)
C(1)-C(4)	1.431(14)	C(60)-C(61)	1.32(2)
C(1)-C(5)	1.511(11)	C(61)-C(62)	1.406(13)

C(1)-C(3)	1.505(14)	C(63)-C(64)	1.531(13)
C(1)-C(2)	1.66(2)	C(65)-C(66)	1.455(14)
C(5)-C(10)	1.371(11)	C(67)-C(68)	1.40(2)
C(5)-C(6)	1.397(11)	B(1)-F(2)	1.329(11)
C(6)-C(7)	1.345(11)	B(1)-F(4)	1.318(11)
C(7)-C(8)	1.361(11)	B(1)-F(3)	1.336(12)
C(8)-C(9)	1.365(11)	B(1)-F(1)	1.357(13)
C(8)-C(11)	1.514(11)	B(2)-F(8)	1.319(11)
C(9)-C(10)	1.390(11)	B(2)-F(6)	1.362(13)
C(12)-C(13)	1.377(9)	B(2)-F(7)	1.364(13)
C(13)-C(14)	1.375(9)	B(2)-F(5)	1.350(12)
C(14)-C(15)	1.397(9)	B(3)-F(10)	1.33(2)
C(14)-C(17)	1.494(8)	B(3)-F(12)	1.35(2)
C(15)-C(16)	1.381(10)	B(3)-F(9)	1.35(2)
C(17)-C(21)	1.383(8)	B(3)-F(11)	1.36(2)
C(17)-C(18)	1.385(9)	B(3A)-F(12A)	1.30(2)
C(18)-C(19)	1.374(9)	B(3A)-F(11A)	1.35(2)
C(20)-C(21)	1.379(9)	B(3A)-F(9A)	1.34(2)
C(22)-C(23)	1.505(9)	B(3A)-F(10A)	1.33(2)
C(24)-C(25)	1.391(9)	B(4)-F(16)	1.35(2)
C(25)-C(26)	1.384(9)	B(4)-F(15)	1.35(2)
C(26)-C(27)	1.380(9)	B(4)-F(14)	1.33(2)
C(26)-C(29)	1.510(8)	B(4)-F(13)	1.37(2)
C(27)-C(28)	1.361(9)		

Bonds	Angles (°)	Bonds	Angles (°)
C(50)-O(1)-C(51)	118.8(9)	C(39)-C(38)-C(37)	115.3(9)
C(53)-O(2)-C(52)	118.2(8)	C(39)-C(38)-C(41)	120.6(7)
C(54)-O(3)-C(55)	124.6(8)	C(37)-C(38)-C(41)	124.1(9)
C(56)-O(4)-C(57)	121.7(9)	C(38)-C(39)-C(40)	122.6(8)
C(62)-O(5)-C(63)	117.1(7)	C(35)-C(40)-C(39)	120.6(9)
C(65)-O(6)-C(64)	115.4(7)	C(42)-C(41)-C(38)	110.8(8)
C(66)-O(7)-C(67)	117.8(8)	C(42)-C(41)-C(44)	108.2(9)
C(45)-O(8)-C(68)	112.4(10)	C(38)-C(41)-C(44)	109.7(8)
C(16)-N(1)-C(12)	120.0(6)	C(42)-C(41)-C(43)	110.3(10)
C(16)-N(1)-C(11)	122.2(7)	C(38)-C(41)-C(43)	112.6(8)
C(12)-N(1)-C(11)	117.8(7)	C(44)-C(41)-C(43)	105.1(9)
C(19)-N(2)-C(20)	120.2(6)	O(8)-C(45)-C(46)	128.4(14)
C(19)-N(2)-C(22)	120.2(6)	O(8)-C(45)-C(50)	115.0(10)
C(20)-N(2)-C(22)	119.6(6)	C(46)-C(45)-C(50)	116.6(12)
C(24)-N(3)-C(28)	119.7(5)	C(47)-C(46)-C(45)	127(2)
C(24)-N(3)-C(23)	119.3(6)	C(46)-C(47)-C(48)	117(2)
C(28)-N(3)-C(23)	121.0(6)	C(47)-C(48)-C(49)	122(2)
C(32)-N(4)-C(31)	121.2(6)	C(48)-C(49)-C(50)	116(2)
C(32)-N(4)-C(34)	119.3(7)	C(45)-C(50)-C(49)	120.7(12)
C(31)-N(4)-C(34)	119.4(6)	C(45)-C(50)-O(1)	118.4(9)

C(4)-C(1)-C(5)	114.7(8)	C(49)-C(50)-O(1)	120.9(13)
C(4)-C(1)-C(3)	111.8(11)	O(1)-C(51)-C(52)	107.6(9)
C(5)-C(1)-C(3)	111.3(8)	O(2)-C(52)-C(51)	114.0(8)
C(4)-C(1)-C(2)	105.0(11)	O(2)-C(53)-C(54)	121.3(9)
C(5)-C(1)-C(2)	106.3(7)	O(3)-C(54)-C(53)	122.7(9)
C(3)-C(1)-C(2)	107.1(10)	C(56)-C(55)-O(3)	118.6(10)
C(10)-C(5)-C(6)	115.3(8)	C(55)-C(56)-O(4)	121.5(11)
C(10)-C(5)-C(1)	123.3(7)	C(62)-C(57)-C(58)	119.5(10)
C(6)-C(5)-C(1)	121.4(7)	C(62)-C(57)-O(4)	118.1(8)
C(7)-C(6)-C(5)	122.2(8)	C(58)-C(57)-O(4)	122.4(11)
C(8)-C(7)-C(6)	122.9(8)	C(57)-C(58)-C(59)	120.0(11)
C(7)-C(8)-C(9)	116.0(7)	C(58)-C(59)-C(60)	119.6(12)
C(7)-C(8)-C(11)	123.1(8)	C(61)-C(60)-C(59)	118.8(12)
C(9)-C(8)-C(11)	120.9(8)	C(60)-C(61)-C(62)	122.5(12)
C(8)-C(9)-C(10)	122.2(7)	C(57)-C(62)-O(5)	116.5(8)
C(5)-C(10)-C(9)	121.3(8)	C(57)-C(62)-C(61)	119.7(10)
C(8)-C(11)-N(1)	109.3(6)	O(5)-C(62)-C(61)	123.8(10)
N(1)-C(12)-C(13)	121.0(7)	O(5)-C(63)-C(64)	106.7(7)
C(14)-C(13)-C(12)	120.2(7)	O(6)-C(64)-C(63)	114.7(7)
C(13)-C(14)-C(15)	117.7(6)	O(6)-C(65)-C(66)	111.5(8)
C(13)-C(14)-C(17)	121.9(6)	O(7)-C(66)-C(65)	112.9(9)
C(15)-C(14)-C(17)	120.4(6)	C(68)-C(67)-O(7)	113.3(9)
C(16)-C(15)-C(14)	119.7(7)	C(67)-C(68)-O(8)	110.0(10)
N(1)-C(16)-C(15)	121.4(7)	F(2)-B(1)-F(4)	111.6(9)
C(21)-C(17)-C(18)	117.1(6)	F(2)-B(1)-F(3)	110.9(11)
C(21)-C(17)-C(14)	121.6(6)	F(4)-B(1)-F(3)	109.8(9)
C(18)-C(17)-C(14)	121.3(6)	F(2)-B(1)-F(1)	108.5(10)
C(19)-C(18)-C(17)	120.9(6)	F(4)-B(1)-F(1)	114.5(11)
N(2)-C(19)-C(18)	120.6(6)	F(3)-B(1)-F(1)	101.1(9)
N(2)-C(20)-C(21)	122.1(6)	F(8)-B(2)-F(6)	111.5(11)
C(20)-C(21)-C(17)	119.1(6)	F(8)-B(2)-F(7)	110.0(9)
N(2)-C(22)-C(23)	108.9(5)	F(6)-B(2)-F(7)	104.2(10)
N(3)-C(23)-C(22)	110.1(5)	F(8)-B(2)-F(5)	115.3(9)
N(3)-C(24)-C(25)	122.0(6)	F(6)-B(2)-F(5)	107.9(10)
C(26)-C(25)-C(24)	118.1(6)	F(7)-B(2)-F(5)	107.3(11)
C(25)-C(26)-C(27)	118.5(6)	F(10)-B(3)-F(12)	115(2)
C(25)-C(26)-C(29)	119.9(6)	F(10)-B(3)-F(9)	111(2)
C(27)-C(26)-C(29)	121.5(6)	F(12)-B(3)-F(9)	106.8(14)
C(28)-C(27)-C(26)	119.8(6)	F(10)-B(3)-F(11)	109.9(14)
N(3)-C(28)-C(27)	121.6(6)	F(12)-B(3)-F(11)	110(2)
C(30)-C(29)-C(33)	118.2(6)	F(9)-B(3)-F(11)	103(2)
C(30)-C(29)-C(26)	120.7(6)	F(12A)-B(3A)-F(11A)	113(2)
C(33)-C(29)-C(26)	120.9(6)	F(12A)-B(3A)-F(9A)	109(2)
C(31)-C(30)-C(29)	120.7(7)	F(11A)-B(3A)-F(9A)	102.7(13)
N(4)-C(31)-C(30)	119.7(7)	F(12A)-B(3A)-F(10A)	113(2)
N(4)-C(32)-C(33)	119.9(6)	F(11A)-B(3A)-F(10A)	109(2)

C(32)-C(33)-C(29)	120.2(6)	F(9A)-B(3A)-F(10A)	109(2)
C(35)-C(34)-N(4)	111.7(6)	F(16)-B(4)-F(15)	109(2)
C(40)-C(35)-C(36)	117.6(9)	F(16)-B(4)-F(14)	113(2)
C(40)-C(35)-C(34)	121.6(10)	F(15)-B(4)-F(14)	116(2)
C(36)-C(35)-C(34)	120.7(8)	F(16)-B(4)-F(13)	110(2)
C(37)-C(36)-C(35)	121.4(8)	F(15)-B(4)-F(13)	102(2)
C(36)-C(37)-C(38)	122.3(10)	F(14)-B(4)-F(13)	107(2)

Table A-20. Anisotropic displacement parameters ($Å^2 \times 10^3$) for [2]-Rotaxane 7.

Atom	U_{11}	U_{22}	U_{33}	U_{23}	U_{13}	U_{12}
O(1)	138(5)	93(4)	81(4)	1(3)	-27(4)	-40(4)
O(2)	110(5)	154(6)	93(5)	-37(4)	-10(4)	11(4)
O(3)	130(6)	141(6)	109(5)	-6(4)	-41(5)	43(5)
O(4)	108(5)	104(4)	94(4)	0(3)	-36(3)	-4(4)
O(5)	107(4)	99(4)	65(3)	-16(3)	-6(3)	-15(3)
O(6)	99(4)	93(4)	105(5)	-24(3)	-4(3)	-15(3)
O(7)	95(5)	117(5)	131(6)	-14(4)	-31(4)	-5(4)
O(8)	96(4)	135(5)	77(4)	5(3)	-29(3)	-29(4)
N(1)	117(6)	69(4)	76(4)	6(3)	-36(4)	-45(4)
N(2)	69(4)	59(3)	53(3)	4(2)	-16(3)	-24(3)
N(3)	60(4)	59(3)	61(3)	-1(2)	-7(3)	-23(3)
N(4)	76(4)	66(4)	107(5)	-14(3)	-7(3)	-33(3)
C(1)	86(6)	125(7)	80(6)	-13(5)	-17(4)	-16(5)
C(2)	234(16)	223(15)	181(14)	66(12)	-114(12)	-83(13)
C(3)	181(12)	185(11)	100(8)	-36(8)	-43(8)	-23(9)
C(4)	113(10)	410(26)	114(10)	51(12)	-38(7)	-23(12)
C(5)	72(5)	93(5)	73(5)	-23(4)	-1(4)	-24(4)
C(6)	78(6)	162(8)	75(6)	-5(5)	-4(4)	-43(5)
C(7)	83(6)	169(9)	75(6)	-8(6)	-21(5)	-51(6)
C(8)	95(6)	87(5)	79(6)	-2(4)	-25(5)	-51(4)
C(9)	112(7)	104(6)	78(6)	-1(4)	-8(5)	-68(5)
C(10)	74(5)	102(6)	95(6)	-24(5)	-1(5)	-36(4)
C(11)	134(7)	93(5)	96(6)	4(4)	-38(5)	-75(5)
C(12)	90(6)	92(6)	97(6)	-5(4)	-31(4)	-44(5)
C(13)	71(5)	66(4)	88(5)	-4(4)	-19(4)	-20(4)
C(14)	64(4)	58(4)	57(4)	5(3)	-18(3)	-18(3)
C(15)	82(5)	64(4)	102(6)	-8(4)	-26(4)	-24(4)
C(16)	93(6)	57(4)	125(7)	-5(4)	-45(5)	-21(4)
C(17)	62(4)	43(3)	49(3)	-1(3)	-14(3)	-12(3)
C(18)	65(4)	70(4)	71(4)	-2(3)	-12(3)	-29(4)
C(19)	63(5)	61(4)	83(5)	-8(3)	-1(4)	-20(4)
C(20)	64(4)	72(5)	85(5)	0(4)	-23(4)	-22(4)
C(21)	61(5)	62(4)	86(5)	-5(3)	-14(3)	-14(3)

C(22)	90(5)	74(4)	62(4)	0(3)	-12(3)	-48(4)
C(23)	86(5)	71(4)	65(4)	8(3)	-18(4)	-42(4)
C(24)	77(5)	52(4)	85(5)	-6(3)	-10(4)	-18(4)
C(25)	62(4)	56(4)	90(5)	1(3)	-1(3)	-20(3)
C(26)	68(5)	53(4)	57(4)	5(3)	-5(3)	-25(3)
C(27)	58(4)	57(4)	91(5)	2(3)	-6(3)	-18(3)
C(28)	56(4)	70(5)	70(4)	4(3)	1(3)	-18(4)
C(29)	61(4)	59(4)	71(4)	-6(3)	-7(3)	-18(3)
C(30)	70(5)	54(4)	141(7)	3(4)	-21(4)	-22(4)
C(31)	90(6)	56(4)	179(9)	11(5)	-31(6)	-31(4)
C(32)	66(4)	85(5)	84(5)	-5(4)	-20(4)	-28(4)
C(33)	77(5)	67(4)	89(5)	12(4)	-26(4)	-27(4)
C(34)	95(6)	79(5)	129(7)	-21(5)	-16(6)	-47(5)
C(35)	76(6)	61(4)	148(9)	-18(5)	-18(6)	-38(4)
C(36)	63(6)	117(7)	146(9)	-23(6)	-27(6)	-16(5)
C(37)	94(7)	111(7)	140(9)	9(6)	-46(7)	-26(6)
C(38)	69(5)	77(5)	139(8)	21(5)	-35(5)	-27(4)
C(39)	61(5)	89(5)	150(9)	26(5)	-30(6)	-27(4)
C(40)	77(6)	85(5)	121(7)	23(5)	-26(5)	-39(4)
C(41)	94(6)	103(6)	108(7)	11(5)	-21(5)	-30(5)
C(42)	144(10)	127(9)	179(12)	-21(8)	15(8)	-15(8)
C(43)	140(10)	254(16)	169(13)	84(12)	-53(9)	-38(10)
C(44)	110(8)	189(11)	174(11)	25(9)	-5(7)	-80(8)
C(45)	150(10)	129(9)	62(5)	0(5)	-22(6)	-62(9)
C(46)	152(10)	234(14)	78(7)	-5(7)	-27(6)	-111(10)
C(47)	325(29)	406(40)	96(11)	56(18)	-83(17)	-282(29)
C(48)	337(25)	210(16)	86(9)	45(10)	-73(14)	-216(18)
C(49)	264(15)	133(8)	70(6)	15(5)	-38(7)	-107(10)
C(50)	192(11)	113(7)	53(5)	23(5)	-38(6)	-92(8)
C(51)	176(11)	124(8)	67(6)	-23(5)	-10(6)	-20(9)
C(52)	119(8)	171(10)	71(6)	-20(6)	14(5)	-40(7)
C(53)	108(8)	121(7)	103(8)	-19(6)	9(6)	6(6)
C(54)	94(7)	161(10)	130(10)	-29(8)	-22(7)	28(7)
C(55)	173(11)	126(8)	97(8)	-12(7)	-57(7)	40(8)
C(56)	148(10)	191(12)	98(8)	4(8)	-61(7)	27(10)
C(57)	125(8)	111(7)	60(5)	19(5)	-43(5)	-45(7)
C(58)	119(8)	153(10)	87(7)	36(7)	-37(6)	-29(7)
C(59)	207(15)	139(10)	88(7)	23(7)	-57(8)	-94(10)
C(60)	196(14)	127(9)	85(7)	-3(6)	-26(8)	-40(10)
C(61)	152(9)	126(8)	86(6)	-5(6)	-41(6)	-54(7)
C(62)	115(8)	96(6)	60(5)	3(4)	-29(5)	-16(6)
C(63)	123(7)	107(6)	64(5)	-12(4)	2(5)	-18(6)
C(64)	125(8)	100(6)	97(7)	-13(5)	17(6)	-35(6)
C(65)	97(7)	122(8)	124(8)	-43(6)	-6(6)	-10(6)
C(66)	97(8)	127(8)	196(13)	-19(8)	-45(9)	3(7)
C(67)	127(9)	134(9)	174(13)	45(9)	-67(9)	-17(7)

C(68)	147(12)	213(15)	124(10)	34(9)	-62(8)	-73(11)
B(1)	99(7)	77(6)	159(10)	6(5)	13(7)	-5(5)
F(1)	357(14)	217(9)	180(7)	-70(6)	44(7)	-117(9)
F(2)	107(5)	208(8)	359(13)	17(7)	39(6)	-52(5)
F(3)	237(9)	149(6)	209(7)	56(5)	-9(6)	30(5)
F(4)	101(4)	88(3)	228(7)	2(4)	32(4)	1(3)
B(2)	100(7)	186(10)	110(8)	48(9)	-27(6)	-55(7)
F(5)	113(5)	404(13)	154(6)	6(7)	-4(4)	-70(6)
F(6)	340(12)	180(6)	155(7)	61(5)	-10(7)	16(6)
F(7)	278(10)	324(10)	170(7)	-21(7)	6(7)	-200(9)
F(8)	164(6)	246(8)	116(4)	54(5)	-38(4)	-60(5)
B(3)	24(8)	108(14)	239(17)	-22(12)	64(10)	-3(8)
F(9)	145(11)	159(11)	210(13)	46(10)	-29(10)	-22(9)
F(10)	147(13)	192(15)	171(11)	23(9)	-17(9)	27(10)
F(11)	119(11)	192(15)	226(15)	33(12)	-48(11)	-21(10)
F(12)	85(10)	173(16)	373(28)	6(18)	-36(13)	52(11)
B(3A)	102(15)	207(20)	178(16)	81(13)	-91(14)	40(10)
F(9A)	109(9)	172(11)	256(15)	76(11)	-45(10)	1(8)
F(10A)	299(28)	346(30)	203(15)	10(15)	-23(17)	-4(22)
F(11A)	117(11)	181(16)	328(23)	67(16)	-64(14)	-15(10)
F(12A)	113(12)	159(16)	451(35)	30(20)	-76(19)	58(11)
B(4)	274(23)	464(40)	271(20)	-61(17)	-135(24)	-99(15)
F(13)	312(16)	623(39)	621(36)	-121(26)	-38(22)	-205(22)
F(14)	406(21)	458(22)	208(11)	-77(12)	-25(12)	-55(14)
F(15)	289(16)	990(46)	194(11)	-77(16)	-53(12)	-154(19)
F(16)	308(14)	353(18)	676(34)	-131(19)	-161(17)	-83(14)
O(1W)	400(21)	144(8)	351(19)	-65(10)	6(15)	-60(11)
O(2W)	255(18)	222(15)	849(57)	46(23)	-111(26)	-32(13)
O(3W)	526(35)	273(17)	376(26)	71(17)	-87(24)	60(19)

The anisotropic displacement factor exponent takes the form: $-2\pi^2[h^2 a^{*2} U11 + ... + 2hka^*b^*U12]$

Table A-20. Hydrogen coordinates (x 10^4) and isotropic displacement parameters ($Å^2$ x 10^3) for [2]-Rotaxane 7.

Atom	x	y	z	U(eq)
H(2A)	8877(13)	6501(10)	5908(9)	302
H(2B)	9858(13)	6219(10)	6287(9)	302
H(2C)	9873(13)	6023(10)	5398(9)	302
H(3A)	8735(10)	7974(8)	6273(7)	234
H(3B)	9657(10)	8358(8)	6070(7)	234
H(3C)	9690(10)	7627(8)	6674(7)	234

H(4A)	11204(9)	6908(13)	5877(8)	330
H(4B)	11186(9)	7559(13)	5189(8)	330
H(4C)	11212(9)	6663(13)	5004(8)	330
H(6A)	7973(6)	7663(6)	5299(5)	124
H(7A)	7241(7)	8107(6)	4232(5)	125
H(9A)	9866(7)	8050(5)	2931(5)	110
H(10A)	10644(6)	7576(5)	4007(5)	106
H(11A)	8475(7)	8510(5)	2289(5)	116
H(11B)	7513(7)	8979(5)	2849(5)	116
H(12A)	8623(6)	6981(5)	2271(5)	105
H(13A)	7836(5)	6040(4)	1947(4)	88
H(15A)	5202(6)	7653(4)	2498(5)	96
H(16A)	6054(7)	8590(4)	2724(5)	105
H(18A)	7100(5)	5278(4)	1535(4)	80
H(19A)	6260(5)	4358(4)	1260(4)	83
H(20A)	3702(5)	5819(4)	2069(4)	86
H(21A)	4478(5)	6762(4)	2406(4)	83
H(22A)	4711(5)	4131(4)	967(4)	84
H(22B)	3693(5)	4678(4)	1387(4)	84
H(23A)	5033(5)	3498(4)	2175(4)	84
H(23B)	4063(5)	4077(4)	2627(4)	84
H(24A)	2469(6)	4009(4)	2249(4)	85
H(25A)	1476(5)	3151(4)	2072(4)	83
H(27A)	3990(5)	1389(4)	1578(4)	83
H(28A)	4899(5)	2307(4)	1680(4)	80
H(30A)	2934(6)	619(4)	2267(5)	104
H(31A)	1907(7)	-262(4)	2363(6)	126
H(32A)	-144(5)	1410(5)	1483(4)	91
H(33A)	835(5)	2320(4)	1419(4)	90
H(34A)	-245(6)	-1(5)	1610(6)	115
H(34B)	490(6)	-605(5)	2097(6)	115
H(36A)	300(7)	-230(6)	3593(8)	129
H(37A)	-851(8)	-73(6)	4717(7)	135
H(39A)	-3027(6)	816(5)	3429(7)	117
H(40A)	-1874(6)	572(5)	2283(6)	109
H(42A)	-3785(10)	1633(7)	5538(8)	236
H(42B)	-3616(10)	1742(7)	4610(8)	236
H(42C)	-2766(10)	1779(7)	5091(8)	236
H(43A)	-2200(10)	-323(10)	5679(9)	285
H(43B)	-3011(10)	340(10)	6188(9)	285
H(43C)	-1961(10)	496(10)	5842(9)	285
H(44A)	-3496(8)	-330(8)	4854(8)	230
H(44B)	-4058(8)	472(8)	4466(8)	230
H(44C)	-4234(8)	352(8)	5392(8)	230
H(46A)	1241(10)	3771(10)	26(6)	170
H(47A)	1173(21)	2569(20)	-330(11)	284

H(48A)	2655(19)	1543(12)	-532(9)	217
H(49A)	4211(12)	1795(7)	-425(5)	173
H(51A)	5496(10)	2473(7)	-817(5)	151
H(51B)	5496(10)	2153(7)	67(5)	151
H(52A)	6850(8)	2726(8)	-509(5)	147
H(52B)	6066(8)	3566(8)	-431(5)	147
H(53A)	7772(8)	2560(6)	523(7)	143
H(53B)	7062(8)	1990(6)	795(7)	143
H(54A)	7506(8)	1970(8)	1798(8)	165
H(54B)	7940(8)	2724(8)	1585(8)	165
H(55A)	6335(10)	2636(7)	3281(7)	170
H(55B)	7478(10)	2568(7)	3020(7)	170
H(56A)	7297(10)	3805(9)	3107(7)	184
H(56B)	6773(10)	3474(9)	3888(7)	184
H(58A)	7221(8)	4923(8)	3686(6)	144
H(59A)	6947(13)	6141(9)	4342(7)	159
H(60A)	5307(14)	6915(8)	4712(6)	162
H(61A)	4025(9)	6449(7)	4464(6)	138
H(63A)	2897(7)	6053(6)	3882(5)	122
H(63B)	3023(7)	5517(6)	4659(5)	122
H(64A)	2662(8)	4444(6)	3973(6)	131
H(64B)	1738(8)	5177(6)	4194(6)	131
H(65A)	1834(8)	6284(6)	2878(6)	141
H(65B)	941(8)	5911(6)	3257(6)	141
H(66A)	913(9)	5374(7)	2088(9)	171
H(66B)	853(9)	6300(7)	1951(9)	171
H(67A)	1369(9)	6041(8)	584(8)	174
H(67B)	2526(9)	5748(8)	299(8)	174
H(68A)	1548(11)	4965(11)	-78(8)	183
H(68B)	1379(11)	4681(11)	816(8)	183

Table A-21. Details of X-ray Data Collection, Solution and Refinement for [2]-Rotaxane **9**.

Empirical formula	$C_{86}H_{86}B_4F_{16}N_4O_8Pd_2S_4$
Crystal	Yellow blocks
Formula weight	1991.87
Temperature	298(2) K
Wavelength, Å	0.71073
Crystal system	Monoclinic
Space group	*Pc* (No.4)
a, Å	17.8929(3)
b, Å	14.3181(2)
c, Å	19.4361(3)
β °	116.800(1)
V, Å^3	4444.5(1)
Z	2
ρ_{calcd}, Mg m^{-3}	1.488
μ, mm^{-1}	0.0589
F(000)	2028
Crystal size, mm	0.26 x 0.30 x 0.32
θ–range for data collection, °	1.27 to 24.00
Limiting indices	$-23 \leq h \leq 23$, $-19 \leq k \leq 12$, $-25 \leq k \leq 25$
Reflections collected	19899
Independent reflections	11604 [R(int) = 0.0500]
Refinement method	Full-matrix least-squares (F^2)
Data / restraints / parameters	11599 / 534 / 1111
Goodness-of-fit on F^2	0.974
Final R indices [$I>2\sigma(I)$]	$R_1 = 0.0569$, $wR_2 = 0.1198$
R indices (all data)	$R_1 = 0.0977$, $wR_2 = 0.1431$
Largest difference peak and hole	0.834 and -0.407 e Å^{-3}

Table A-22. Atomic coordinates (x 10^4) and equivalent isotropic displacement parameters (Å^2 x 10^3) for [2]-Rotaxane **9**.

Atom	x	y	z	U(eq)
Pd(1)	1038(1)	-3916(1)	2301(1)	55(1)
Pd(2)	8151(1)	8916(1)	3510(1)	58(1)
S(1)	-78(4)	-3518(4)	1154(4)	73(2)
S(2)	1960(4)	-4560(4)	3439(3)	61(2)
S(3)	7208(4)	9581(4)	2359(3)	65(2)
S(4)	9263(4)	8528(4)	4655(3)	62(2)
O(1)	2354(10)	2763(11)	2180(9)	86(5)

O(2)	3115(9)	3308(9)	1266(8)	72(4)
O(3)	4585(10)	3127(8)	1003(8)	71(4)
O(4)	6237(9)	2899(10)	2211(9)	74(4)
O(5)	6844(10)	2334(9)	3624(7)	67(4)
O(6)	6027(11)	1729(10)	4547(10)	86(5)
O(7)	4660(10)	1903(10)	4796(8)	79(4)
O(8)	2889(9)	2080(8)	3571(8)	66(4)
N(1)	1671(9)	-2584(9)	2424(8)	53(4)
N(2)	4097(11)	1306(7)	2650(9)	52(4)
N(3)	5006(11)	3727(11)	3088(9)	61(4)
N(4)	7529(10)	7637(9)	3433(9)	57(4)
B(1)	7064(10)	-5640(9)	5918(8)	69(5)
F(1)	6288(7)	-5620(8)	5895(8)	112(4)
F(2)	7209(10)	-4810(7)	5661(8)	107(4)
F(3)	7663(7)	-5818(9)	6648(5)	100(4)
F(4)	7086(9)	-6339(7)	5447(7)	95(4)
B(2)	2147(9)	617(11)	-101(9)	79(5)
F(5)	2890(6)	663(9)	-123(7)	107(4)
F(6)	2059(10)	-238(8)	184(8)	114(5)
F(7)	1511(6)	725(9)	-835(6)	90(3)
F(8)	2081(9)	1288(8)	375(7)	110(5)
B(3)	2787(12)	6212(11)	827(9)	137(6)
F(9)	3466(8)	5719(10)	1219(7)	234(7)
F(10)	2865(13)	7155(8)	870(10)	233(8)
F(11)	2463(9)	5982(10)	102(5)	194(6)
F(12)	2213(13)	6029(9)	1106(11)	224(8)
B(4)	6652(17)	8654(14)	5104(15)	317(13)
F(13)	6272(19)	9189(13)	5379(17)	454(18)
F(14)	6075(15)	8111(16)	4546(15)	370(14)
F(15)	7051(17)	9159(12)	4788(15)	328(13)
F(16)	7225(17)	8077(18)	5632(14)	451(15)
C(1)	359(15)	-5142(13)	2153(14)	67(6)
C(2)	803(15)	-5835(13)	2655(12)	72(7)
C(3)	301(16)	-6713(10)	2557(14)	79(7)
C(4)	-516(12)	-6725(13)	2004(13)	87(7)
C(5)	-818(10)	-5932(15)	1598(12)	81(7)
C(6)	-401(10)	-5254(11)	1642(11)	47(4)
C(7)	-851(11)	-4465(12)	1121(13)	65(5)
C(8)	1715(14)	-5829(12)	3207(12)	73(6)
C(9)	-526(13)	-2426(11)	1283(12)	60(5)
C(10)	-774(14)	-2391(15)	1851(13)	90(6)
C(11)	-959(22)	-1410(23)	1966(19)	204(19)
C(12)	-1156(13)	-788(16)	1426(17)	98(8)
C(13)	-877(18)	-865(18)	935(19)	117(11)
C(14)	-595(14)	-1709(16)	834(15)	96(8)
C(15)	2970(13)	-4435(13)	3614(11)	65(6)

C(16)	3598(23)	-4852(17)	4320(19)	124(11)
C(17)	4507(15)	-4623(22)	4501(16)	143(15)
C(18)	4654(22)	-4093(22)	3955(21)	134(14)
C(19)	4040(16)	-3910(13)	3345(17)	96(7)
C(20)	3254(12)	-4006(13)	3132(12)	78(6)
C(21)	1967(12)	-2152(11)	3023(12)	59(5)
C(22)	2474(15)	-1340(13)	3170(12)	74(7)
C(23)	2550(13)	-971(11)	2520(13)	64(6)
C(24)	2246(11)	-1543(12)	1853(8)	61(5)
C(25)	1776(12)	-2256(12)	1843(9)	63(6)
C(26)	3102(15)	-203(13)	2578(11)	72(6)
C(27)	2944(11)	450(11)	1963(9)	47(4)
C(28)	3426(8)	1191(9)	2028(9)	40(4)
C(29)	4300(14)	789(13)	3240(11)	67(5)
C(30)	3825(14)	-15(12)	3238(12)	67(6)
C(31)	4708(13)	2025(11)	2725(10)	63(5)
C(32)	4508(11)	2874(11)	3083(11)	61(5)
C(33)	4796(14)	4304(13)	2443(10)	59(5)
C(34)	5336(13)	4987(11)	2498(11)	68(6)
C(35)	6040(9)	5157(9)	3157(9)	37(4)
C(36)	6286(12)	4620(11)	3778(11)	64(6)
C(37)	5743(16)	3906(12)	3741(13)	82(7)
C(38)	6551(11)	6044(10)	3256(9)	43(4)
C(39)	6935(12)	6467(10)	3922(11)	66(6)
C(40)	7404(11)	7348(11)	4025(10)	64(5)
C(41)	7165(15)	7074(13)	2742(12)	77(7)
C(42)	6728(12)	6287(11)	2689(11)	60(6)
C(43)	8736(13)	10082(11)	3621(12)	54(5)
C(44)	9586(16)	10085(13)	4173(14)	79(6)
C(45)	10069(13)	11078(11)	4293(12)	80(7)
C(46)	9608(17)	11753(15)	3732(15)	104(10)
C(47)	8790(14)	11600(15)	3184(14)	86(7)
C(48)	8362(10)	10878(14)	3127(12)	61(6)
C(49)	7490(14)	10776(13)	2558(13)	74(7)
C(50)	10056(15)	9282(15)	4671(16)	120(9)
C(51)	6092(15)	9564(12)	2115(13)	70(7)
C(52)	5552(11)	9852(12)	1452(10)	62(5)
C(53)	4752(18)	9774(15)	1216(14)	96(7)
C(54)	4435(21)	9326(20)	1585(22)	126(11)
C(55)	4937(21)	8963(22)	2349(23)	142(15)
C(56)	5862(18)	9146(16)	2614(17)	114(10)
C(57)	9636(15)	7482(15)	4530(12)	76(6)
C(58)	9845(19)	7221(20)	3953(16)	151(13)
C(59)	10286(19)	6510(20)	3914(17)	121(9)
C(60)	10240(21)	5687(20)	4314(23)	158(14)
C(61)	10103(16)	5883(14)	4963(15)	96(8)

C(62)	9726(14)	6752(13)	5058(10)	82(7)
C(63)	2148(11)	1724(9)	3066(10)	74(6)
C(64)	1658(12)	1058(11)	3269(13)	71(5)
C(65)	1019(23)	799(17)	2731(16)	131(12)
C(66)	636(17)	1020(14)	1972(19)	105(10)
C(67)	1053(17)	1694(15)	1704(14)	84(7)
C(68)	1810(15)	2027(12)	2285(15)	73(7)
C(69)	1878(12)	3147(12)	1467(11)	86(6)
C(70)	2372(14)	3595(15)	1224(15)	152(12)
C(71)	3079(18)	3239(16)	477(12)	95(9)
C(72)	3783(14)	2826(16)	508(14)	98(8)
C(73)	5239(14)	2693(16)	933(13)	84(7)
C(74)	6038(9)	3133(8)	1423(7)	72(6)
C(75)	6987(9)	3250(8)	2739(7)	62(6)
C(76)	7415(9)	3887(8)	2604(7)	82(7)
C(77)	8249(13)	4276(14)	3169(13)	78(6)
C(78)	8492(19)	3893(17)	3890(14)	116(11)
C(79)	8039(18)	3255(20)	4003(15)	103(9)
C(80)	7297(15)	2890(15)	3499(10)	71(6)
C(81)	7143(13)	1639(15)	4251(11)	149(11)
C(82)	6648(14)	1166(10)	4386(11)	85(6)
C(83)	6073(14)	1611(16)	5243(13)	80(6)
C(84)	5441(14)	2270(13)	5334(9)	80(8)
C(85)	3989(15)	2373(13)	4845(10)	80(7)
C(86)	3193(11)	1852(11)	4379(10)	81(7)

Table A-23. Bonding parameters for [2]-Rotaxane, **9**.

Bond	Distance (Å)	Bond	Distance (Å)
Pd(1)-C(1)	2.08(2)	C(10)-C(11)	1.48(3)
Pd(1)-N(1)	2.18(2)	C(11)-C(12)	1.30(4)
Pd(1)-S(2)	2.275(6)	C(12)-C(13)	1.27(4)
Pd(1)-S(1)	2.296(7)	C(13)-C(14)	1.36(3)
Pd(2)-C(43)	1.93(2)	C(15)-C(20)	1.39(3)
Pd(2)-N(4)	2.112(12)	C(15)-C(16)	1.45(4)
Pd(2)-S(4)	2.286(6)	C(16)-C(17)	1.53(4)
Pd(2)-S(3)	2.314(6)	C(17)-C(18)	1.42(5)
S(1)-C(9)	1.82(2)	C(18)-C(19)	1.23(4)
S(1)-C(7)	1.92(2)	C(19)-C(20)	1.28(3)
S(2)-C(15)	1.69(2)	C(21)-C(22)	1.42(2)
S(2)-C(8)	1.88(2)	C(22)-C(23)	1.43(3)
S(3)-C(51)	1.83(2)	C(23)-C(24)	1.42(2)
S(3)-C(49)	1.78(2)	C(23)-C(26)	1.45(3)

S(4)-C(57)	1.70(2)	C(24)-C(25)	1.32(2)
S(4)-C(50)	1.77(2)	C(26)-C(30)	1.38(3)
O(1)-C(69)	1.37(2)	C(26)-C(27)	1.44(2)
O(1)-C(68)	1.51(2)	C(27)-C(28)	1.34(2)
O(2)-C(70)	1.36(3)	C(29)-C(30)	1.43(3)
O(2)-C(71)	1.51(3)	C(31)-C(32)	1.521(10)
O(3)-C(73)	1.39(2)	C(33)-C(34)	1.34(2)
O(3)-C(72)	1.39(2)	C(34)-C(35)	1.35(2)
O(4)-C(75)	1.37(2)	C(35)-C(36)	1.33(2)
O(4)-C(74)	1.45(2)	C(35)-C(38)	1.52(2)
O(5)-C(80)	1.24(2)	C(36)-C(37)	1.39(3)
O(5)-C(81)	1.47(2)	C(38)-C(42)	1.32(3)
O(6)-C(83)	1.33(2)	C(38)-C(39)	1.31(2)
O(6)-C(82)	1.52(3)	C(39)-C(40)	1.48(2)
O(7)-C(84)	1.42(2)	C(41)-C(42)	1.35(3)
O(7)-C(85)	1.42(3)	C(43)-C(44)	1.41(3)
O(8)-C(63)	1.34(2)	C(43)-C(48)	1.44(3)
O(8)-C(86)	1.45(2)	C(44)-C(50)	1.49(3)
N(1)-C(21)	1.21(2)	C(44)-C(45)	1.62(3)
N(1)-C(25)	1.31(2)	C(45)-C(46)	1.41(3)
N(2)-C(29)	1.27(2)	C(46)-C(47)	1.39(3)
N(2)-C(28)	1.27(2)	C(47)-C(48)	1.26(3)
N(2)-C(31)	1.46(2)	C(48)-C(49)	1.46(3)
N(3)-C(37)	1.38(3)	C(51)-C(56)	1.35(3)
N(3)-C(33)	1.40(2)	C(51)-C(52)	1.28(3)
N(3)-C(32)	1.51(2)	C(52)-C(53)	1.30(3)
N(4)-C(40)	1.33(2)	C(53)-C(54)	1.27(4)
N(4)-C(41)	1.44(2)	C(54)-C(55)	1.44(4)
B(1)-F(2)	1.359(13)	C(55)-C(56)	1.52(4)
B(1)-F(3)	1.361(14)	C(57)-C(58)	1.38(3)
B(1)-F(4)	1.368(13)	C(57)-C(62)	1.42(3)
B(1)-F(1)	1.371(14)	C(58)-C(59)	1.31(3)
B(2)-F(5)	1.352(14)	C(59)-C(60)	1.44(4)
B(2)-F(7)	1.374(14)	C(60)-C(61)	1.42(4)
B(2)-F(8)	1.374(14)	C(61)-C(62)	1.47(3)
B(2)-F(6)	1.380(14)	C(63)-C(68)	1.43(3)
B(3)-F(11)	1.30(2)	C(63)-C(64)	1.46(2)
B(3)-F(9)	1.31(2)	C(64)-C(65)	1.21(3)
B(3)-F(10)	1.36(2)	C(65)-C(66)	1.35(4)
B(3)-F(12)	1.39(2)	C(66)-C(67)	1.45(3)
B(4)-F(13)	1.29(2)	C(67)-C(68)	1.40(3)
B(4)-F(15)	1.34(2)	C(69)-C(70)	1.34(3)
B(4)-F(16)	1.36(2)	C(71)-C(72)	1.37(3)
B(4)-F(14)	1.36(2)	C(73)-C(74)	1.46(3)
C(1)-C(6)	1.28(3)	C(75)-C(76)	1.29
C(1)-C(2)	1.37(3)	C(75)-C(80)	1.42(2)

C(2)-C(8)	1.49(3)	C(76)-C(77)	1.50(2)
C(2)-C(3)	1.51(3)	C(77)-C(78)	1.38(3)
C(3)-C(4)	1.37(3)	C(78)-C(79)	1.31(4)
C(4)-C(5)	1.35(3)	C(79)-C(80)	1.35(3)
C(5)-C(6)	1.20(2)	C(81)-C(82)	1.23(3)
C(6)-C(7)	1.49(2)	C(83)-C(84)	1.54(3)
C(9)-C(14)	1.32(3)	C(85)-C(86)	1.50(3)
C(9)-C(10)	1.36(3)		

Bonds	Angle (°)	Bonds	Angle (°)
C(1)-Pd(1)-N(1)	176.3(7)	C(19)-C(18)-C(17)	116(3)
C(1)-Pd(1)-S(2)	85.1(7)	C(18)-C(19)-C(20)	132(3)
N(1)-Pd(1)-S(2)	97.8(4)	C(19)-C(20)-C(15)	121(2)
C(1)-Pd(1)-S(1)	82.9(7)	N(1)-C(21)-C(22)	125(2)
N(1)-Pd(1)-S(1)	94.1(4)	C(21)-C(22)-C(23)	115(2)
S(2)-Pd(1)-S(1)	167.7(2)	C(24)-C(23)-C(22)	116(2)
C(43)-Pd(2)-N(4)	178.0(8)	C(24)-C(23)-C(26)	118(2)
C(43)-Pd(2)-S(4)	84.9(6)	C(22)-C(23)-C(26)	123(2)
N(4)-Pd(2)-S(4)	93.3(5)	C(25)-C(24)-C(23)	116(2)
C(43)-Pd(2)-S(3)	82.8(6)	C(24)-C(25)-N(1)	127(2)
N(4)-Pd(2)-S(3)	99.0(5)	C(30)-C(26)-C(27)	113(2)
S(4)-Pd(2)-S(3)	167.5(2)	C(30)-C(26)-C(23)	123(2)
C(9)-S(1)-C(7)	104.8(9)	C(27)-C(26)-C(23)	124(2)
C(9)-S(1)-Pd(1)	108.8(7)	C(28)-C(27)-C(26)	124(2)
C(7)-S(1)-Pd(1)	98.9(7)	N(2)-C(28)-C(27)	119(2)
C(15)-S(2)-C(8)	105.3(10)	N(2)-C(29)-C(30)	122(2)
C(15)-S(2)-Pd(1)	113.2(8)	C(26)-C(30)-C(29)	118(2)
C(8)-S(2)-Pd(1)	99.8(6)	N(2)-C(31)-C(32)	106.8(11)
C(51)-S(3)-C(49)	103.7(9)	C(31)-C(32)-N(3)	113.0(10)
C(51)-S(3)-Pd(2)	118.6(8)	C(34)-C(33)-N(3)	118(2)
C(49)-S(3)-Pd(2)	100.0(8)	C(33)-C(34)-C(35)	122(2)
C(57)-S(4)-C(50)	100.2(12)	C(36)-C(35)-C(34)	123(2)
C(57)-S(4)-Pd(2)	107.5(8)	C(36)-C(35)-C(38)	115.6(14)
C(50)-S(4)-Pd(2)	102.0(8)	C(34)-C(35)-C(38)	121.3(14)
C(69)-O(1)-C(68)	106(2)	C(35)-C(36)-C(37)	116(2)
C(70)-O(2)-C(71)	111(2)	C(36)-C(37)-N(3)	123(2)
C(73)-O(3)-C(72)	117(2)	C(42)-C(38)-C(39)	119(2)
C(75)-O(4)-C(74)	113.5(13)	C(42)-C(38)-C(35)	117.9(14)
C(80)-O(5)-C(81)	125(2)	C(39)-C(38)-C(35)	122(2)
C(83)-O(6)-C(82)	115(2)	C(38)-C(39)-C(40)	123(2)
C(84)-O(7)-C(85)	111(2)	N(4)-C(40)-C(39)	117(2)
C(63)-O(8)-C(86)	118.1(14)	C(42)-C(41)-N(4)	123(2)
C(21)-N(1)-C(25)	118(2)	C(38)-C(42)-C(41)	120(2)
C(21)-N(1)-Pd(1)	122.2(12)	C(44)-C(43)-C(48)	121(2)
C(25)-N(1)-Pd(1)	119.3(12)	C(44)-C(43)-Pd(2)	115.5(14)
C(29)-N(2)-C(28)	123(2)	C(48)-C(43)-Pd(2)	123(2)

C(29)-N(2)-C(31)	115(2)	C(43)-C(44)-C(50)	126(2)
C(28)-N(2)-C(31)	121.9(14)	C(43)-C(44)-C(45)	116(2)
C(37)-N(3)-C(33)	118(2)	C(50)-C(44)-C(45)	118(2)
C(37)-N(3)-C(32)	118(2)	C(46)-C(45)-C(44)	114(2)
C(33)-N(3)-C(32)	123(2)	C(47)-C(46)-C(45)	122(2)
C(40)-N(4)-C(41)	116.6(14)	C(48)-C(47)-C(46)	126(2)
C(40)-N(4)-Pd(2)	119.7(11)	C(47)-C(48)-C(43)	120(2)
C(41)-N(4)-Pd(2)	123.6(12)	C(47)-C(48)-C(49)	123(2)
F(2)-B(1)-F(3)	110.8(13)	C(43)-C(48)-C(49)	116(2)
F(2)-B(1)-F(4)	109.1(10)	C(48)-C(49)-S(3)	111(2)
F(3)-B(1)-F(4)	108.3(11)	C(44)-C(50)-S(4)	104(2)
F(2)-B(1)-F(1)	109.1(11)	C(56)-C(51)-C(52)	122(2)
F(3)-B(1)-F(1)	110.4(11)	C(56)-C(51)-S(3)	118(2)
F(4)-B(1)-F(1)	109.2(12)	C(52)-C(51)-S(3)	120(2)
F(5)-B(2)-F(7)	109.0(12)	C(53)-C(52)-C(51)	123(2)
F(5)-B(2)-F(8)	111.8(11)	C(54)-C(53)-C(52)	123(3)
F(7)-B(2)-F(8)	109.7(13)	C(53)-C(54)-C(55)	122(3)
F(5)-B(2)-F(6)	110.3(13)	C(54)-C(55)-C(56)	111(3)
F(7)-B(2)-F(6)	109.0(10)	C(51)-C(56)-C(55)	118(3)
F(8)-B(2)-F(6)	106.9(12)	C(58)-C(57)-C(62)	114(2)
F(11)-B(3)-F(9)	109.7(13)	C(58)-C(57)-S(4)	128(2)
F(11)-B(3)-F(10)	107.6(12)	C(62)-C(57)-S(4)	118(2)
F(9)-B(3)-F(10)	117(2)	C(59)-C(58)-C(57)	130(2)
F(11)-B(3)-F(12)	109(2)	C(58)-C(59)-C(60)	115(3)
F(9)-B(3)-F(12)	109.0(13)	C(61)-C(60)-C(59)	113(3)
F(10)-B(3)-F(12)	103.7(12)	C(60)-C(61)-C(62)	124(2)
F(13)-B(4)-F(15)	111(2)	C(57)-C(62)-C(61)	116(2)
F(13)-B(4)-F(16)	114(2)	O(8)-C(63)-C(68)	118(2)
F(15)-B(4)-F(16)	107(2)	O(8)-C(63)-C(64)	124.3(14)
F(13)-B(4)-F(14)	109(2)	C(68)-C(63)-C(64)	118(2)
F(15)-B(4)-F(14)	108(2)	C(65)-C(64)-C(63)	114(2)
F(16)-B(4)-F(14)	107(2)	C(64)-C(65)-C(66)	133(3)
C(6)-C(1)-C(2)	122(2)	C(65)-C(66)-C(67)	117(3)
C(6)-C(1)-Pd(1)	124.2(14)	C(68)-C(67)-C(66)	114(2)
C(2)-C(1)-Pd(1)	113(2)	C(67)-C(68)-C(63)	123(2)
C(1)-C(2)-C(8)	127(2)	C(67)-C(68)-O(1)	125(2)
C(1)-C(2)-C(3)	113(2)	C(63)-C(68)-O(1)	111(2)
C(8)-C(2)-C(3)	119(2)	C(70)-C(69)-O(1)	110(2)
C(4)-C(3)-C(2)	118(2)	C(69)-C(70)-O(2)	128(2)
C(5)-C(4)-C(3)	117(2)	C(72)-C(71)-O(2)	112(2)
C(6)-C(5)-C(4)	124(2)	C(71)-C(72)-O(3)	123(2)
C(5)-C(6)-C(1)	124(2)	O(3)-C(73)-C(74)	111(2)
C(5)-C(6)-C(7)	116(2)	O(4)-C(74)-C(73)	107.0(14)
C(1)-C(6)-C(7)	119(2)	C(76)-C(75)-O(4)	125.5(8)
C(6)-C(7)-S(1)	110.8(12)	C(76)-C(75)-C(80)	118.5(12)
C(2)-C(8)-S(2)	103.8(13)	O(4)-C(75)-C(80)	116(2)

C(14)-C(9)-C(10)	123(2)	C(75)-C(76)-C(77)	126.7(10)
C(14)-C(9)-S(1)	119(2)	C(78)-C(77)-C(76)	110(2)
C(10)-C(9)-S(1)	118(2)	C(79)-C(78)-C(77)	121(3)
C(9)-C(10)-C(11)	109(2)	C(78)-C(79)-C(80)	129(3)
C(12)-C(11)-C(10)	122(3)	O(5)-C(80)-C(79)	129(2)
C(11)-C(12)-C(13)	120(2)	O(5)-C(80)-C(75)	117(2)
C(12)-C(13)-C(14)	119(3)	C(79)-C(80)-C(75)	114(2)
C(9)-C(14)-C(13)	122(2)	C(82)-C(81)-O(5)	121(2)
C(20)-C(15)-C(16)	117(2)	C(81)-C(82)-O(6)	114(2)
C(20)-C(15)-S(2)	126(2)	O(6)-C(83)-C(84)	109(2)
C(16)-C(15)-S(2)	117(2)	O(7)-C(84)-C(83)	103(2)
C(15)-C(16)-C(17)	115(3)	O(7)-C(85)-C(86)	109(2)
C(16)-C(17)-C(18)	118(2)	O(8)-C(86)-C(85)	109.5(13)

Table A-24. Anisotropic displacement parameters ($Å^2 \times 10^3$) for [2]-Rotaxane **9**.

Atom	U_{11}	U_{22}	U_{33}	U_{23}	U_{13}	U_{12}
Pd(1)	58(1)	43(1)	64(1)	4(1)	28(1)	-2(1)
Pd(2)	73(1)	39(1)	71(1)	3(1)	41(1)	-2(1)
S(1)	78(4)	63(4)	84(4)	13(3)	42(4)	-7(3)
S(2)	77(4)	57(3)	64(4)	4(3)	44(3)	13(3)
S(3)	74(4)	49(3)	67(4)	-5(3)	29(3)	3(3)
S(4)	64(4)	55(3)	62(4)	7(3)	22(3)	0(3)
O(1)	85(11)	103(11)	78(11)	35(8)	44(9)	31(8)
O(2)	78(10)	63(9)	62(9)	35(7)	18(7)	2(7)
O(3)	98(12)	45(7)	60(9)	-9(6)	27(8)	-33(7)
O(4)	63(10)	87(10)	70(10)	16(8)	27(8)	8(7)
O(5)	109(12)	51(7)	41(7)	9(5)	34(8)	9(7)
O(6)	123(13)	77(10)	85(11)	22(8)	71(10)	7(9)
O(7)	69(10)	119(11)	57(9)	-4(7)	34(8)	8(8)
O(8)	105(12)	48(7)	42(8)	10(6)	32(8)	4(7)
N(1)	67(10)	45(8)	34(8)	9(6)	11(7)	11(6)
N(2)	92(12)	9(5)	56(10)	3(6)	35(9)	-17(6)
N(3)	62(10)	83(10)	38(9)	-13(7)	23(8)	-4(7)
N(4)	78(10)	37(7)	87(11)	-20(7)	64(9)	-26(6)
B(1)	113(11)	65(9)	55(9)	18(7)	63(9)	34(10)
F(1)	105(8)	102(8)	142(12)	5(8)	66(8)	19(7)
F(2)	167(12)	66(6)	95(9)	6(6)	66(9)	-11(7)
F(3)	124(9)	136(10)	48(6)	15(5)	45(6)	15(8)
F(4)	154(11)	67(6)	85(8)	-30(6)	72(8)	-19(7)
B(2)	71(10)	89(12)	64(11)	-25(7)	20(8)	-57(10)
F(5)	61(6)	170(11)	70(8)	7(7)	10(5)	-24(7)
F(6)	144(11)	82(7)	106(10)	2(6)	47(9)	-29(7)

F(7)	61(6)	116(8)	74(7)	-16(6)	14(5)	-5(6)
F(8)	125(11)	96(8)	69(7)	-11(6)	9(7)	20(7)
B(3)	294(20)	72(9)	96(9)	30(8)	134(13)	57(12)
F(9)	245(13)	183(11)	146(11)	11(9)	-26(9)	29(9)
F(10)	463(24)	88(6)	308(18)	-1(8)	316(18)	-11(9)
F(11)	256(14)	250(13)	67(5)	24(6)	64(7)	125(11)
F(12)	476(21)	78(7)	277(16)	14(9)	308(18)	13(10)
B(4)	689(42)	37(13)	427(38)	-42(13)	430(24)	-1(15)
F(13)	938(54)	161(15)	594(38)	-78(21)	639(38)	20(24)
F(14)	585(34)	238(21)	520(33)	-134(20)	456(28)	-68(20)
F(15)	671(40)	91(10)	406(28)	-47(12)	405(29)	-35(15)
F(16)	778(46)	357(30)	412(31)	113(22)	438(29)	91(27)
C(1)	87(16)	45(11)	108(17)	25(11)	78(14)	14(10)
C(2)	122(18)	45(11)	69(14)	-14(10)	59(14)	-25(11)
C(3)	130(20)	17(7)	133(18)	1(8)	96(17)	-17(9)
C(4)	52(12)	52(12)	139(18)	-25(11)	28(12)	-34(9)
C(5)	20(7)	100(16)	100(13)	-24(10)	8(7)	5(8)
C(6)	22(8)	36(7)	83(11)	-3(7)	23(8)	-24(6)
C(7)	46(9)	44(8)	109(14)	-4(8)	38(10)	-10(6)
C(8)	110(17)	38(10)	60(12)	11(8)	29(12)	9(9)
C(9)	73(13)	31(8)	77(14)	10(8)	35(11)	3(7)
C(10)	109(15)	82(11)	114(16)	0(10)	81(13)	21(10)
C(11)	261(37)	217(32)	200(32)	104(25)	163(29)	184(29)
C(12)	61(11)	90(16)	124(21)	4(14)	25(12)	45(10)
C(13)	98(21)	75(16)	160(28)	28(16)	42(20)	14(14)
C(14)	91(15)	81(15)	145(20)	-38(13)	78(15)	-28(11)
C(15)	73(12)	58(10)	37(9)	-10(7)	0(8)	13(8)
C(16)	187(32)	71(18)	144(27)	-31(16)	102(26)	-23(18)
C(17)	54(15)	168(26)	101(20)	-89(18)	-60(14)	56(16)
C(18)	121(28)	143(27)	161(35)	-57(23)	83(25)	-39(20)
C(19)	83(16)	62(10)	138(20)	13(11)	45(14)	18(10)
C(20)	52(11)	113(14)	98(14)	24(10)	59(10)	31(9)
C(21)	86(13)	37(9)	69(14)	6(9)	49(11)	-31(9)
C(22)	134(19)	56(12)	78(13)	-3(9)	88(14)	-12(11)
C(23)	83(12)	30(9)	107(16)	8(9)	67(12)	0(8)
C(24)	65(11)	77(12)	22(8)	-31(7)	3(7)	-33(9)
C(25)	74(12)	56(10)	25(8)	-17(7)	-7(7)	8(8)
C(26)	133(18)	53(11)	45(11)	-24(8)	53(12)	-4(11)
C(27)	62(10)	48(9)	36(8)	18(7)	26(8)	6(7)
C(28)	32(7)	33(8)	34(9)	-4(6)	-4(7)	-20(6)
C(29)	90(13)	63(12)	38(10)	-13(8)	21(9)	-18(8)
C(30)	106(17)	55(12)	60(13)	24(9)	54(13)	5(11)
C(31)	116(15)	38(9)	37(9)	-10(7)	37(10)	-1(9)
C(32)	60(10)	40(10)	90(14)	-2(8)	38(10)	-35(9)
C(33)	83(12)	49(9)	25(8)	20(6)	6(7)	-13(8)
C(34)	99(16)	41(10)	42(10)	-17(7)	13(10)	-34(10)

C(35)	40(8)	27(7)	42(9)	10(6)	17(7)	-7(6)
C(36)	86(13)	41(9)	73(13)	-32(8)	44(11)	-35(8)
C(37)	151(20)	39(10)	79(15)	19(9)	72(15)	19(11)
C(38)	64(10)	34(8)	22(8)	-7(6)	13(7)	0(7)
C(39)	112(14)	29(8)	105(15)	19(8)	93(13)	9(8)
C(40)	85(11)	42(8)	104(13)	-21(7)	77(11)	-29(7)
C(41)	126(19)	57(12)	70(14)	-4(10)	62(14)	14(12)
C(42)	77(13)	33(10)	54(12)	-10(7)	15(9)	-10(8)
C(43)	64(13)	33(9)	66(12)	-6(8)	31(10)	-17(8)
C(44)	101(16)	49(10)	106(15)	22(9)	64(13)	13(9)
C(45)	142(16)	32(7)	101(13)	-7(8)	85(12)	-40(8)
C(46)	159(24)	62(13)	170(25)	26(13)	143(22)	7(14)
C(47)	61(14)	99(17)	104(16)	35(12)	41(12)	28(12)
C(48)	30(9)	68(13)	96(15)	10(11)	40(10)	4(8)
C(49)	98(17)	47(11)	112(17)	-4(10)	79(15)	-7(10)
C(50)	97(15)	88(14)	144(20)	63(13)	28(14)	-23(11)
C(51)	124(17)	32(7)	95(16)	9(8)	86(15)	30(8)
C(52)	39(10)	80(12)	39(10)	-2(9)	-7(8)	31(8)
C(53)	114(20)	88(13)	109(15)	-21(10)	70(15)	0(12)
C(54)	127(22)	90(15)	198(31)	-25(18)	106(22)	23(14)
C(55)	111(25)	176(27)	206(39)	-63(26)	129(28)	-18(19)
C(56)	105(20)	66(12)	117(21)	-19(11)	1(15)	28(11)
C(57)	79(14)	100(15)	44(12)	6(10)	22(11)	13(11)
C(58)	202(28)	164(22)	138(22)	114(17)	120(22)	119(20)
C(59)	123(19)	128(20)	130(22)	-24(17)	73(17)	19(15)
C(60)	214(32)	89(17)	199(34)	-44(20)	117(26)	-36(17)
C(61)	120(20)	37(11)	98(16)	-15(10)	20(14)	-33(12)
C(62)	131(17)	58(11)	40(9)	8(7)	22(10)	-26(10)
C(63)	110(18)	41(11)	61(14)	-6(9)	30(13)	-6(10)
C(64)	75(12)	50(10)	100(14)	16(9)	49(12)	1(8)
C(65)	215(34)	79(17)	85(19)	34(14)	56(20)	32(19)
C(66)	95(16)	53(12)	187(29)	2(13)	81(18)	-11(10)
C(67)	113(19)	68(13)	62(12)	-13(10)	32(13)	10(12)
C(68)	95(16)	33(9)	119(19)	17(10)	72(14)	3(9)
C(69)	89(12)	71(9)	95(14)	-37(10)	37(11)	-22(8)
C(70)	115(18)	174(21)	199(27)	148(20)	98(19)	102(16)
C(71)	145(22)	80(13)	48(11)	25(9)	32(12)	-33(12)
C(72)	89(18)	102(16)	116(19)	9(13)	58(16)	14(13)
C(73)	90(17)	92(16)	96(17)	-1(12)	66(15)	10(12)
C(74)	83(14)	78(13)	56(14)	25(10)	31(11)	36(11)
C(75)	77(14)	71(13)	59(13)	20(10)	48(12)	33(11)
C(76)	124(19)	70(13)	49(11)	6(9)	36(11)	15(12)
C(77)	86(13)	58(11)	89(16)	-19(10)	38(12)	-27(10)
C(78)	156(25)	105(20)	67(15)	-32(13)	32(15)	-33(16)
C(79)	80(17)	122(21)	73(16)	0(13)	4(14)	7(14)
C(80)	76(15)	96(16)	36(10)	-6(10)	22(10)	24(12)

C(81)	129(16)	208(20)	181(20)	181(18)	133(16)	121(15)
C(82)	129(16)	32(6)	68(9)	2(6)	21(10)	-12(8)
C(83)	61(12)	97(13)	72(14)	4(10)	21(10)	-7(9)
C(84)	127(19)	76(12)	21(8)	-17(7)	20(10)	-50(12)
C(85)	134(21)	59(11)	25(9)	4(8)	18(11)	-7(11)
C(86)	110(17)	77(14)	78(15)	-9(11)	62(14)	-30(11)

The anisotropic displacement factor exponent takes the form: $-2\pi^2[h^2\,a^{*2}\,U11 + ... + 2hka^*b^*U12]$

Table A-25. Hydrogen coordinates (x 10^4) and isotropic displacement parameters ($Å^2$ x 10^3) for [2]-Rotaxane **9**.

Atom	x	y	z	U(eq)
H(3A)	539(16)	-7233(10)	2865(14)	95
H(4A)	-847(12)	-7256(13)	1912(13)	104
H(5A)	-1387(10)	-5907(15)	1261(12)	97
H(7A)	-1250(11)	-4199(12)	1276(13)	78
H(7B)	-1158(11)	-4694(12)	597(13)	78
H(8A)	2045(14)	-6089(12)	2971(12)	88
H(8B)	1822(14)	-6184(12)	3667(12)	88
H(10A)	-820(14)	-2903(15)	2124(13)	108
H(11A)	-934(22)	-1236(23)	2437(19)	245
H(12A)	-1500(13)	-288(16)	1400(17)	117
H(13A)	-865(18)	-351(18)	647(19)	141
H(14A)	-446(14)	-1783(16)	436(15)	115
H(16A)	3462(23)	-5228(17)	4637(19)	148
H(17A)	4950(15)	-4826(22)	4957(16)	172
H(18A)	5189(22)	-3896(22)	4055(21)	161
H(19A)	4167(16)	-3657(13)	2970(17)	115
H(20A)	2869(12)	-3787(13)	2652(12)	94
H(21A)	1855(12)	-2368(11)	3418(12)	71
H(22A)	2738(15)	-1067(13)	3656(12)	89
H(24A)	2371(11)	-1421(12)	1446(8)	73
H(25A)	1488(12)	-2560(12)	1373(9)	75
H(27A)	2477(11)	350(11)	1493(9)	57
H(28A)	3274(8)	1615(9)	1625(9)	48
H(29A)	4776(14)	941(13)	3690(11)	80
H(30A)	3998(14)	-399(12)	3669(12)	81
H(31A)	4666(13)	2181(11)	2223(10)	75
H(31B)	5271(13)	1806(11)	3052(10)	75
H(32A)	4623(11)	2727(11)	3608(11)	74
H(32B)	3916(11)	3015(11)	2797(11)	74

H(33A)	4301(14)	4217(13)	1994(10)	71
H(34A)	5221(13)	5355(11)	2068(11)	81
H(36A)	6793(12)	4716(11)	4213(11)	76
H(37A)	5881(16)	3533(12)	4173(13)	99
H(39A)	6912(12)	6201(10)	4349(11)	79
H(40A)	7603(11)	7686(11)	4483(10)	77
H(41A)	7234(15)	7262(13)	2317(12)	93
H(42A)	6550(12)	5913(11)	2252(11)	72
H(45A)	10598(13)	11191(11)	4693(12)	96
H(46A)	9863(17)	12319(15)	3730(15)	125
H(47A)	8532(14)	12073(15)	2825(14)	104
H(49A)	7402(14)	11090(13)	2086(13)	89
H(49B)	7132(14)	11070(13)	2750(13)	89
H(50A)	10418(15)	9489(15)	5192(16)	144
H(50B)	10393(15)	8973(15)	4464(16)	144
H(52A)	5742(11)	10127(12)	1126(10)	75
H(53A)	4393(18)	10060(15)	755(14)	115
H(54A)	3859(21)	9230(20)	1355(22)	151
H(55A)	4721(21)	8655(22)	2642(23)	171
H(56A)	6260(18)	8975(16)	3105(17)	137
H(58A)	9640(19)	7612(20)	3525(16)	181
H(59A)	10606(19)	6538(20)	3647(17)	145
H(60A)	10295(21)	5085(20)	4163(23)	190
H(61A)	10261(16)	5436(14)	5350(15)	115
H(62A)	9555(14)	6821(13)	5442(10)	99
H(64A)	1825(12)	851(11)	3771(13)	85
H(65A)	730(23)	354(17)	2867(16)	157
H(66A)	127(17)	752(14)	1637(19)	127
H(67A)	837(17)	1886(15)	1193(14)	101
H(69A)	1571(12)	2658(12)	1103(11)	104
H(69B)	1477(12)	3580(12)	1496(11)	104
H(70A)	2487(14)	4196(15)	1481(15)	183
H(70B)	2019(14)	3723(15)	682(15)	183
H(71A)	2591(18)	2879(16)	142(12)	115
H(71B)	3022(18)	3861(16)	260(12)	115
H(72A)	3735(14)	2854(16)	-9(14)	117
H(72B)	3754(14)	2171(16)	621(14)	117
H(73A)	5141(14)	2723(16)	400(13)	101
H(73B)	5260(14)	2040(16)	1073(13)	101
H(74A)	6471(9)	2902(8)	1296(7)	87
H(74B)	5998(9)	3804(8)	1351(7)	87
H(76A)	7185(9)	4131(8)	2108(7)	98
H(77A)	8557(13)	4712(14)	3049(13)	94
H(78A)	8987(19)	4093(17)	4301(14)	139
H(79A)	8257(18)	3018(20)	4502(15)	124
H(81A)	7501(13)	1207(15)	4153(11)	179

H(81B)	7497(13)	1969(15)	4723(11)	179
H(82A)	6964(14)	769(10)	4827(11)	102
H(82B)	6339(14)	762(10)	3948(11)	102
H(83A)	6635(14)	1749(16)	5635(13)	96
H(83B)	5946(14)	968(16)	5307(13)	96
H(84A)	5498(14)	2248(13)	5854(9)	96
H(84B)	5512(14)	2909(13)	5209(9)	96
H(85A)	3945(15)	3004(13)	4650(10)	96
H(85B)	4091(15)	2407(13)	5378(10)	96
H(86A)	3293(11)	1185(11)	4454(10)	98
H(86B)	2776(11)	2021(11)	4547(10)	98

Table A-26. Details of X-ray Data Collection, Solution and Refinement for [2]-Rotaxane, Molecular Shuttle **17**.

Empirical formula	$C_{68}H_{84}B_5F_{20}N_5O_8$
Formula weight	1533.45
Temperature, K	293(2)
Wavelength, Å	0.71073
Crystal system	Monoclinic
Space group	*Cc* (No. 9)
a, Å	40.78(2)
b, Å	15.808(5)
c, Å	12.336(4)
β, °	98.48(2)
V, Å^3	7866(5)
Z	4
ρ_{calcd}, Mg m^{-3}	1.295
μ, mm^{-1}	0.115
F(000)	3184
Crystal size, mm	0.22 x 0.24 x 0.38
θ–range for data collection, °	2.02 to 23.50
Limiting indices	$-45 \le h \le 42$, $-9 \le k \le 17$, $-13 \le l \le 12$
Reflections collected	16889
Independent reflections	10068 [R(int) = 0.0631]
Refinement method	Full-matrix least-squares on F^2
Data / restraints / parameters	10068 / 369 / 1001
Goodness-of-fit on F^2	0.929
Final R indices [I>2σ(I)]	$R_1 = 0.0997$, $wR_2 = 0.2451$
R indices (all data)	$R_1 = 0.1982$, $wR_2 = 0.2999$
Largest differences; peak and hole	0.516 and -0.274 eÅ^{-3}

Table A-27. Atomic coordinates (x 10^4) and equivalent isotropic displacement parameters ($Å^2$ x 10^3) for [2]-Rotaxane, Molecular Shuttle **17**.

Atom	x	y	z	U(eq)
C(1)	6892(4)	3585(12)	9767(13)	130(5)
C(2)	7113(6)	4323(18)	10230(20)	227(11)
C(3)	6602(6)	4126(15)	9290(19)	213(11)
C(4)	6884(8)	3090(20)	10893(18)	300(20)
C(5)	7075(4)	3122(14)	8944(15)	125(6)
C(6)	7120(5)	3566(18)	8050(20)	173(11)
C(7)	7245(6)	3248(14)	7210(20)	162(10)
N(1)	7351(3)	2432(14)	7247(18)	155(6)
C(8)	7352(4)	2002(14)	8250(20)	160(7)
C(9)	7180(4)	2381(12)	9104(12)	117(5)
C(10)	7543(4)	1950(18)	6500(16)	198(10)
C(11)	7363(5)	1144(13)	6146(17)	188(9)
N(2)	7050(4)	1291(11)	5230(20)	181(8)
C(12)	6786(5)	1253(11)	5742(12)	132(6)
C(13)	6471(3)	1348(9)	5090(13)	105(4)
C(14)	6438(4)	1512(8)	4028(11)	94(4)
C(15)	6749(4)	1617(11)	3694(13)	136(6)
C(16)	7015(5)	1490(20)	4242(14)	270(20)
C(17)	6115(3)	1608(6)	3360(10)	69(3)
C(18)	5824(3)	1452(7)	3652(9)	74(3)
C(19)	5531(3)	1580(6)	3073(8)	68(3)
N(3)	5507(2)	1886(5)	2058(6)	58(2)
C(20)	5780(3)	2050(7)	1659(9)	68(3)
C(21)	6087(3)	1848(7)	2245(11)	88(4)
C(22)	5174(3)	2033(8)	1408(8)	69(3)
C(23)	5091(2)	2970(7)	1488(7)	56(3)
N(4)	4761(2)	3114(5)	828(6)	56(2)
C(24)	4495(3)	2979(7)	1318(8)	72(3)
C(25)	4170(3)	3045(6)	731(8)	69(3)
C(26)	4136(2)	3326(6)	-346(7)	56(3)
C(27)	4419(3)	3516(7)	-822(7)	68(3)
C(28)	4736(3)	3385(6)	-200(7)	63(3)
C(29)	3805(3)	3413(7)	-1009(8)	71(3)
C(30)	3551(3)	2903(8)	-726(9)	89(3)
C(31)	3256(3)	2943(12)	-1483(16)	130(5)
N(5)	3221(3)	3391(8)	-2423(9)	93(3)
C(32)	3463(4)	3844(9)	-2622(12)	106(4)
C(33)	3757(4)	3854(8)	-2017(12)	106(4)
C(34)	2902(3)	3260(9)	-3224(10)	106(4)
C(35)	2967(4)	2596(14)	-4172(12)	124(6)
C(36)	3097(3)	2952(10)	-4999(14)	112(4)
C(37)	3181(4)	2310(19)	-5780(12)	143(7)

C(38)	3153(4)	1462(11)	-5636(19)	118(6)
C(39)	3010(5)	1182(11)	-4769(16)	129(5)
C(40)	2940(4)	1772(12)	-4031(14)	117(5)
C(41)	3264(4)	905(11)	-6517(15)	138(6)
C(42)	3224(4)	-106(15)	-6080(20)	213(11)
C(43)	3047(9)	970(30)	-7510(20)	440(40)
C(44)	3634(5)	1054(15)	-6524(16)	193(10)
O(1)	4438(2)	1122(4)	-171(6)	75(2)
O(2)	4474(2)	1153(4)	2238(5)	77(2)
O(3)	4809(2)	2312(4)	3690(5)	69(2)
O(4)	5418(2)	3262(5)	4255(5)	84(2)
O(5)	5817(2)	3852(4)	2979(5)	75(2)
O(6)	5790(2)	3904(5)	571(5)	77(2)
O(7)	5457(2)	2708(5)	-818(6)	84(2)
O(8)	4849(2)	1769(4)	-1415(5)	77(2)
C(45)	4520(3)	1696(7)	-1881(9)	70(3)
C(46)	4407(3)	1956(7)	-2985(9)	78(3)
C(47)	4087(5)	1857(9)	-3388(11)	114(5)
C(48)	3858(3)	1488(8)	-2694(14)	102(5)
C(49)	3978(3)	1240(8)	-1586(9)	81(3)
C(50)	4301(3)	1326(7)	-1200(8)	65(3)
C(51)	4234(2)	710(6)	486(7)	60(3)
C(52)	4424(3)	425(8)	1539(8)	82(3)
C(53)	4612(3)	898(7)	3303(9)	96(4)
C(54)	4602(3)	1681(9)	4037(9)	97(4)
C(55)	4868(3)	2978(8)	4420(9)	94(4)
C(56)	5194(3)	3066(8)	5015(10)	94(4)
C(57)	5739(3)	3343(6)	4707(8)	61(3)
C(58)	5880(5)	3099(8)	5762(10)	107(5)
C(59)	6200(4)	3170(8)	6144(10)	81(4)
C(60)	6394(4)	3447(10)	5531(11)	114(5)
C(61)	6276(3)	3706(7)	4502(10)	82(4)
C(62)	5953(3)	3643(6)	4053(10)	74(3)
C(63)	6016(3)	4377(8)	2370(9)	88(4)
C(64)	5818(3)	4603(7)	1284(9)	87(4)
C(65)	5628(3)	4092(10)	-512(8)	102(4)
C(66)	5617(3)	3405(8)	-1208(9)	83(3)
C(67)	5421(4)	1928(8)	-1535(10)	102(4)
C(68)	5096(3)	1959(9)	-2153(8)	99(4)
B(1)	4789(4)	5279(7)	1980(10)	134(5)
F(1)	4563(3)	4836(7)	2240(9)	246(6)
F(2)	5008(4)	5358(14)	2832(12)	400(11)
F(3)	4690(4)	6037(6)	1765(11)	287(8)
F(4)	4930(3)	4983(6)	1220(11)	234(6)
B(2)	3821(8)	4270(30)	4700(40)	650(40)
F(5)	3519(7)	4510(30)	4490(40)	600(40)

F(6)	3810(14)	3470(30)	4840(50)	700(40)
F(7)	3994(7)	4320(30)	3910(40)	610(40)
F(8)	3952(8)	4650(30)	5550(40)	630(40)
B(3)	5486(3)	296(8)	6015(9)	90(4)
F(9)	5537(4)	-265(8)	5328(11)	282(9)
F(10)	5347(4)	944(7)	5508(9)	244(8)
F(11)	5769(4)	594(16)	6437(16)	396(16)
F(12)	5346(3)	11(6)	6826(7)	172(4)
B(4)	2826(9)	4835(17)	-5870(20)	530(30)
F(13)	2757(12)	4107(17)	-5530(30)	480(30)
F(14)	2548(9)	5186(13)	-5850(20)	430(20)
F(15)	3030(10)	5240(20)	-5170(20)	420(20)
F(16)	2874(6)	4805(16)	-6860(20)	400(20)
B(5)	2381(5)	-1389(11)	3955(15)	166(10)
F(17)	2103(4)	-1558(11)	4222(18)	306(11)
F(18)	2359(5)	-733(11)	3325(14)	290(8)
F(19)	2560(6)	-1129(12)	4822(11)	344(13)
F(20)	2502(4)	-2031(11)	3522(18)	327(12)
O(1W)	6965(5)	837(7)	1099(13)	229(7)
O(2W)	1910(8)	4650(20)	-7110(50)	350(30)
O(3W)	6236(5)	1009(14)	-115(14)	261(8)
O(4W)	3422(2)	6596(8)	-3142(7)	157(4)
O(5W)	6301(6)	-1020(50)	2761(18)	430(40)

Table A-28. Bonding parameters for [2]-Rotaxane, Molecular Shuttle **17**.

Bond	Distance (Å)	Bond	Distance (Å)
C(1)-C(3)	1.51(2)	O(1)-C(50)	1.348(12)
C(1)-C(2)	1.54(3)	O(1)-C(51)	1.402(11)
C(1)-C(5)	1.53(2)	O(2)-C(53)	1.409(12)
C(1)-C(4)	1.60(3)	O(2)-C(52)	1.434(12)
C(5)-C(9)	1.25(2)	O(3)-C(55)	1.384(11)
C(5)-C(6)	1.34(2)	O(3)-C(54)	1.411(13)
C(6)-C(7)	1.32(3)	O(4)-C(57)	1.351(12)
C(7)-N(1)	1.36(2)	O(4)-C(56)	1.437(12)
N(1)-C(8)	1.41(2)	O(5)-C(62)	1.398(13)
N(1)-C(10)	1.50(2)	O(5)-C(63)	1.446(12)
C(8)-C(9)	1.48(2)	O(6)-C(64)	1.407(11)
C(10)-C(11)	1.50(3)	O(6)-C(65)	1.432(12)
C(11)-N(2)	1.59(2)	O(7)-C(66)	1.401(12)
N(2)-C(16)	1.25(3)	O(7)-C(67)	1.511(14)
N(2)-C(12)	1.33(2)	O(8)-C(45)	1.383(12)
C(12)-C(13)	1.418(19)	O(8)-C(68)	1.486(14)
C(13)-C(14)	1.324(17)	C(45)-C(46)	1.431(15)

C(14)-C(15)	1.400(19)	C(45)-C(50)	1.439(15)
C(14)-C(17)	1.456(17)	C(46)-C(47)	1.333(18)
C(15)-C(16)	1.20(2)	C(47)-C(48)	1.48(2)
C(17)-C(18)	1.316(14)	C(48)-C(49)	1.436(18)
C(17)-C(21)	1.415(16)	C(49)-C(50)	1.341(14)
C(18)-C(19)	1.313(13)	C(51)-C(52)	1.482(13)
C(19)-N(3)	1.333(12)	C(53)-C(54)	1.538(16)
N(3)-C(20)	1.308(12)	C(55)-C(56)	1.426(15)
N(3)-C(22)	1.493(12)	C(57)-C(62)	1.358(13)
C(20)-C(21)	1.385(15)	C(57)-C(58)	1.397(16)
C(22)-C(23)	1.526(11)	C(58)-C(59)	1.329(18)
C(23)-N(4)	1.483(12)	C(59)-C(60)	1.250(18)
N(4)-C(28)	1.328(11)	C(60)-C(61)	1.352(15)
N(4)-C(24)	1.336(12)	C(61)-C(62)	1.356(14)
C(24)-C(25)	1.418(14)	C(63)-C(64)	1.501(15)
C(25)-C(26)	1.389(12)	C(65)-C(66)	1.380(16)
C(26)-C(27)	1.399(13)	C(67)-C(68)	1.428(16)
C(26)-C(29)	1.479(13)	B(1)-F(1)	1.236(11)
C(27)-C(28)	1.419(13)	B(1)-F(4)	1.261(11)
C(29)-C(30)	1.397(15)	B(1)-F(2)	1.280(12)
C(29)-C(33)	1.414(16)	B(1)-F(3)	1.279(11)
C(30)-C(31)	1.413(18)	B(2)-F(8)	1.269(15)
C(31)-N(5)	1.35(2)	B(2)-F(6)	1.270(15)
N(5)-C(32)	1.271(15)	B(2)-F(7)	1.279(15)
N(5)-C(34)	1.526(15)	B(2)-F(5)	1.283(15)
C(32)-C(33)	1.316(17)	B(3)-F(9)	1.264(11)
C(34)-C(35)	1.62(2)	B(3)-F(11)	1.282(12)
C(35)-C(40)	1.321(19)	B(3)-F(10)	1.288(11)
C(35)-C(36)	1.342(19)	B(3)-F(12)	1.303(10)
C(36)-C(37)	1.47(2)	B(4)-F(14)	1.266(15)
C(37)-C(38)	1.36(2)	B(4)-F(16)	1.268(14)
C(38)-C(39)	1.36(2)	B(4)-F(13)	1.272(15)
C(38)-C(41)	1.52(2)	B(4)-F(15)	1.274(14)
C(39)-C(40)	1.36(2)	B(5)-F(17)	1.253(13)
C(41)-C(43)	1.40(2)	B(5)-F(19)	1.272(13)
C(41)-C(44)	1.53(2)	B(5)-F(20)	1.278(13)
C(41)-C(42)	1.70(3)	B(5)-F(18)	1.292(13)

Bonds	Angle (°)	Bonds	Angle (°)
C(3)-C(1)-C(2)	95.7(19)	C(43)-C(41)-C(42)	105(2)
C(3)-C(1)-C(5)	116.4(15)	C(38)-C(41)-C(42)	105.6(17)
C(2)-C(1)-C(5)	107.0(15)	C(44)-C(41)-C(42)	106.6(13)
C(3)-C(1)-C(4)	120.2(18)	C(50)-O(1)-C(51)	117.2(8)
C(2)-C(1)-C(4)	98(2)	C(53)-O(2)-C(52)	109.4(8)
C(5)-C(1)-C(4)	114.4(16)	C(55)-O(3)-C(54)	113.3(8)
C(9)-C(5)-C(6)	122(2)	C(57)-O(4)-C(56)	114.9(8)

C(9)-C(5)-C(1)	122.0(17)	C(62)-O(5)-C(63)	117.0(8)
C(6)-C(5)-C(1)	115.8(19)	C(64)-O(6)-C(65)	113.9(9)
C(7)-C(6)-C(5)	124(3)	C(66)-O(7)-C(67)	116.8(9)
C(6)-C(7)-N(1)	120(2)	C(45)-O(8)-C(68)	117.8(8)
C(7)-N(1)-C(8)	116(2)	O(8)-C(45)-C(46)	122.0(10)
C(7)-N(1)-C(10)	131(3)	O(8)-C(45)-C(50)	116.0(9)
C(8)-N(1)-C(10)	111(2)	C(46)-C(45)-C(50)	122.0(10)
N(1)-C(8)-C(9)	119.2(18)	C(47)-C(46)-C(45)	118.9(12)
C(5)-C(9)-C(8)	117.1(18)	C(46)-C(47)-C(48)	119.7(12)
N(1)-C(10)-C(11)	109.4(16)	C(49)-C(48)-C(47)	120.3(11)
C(10)-C(11)-N(2)	112.9(16)	C(50)-C(49)-C(48)	119.2(11)
C(16)-N(2)-C(12)	119.3(14)	C(49)-C(50)-O(1)	124.0(11)
C(16)-N(2)-C(11)	134(2)	C(49)-C(50)-C(45)	119.8(10)
C(12)-N(2)-C(11)	106(2)	O(1)-C(50)-C(45)	116.2(10)
N(2)-C(12)-C(13)	117.1(15)	O(1)-C(51)-C(52)	111.7(8)
C(14)-C(13)-C(12)	122.2(15)	O(2)-C(52)-C(51)	107.1(9)
C(13)-C(14)-C(15)	110.6(13)	O(2)-C(53)-C(54)	106.2(9)
C(13)-C(14)-C(17)	122.1(15)	O(3)-C(54)-C(53)	108.8(8)
C(15)-C(14)-C(17)	127.2(13)	O(3)-C(55)-C(56)	118.0(10)
C(16)-C(15)-C(14)	126.4(16)	C(55)-C(56)-O(4)	108.6(10)
C(15)-C(16)-N(2)	124(2)	O(4)-C(57)-C(62)	117.1(10)
C(18)-C(17)-C(21)	111.7(11)	O(4)-C(57)-C(58)	126.8(11)
C(18)-C(17)-C(14)	127.2(13)	C(62)-C(57)-C(58)	115.9(12)
C(21)-C(17)-C(14)	121.0(13)	C(59)-C(58)-C(57)	123.8(12)
C(19)-C(18)-C(17)	127.4(12)	C(60)-C(59)-C(58)	119.4(12)
C(18)-C(19)-N(3)	120.1(11)	C(59)-C(60)-C(61)	120.4(16)
C(20)-N(3)-C(19)	118.5(10)	C(60)-C(61)-C(62)	123.4(14)
C(20)-N(3)-C(22)	121.8(9)	C(61)-C(62)-C(57)	117.0(12)
C(19)-N(3)-C(22)	119.7(10)	C(61)-C(62)-O(5)	126.5(10)
N(3)-C(20)-C(21)	120.7(11)	C(57)-C(62)-O(5)	116.5(11)
C(20)-C(21)-C(17)	120.5(11)	O(5)-C(63)-C(64)	109.3(9)
N(3)-C(22)-C(23)	108.0(7)	O(6)-C(64)-C(63)	110.8(9)
N(4)-C(23)-C(22)	107.8(6)	C(66)-C(65)-O(6)	112.7(12)
C(28)-N(4)-C(24)	122.1(8)	C(65)-C(66)-O(7)	112.2(10)
C(28)-N(4)-C(23)	120.6(8)	C(68)-C(67)-O(7)	106.7(10)
C(24)-N(4)-C(23)	117.3(8)	C(67)-C(68)-O(8)	109.1(9)
N(4)-C(24)-C(25)	121.2(9)	F(1)-B(1)-F(4)	114.9(9)
C(26)-C(25)-C(24)	117.7(9)	F(1)-B(1)-F(2)	107.3(11)
C(25)-C(26)-C(27)	120.0(9)	F(4)-B(1)-F(2)	107.8(12)
C(25)-C(26)-C(29)	120.7(9)	F(1)-B(1)-F(3)	111.2(12)
C(27)-C(26)-C(29)	119.3(8)	F(4)-B(1)-F(3)	111.0(10)
C(26)-C(27)-C(28)	118.9(8)	F(2)-B(1)-F(3)	103.9(10)
N(4)-C(28)-C(27)	119.9(9)	F(8)-B(2)-F(6)	112(3)
C(30)-C(29)-C(33)	119.5(11)	F(8)-B(2)-F(7)	113(3)
C(30)-C(29)-C(26)	117.3(10)	F(6)-B(2)-F(7)	102(2)
C(33)-C(29)-C(26)	122.0(11)	F(8)-B(2)-F(5)	107(2)

C(29)-C(30)-C(31)	113.6(13)	F(6)-B(2)-F(5)	106(2)
N(5)-C(31)-C(30)	124.3(13)	F(7)-B(2)-F(5)	117(3)
C(32)-N(5)-C(31)	118.4(12)	F(9)-B(3)-F(11)	107.7(14)
C(32)-N(5)-C(34)	124.2(12)	F(9)-B(3)-F(10)	109.7(12)
C(31)-N(5)-C(34)	117.2(12)	F(11)-B(3)-F(10)	102.1(15)
N(5)-C(32)-C(33)	124.4(13)	F(9)-B(3)-F(12)	114.0(12)
C(32)-C(33)-C(29)	119.3(13)	F(11)-B(3)-F(12)	106.5(14)
N(5)-C(34)-C(35)	110.0(10)	F(10)-B(3)-F(12)	115.8(10)
C(40)-C(35)-C(36)	124.3(18)	F(14)-B(4)-F(16)	108(2)
C(40)-C(35)-C(34)	121.2(14)	F(14)-B(4)-F(13)	98(2)
C(36)-C(35)-C(34)	113.7(17)	F(16)-B(4)-F(13)	111(2)
C(35)-C(36)-C(37)	111.3(16)	F(14)-B(4)-F(15)	105(2)
C(38)-C(37)-C(36)	124.2(16)	F(16)-B(4)-F(15)	120(2)
C(37)-C(38)-C(39)	118.5(16)	F(13)-B(4)-F(15)	112(2)
C(37)-C(38)-C(41)	116(2)	F(17)-B(5)-F(19)	106.1(17)
C(39)-C(38)-C(41)	125.4(18)	F(17)-B(5)-F(20)	111.1(15)
C(40)-C(39)-C(38)	117.2(18)	F(19)-B(5)-F(20)	113.5(18)
C(35)-C(40)-C(39)	123.9(19)	F(17)-B(5)-F(18)	110.1(18)
C(43)-C(41)-C(38)	111.2(13)	F(19)-B(5)-F(18)	103.1(15)
C(43)-C(41)-C(44)	119(3)	F(20)-B(5)-F(18)	112.5(17)
C(38)-C(41)-C(44)	108.3(13)		

Table A-29. Anisotropic displacement parameters ($Å^2 \times 10^3$) for [2]-Rotaxane, Molecular Shuttle **17**.

Atom	U_{11}	U_{22}	U_{33}	U_{23}	U_{13}	U_{12}
C(1)	106(13)	157(15)	125(12)	17(11)	11(10)	-11(10)
C(2)	180(20)	260(30)	240(20)	-120(20)	42(17)	-40(20)
C(3)	200(20)	240(20)	186(18)	-2(17)	-47(15)	100(19)
C(4)	290(30)	470(60)	129(17)	-40(20)	-24(19)	140(40)
C(5)	77(10)	154(18)	142(15)	53(12)	9(9)	12(10)
C(6)	117(16)	260(30)	164(18)	-20(20)	72(14)	-32(14)
C(7)	117(15)	121(16)	210(20)	53(15)	-95(16)	-19(12)
N(1)	79(10)	183(19)	191(17)	-3(14)	-23(10)	13(10)
C(8)	64(11)	195(19)	197(19)	-8(19)	-59(12)	-8(11)
C(9)	139(13)	112(12)	89(9)	-2(8)	-22(9)	29(10)
C(10)	39(10)	380(30)	175(16)	-79(18)	21(9)	12(14)
C(11)	140(17)	190(20)	196(17)	-22(14)	-96(14)	41(13)
N(2)	57(10)	190(15)	270(20)	-60(14)	-57(12)	52(9)
C(12)	113(15)	176(16)	91(9)	-21(9)	-41(10)	51(12)
C(13)	64(9)	125(12)	119(12)	12(8)	-5(8)	-1(7)
C(14)	128(14)	78(9)	70(9)	-16(6)	-8(8)	18(8)
C(15)	76(12)	210(18)	116(11)	47(11)	-8(10)	-23(10)
C(16)	66(13)	660(60)	67(10)	31(18)	-25(9)	23(18)

C(17)	60(9)	50(7)	93(9)	8(6)	-4(7)	-4(5)
C(18)	64(9)	84(9)	70(7)	-16(6)	1(7)	-5(6)
C(19)	80(10)	78(8)	46(6)	5(5)	11(6)	-19(6)
N(3)	67(7)	42(5)	64(6)	-4(4)	2(5)	1(4)
C(20)	43(8)	87(8)	73(7)	7(6)	4(6)	-3(6)
C(21)	74(10)	92(9)	105(10)	2(7)	32(7)	-5(7)
C(22)	67(8)	74(9)	64(7)	5(5)	3(6)	5(5)
C(23)	58(7)	61(8)	49(6)	10(4)	11(5)	-6(5)
N(4)	63(6)	48(5)	59(6)	0(4)	14(5)	-10(4)
C(24)	80(9)	93(9)	45(6)	13(5)	15(6)	-5(6)
C(25)	86(9)	66(7)	60(7)	13(5)	25(6)	-13(6)
C(26)	60(7)	79(7)	30(5)	-5(4)	10(5)	12(5)
C(27)	81(9)	83(8)	39(5)	1(5)	4(6)	-4(6)
C(28)	64(8)	90(8)	37(6)	5(5)	16(5)	13(6)
C(29)	58(8)	92(9)	60(7)	7(6)	7(5)	2(6)
C(30)	52(8)	125(10)	83(7)	-11(7)	-12(6)	-6(7)
C(31)	62(10)	173(15)	161(15)	-42(12)	35(10)	-3(8)
N(5)	71(8)	114(9)	89(7)	4(6)	-2(6)	-8(6)
C(32)	73(10)	117(11)	112(9)	15(8)	-41(8)	-21(8)
C(33)	120(13)	66(9)	130(12)	12(7)	7(10)	-17(7)
C(34)	58(8)	160(13)	95(9)	11(8)	-5(6)	8(7)
C(35)	95(11)	180(20)	101(11)	24(11)	11(8)	-22(11)
C(36)	51(8)	137(12)	139(13)	0(11)	-20(8)	-13(7)
C(37)	86(11)	260(30)	79(9)	-15(13)	-2(7)	6(13)
C(38)	73(10)	69(11)	200(20)	-41(12)	-13(10)	8(8)
C(39)	129(14)	100(13)	160(14)	-4(12)	33(11)	46(10)
C(40)	134(13)	78(11)	134(12)	13(10)	2(10)	1(9)
C(41)	69(10)	134(15)	198(16)	-68(12)	-24(9)	28(9)
C(42)	99(13)	190(20)	360(30)	-140(20)	85(15)	-26(11)
C(43)	450(50)	580(60)	220(20)	-280(40)	-190(30)	380(50)
C(44)	124(17)	280(30)	181(17)	-21(16)	46(12)	109(16)
O(1)	77(5)	66(5)	82(5)	-5(4)	13(4)	-25(4)
O(2)	124(6)	55(5)	48(4)	-7(3)	2(4)	-24(4)
O(3)	95(5)	72(5)	45(3)	-5(3)	27(3)	-41(4)
O(4)	91(6)	113(7)	56(4)	-9(4)	38(4)	-34(5)
O(5)	87(5)	92(6)	45(4)	-1(4)	4(4)	-10(4)
O(6)	87(5)	86(6)	61(5)	7(4)	17(4)	6(4)
O(7)	90(6)	91(6)	72(4)	-12(5)	17(4)	-2(4)
O(8)	90(6)	73(5)	65(4)	-20(4)	6(4)	-13(4)
C(45)	76(9)	65(8)	64(7)	-10(6)	-3(6)	-25(6)
C(46)	90(10)	72(8)	65(7)	-2(5)	-6(6)	-21(6)
C(47)	147(16)	105(12)	79(9)	-1(8)	-21(10)	-5(10)
C(48)	75(9)	70(9)	153(14)	-57(9)	-6(9)	-10(7)
C(49)	70(10)	113(10)	60(7)	-23(6)	12(7)	-25(6)
C(50)	71(9)	78(8)	43(6)	-6(5)	-4(6)	27(6)
C(51)	77(7)	42(6)	61(6)	-7(5)	9(5)	-24(5)

C(52)	86(9)	93(10)	71(7)	7(7)	22(6)	-29(6)
C(53)	149(12)	52(8)	87(9)	12(7)	12(7)	-48(7)
C(54)	118(10)	130(12)	48(6)	-5(7)	34(6)	-20(8)
C(55)	68(9)	125(10)	100(8)	-69(8)	48(7)	-38(7)
C(56)	96(10)	88(9)	109(9)	-37(7)	56(8)	-42(7)
C(57)	73(9)	47(7)	70(8)	-9(5)	30(6)	-9(5)
C(58)	183(17)	104(11)	37(7)	9(6)	29(8)	-14(10)
C(59)	110(11)	78(9)	46(7)	3(6)	-23(8)	-1(7)
C(60)	153(14)	120(12)	58(8)	25(8)	-14(9)	31(10)
C(61)	88(11)	58(8)	94(9)	-11(6)	-14(7)	-3(6)
C(62)	82(10)	52(7)	88(9)	3(6)	14(8)	-30(6)
C(63)	85(9)	103(10)	80(8)	7(7)	23(7)	-24(7)
C(64)	134(11)	48(8)	78(8)	-11(6)	15(7)	-23(6)
C(65)	113(11)	165(14)	31(6)	9(8)	23(6)	-36(9)
C(66)	100(9)	94(9)	53(7)	7(7)	2(6)	-32(7)
C(67)	135(13)	97(10)	69(7)	9(7)	3(8)	21(8)
C(68)	127(12)	130(11)	41(6)	-25(6)	14(7)	27(8)
B(1)	275(18)	28(7)	104(11)	-43(7)	48(8)	-60(8)
F(1)	360(15)	184(10)	223(11)	-66(8)	142(10)	-154(11)
F(2)	290(19)	540(30)	324(18)	-150(20)	-92(14)	-26(19)
F(3)	530(20)	91(6)	305(13)	43(8)	298(14)	101(10)
F(4)	266(13)	136(9)	332(14)	-120(10)	150(11)	-26(8)
B(2)	280(30)	750(60)	830(60)	700(60)	-200(40)	-120(40)
F(5)	260(30)	710(60)	750(70)	660(60)	-170(30)	-160(30)
F(6)	520(60)	730(60)	820(80)	630(60)	-20(60)	-20(40)
F(7)	190(20)	710(70)	850(70)	600(60)	-220(30)	-150(30)
F(8)	190(30)	790(70)	840(60)	660(60)	-160(40)	-110(40)
B(3)	69(10)	128(14)	73(9)	12(9)	14(7)	-8(8)
F(9)	490(30)	162(10)	231(12)	-119(10)	163(15)	-38(12)
F(10)	392(19)	188(11)	188(10)	126(9)	164(11)	148(12)
F(11)	179(15)	630(40)	340(20)	-160(30)	-92(16)	-30(20)
F(12)	257(12)	148(8)	133(6)	63(6)	102(7)	34(7)
B(4)	730(50)	290(30)	520(30)	250(30)	-130(30)	-230(30)
F(13)	770(70)	230(30)	400(40)	210(30)	-70(40)	-140(30)
F(14)	770(50)	132(16)	270(30)	46(19)	-320(30)	-210(30)
F(15)	540(40)	350(40)	380(30)	190(30)	60(30)	-200(40)
F(16)	340(30)	300(30)	440(30)	320(20)	-310(20)	-290(20)
B(5)	200(30)	160(20)	150(20)	68(18)	83(19)	50(20)
F(17)	219(16)	273(17)	470(30)	-141(18)	210(19)	-50(12)
F(18)	380(20)	227(16)	259(16)	31(13)	34(15)	-4(14)
F(19)	570(40)	330(20)	107(8)	28(10)	-32(13)	0(20)
F(20)	248(19)	293(19)	490(30)	-37(19)	230(20)	39(13)
O(1W)	360(20)	72(8)	268(15)	-15(8)	82(14)	-34(9)
O(2W)	170(30)	230(40)	690(90)	160(50)	180(40)	70(30)
O(3W)	255(18)	330(20)	225(14)	-36(14)	128(13)	1(14)
O(4W)	111(7)	273(13)	90(5)	-24(7)	30(5)	20(7)

O(5W)	85(18)	1130(140)	82(14)	-110(30)	-3(11)	20(30)

Table A-30. Hydrogen coordinates (x 10^4) and isotropic displacement parameters ($Å^2$ x 10^3) for [2]-Rotaxane, Molecular Shuttle **17**.

Atom	x	y	z	U(eq)
H(2A)	7318	4106	10614	341
H(2B)	7003	4642	10734	341
H(2C)	7158	4683	9646	341
H(3A)	6438	3779	8863	319
H(3B)	6676	4554	8829	319
H(3C)	6507	4390	9872	319
H(4A)	6754	2581	10751	452
H(4B)	6787	3440	11392	452
H(4C)	7106	2939	11209	452
H(6A)	7060	4133	8019	208
H(7A)	7261	3580	6601	195
H(8A)	7460	1485	8374	192
H(9A)	7150	2084	9732	141
H(10A)	7763	1820	6879	238
H(10B)	7566	2291	5862	238
H(11A)	7290	880	6778	226
H(11B)	7515	758	5865	226
H(12A)	6806	1168	6495	159
H(13A)	6282	1293	5420	125
H(15A)	6751	1800	2978	164
H(16A)	7204	1550	3909	322
H(18A)	5825	1225	4348	89
H(19A)	5340	1457	3371	81
H(20A)	5769	2304	974	82
H(21A)	6275	1871	1903	106
H(22A)	5009	1691	1696	83
H(22B)	5175	1876	648	83
H(23A)	5086	3125	2246	67
H(23B)	5257	3312	1209	67
H(24A)	4523	2840	2059	86
H(25A)	3985	2905	1056	83
H(27A)	4398	3724	-1534	82
H(28A)	4926	3489	-513	75
H(30A)	3574	2568	-99	107
H(31A)	3073	2641	-1322	156
H(32A)	3429	4192	-3236	128
H(33A)	3931	4149	-2250	128
H(34A)	2828	3797	-3554	127

H(34B)	2730	3045	-2834	127
H(36A)	3130	3531	-5071	135
H(37A)	3257	2497	-6412	171
H(39A)	2962	612	-4687	154
H(40A)	2869	1583	-3390	141
H(42A)	3358	-182	-5383	320
H(42B)	3296	-490	-6604	320
H(42C)	2996	-216	-6023	320
H(43A)	3117	597	-8040	660
H(43B)	3047	1543	-7772	660
H(43C)	2826	823	-7390	660
H(44A)	3753	959	-5803	290
H(44B)	3669	1626	-6744	290
H(44C)	3713	670	-7031	290
H(46A)	4553	2190	-3412	93
H(47A)	4009	2019	-4105	137
H(48A)	3636	1416	-2976	122
H(49A)	3833	1023	-1142	97
H(51A)	4131	224	93	72
H(51B)	4060	1092	631	72
H(52A)	4302	-6	1870	99
H(52B)	4636	190	1421	99
H(53A)	4838	705	3315	115
H(53B)	4483	441	3554	115
H(54A)	4377	1890	3986	116
H(54B)	4679	1533	4795	116
H(55A)	4715	2927	4949	113
H(55B)	4814	3498	4017	113
H(56A)	5260	2545	5399	112
H(56B)	5197	3516	5552	112
H(58A)	5741	2874	6223	128
H(59A)	6280	3015	6862	98
H(60A)	6620	3476	5784	136
H(61A)	6424	3940	4081	99
H(63A)	6215	4076	2256	106
H(63B)	6081	4888	2781	106
H(64A)	5599	4789	1394	104
H(64B)	5925	5067	959	104
H(65A)	5403	4278	-472	122
H(65B)	5743	4553	-811	122
H(66A)	5841	3246	-1294	100
H(66B)	5502	3565	-1923	100
H(67A)	5587	1926	-2021	122
H(67B)	5448	1421	-1088	122
H(68A)	5078	1548	-2742	119
H(68B)	5055	2516	-2473	119

Table A-31. Details of X-ray Data Collection, Solution and Refinement for [3]Rotaxane **14**.

Empirical formula	$C_{110}H_{126}F_{18}N_6O_{34}S_6$
Formula weight	2610.53
Temperature, K	293(2)
Wavelength, Å	0.71073
Crystal system	Monoclinic
Space group	$P2_1/n$ (No. 14)
a, Å	16.892(4)
b, Å	14.926(7)
c, Å	25.494(13)
β, °	107.94(2)
V, Å^3	6115(4)
Z	2
ρ_{calcd}, Mg m^{-3}	1.418
μ, mm^{-1}	0.219
F(000)	2716
Crystal size, mm	0.24 x 0.30 x 0.34
θ–range for data collection, °	1.60 to 23.00
Limiting indices	$-18 \le h \le 17$, $-16 \le k \le 16$, $-28 \le l \le 26$
Reflections collected	24910
Independent reflections	8401 [R(int) = 0.0583]
Refinement method	Full-matrix least-squares on F^2
Data / restraints / parameters	8401 / 0 / 820
Goodness-of-fit on F^2	1.212
Final R indices [$I>2\sigma(I)$]	$R_1 = 0.1368$, $wR_2 = 0.3516$
R indices (all data)	$R_1 = 0.2204$, $wR_2 = 0.3959$
Largest differences; peak and hole	0.482 and -0.503 eÅ^{-3}

Table A-32. Atomic coordinates (x 10^4) and equivalent isotropic displacement parameters (Å^2 x 10^3) for [3]-Rotaxane, **14**.

Atom	x	y	z	U(eq)
O(1)	8248(4)	3610(4)	429(3)	113(2)
O(2)	6573(3)	3863(4)	495(3)	102(2)
O(3)	5689(7)	3265(6)	1205(5)	187(4)
O(4)	5476(3)	1412(5)	1512(2)	112(2)
O(5)	6528(4)	87(4)	1772(3)	114(2)
O(6)	8328(4)	143(5)	1853(3)	121(2)
O(7)	8867(4)	410(4)	936(4)	126(2)
O(8)	9285(3)	2290(4)	761(2)	89(2)
N(1)	11842(4)	5198(6)	2589(3)	91(2)

N(2)	8183(3)	2700(4)	1744(2)	64(2)
N(3)	6738(3)	1321(3)	645(2)	57(1)
C(1)	12798(5)	7336(6)	4897(4)	93(2)
C(2)	12360(20)	6686(17)	5164(11)	117(9)
C(2A)	13060(30)	6673(18)	5403(10)	162(12)
C(3)	12440(30)	8247(16)	4855(10)	134(8)
C(3A)	11800(20)	7560(40)	4867(14)	233(19)
C(4)	13766(11)	7393(18)	5251(8)	108(6)
C(4A)	13330(30)	8143(19)	5028(12)	162(12)
C(5)	12779(5)	6945(6)	4354(4)	79(2)
C(6)	13050(5)	6117(6)	4290(4)	89(2)
C(7)	13029(5)	5726(6)	3818(5)	99(3)
C(8)	12727(5)	6183(7)	3337(4)	86(2)
C(9)	12412(5)	7047(6)	3355(4)	95(3)
C(10)	12441(5)	7434(6)	3868(4)	88(2)
C(11)	12626(5)	5802(7)	2751(4)	124(4)
C(12)	11875(5)	4318(8)	2667(4)	113(3)
C(13)	11149(5)	3846(6)	2514(4)	106(3)
C(14)	10396(4)	4238(6)	2296(3)	78(2)
C(15)	10374(5)	5138(6)	2234(3)	94(2)
C(16)	11135(8)	5643(6)	2373(4)	108(3)
C(17)	9616(4)	3692(5)	2120(3)	65(2)
C(18)	9609(4)	2801(6)	2239(3)	87(2)
C(19)	8897(5)	2313(5)	2043(3)	86(2)
C(20)	8167(4)	3556(5)	1654(3)	77(2)
C(21)	8856(5)	4077(5)	1838(3)	87(2)
C(22)	7444(4)	2123(5)	1488(3)	76(2)
C(23)	7481(4)	1864(4)	936(3)	65(2)
C(24)	6790(4)	430(5)	689(3)	68(2)
C(25)	6112(4)	-99(4)	445(3)	62(2)
C(26)	5365(3)	282(4)	137(2)	50(2)
C(27)	5345(4)	1222(4)	99(3)	68(2)
C(28)	6020(4)	1709(4)	348(3)	70(2)
C(29)	9610(5)	3119(6)	770(3)	83(2)
C(30)	10442(6)	3315(7)	963(4)	102(3)
C(31)	10751(9)	4147(13)	983(6)	140(5)
C(32)	10260(12)	4811(11)	814(6)	154(5)
C(33)	9386(9)	4713(7)	616(5)	138(4)
C(34)	9058(6)	3844(6)	592(4)	97(3)
C(35)	7629(9)	4275(11)	137(7)	214(8)
C(36)	6875(8)	4147(10)	93(6)	180(6)
C(37)	5922(7)	4383(6)	634(5)	132(4)
C(38)	5658(9)	3973(12)	1016(8)	188(7)
C(39)	5378(8)	2969(9)	1640(6)	148(4)
C(40)	4950(7)	2157(8)	1515(6)	140(4)
C(41)	5153(7)	564(8)	1451(4)	107(3)

C(42)	4261(6)	417(10)	1236(4)	115(3)
C(43)	4009(9)	-417(12)	1173(5)	136(4)
C(44)	4571(12)	-1127(9)	1301(5)	148(5)
C(45)	5408(8)	-960(10)	1500(5)	129(4)
C(46)	5705(7)	-156(8)	1589(4)	97(3)
C(47)	7104(7)	-640(8)	1963(5)	136(4)
C(48)	7964(7)	-196(10)	2209(6)	172(6)
C(49)	8930(7)	-424(7)	1755(6)	155(5)
C(50)	9363(6)	39(10)	1417(6)	149(4)
C(51)	9346(8)	699(7)	628(6)	159(5)
C(52)	9836(6)	1559(7)	785(5)	126(4)
S(1)	10768(2)	912(3)	3212(2)	177(2)
O(9)	10891(13)	1433(11)	3761(5)	329(10)
O(10)	9955(6)	547(10)	3005(5)	263(6)
O(11)	11027(6)	1425(7)	2821(6)	249(6)
S(2)	3834(3)	2937(3)	3421(3)	198(2)
O(12)	4613(8)	2453(11)	3521(9)	368(11)
O(13)	3106(7)	2547(7)	2993(5)	223(5)
O(14)	3817(6)	3814(7)	3391(6)	225(5)
S(3)	7668(4)	1592(5)	3299(3)	246(3)
O(15)	8076(9)	2072(10)	3739(5)	280(7)
O(16)	7553(10)	629(8)	3300(7)	289(8)
O(17)	7688(9)	2027(8)	2774(4)	258(6)
C(53)	11465(7)	53(10)	3397(6)	143(5)
F(1)	11392(6)	-452(6)	3794(4)	211(4)
F(2)	12228(6)	261(8)	3512(5)	257(5)
F(3)	11392(10)	-534(8)	2974(6)	295(7)
C(54)	3760(30)	2860(20)	4009(9)	440(30)
F(4)	2870(8)	3069(9)	4047(6)	288(6)
F(5)	3508(12)	1831(12)	4051(11)	401(13)
F(6)	4199(10)	3130(20)	4396(7)	464(18)
C(55)	6671(12)	1732(15)	3200(10)	210(10)
F(7)	6383(13)	1410(10)	3612(8)	355(12)
F(8)	6248(11)	1403(10)	2802(6)	331(9)
F(9)	6535(14)	2533(12)	3222(8)	386(11)
O(1W)	9776(7)	1840(6)	4386(5)	211(4)

Table A-33. Bonding parameters for [3]-Rotaxane, **14**.

Bond	Distance (Å)	Bond	Distance (Å)
O(1)-C(34)	1.348(9)	C(17)-C(18)	1.365(10)
O(1)-C(35)	1.467(11)	C(17)-C(21)	1.387(9)
O(2)-C(36)	1.346(13)	C(18)-C(19)	1.363(9)
O(2)-C(37)	1.477(11)	C(20)-C(21)	1.358(9)

O(3)-C(38)	1.156(14)	C(22)-C(23)	1.477(9)
O(3)-C(39)	1.437(14)	C(24)-C(25)	1.373(8)
O(4)-C(41)	1.368(10)	C(25)-C(26)	1.387(8)
O(4)-C(40)	1.425(11)	C(26)-C(27)	1.406(8)
O(5)-C(46)	1.371(12)	C(26)-C(26)'	1.478(11)
O(5)-C(47)	1.438(10)	C(27)-C(28)	1.337(8)
O(6)-C(48)	1.343(13)	C(29)-C(30)	1.369(11)
O(6)-C(49)	1.403(11)	C(29)-C(34)	1.409(11)
O(7)-C(51)	1.359(11)	C(30)-C(31)	1.343(15)
O(7)-C(50)	1.370(14)	C(31)-C(32)	1.279(16)
O(8)-C(29)	1.351(9)	C(32)-C(33)	1.413(17)
O(8)-C(52)	1.423(9)	C(33)-C(34)	1.404(13)
N(1)-C(16)	1.328(11)	C(35)-C(36)	1.258(14)
N(1)-C(12)	1.327(11)	C(37)-C(38)	1.338(15)
N(1)-C(11)	1.549(9)	C(39)-C(40)	1.396(13)
N(2)-C(20)	1.298(8)	C(41)-C(46)	1.395(13)
N(2)-C(19)	1.342(9)	C(41)-C(42)	1.454(13)
N(2)-C(22)	1.492(8)	C(42)-C(43)	1.309(14)
N(3)-C(24)	1.334(8)	C(43)-C(44)	1.393(16)
N(3)-C(28)	1.347(8)	C(44)-C(45)	1.369(16)
N(3)-C(23)	1.486(7)	C(45)-C(46)	1.294(13)
C(1)-C(3)	1.48(3)	C(47)-C(48)	1.544(15)
C(1)-C(4A)	1.47(2)	C(49)-C(50)	1.464(16)
C(1)-C(5)	1.494(11)	C(51)-C(52)	1.514(14)
C(1)-C(2)	1.51(2)	S(1)-O(10)	1.420(9)
C(1)-C(2A)	1.58(2)	S(1)-O(11)	1.429(8)
C(1)-C(4)	1.61(2)	S(1)-O(9)	1.557(12)
C(1)-C(3A)	1.69(3)	S(1)-C(53)	1.706(13)
C(2)-C(2A)	1.16(3)	S(2)-O(14)	1.311(10)
C(2)-C(3A)	1.65(5)	S(2)-O(12)	1.454(11)
C(2A)-C(4)	1.73(4)	S(2)-O(13)	1.489(10)
C(3)-C(4A)	1.43(4)	S(2)-C(54)	1.55(3)
C(3)-C(3A)	1.50(5)	S(3)-O(15)	1.331(10)
C(4)-C(4A)	1.37(4)	S(3)-O(16)	1.449(11)
C(5)-C(6)	1.346(11)	S(3)-O(17)	1.497(11)
C(5)-C(10)	1.398(11)	S(3)-C(55)	1.64(2)
C(6)-C(7)	1.328(11)	C(53)-F(2)	1.269(12)
C(7)-C(8)	1.358(12)	C(53)-F(1)	1.297(11)
C(8)-C(9)	1.400(12)	C(53)-F(3)	1.366(16)
C(8)-C(11)	1.558(12)	C(54)-F(6)	1.11(2)
C(9)-C(10)	1.417(11)	C(54)-F(4)	1.57(4)
C(12)-C(13)	1.363(11)	C(54)-F(5)	1.60(5)
C(13)-C(14)	1.353(10)	C(55)-F(8)	1.154(16)
C(14)-C(15)	1.352(10)	C(55)-F(9)	1.22(2)
C(14)-C(17)	1.497(9)	C(55)-F(7)	1.37(3)
C(15)-C(16)	1.438(11)		

Bonds	Angle (°)	Bonds	Angle (°)
C(34)-O(1)-C(35)	118.6(9)	N(2)-C(20)-C(21)	122.2(7)
C(36)-O(2)-C(37)	120.1(9)	C(20)-C(21)-C(17)	120.0(7)
C(38)-O(3)-C(39)	128.5(10)	C(23)-C(22)-N(2)	107.1(5)
C(41)-O(4)-C(40)	119.8(8)	C(22)-C(23)-N(3)	110.0(5)
C(46)-O(5)-C(47)	115.1(8)	N(3)-C(24)-C(25)	120.7(6)
C(48)-O(6)-C(49)	113.6(9)	C(24)-C(25)-C(26)	120.5(6)
C(51)-O(7)-C(50)	109.7(10)	C(25)-C(26)-C(27)	116.5(5)
C(29)-O(8)-C(52)	116.4(6)	C(25)-C(26)-C(26)'	121.0(7)
C(16)-N(1)-C(12)	123.3(7)	C(27)-C(26)-C(26)'	122.5(7)
C(16)-N(1)-C(11)	113.8(9)	C(28)-C(27)-C(26)	120.8(6)
C(12)-N(1)-C(11)	122.9(9)	C(27)-C(28)-N(3)	121.4(6)
C(20)-N(2)-C(19)	119.4(6)	O(8)-C(29)-C(30)	124.6(8)
C(20)-N(2)-C(22)	121.4(6)	O(8)-C(29)-C(34)	118.2(7)
C(19)-N(2)-C(22)	119.0(6)	C(30)-C(29)-C(34)	117.1(9)
C(24)-N(3)-C(28)	120.1(5)	C(31)-C(30)-C(29)	123.7(11)
C(24)-N(3)-C(23)	118.6(6)	C(32)-C(31)-C(30)	120.0(13)
C(28)-N(3)-C(23)	121.4(5)	C(31)-C(32)-C(33)	122.5(13)
C(3)-C(1)-C(4A)	57.8(17)	C(34)-C(33)-C(32)	117.7(11)
C(3)-C(1)-C(5)	113.5(12)	O(1)-C(34)-C(33)	126.9(10)
C(4A)-C(1)-C(5)	111.6(11)	O(1)-C(34)-C(29)	114.1(7)
C(3)-C(1)-C(2)	112.4(18)	C(33)-C(34)-C(29)	118.9(9)
C(4A)-C(1)-C(2)	140.5(14)	C(36)-C(35)-O(1)	119.1(12)
C(5)-C(1)-C(2)	107.2(10)	C(35)-C(36)-O(2)	126.1(11)
C(3)-C(1)-C(2A)	130.1(16)	C(38)-C(37)-O(2)	112.0(8)
C(4A)-C(1)-C(2A)	109(2)	O(3)-C(38)-C(37)	137.7(13)
C(5)-C(1)-C(2A)	115.7(13)	C(40)-C(39)-O(3)	112.1(11)
C(2)-C(1)-C(2A)	44.1(13)	C(39)-C(40)-O(4)	113.5(10)
C(3)-C(1)-C(4)	108.1(17)	O(4)-C(41)-C(46)	118.2(10)
C(4A)-C(1)-C(4)	52.4(17)	O(4)-C(41)-C(42)	120.8(11)
C(5)-C(1)-C(4)	105.6(9)	C(46)-C(41)-C(42)	121.0(10)
C(2)-C(1)-C(4)	109.8(17)	C(43)-C(42)-C(41)	116.6(11)
C(2A)-C(1)-C(4)	65.9(18)	C(42)-C(43)-C(44)	121.6(13)
C(3)-C(1)-C(3A)	56(2)	C(45)-C(44)-C(43)	119.9(12)
C(4A)-C(1)-C(3A)	112(3)	C(46)-C(45)-C(44)	122.3(13)
C(5)-C(1)-C(3A)	107.2(12)	C(45)-C(46)-O(5)	127.1(10)
C(2)-C(1)-C(3A)	62(2)	C(45)-C(46)-C(41)	118.5(11)
C(2A)-C(1)-C(3A)	101(2)	O(5)-C(46)-C(41)	114.2(10)
C(4)-C(1)-C(3A)	147.1(14)	O(5)-C(47)-C(48)	105.5(9)
C(2A)-C(2)-C(1)	71.3(17)	O(6)-C(48)-C(47)	117.1(10)
C(2A)-C(2)-C(3A)	127(3)	O(6)-C(49)-C(50)	109.9(8)
C(1)-C(2)-C(3A)	64.8(19)	O(7)-C(50)-C(49)	116.1(9)
C(2)-C(2A)-C(1)	64.7(17)	O(7)-C(51)-C(52)	119.5(10)
C(2)-C(2A)-C(4)	122(2)	O(8)-C(52)-C(51)	109.9(7)
C(1)-C(2A)-C(4)	57.9(12)	O(10)-S(1)-O(11)	114.5(8)
C(4A)-C(3)-C(1)	61.0(15)	O(10)-S(1)-O(9)	111.9(10)

C(4A)-C(3)-C(3A)	128(3)	O(11)-S(1)-O(9)	112.0(10)
C(1)-C(3)-C(3A)	69.3(18)	O(10)-S(1)-C(53)	108.7(8)
C(3)-C(3A)-C(2)	103.7(19)	O(11)-S(1)-C(53)	105.2(5)
C(3)-C(3A)-C(1)	54.6(14)	O(9)-S(1)-C(53)	103.7(8)
C(2)-C(3A)-C(1)	53.5(11)	O(14)-S(2)-O(12)	120.6(9)
C(4A)-C(4)-C(1)	58.8(14)	O(14)-S(2)-O(13)	110.4(8)
C(4A)-C(4)-C(2A)	106(2)	O(12)-S(2)-O(13)	115.7(9)
C(1)-C(4)-C(2A)	56.2(13)	O(14)-S(2)-C(54)	97.3(14)
C(4)-C(4A)-C(3)	127(2)	O(12)-S(2)-C(54)	97.6(14)
C(4)-C(4A)-C(1)	68.8(14)	O(13)-S(2)-C(54)	112.7(18)
C(3)-C(4A)-C(1)	61.2(15)	O(15)-S(3)-O(16)	124.6(12)
C(6)-C(5)-C(10)	115.6(8)	O(15)-S(3)-O(17)	111.8(11)
C(6)-C(5)-C(1)	124.1(9)	O(16)-S(3)-O(17)	118.1(9)
C(10)-C(5)-C(1)	120.3(8)	O(15)-S(3)-C(55)	107.6(10)
C(7)-C(6)-C(5)	126.7(9)	O(16)-S(3)-C(55)	89.7(12)
C(6)-C(7)-C(8)	119.7(9)	O(17)-S(3)-C(55)	96.3(13)
C(7)-C(8)-C(9)	118.2(8)	F(2)-C(53)-F(1)	107.2(10)
C(7)-C(8)-C(11)	125.6(10)	F(2)-C(53)-F(3)	100.2(13)
C(9)-C(8)-C(11)	116.0(10)	F(1)-C(53)-F(3)	103.7(13)
C(8)-C(9)-C(10)	120.1(8)	F(2)-C(53)-S(1)	116.4(10)
C(5)-C(10)-C(9)	119.6(8)	F(1)-C(53)-S(1)	115.4(10)
N(1)-C(11)-C(8)	107.5(6)	F(3)-C(53)-S(1)	112.2(10)
N(1)-C(12)-C(13)	118.4(9)	F(6)-C(54)-S(2)	127(5)
C(14)-C(13)-C(12)	122.9(9)	F(6)-C(54)-F(4)	105(2)
C(15)-C(14)-C(13)	117.8(7)	S(2)-C(54)-F(4)	114.3(12)
C(15)-C(14)-C(17)	121.0(7)	F(6)-C(54)-F(5)	114(3)
C(13)-C(14)-C(17)	121.1(8)	S(2)-C(54)-F(5)	103.9(15)
C(14)-C(15)-C(16)	120.0(8)	F(4)-C(54)-F(5)	85(3)
N(1)-C(16)-C(15)	117.5(8)	F(8)-C(55)-F(9)	113(2)
C(18)-C(17)-C(21)	116.7(6)	F(8)-C(55)-F(7)	105(2)
C(18)-C(17)-C(14)	122.0(7)	F(9)-C(55)-F(7)	101(2)
C(21)-C(17)-C(14)	121.2(7)	F(8)-C(55)-S(3)	114(2)
C(19)-C(18)-C(17)	120.4(7)	F(9)-C(55)-S(3)	108.5(19)
N(2)-C(19)-C(18)	121.0(7)	F(7)-C(55)-S(3)	115.2(18)

Table A-34. Anisotropic displacement parameters ($Å^2 \times 10^3$) for [3]-Rotaxane **14**.

Atom	U_{11}	U_{22}	U_{33}	U_{23}	U_{13}	U_{12}
O(1)	92(4)	115(4)	126(5)	49(4)	26(3)	15(4)
O(2)	70(3)	96(4)	132(5)	31(4)	17(3)	12(3)
O(3)	270(11)	96(5)	253(11)	44(6)	167(9)	66(6)
O(4)	84(4)	153(6)	99(5)	14(4)	29(3)	49(4)
O(5)	86(4)	150(5)	105(5)	26(4)	28(3)	36(4)
O(6)	92(4)	150(5)	121(5)	43(4)	36(4)	31(4)

O(7)	92(5)	97(4)	194(8)	25(4)	52(5)	21(3)
O(8)	60(3)	85(3)	129(5)	9(3)	38(3)	9(3)
N(1)	66(5)	132(7)	75(5)	-28(5)	22(4)	-15(5)
N(2)	41(3)	69(4)	75(4)	-12(3)	6(3)	-3(3)
N(3)	50(3)	51(3)	67(4)	-15(3)	13(3)	-11(3)
C(1)	106(7)	92(6)	81(6)	-25(5)	29(5)	-15(5)
C(2)	170(20)	127(17)	82(17)	-17(15)	79(16)	-60(20)
C(2A)	280(40)	118(17)	66(16)	27(13)	23(19)	-40(20)
C(3)	170(30)	110(18)	130(20)	-21(14)	50(20)	-3(18)
C(3A)	140(30)	420(60)	140(30)	-60(30)	37(19)	90(40)
C(4)	95(14)	131(16)	89(14)	-29(13)	16(10)	-6(12)
C(4A)	260(40)	113(19)	130(20)	-72(17)	80(20)	-100(20)
C(5)	79(5)	85(6)	73(6)	-18(5)	25(4)	-23(4)
C(6)	90(6)	97(7)	75(7)	-22(5)	18(4)	-16(5)
C(7)	85(6)	93(6)	119(9)	-12(7)	32(6)	-12(5)
C(8)	68(5)	95(6)	102(8)	-40(6)	38(5)	-30(5)
C(9)	80(6)	114(7)	81(7)	0(6)	12(4)	-39(5)
C(10)	91(6)	88(5)	84(7)	-21(6)	26(5)	-26(4)
C(11)	90(6)	173(9)	124(8)	-77(7)	54(5)	-73(6)
C(12)	75(6)	125(8)	131(9)	-34(7)	19(5)	11(6)
C(13)	59(5)	115(6)	129(8)	-51(6)	4(5)	-33(5)
C(14)	55(5)	101(6)	73(5)	-18(4)	10(4)	-17(4)
C(15)	71(5)	94(6)	104(7)	2(5)	10(4)	-19(5)
C(16)	137(9)	94(6)	85(7)	-12(5)	21(6)	-29(7)
C(17)	61(5)	68(5)	55(4)	-16(4)	2(3)	-13(4)
C(18)	60(5)	95(6)	88(6)	-1(5)	-2(4)	-6(4)
C(19)	75(6)	68(4)	100(6)	-10(4)	7(4)	-21(4)
C(20)	50(4)	75(5)	90(6)	-20(4)	-3(4)	-3(4)
C(21)	82(6)	66(4)	98(6)	-21(4)	4(5)	-2(4)
C(22)	46(4)	82(5)	89(6)	-14(4)	3(4)	-16(3)
C(23)	47(4)	69(4)	79(5)	-27(4)	18(3)	-23(3)
C(24)	49(4)	72(5)	76(5)	-5(4)	8(3)	2(4)
C(25)	52(4)	47(3)	77(5)	-9(3)	6(3)	-3(3)
C(26)	43(4)	55(4)	50(4)	-9(3)	11(3)	-5(3)
C(27)	50(4)	48(4)	91(5)	-4(4)	0(3)	-2(3)
C(28)	64(5)	49(4)	89(5)	-9(4)	11(4)	0(4)
C(29)	69(6)	105(6)	85(6)	-8(5)	40(4)	3(5)
C(30)	81(7)	126(8)	108(7)	-23(6)	42(5)	-25(6)
C(31)	111(10)	192(14)	129(10)	-31(10)	56(8)	-37(10)
C(32)	175(15)	160(13)	153(12)	-25(10)	88(11)	-82(11)
C(33)	175(12)	103(8)	156(11)	40(7)	79(9)	11(8)
C(34)	80(6)	102(7)	118(7)	17(5)	44(5)	-14(5)
C(35)	140(12)	267(16)	236(17)	180(14)	63(11)	100(12)
C(36)	97(9)	256(16)	169(12)	122(11)	16(9)	52(9)
C(37)	115(8)	75(6)	174(11)	8(6)	-3(7)	42(6)
C(38)	188(13)	152(13)	290(20)	64(13)	169(14)	56(10)

C(39)	168(11)	135(10)	180(12)	3(9)	109(10)	37(8)
C(40)	124(9)	118(8)	181(12)	4(8)	49(8)	22(8)
C(41)	137(10)	109(8)	88(7)	-11(6)	52(6)	-29(8)
C(42)	86(7)	180(12)	86(7)	18(7)	38(5)	16(7)
C(43)	158(11)	149(11)	124(10)	-14(9)	77(8)	-46(11)
C(44)	221(16)	121(9)	133(10)	28(8)	99(11)	-23(11)
C(45)	120(9)	152(12)	130(9)	19(8)	61(7)	-31(8)
C(46)	110(8)	103(7)	90(7)	23(6)	50(6)	23(7)
C(47)	136(10)	159(9)	121(9)	67(7)	53(7)	39(8)
C(48)	99(9)	214(13)	168(12)	112(10)	-10(8)	43(8)
C(49)	87(7)	101(7)	258(16)	36(8)	26(9)	45(6)
C(50)	64(7)	215(13)	169(12)	-20(10)	36(7)	29(8)
C(51)	157(10)	106(8)	260(16)	11(9)	132(11)	16(7)
C(52)	91(6)	119(8)	187(11)	1(7)	73(7)	17(6)
S(1)	137(3)	179(3)	219(5)	87(3)	60(3)	29(2)
O(9)	510(30)	339(17)	150(10)	-27(11)	115(13)	161(17)
O(10)	107(7)	408(17)	245(12)	73(11)	10(7)	-72(9)
O(11)	213(9)	227(9)	362(16)	203(11)	172(10)	109(8)
S(2)	183(4)	123(3)	286(7)	-17(3)	69(4)	-13(3)
O(12)	161(9)	303(15)	630(30)	-83(18)	102(13)	109(10)
O(13)	222(10)	183(8)	223(11)	-59(8)	9(8)	-56(8)
O(14)	198(10)	134(8)	319(16)	-35(8)	44(9)	19(6)
S(3)	228(6)	275(7)	223(7)	-61(6)	53(5)	32(5)
O(15)	262(13)	382(18)	144(9)	-144(11)	-14(8)	-2(12)
O(16)	348(19)	142(8)	380(20)	29(11)	118(15)	-53(10)
O(17)	402(17)	309(14)	97(7)	5(8)	128(9)	-77(11)
C(53)	96(8)	205(13)	124(10)	99(10)	26(7)	-3(8)
F(1)	264(9)	199(7)	194(8)	84(6)	104(7)	60(6)
F(2)	122(6)	302(11)	325(14)	117(10)	38(7)	49(7)
F(3)	490(20)	227(10)	193(10)	-16(8)	148(12)	-35(11)
C(54)	600(60)	460(50)	97(13)	-140(20)	-140(20)	370(40)
F(4)	266(12)	314(14)	317(16)	29(11)	141(11)	81(10)
F(5)	400(20)	307(16)	580(40)	210(20)	280(20)	117(17)
F(6)	294(16)	870(50)	173(12)	-160(20)	-10(10)	140(20)
C(55)	177(17)	163(16)	220(20)	-86(16)	-43(14)	-7(13)
F(7)	570(30)	241(13)	308(19)	-9(11)	220(20)	-90(14)
F(8)	400(20)	321(16)	241(14)	6(12)	54(13)	-195(16)
F(9)	550(30)	213(12)	420(20)	-64(14)	190(20)	-45(15)
O(1W)	206(9)	185(8)	213(10)	19(7)	21(7)	-29(7)

Table A-35. Hydrogen coordinates (x 10^4) and isotropic displacement parameters ($Å^2$ x 10^3) for [3]-Rotaxane **14**.

Atom	x	y	z	U(eq)
H(6A)	13275	5783	4609	107
H(7A)	13220	5142	3816	118
H(9A)	12184	7366	3030	113
H(10A)	12237	8009	3882	106
H(11A)	12561	6287	2488	149
H(11B)	13113	5456	2754	149
H(12A)	12381	4030	2823	136
H(13A)	11172	3227	2560	128
H(15A)	9865	5431	2100	112
H(16A)	11134	6258	2313	130
H(18A)	10094	2525	2455	104
H(19A)	8906	1702	2116	103
H(20A)	7666	3822	1456	93
H(21A)	8820	4691	1775	105
H(22A)	7456	1595	1711	91
H(22B)	6935	2450	1455	91
H(23A)	7982	1519	974	78
H(23B)	7500	2397	723	78
H(24A)	7292	165	886	82
H(25A)	6153	-718	488	74
H(27A)	4856	1508	-102	82
H(28A)	5993	2330	316	84
H(30A)	10814	2844	1087	123
H(31A)	11322	4241	1119	168
H(32A)	10486	5381	822	185
H(33A)	9039	5207	506	166
H(35A)	7789	4847	321	256
H(35B)	7671	4336	-232	256
H(36A)	6672	3725	-208	216
H(36B)	6596	4710	-36	216
H(37A)	6141	4969	770	158
H(37B)	5455	4471	303	158
H(38A)	5883	4348	1338	226
H(38B)	5065	4097	893	226
H(39A)	5840	2899	1976	178
H(39B)	5008	3421	1706	178
H(40A)	4536	2206	1155	169
H(40B)	4660	2048	1783	169
H(42A)	3887	892	1147	137
H(43A)	3442	-539	1039	163
H(44A)	4378	-1714	1253	178
H(45A)	5775	-1441	1573	155

H(47A)	7104	-1032	1659	163
H(47B)	6957	-988	2241	163
H(48A)	7906	284	2451	206
H(48B)	8338	-637	2436	206
H(49A)	8666	-961	1568	186
H(49B)	9328	-599	2104	186
H(50A)	9702	511	1637	179
H(50B)	9737	-384	1326	179
H(51A)	8985	766	252	191
H(51B)	9738	226	626	191
H(52A)	10221	1507	1155	151
H(52B)	10157	1666	534	151

REFERENCES

1. Pedersen, C. J. *J. Am. Chem. Soc.* **1967**, *89*, 7017.
2. Pedersen, C. J. *Angew. Chem. Int. Ed. Engl.* **1988**, *27*, 1021.
3. Lehn, J. M. *Angew. Chem. Int. Ed. Engl.* **1988**, *27*, 89.
4. Cram, D. J. *Angew. Chem. Int. Ed. Engl.* **1988**, *27*, 1009.
5. Schill, G. *Catenanes, Rotaxanes and Knots*; Academic: New York, 1971.
6. Ashton, P. R.; Baxter, I.; Fyfe, M. C. T.; Raymo, F. M.; Spencer,N.; Stoddart, J. F.; White, A. J. P.; Williams, D. J. *J. Amer. Chem. Soc.* **1998**, *120*, 2297.
7. Note that Stoddart and Amabilino published an extensive 100-page review of this area four years ago. The last four years has seen roughly the same amount of activity. Stoddart, J. F.; Amabilino, D. B. *Chem. Rev.* **1995**, *95*, 2725.
8. Lüttringhaus, A.; Cramer, F.; Prinzbach, H.; Henglein, F. M. *Liebigs Ann. Chem.* **1958**, *613*, 185.
9. Harrison, I. T.; Harrison, S. *J. Amer. Chem. Soc.* **1967**, *89*, 5723.
10. Harrison, I. T. *J. Chem. Soc., Chem. Commun.* **1972**, 231.
11. Harrison, I. T. *J. Chem. Soc., Perkin Trans. 1* **1974**, 301.
12. Agam, G.; Zilkha A. *J. Amer. Chem. Soc.* **1976**, *98*, 5206.
13. Agam, G.; Zilkha A. *J. Amer. Chem. Soc.* **1976**, *98*, 5214.
14. Gibson, H. W.; *Large Ring Molecules*; Semlyen, J. A. (Ed.); Wiley: New York, 1996.
15. Logeman, E.; Rissler, K.; Schill, G.; Fritz, H. *Chem. Ber.* **1981**, *114*, 2245.
16. Schill, G.; Zollenkopf, H. *Liebigs Ann. Chem.* **1969**, *721*, 53.
17. Gibson, H. W.; Bheda, M. C.; Engen, P. T. *Prog. Polym. Sci.* **1994**, *19*, 843.

18. Ashton, P. R.; Grognuz, M.; Slawin, A. M. Z.; Stoddart, J. F.; Williams, D. J. *Tetrahedron Lett.* **1991**, *32(43)*, 6235.

19. *Cyclodextrins*; Szejtli, J., Osa, T., Eds. Comprehensive Supramolecular Chemistry Series; Atwood, J. L., Davies, J. E. D., MacNicol, D. D., Vögtle, F., Eds; Elsevier: Oxford, U.K., 1996; Vol. 3.

20. Stoddart, J. F.; Nepogodiev, S. A. *Chem. Rev.* **1998**, *98*, 1959.

21. Ogino, H. *J. Amer. Chem. Soc.* **1981**, *103*, 1303.

22. Yamanari, K.; Shimura, Y. *Bull. Chem. Soc. Jpn.* **1983**, *56*, 2283.

23. Wylie, R. S.; Macartney, D. H. *J. Amer. Chem. Soc.* **1992**, *114*, 3136.

24. Wylie, R. S.; Macartney, D. H. *Supramol. Chem.* **1993**, *3*, 29.

25. Macartney, D. H.; Wadding, C. A. *Inorg. Chem.* **1994**, *33*, 5912.

26. Lyon, A. P.; Macartney, D. H. *Inorg. Chem.* **1997**, *36*, 729.

27. Tamura, M.; Ueno, A. *Chem. Lett.* **1998**, 369.

28. Harada, A.; Li, J.; Kamachi, M. *J. Chem. Soc., Chem. Commun.* **1997**, 1413.

29. Anderson, S.; Claridge, T. D. W.; Anderson, H. L. *Angew. Chem. Int. Ed. Engl.* **1997**, *36*, 1310.

30. Jeon, Y.-M.; Whang, D.; Kim, J.; Kim, K. *Chem. Lett.* **1996**, 503.

31. Jeon, Y.-M.; Whang, D.; Heo, J.; Kim, K. *J. Amer. Chem. Soc.* **1996**, *118*, 11333.

32. Whang, D.; Kim, K. *J. Amer. Chem. Soc.* **1997**, *119*, 451.

33. Jeon, Y.-M.; Whang, D.; Kim, C.-A.; Kim, K. *J. Chem. Soc., Chem. Commun.* **1997**, 2361.

34. Whang, D.; Park, K.-M.; Heo, J.; Ashton, P.; Kim, K. *J. Amer. Chem. Soc.* **1998**, *120*, 4899.

35. Mock, W. L.; Shih, N.-Y. *J. Org. Chem.* **1983**, *48*, 3618.

36. Mock, W. L.; Shih, N.-Y. *J. Org. Chem.* **1986**, *51*, 4440.

37. Ashton, P. R.; Campbell, P. J.; Chrystal, E. J. T.; Glink, P. T.; Menzer, S.; Philp, D.; Spencer, N.; Stoddart, J. F.; Tasker, P. A.; Williams, D. J. *Angew. Chem. Int. Ed. Engl.* **1995**, *34*, 1865.

38. Ashton, P. R.; Chrystal, E. J. T.; Glink, P. T.; Menzer, S.; Schiavo, C.; Stoddart, J. F.; Tasker, P. A.; Williams, D. J. *Angew. Chem. Int. Ed. Engl.* **1995**, *34*, 1869.

39. Ashton, P. R.; Chrystal, E. J. T.; Glink, P. T.; Menzer, S.; Schiavo,C.; Spencer, N.; Stoddart, J. F.; Tasker, P. A.;White, A. J. P.; Williams, D. J. *Chem. Eur. J.* **1996**, *2*, 709.

40. Ashton, P. R.; Fyfe, M. C. T.; Glink, P. T.; Menzer, S.; Stoddart, J. F.; White, A. J. P.; Williams, D. J. *J. Amer. Chem. Soc.* **1997**, *119*, 12514.

41. Ashton, P. R.; Ballardini, R.; Balzani, V.; Gomezlopez, M.; Lawrence, S. E.; Martinezdiaz, M. V.; Montalti, M.; Piersanti, A.; Prodi, L.; Stoddart, J. F.; Williams, D. J. *J. Amer. Chem. Soc.* **1997**, *119*, 10641.

42. Ashton, P. R.; Baxter, I.; Fyfe, M. C. T.; Raymo, F. M.; Spencer, N.; Stoddart, J. F.; White, A. J. P.; Williams, D. J. *J. Amer. Chem. Soc.* **1998**, *120*, 2297.

43. Ashton, P. R.; Glink, P. T.; Stoddart, J. F.; Tasker, P. A.; White, A. J. P.; Williams, D. J. *Chem. Eur. J.* **1996**, *2*, 729.

44. Kolchinski, A. G.; Alcock, N. W.; Busch, D. H. *J. Chem. Soc., Chem. Commun.* **1995**, 1289.

45. Kolchinski, A. G.; Alcock, N. W.; Roesner, R. A.; Busch, D. H. *J. Chem. Soc., Chem. Commun.* **1998**, 1437.

46. Hunter, C. A. *J. Amer. Chem. Soc.* **1992**, *114*, 5303.

47. Hunter, C. A.; Purvis, D. H. *Angew. Chem. Int. Ed. Engl.* **1992**, *31*, 792.

48. Carver, F. J.; Hunter, C. A.; Shannon, R. J. *J. Chem. Soc., Chem. Commun.* **1994**, 1277.

49. Vögtle, F.; Meier, S.; Hoss, R. *Angew. Chem. Int. Ed. Engl.* **1992**, *31*, 1619.

50. Brodesser, G.; Güther, R.; Hoss, R.; Meier, S.; Ottens-Hildebrandt, S.; Schmitz, J.; Vögtle, F. *Pure Appl. Chem.* **1993**, *65*, 2325.

51. Vögtle, F.; Dünnwald, T.; Schmidt, T. *Acc. Chem. Res.* **1996**, *29*, 451.

52. Händel, M.; Plevoets, M.; Gestermann, S.; Vögtle, F. *Angew. Chem. Int. Ed. Engl.* **1997**, *36*, 1199.

53. Johnston, A. G.; Leigh, D. A.; Murphy, A.; Smart, J. P.; Slawin, A. M. Z. *J. Amer. Chem. Soc.* **1996**, *118*, 10662.

54. Leigh, D. A.; Murphy, A.; Smart, J. P.; Slawin, A. M. Z. *Angew. Chem. Int. Ed. Engl.* **1997**, *36*, 728.

55. Lane, A. S.; Leigh, D. A.; Murphy, A. *J. Amer. Chem. Soc.* **1997**, *119*, 11092.

56. Dietrich-Buchecker, C. O.; Sauvage, J. -P.; Kintzinger, J. P. *Tetrahedron Lett.* **1983**, *24*, 5095.

57. Dietrich-Buchecker, C. O.; Sauvage, J. -P. *Bioorg. Chem. Front.* **1991**, *2*, 195.

58. Wu, C.; Lecavalier, P. R.; Shen, Y. X.; Gibson, H. W. *Chem. Mater.* **1991**, *3*, 569.

59. Gavinã, P.; Sauvage, J.-P. *Tetrahedron Lett.* **1997**, *38*, 3521.

60. Armaroli, N.; Diederich, F.; Dietrich-Buchecker, C. O.; Flamigni, L.; Marconi, G.; Nierengarten, J.-F.; Sauvage, J.-P. *Chem. Eur. J.* **1998**, *4*, 406.

61. Chambron, J.-C.; Heitz, V.; Sauvage, J.-P. *Bull. Soc. Chim. Fr.* **1995**, *132*, 340.

62. Cárdenas, D. J.; Gavinã, P.; Sauvage, J.-P. *J. Chem. Soc., Chem. Commun.* **1996**, 1915.

63. Solladie, N.; Chambron, J.-C.; Dietrich-Buchecker, C. O.; Sauvage, J.-P. *Angew. Chem. Int. Ed. Engl.* **1996**, *35*, 906.

64. Chambron, J.-C.; Heitz, V.; Sauvage, J.-P. *J. Chem. Soc., Chem. Commun.* **1992**, 1131.

65. Linke, M.; Chambron, J.-C.; Heitz, V.; Sauvage, J.-P. *J. Amer. Chem. Soc.* **1997**, *119*, 11329.

66. Diederich, F.; Dietrich-Buchecker, C. O.; Nierengarten, J.-F.; Sauvage, J.-P. *J. Chem. Soc., Chem. Commun.* **1995**, 781.

67. Allwood, B. L.; Spencer, N.; Shariari-Zavareh, H.; Stoddart, J. F.; Wiliams, D. J. *J. Chem. Soc., Chem. Commun.* **1987**, 1064.

68. Hunter, C. A.; Sanders, J. K. M. *J. Amer. Chem. Soc.* **1990**, *112*, 5525.

69. Hunter, C. A. *Chem. Soc. Rev.* **1994**, *23*, 101.

70. Jorgensen, W. L.; Severance, D. L. *J. Amer. Chem. Soc.* **1990**, *112*, 4768.

71. Ashton, P. R.; Philp, D.; Reddington, M. V.; Slawin, A. M. Z.; Spencer, N.; Stoddart, J. F.; Williams, D. J. *J. Chem. Soc., Chem. Commun.* **1991**, 1680.

72. Ashton, P. R.; Philp, D.; Spencer, N.; Stoddart, J. F. *J. Chem. Soc., Chem. Commun.* **1992**, 1124.

73. Ashton, P. R.; Philp, D.; Bêlohradský, M.; Stoddart, J. F. *J. Chem. Soc., Chem. Commun.* **1993**, 1269.

74. Ambilino, D.B.; Ashton, P. R.; Bêlohradský, M.; Raymo, F. M.; Stoddart, J. F. *J. Chem. Soc., Chem. Commun.* **1995**, 747.

75. Ashton, P. R.; Philp, D.; Bêlohradský, M.; Stoddart, J. F. *J. Chem. Soc., Chem. Commun.* **1993**, 1274.

76. Ambilino, D.B.; Ashton, P. R.; Bêlohradský, M.; Raymo, F. M.; Stoddart, J. F. *J. Chem. Soc., Chem. Commun.* **1995**, 751.

77. Ballardini, R.; Balzani, V.; Credi, A.; Gandolfini, M. T.; Langford, S. J.; Menzer, S.; Prodi, L.; Stoddart, J. F.; Venturi, M.; Williams, D. J. *Angew. Chem. Int. Ed. Engl.* **1996**, *35*, 978.

78. Ashton, P. R.; Odel, B.; Reddington, M. V.; Slawin, A. M. Z.; Stoddart, J. F.; Williams, D. J. *Angew. Chem. Int. Ed. Engl.* **1988**, *27*, 1550.

79. Anelli, P. L.; Ashton, P. R.; Spencer, N.; Slawin, A. M. Z.; Stoddart, J. F.; Williams, D. J. *Angew. Chem. Int. Ed. Engl.* **1991**, *30*, 1036.

80. Ashton, P. R.; Philp, D.; Spencer, N.; Stoddart, J. F.; Williams, D. J. . *J. Chem. Soc., Chem. Commun.* **1994**, 181.

81. Ashton, P. R.; Philp, D.; Spencer, N.; Stoddart, J. F. *J. Chem. Soc., Chem. Commun.* **1991**, 1677.

82. Reddington, M. V.; Slawin, A. M. Z.; Spencer, N.; Stoddart, J. F.; Vicent, C.; Williams, D. J. *J. Chem. Soc., Chem. Commun.* **1991**, 630.

83. Anelli, P. L.; Ashton, P. R.; Ballardini, R.; Balzani, V.; Delgado, M.; Gandolfi, M. T.; Goodnow, T. T.; Kaifer, A. E.; Philp, D.; Pietraszkiewicz, M.; Prodi, L.; Reddington, M. V.; Slawin, A. M. Z.; Spencer, N.; Stoddart, J. F.; Vicent, C.; Williams, D. J. *J. Amer. Chem. Soc.* **1992**, *114*, 193.

84. Ashton, P. R.; Grognuz, M.; Slawin, A. M. Z.; Stoddart, J. F.; Williams, D. J. *Tetrahedron Lett.* **1991**, *32*, 6235.

85. Raymo, F. M.; Stoddart, J. F *Chem. Rev.* **1999**, *99*, 1643.

86. Chambron, J.-C.; Sauvage, J.-P. *Chem. Eur. J.* **1998**, *4*, 1362.

87. Collier, C. P.; Wong, E. W.; Belohradsky; Raymo, F. M.; Stoddart, J. F.; Kuekes, P. J.; Williams, R. S.; Heath, J. R. *Science* **1999**, *285*, 391.

88. Colquhoun, H. M.; Goodings, E. P.; Maud, J. M.; Stoddart, J. F.; Wolstenholme, J. B.; Williams, D. J. *J. Chem. Soc., Perkin Trans. II* **1985**, 607.

89. Allwood, B. L.; Spencer, N.; Shahriari-Zavareh, H.; Stoddart, J. F.; Williams, D. J. *J. Chem. Soc., Chem. Commun.* **1987**, 1061.

90. Allwood, B. L.; Shahriari-Zavareh, H.; Stoddart, J. F.; Williams, D. J. *J. Chem. Soc., Chem. Commun.* **1987**, 1058.

91. Slawin, A. M. Z.; Spencer, N.; Stoddart, J. F.; Williams, D. J. *J. Chem. Soc., Chem. Commun.* **1987**, 1070.

92. Ashton, P. R.; Langford, S. J.; Spencer, N.; Stoddart, J. F.; White, A. J. P.; Williams, D. J. *J. Chem. Soc., Chem. Commun.* **1987**, 1058.

93. Furniss, B. S.; Hannaford, A. J.; Smith, P. W. G.; Tatchell, A. R. *Vogel's Textbook of Practical Organic Chemistry(5th Ed.)*; Wiley: New York, 1989.

94. Singh, S. K.; Summers, L. A. *Z. Naturforsch.* **1986**, *41b*, 239.

95. Reinhoudt, D. N.; De Jong, F.; Tomassen, H. P. M. *Tetrahedron Lett.* **1979**, *22*, 2067.

96. Katritzky, A. R.; Mokrosz, M. J. *Heterocycles*, **1984**, *22*, 505.

97. Ikegami, Y.; Muramatsu, T.; Hamaya, K. *J. Amer. Chem. Soc.* **1989**, *111*, 5782.

98. Zoltewicz, E. R.; Deady, A. T. *Adv. Heterocycl. Chem.* **1978**, *22*, 71.

99. Hynes, M. J. *J. Chem. Soc., Dalton Trans.* **1993**, 311.

100. Blandamer, M. J.; Burgess, J.; Robertson, R. E.; Scott, J. M. W. *Chem. Rev.* **1982**, *82*, 259.

101. Stauffer, D. A.; Barrans, Jr., R. E.; Dougherty, D. A. *J. Org. Chem.* **1990**, *55*, 2762.

102. Privalov, P. L.; Gill, S. J. *Adv. Prot. Chem.* **1988**, *39*, 191.

103. Hanson, I. R.; Hughes, D. L.; Truter, M. R. *J. Chem. Soc., Perkin Trans. II* **1976**, 972.

104. Loeb, S. J.; Murphy, S. L.; Wisner, J. A. *Crystal Engineering* **1999**, *2*, 27-35.

105. Kickham, J. E.; Loeb, S. J.; Murphy, S. L. *Chem. Eur. J.* **1997**, *3*, 1203.

106. See for example: Ashton, P. R.; Claessens, C. G.; Hayes, W.; Menzer, S.; Stoddart, J. F.; White, A. J. P.; Williams, D. J. *Angew. Chem. Int. Ed. Engl.* **1995**, *34*, 1862.

107. Anelli, P. L.; Asakawa, M.; Ashton, P. R.; Bissell, R. A.; Clavier, G.; Gorski, R.; Kaifer, A. E.; Langford, S. J.; Mattersteig, G.; Menzer, S.; Philp, D.; Slawin, A. M. Z.; Spencer, N.; Stoddart, J. F.; Tolley, M. S.; Williams, D. J *Chem. Eur. J.* **1997**, *3*, 1113.

108. Bissel, R. A.; Cordova, E.; Kaifer, A. E.; Stoddart, J. F. *Nature (London)* **1994**, *369*, 133.

109. Sutherland, I. O. *Annu. Rep. NMR Spectrosc.* **1971**, *4*, 71.

Curriculum Vitae

Name	James A. Wisner
Date of Birth	August 27th, 1969
Place of Birth	Toronto, Ontario, Canada
Citizenship	Canadian
Education	B.Sc., Honours Chemistry, 1994 University of Waterloo Ph.D., Chemistry, 1999 University of Windsor
Professional Work History	Teaching Assistant University of Windsor, Windsor, Ontario, Canada Sept., 1994 - present Research Assistant University of Windsor, Windsor, Ontario, Canada Sept., 1994 - present Research Chemist (Organic Synthesis) Steroids Ltd., Chicago, IL, USA May, 1992 - Jan., 1993 Research Assistant (Analytical Method Development) Occupational Hazards and Investigation, Health and Welfare Canada, Ottawa, Canada Jan., 1991 - Apr., 1991 Sept., 1991 - Dec., 1991 Research Assistant (Bacterial/Viral Pesticide Efficacy) Harrow Research Station, Agriculture Canada, Harrow, Ontario, Canada May, 1990 - August, 1990

Scholarships and Awards

Natural Sciences and Engineering Research Council of Canada Post-doctoral Fellowship (Pending)

University of Windsor Summer Research Scholarship (1999)

Ontario Graduate Scholarship (1998)

University of Windsor Tuition Scholarship (1998)

Ontario Graduate Scholarship (1997)

University of Windsor Tuition Scholarship (1997)

University of Windsor Tuition Scholarship (1996)

Publications in Refereed Journals

Loeb, S. J., Murphy, S. L., and Wisner, J. A. "Crystal Engineering with Molecular Rods: Binuclear Complexes of Bridging, Nitrogen Donor Ligands Capped by Organopalladium Fragments" *Crystal Engineering* **1999**, *2*, 27-35.

Loeb, S. J., and Wisner, J. A. "1,2-Bis(4,4'-dipyridinium)ethane. A Versatile Dication for the Formation of [2]Rotaxanes with Dibenzo-24-crown-8 ether" *Chem. Comm.* **1998**, 2757-2756.

Loeb, S. J., and Wisner, J. A. "A New Motif for the Self-assembly of [2]Pseudorotaxanes. 1,2-Bis(pyridinium)ethane 'Axles' and 24-Crown-8 ether 'wheels'" *Angew. Chem. Int. Ed. Engl.* **1998**, *37*, 2838-2840.

Loeb, S. J., Shimizu, G. K. H., and Wisner, J. A. "Mono- Versus Dipalladation of a Durene Based Thioether Ligand. Structures of $[PdCl((t\text{-}BuSCH_2)_4C_6H)]$ and $[Pd_2((t\text{-}BuSCH_2)_4C_6H)(MeCN)_2][BF_4]_2$" *Organometallics* **1998**, *17*, 2324-2327.

Gugelchuck, M. M., and Wisner J. A. "Density Functional Study of Intermediates in the Nickel-Catalyzed Homo-Diels-Alder Reaction of Norbornadiene with Alkenes" *Organometallics* **1995**, *14*, 1834-1839.

Conference Presentations

Loeb, S. J., Wisner, J. A* "1,2-Bis(pyridinium)ethane Ligands in the Construction of Interlocked and Interpenetrated Molecules" 82nd Canadian Chemical Conference and Exhibition, Toronto, Ontario, Canada, 1999.

Hall, J. R., Loeb, S. J.*, Wisner, J. A. "Self-Assembly with Oganopalladium Building Blocks" 217th American Chemical Society Conference, Anaheim, USA, 1999.

Corrent, S. S., Kickham, J. E., Murphy, S. L., Loeb, S. J.*, Wisner, J. A. "Second Sphere Coordination" 216th American Chemical Society Conference, Boston, USA, 1998.

Loeb, S. J.*, Wisner, J. A. "A New Motif for the Self-assembly of [2]Rotaxanes" XXIII International Symposium on Macrocyclic Chemistry, Turtle Bay, USA, 1998.

Loeb, S. J.*, Wisner, J. A. "A New Motif for the Self-assembly of [2]Rotaxanes" 81st Canadian Chemical Conference and Exhibition, Whistler, British Columbia, 1998.